

EXPRESSION PROFILING OF *THERMOPLASMA VOLCANIUM* GSS1 UNDER STRESS  
CONDITIONS WITH SPECIFIC EMPHASIS ON PROTEASOME ASSOCIATED  
REGULATORY VAT GENES

A THESIS SUBMITTED TO  
THE GRADUATE SCHOOL OF NATURAL AND APPLIED SCIENCES  
OF  
MIDDLE EAST TECHNICAL UNIVERSITY

BY

TÜLAY YILMAZ

IN PARTIAL FULFILLMENT OF THE REQUIREMENTS  
FOR  
THE DEGREE OF MASTER OF SCIENCE  
IN  
BIOLOGY

MAY 2013



Approval of the thesis:

**EXPRESSION PROFILING OF *THERMOPLASMA VOLCANIUM* GSS1 UNDER  
STRESS CONDITIONS WITH SPECIFIC EMPHASIS ON PROTEASOME  
ASSOCIATED REGULATORY VAT GENES**

submitted by **TÜLAY YILMAZ** in partial fulfillment of the requirements of the degree of  
**Master of Science in Biology Department, Middle East Technical University** by,

Prof. Dr. Canan Özgen  
Dean, Graduate School of **Natural and Applied Sciences** \_\_\_\_\_

Prof. Dr. Gülay Özcengiz  
Head of Department, **Biology** \_\_\_\_\_

Prof. Dr. Semra Kocabıyık  
Supervisor, **Biology Department, METU** \_\_\_\_\_

**Examining Committee Members:**

Prof. Dr. Emel Arınç  
Biology Dept., METU \_\_\_\_\_

Prof. Dr. Semra Kocabıyık  
Biology Dept., METU \_\_\_\_\_

Prof. Dr. Fatih İzgü  
Biology Dept., METU \_\_\_\_\_

Assoc. Prof. Dr. Tülin Yanık  
Biology Dept., METU \_\_\_\_\_

Assoc. Prof. Dr. Ayşen Tezcaner  
Engineering Dept., METU \_\_\_\_\_

**Date:** 02.05.2013  
\_\_\_\_\_

**I hereby declare that all information in this document has been obtained and presented in accordance with academic rules and ethical conduct. I also declare that, as required by these rules and conduct, I have fully cited and referenced all material and results that are not original to this work.**

Name, Last name: Tülay YILMAZ

Signature:

## ABSTRACT

### EXPRESSION PROFILING OF *THERMOPLASMA VOLCANIUM* GSS1 UNDER STRESS CONDITIONS WITH SPECIFIC EMPHASIS ON PROTEASOME ASSOCIATED REGULATORY VAT GENES

Yılmaz, Tülay

M.Sc., Department of Biology

Supervisor: Prof. Dr. Semra Kocabıyık

May 2013, 150 pages

In this study differential expression of the two proteasome associated VAT genes (TVNO382 and TVN0947) of *Thermoplasma volcanium* GSS1 (*Tpv*) cells challenged by extracellular stresses, *i.e.*, pH, heat-shock and hydrogen peroxide were investigated using quantitative RT-PCR and Western blotting/hybridization techniques. We also performed a comprehensive transcriptome analysis of the *Tpv* as response to environmental stresses by genome-wide expression arrays. Quantitative RT-PCR analyses revealed that VAT genes elicited specific response under heat-shock (at 65°C and 70°C), pH stress (at pH 4.0) and oxidative stress (at 0.02 mM H<sub>2</sub>O<sub>2</sub>) over 120 min. Western hybridization corroborated the qRT-PCR results at protein level. These results suggested a critical role for VAT proteins possibly in association with the 20S proteasome in *Tpv* cells for adaptation to external stress, especially heat-shock. Microarray analyses revealed that *Tpv* cells' gene expression over 60 min stress exposure was essentially down-regulated. Within this group of genes those functionally linked to energy production and conversion, transcription and translation were significantly and extensively inhibited. Response to heat stress (at 65°C) could be linked to elevated expression of genes encoding heat-shock related genes (*e.g.* GrpE) whereas the stress response to pH and oxidative stresses was characterized by up-regulation of membrane and transport related genes. Among the stress responsive genes sugar permease (TVN1145) and GrpE (TVN0489) genes were selected for verification of the microarray data by qRT-PCR technique. The results demonstrated a consistent trend in the expression patterns of the selected genes by two techniques. Collectively, our results suggest that the transcription and translation are retarded to prevent error prone synthesis of proteins and to avoid energy requiring synthetic processes. The energy balance may be maintained by activation of carbohydrate transport and metabolism under all stress conditions. *Tpv* also modulates stress specific genes (*e.g.*, GrpE-Heat-shock, redoxins-Oxidative stress, transporters-pH stress) as part of its stress defense mechanism(s).

Key words: Archaea, heat/pH/oxidative stress, *Thermoplasma volcanium*, VAT, microarray

## ÖZ

### ***THERMOPLASMA VOLCANIUM* GSS1'İN STRES KOŞULLARI ALTINDA PROTEAZOMA İLİŞKİN DÜZENLEYİCİ VAT GENLERİ AĞIRLIKLIL OLMAK ÜZERE GEN ANLATIM PROFİLİNİN BELİRLENMESİ**

Yılmaz, Tülay

Yüksek Lisans, Biyoloji Bölümü

Tez yöneticisi: Prof. Dr. Semra Kocabıyık

Mayıs 2013, 150 Sayfa

*Thermoplasma volcanium* (*Tpv*) GSS1'in dış stres etkenleri olan; pH, ısı-şoku ve hidrojen peroksit ile tetiklendiğinde proteasoma ilişkin iki VAT geninin anlatımında oluşan farklılıklar nicel RT-PCR ve Western aktarım ve hibritleme teknikleri ile incelenmiştir. Ayrıca genom boyutunda mikrodizinler aracılığı ile *Tpv*'nin çevresel streslere tepkisinin geniş kapsamlı transkriptom düzeyinde analizi yapılmıştır. Nicel RT-PCR analizleri göstermiştir ki, VAT genleri ısı şoku (65°C ve 70°C), pH stresi (pH 4.0) ve oksidatif strese (0.02 mM H<sub>2</sub>O<sub>2</sub>) 120 dakika boyunca maruz bırakıldıklarında özgün stres yanıtı oluşturmuşlardır. Western hibritleme qRT-PCR sonuçlarını doğrulamıştır. Bu sonuçlar *Tpv* hücrelerinde VAT proteininin muhtemelen proteasomla birlikte çevresel strese özellikle ısı-şokuna uyumda, kritik bir role sahip olduğunu göstermektedir. Mikroarray analizi sonuçları *Tpv* hücrelerinde genlerin strese maruz kaldıkları 60 dakika boyunca çoğunlukla anlatımlarının düştüğünü ortaya çıkartmıştır. Bu grup genler içinde işlevsel olarak enerji üretimi ve dönüşümü, transkripsiyon ve translasyon ile bağlantılı olanlar geniş kapsamlı ve önemli ölçüde inhibe olmuşlardır. Isı-şoku yanıtı, ısı-şoku bağlantılı genlerin (örneğin, GrpE) anlatımının artması ile ilişkilendirilebilirken, pH ve oksidatif strese yanıtı membran ve transport ile bağlantılı genlerin anlatımının artması ile karakterize edilmişlerdir. Strese tepki gösteren genler arasından seçilen şeker permeaz ve GrpE genleri mikrodizin verisini doğrulamak için qRT-PCR ile analiz edilmişlerdir. Bu sonuçlar seçilen genlerin her iki teknikle belirlenen anlatım örüntülerinin tutarlı olduğunu göstermiştir. Toplu olarak bu sonuçlar öneriyor ki, tüm stres koşullarında hata eğilimli protein sentezini önlemek ve enerji gerektiren sentetik süreçlerden kaçınmak için transkripsiyon ve translasyonun engellenmektedir. Tüm stres koşullarında enerji dengesinin sürdürülebilirliği karbonhidrat taşıma ve metabolizmasının aktivasyonu ile sağlanmıştır. *Tpv* ayrıca stresten korunma mekanizmasının bir parçası olarak strese özgü genleri de (ör, GrpE-Isı-şoku, redoksinler-Oksidatif stres, Taşıyıcılar-pH stres) düzenlemektedir.

Anahtar kelimeler: Arkea, ısı/pH/oksidatif stres, *Thermoplasma volcanium*, VAT, mikroarray

**To my family,**

## ACKNOWLEDGEMENTS

Foremost, I would like to express my great appreciation to my supervisor Prof. Dr. Semra Kocabıyık for her valuable and constructive suggestions during the planning and development of this research work. Her willingness to give her time so generously has been very much appreciated. Her guidance helped me in all steps of this thesis. It would have not been possible to finish without her help.

Secondly, I want to thank dear professors Prof. Dr. Emel Arınç, Prof. Dr. Fatih İzgü, Assoc. Prof. Dr. Tülin Yanık and Assoc. Prof. Dr. Ayşen Tezcaner for their valuable contributions.

I wish to thank to my lab partners, Ilir Sheraj and Esra Yetişgin for their help.

I would like to thank to my beloved, Paul J. Swenson, for his unequivocal support, and great patience at all times.

I'm thankful to my great friends Yiğit Ozan Çolak, Erkan Arslan, Güler Bozok, Negar Taghavi and Kaveh Dehganian for sharing all my happy and distressed moments. I also thank to Gül Açıkgöz Çakmak, for reminding me the potential in me whenever I felt down. I'm lucky to meet you all in different periods of my life.

And the last but not least I would like to thank to my mother, İsmınaz Yılmaz for her peerless support in every stage of my life, I would be nothing without her help. I also thank to my father Faruk Yılmaz and brother Tümay Evren Yılmaz for being there whenever I needed.

I would like to thank for the financial support for the project and student fellowship of ODTÜ-BAP-07-02-2012-101 and TUBİTAK/TBAG109T946, respectively.

## TABLE OF CONTENTS

ABSTRACT .....	v
ÖZ.....	vi
ACKNOWLEDGEMENTS .....	viii
TABLE OF CONTENTS .....	ix
LIST OF TABLES .....	xiii
LIST OF FIGURES.....	xv
LIST OF ABBREVIATIONS .....	xix

### CHAPTERS

1. INTRODUCTION .....	1
1.1 Life in Extreme Conditions.....	1
1.2 Benefits of Studying with Archaea .....	2
1.3 Stress and Stress Response.....	2
1.4 Proteasomes at a Glance.....	3
1.4.1 The 20S Proteasome.....	4
1.4.1.1 Distribution and Subunit Composition of the 20S Proteasome .....	4
1.4.1.2 Structure of the Proteasome.....	5
1.4.2 The 26S Proteasome.....	7
1.4.2.1 Structure of the 26S Proteasome.....	7
1.4.2.2 The Ubiquitin-Proteasome System (UPS) .....	8
1.4.2.3 Multistep Mechanism of the 26S Proteasome .....	9
1.5 Proteasome Assisting Complexes.....	10
1.5.1 AAA+ Superfamily .....	10
1.5.1.1 Archaeal PAN Complex .....	11
1.5.1.2 Eukaryotic Cdc48/p97 .....	12
1.5.1.3 <i>Thermoplasma</i> VAT Protein.....	13
1.6 Proteasome, PAN and VAT Involvement in Stress Response.....	15
1.7 A Study from a Specific Gene to a Genome-Wide Analysis.....	16
1.7.1 Microarray Technology .....	16
1.8 <i>Thermoplasma volcanium</i> as a Model Organism .....	20
1.9 Aim of the Study.....	20
2. MATERIALS AND METHODS.....	23
2.1 Materials.....	23
2.2 2.1.1 Chemicals, Enzymes and Kits.....	23

2.1.2 Buffers and Solutions .....	23
2.1.3 Molecular Size Markers and Ladders .....	23
2.2 Strain and Medium .....	24
2.2.1 Archaeal Strain .....	24
2.2.2 Growth and Maintenance .....	24
2.3 Methods .....	24
2.3.1 Growth of <i>T. volcanium</i> Cells for Transcription Induction under Stress .....	24
2.3.1.1 Heat Stress .....	24
2.3.1.2 pH Stress .....	25
2.3.1.3 Oxidative Stress .....	25
2.3.2 RNA Isolation .....	25
2.3.2.1 RNeasy Mini Kit Protocol .....	25
2.3.2.2 RNA All Prep Kit Protocol .....	26
2.3.3 Agarose Gel Electrophoresis of Stress Exposed RNA Samples .....	26
2.3.4 Real-Time Reverse Transcription PCR .....	27
2.3.4.1 Reverse Transcription PCR .....	27
2.3.4.2 The Real-Time PCR .....	28
2.3.5 Detection of the VAT Protein by Western Blot Analysis .....	28
2.3.5.1 Purification of Total Protein .....	29
2.3.5.2 Biotin Labeling of the Antibody .....	29
2.3.5.3 SDS Polyacrylamide Gel Electrophoresis of the Purified Total Protein .....	29
2.3.5.4 Western Blotting .....	30
2.3.5.5 Immunodetection .....	30
2.3.6 Microarray .....	31
3. RESULTS .....	33
3.1 RNA Isolation, Concentration and Quality Check .....	33
3.2 Reverse Transcription and Quantitative Real-Time PCR for Expression Analysis of TVN0382 .....	36
3.2.1 Time-Course Differential Expression of TVN0382 Gene under Heat Stress .....	38
3.2.2 Fold Difference Analysis of Time-Course Expression of TVN0382 Gene under Heat Shock .....	40
3.2.3 Time-Course Differential Expression of TVN0382 Gene under pH Stress .....	41
3.2.4 Fold Difference Analysis of Time-Course Expression of TVN0382 Gene under pH Stress .....	44
3.2.5 Time-Course Differential Expression of TVN0382 Gene under Oxidative Stress .....	45
3.2.6 Fold Difference Analysis of Time-Course Expression of TVN0382 Gene under Oxidative Stress .....	48
3.3 Reverse Transcription and Quantitative Real-Time PCR for Expression Analysis of TVN0947 .....	49
3.3.1 Time-Course Differential Expression of TVN0947 Gene under Heat Stress .....	51

3.3.2	Fold Difference Analysis of Time-Course Expression of TVN0947 Gene under Heat Shock .....	53
3.3.3	Time-Course Differential Expression of TVN0947 Gene under pH Stress.....	54
3.3.4	Fold Difference Analysis of Time-Course Expression of TVN0947 Gene under pH Stress .....	57
3.3.5	Time-Course Differential Expression of TVN0947 Gene under Oxidative Stress .....	58
3.3.6	Fold Difference Analysis of Time-Course Expression of TVN0947 Gene under Oxidative Stress.....	61
3.4	Expression Analysis of VAT Genes at Translation Level under Stress Conditions by Western Blot Hybridization Assay .....	62
3.5	Whole Genome Microarray Analysis of <i>Thermoplasma volcanium</i> GSS 1 Response to Heat shock, pH and Oxidative Stress .....	65
3.5.1	RNA Isolation of Stress Induced Cells for Microarray Study .....	65
3.5.2	Quality Assessment of Microarray Data and Normalization .....	67
3.5.3	Microarray Data Analysis .....	71
3.5.3.1	Heat Stress .....	71
3.5.3.2	pH Stress.....	76
3.5.3.3	Oxidative Stress.....	83
3.6	Validation of Microarray Results Using Real-Time Quantitative PCR .....	90
3.7	Reverse Transcription and Quantitative Real-Time PCR for Expression Analysis of TVN0489 .....	93
3.7.1	Time-Course Differential Expression of TVN0489 Gene under Heat Stress ...	93
3.7.2	Fold Difference Analysis of Time-Course Expression of TVN0489 Gene under Heat Shock .....	95
3.7.3	Time-Course Differential Expression of TVN0947 Gene under pH Stress.....	96
3.7.4	Fold Difference Analysis of Time-Course Expression of TVN0489 Gene under pH Stress .....	97
3.7.5	Time-Course Differential Expression of TVN0489 Gene under Oxidative Stress .....	98
3.7.6	Fold Difference Analysis of Time-Course Expression of TVN0489 Gene under Oxidative Stress.....	99
3.8	Reverse Transcription and Quantitative Real-Time PCR for Expression Analysis of TVN1145 .....	100
3.8.1	Time-Course Differential Expression of TVN1145 Gene under Heat Stress .	100
3.8.2	Fold Difference Analysis of Time-Course Expression of TVN1145 Gene under Heat Shock .....	101
3.8.3	Time-Course Differential Expression of TVN1145 Gene under pH Stress....	103
3.8.4	Fold Difference Analysis of Time-Course Expression of TVN1145 Gene under pH Stress .....	104
3.8.5	Time-Course Differential Expression of TVN1145 Gene under Oxidative Stress .....	105
3.8.6	Fold Difference Analysis of Time-Course Expression of TVN1145 Gene under Oxidative Stress.....	106

4. DISCUSSION .....	107
5. CONCLUSION .....	119
REFERENCES .....	121
APPENDICES .....	131
A. BUFFERS AND SOLUTIONS .....	131
B. LADDER IMAGES .....	135
C. AMPLIFICATION AND MELTING CURVES .....	137

## LIST OF TABLES

### TABLES

Table 2.1 Gene specific reverse primers (RP) for cDNA synthesis.....	27
Table 2.2 Gene specific forward (Fp) and reverse primers (Rp) for qRT-PCR.....	28
Table 2.3 Flow chart for NimbleGen gene expression array .....	32
Table 3.1 Concentrations of the RNA samples and $A_{260}/A_{280}$ ratio .....	36
Table 3.2 Representative Ct values and mean value of at least three melting temperatures from heat shock experiments for TVN0382 gene.....	38
Table 3.3 Fold differences of TVN0382 gene expression under heat shock .....	40
Table 3.4 Representative Ct values and mean value of at least three melting temperatures from pH stress experiments for TVN0382 gene.....	42
Table 3.5 Fold differences of TVN0382 gene expression under pH stress.....	44
Table 3.6 Representative Ct values and mean value of at least three melting temperatures from oxidative stress experiments for TVN0382 gene.....	46
Table 3.7 Fold differences of TVN0382 gene expression under oxidative stress.....	48
Table 3.8 Representative Ct values and mean value of at least three melting temperatures from heat shock experiments for TVN0947 gene.....	51
Table 3.9 Fold differences of TVN0947 gene expression under heat shock .....	53
Table 3.10 Representative Ct values and mean value of at least three melting temperatures from pH stress experiments for TVN0947 gene.....	55
Table 3.11 Fold differences of TVN0947 gene expression under pH stress.....	57
Table 3.12 Representative Ct values and mean value of at least three melting temperatures from oxidative stress experiments for TVN0947 gene.....	59
Table 3.13 Fold differences of TVN0947 gene expression under oxidative stress.....	61
Table 3.14 Concentrations of the RNA samples .....	65
Table 3.15 Concentrations of the double stranded cDNA samples.....	66
Table 3.16 Number of genes differentially expressed in total of 1501 genes under heat shock.....	71
Table 3.17 Differentially expressed genes of <i>Tpv</i> cells under heat shock .....	73
Table 3.18 Number of genes differentially expressed in total of 1501 genes under pH stress .....	76
Table 3.19 Differentially expressed genes of <i>Tpv</i> cells under pH stress.....	78
Table 3.20 Number of genes differentially expressed in total of 1501 genes under oxidative stress .....	83
Table 3.21 Differentially expressed genes of <i>Tpv</i> cells under oxidative stress.....	85
Table 3.22 Representative Ct values and mean value of at least two melting temperatures from heat shock experiments for TVN0489 gene .....	93

Table 3.23 Fold differences of TVN0489 gene expression under heat shock.....	95
Table 3.24 Representative Ct values and mean value of at least two melting temperatures from pH stress experiments for TVN0489 gene .....	96
Table 3.25 Fold differences of TVN0489 gene expression under pH stress.....	97
Table 3.26 Representative Ct values and mean value of at least two melting temperatures from oxidative stress experiments for TVN0489 gene .....	98
Table 3.27 Fold differences of TVN0489 gene expression under oxidative stress .....	99
Table 3.28 Representative Ct values and mean value of at least two melting temperatures from heat shock experiments for TVN1145 gene .....	100
Table 3.29 Fold differences of TVN1145 gene expression under heat shock.....	102
Table 3.30 Representative Ct values and mean value of at least two melting temperatures from pH stress experiments for TVN1145 gene .....	103
Table 3.31 Fold differences of TVN01145 gene expression under pH stress .....	104
Table 3.32 Representative Ct values and mean value of at least two melting temperatures from oxidative stress experiments for TVN1145 gene .....	105
Table 3.33 Fold differences of TVN1145 gene expression under oxidative stress .....	106

## LIST OF FIGURES

### FIGURES

Figure 1.1 Transmission electron microscopy of the negatively stained recombinant <i>Tpv</i> 20S proteasome .....	5
Figure 1.2 Structure comparisons of the eubacterial, archaeal and eukaryotic 20S proteasome complexes .....	6
Figure 1.3 The 26S proteasome composition.....	7
Figure 1.4 Protein degradation process by the 26S proteasome.....	10
Figure 1.5 Electron micrograph of negatively stained VAT protein particles .....	14
Figure 1.6 The synthesis of microarrays using NimbleGen MAS technology .....	18
Figure 3.1 Gel electrophoresis of RNA samples isolated from <i>Tpv</i> cells under heat shock.....	33
Figure 3.2 Gel electrophoresis of RNA samples isolated from <i>Tpv</i> cells under pH stress .....	34
Figure 3.3 Gel electrophoresis of RNA samples isolated from <i>Tpv</i> cells under oxidative stress .....	34
Figure 3.4 Gel electrophoresis of control RNA samples isolated from <i>Tpv</i> cells under optimum conditions .....	35
Figure 3.5 The sequence of TVN0382 gene (1128 bp).....	37
Figure 3.6 Agarose gel electrophoresis of cDNA samples of VAT gene, TVN0382 .....	37
Figure 3.7 Real-time PCR amplification and melting curves for TVN0382 gene.....	39
Figure 3.8 Real-time PCR amplification and melting curves for TVN0382 gene.....	39
Figure 3.9 Relative mRNA expression of TVN0382 gene determined by quantitative real-time PCR analysis under heat shock at 65°C and 70°C .....	41
Figure 3.10 Real-time PCR amplification and melting curves for TVN0382 gene .....	43
Figure 3.11 Real-time PCR amplification and melting curves for TVN0382 gene .....	43
Figure 3.12 Relative mRNA expression of TVN0382 gene determined by quantitative real-time PCR analysis under pH stress at pH 3.6, 4.0, 4.5 and 5.0.....	45
Figure 3.13 Real-time PCR amplification and melting curves for TVN0382 gene .....	47
Figure 3.14 Real-time PCR amplification and melting curves for TVN0382 gene .....	47
Figure 3.15 Relative mRNA expression of TVN0382 gene determined by quantitative real-time PCR analysis under oxidative stress at 0.01 mM, 0.02 mM, 0.03 mM and 0.05 mM.....	49
Figure 3.16 Agarose gel electrophoresis of cDNA samples of VAT gene, TVN0947 .....	49
Figure 3.17 The sequence of TVN0947 gene (2238 bp).....	50
Figure 3.18 Real-time PCR amplification and melting curves for TVN0947 gene .....	52
Figure 3.19 Real-time PCR amplification and melting curves for TVN0947 gene .....	52

Figure 3.20 Relative mRNA expression of TVN0947 gene determined by quantitative real-time PCR analysis under heat shock at 65°C and 70°C .....	54
Figure 3.21 Real-time PCR amplification and melting curves for TVN0947 gene .....	56
Figure 3.22 Real-time PCR amplification and melting curves for TVN0947 gene .....	56
Figure 3.23 Relative mRNA expression of TVN0947 gene determined by quantitative real-time PCR analysis under pH stress at pH 3.6, 4.0, 4.5 and 5.0 .....	58
Figure 3.24 Real-time PCR amplification and melting curves for TVN0947 gene .....	60
Figure 3.25 Real-time PCR amplification and melting curves for TVN0947 gene .....	60
Figure 3.26 Relative mRNA expression of TVN0947 gene determined by quantitative real-time PCR analysis under oxidative stress at 0.01 mM, 0.02 mM, 0.03 mM and 0.05 mM .....	62
Figure 3.27 Clustel Q (1.1.0) multiple sequence alignment of subject TVN0382 versus object partial VCP protein .....	63
Figure 3.28 Clustel Q (1.1.0) multiple sequence alignment of subject TVN0947 versus object partial VCP protein .....	63
Figure 3.29 Western blot hybridization analyses of <i>Tpv</i> protein extracts from control and stress exposed cultures for 60 min .....	64
Figure 3.30 Western blot hybridization analyses of <i>Tpv</i> protein extracts from control and stress exposed cultures for 120 min .....	64
Figure 3.31 Formaldehyde agarose gel (1.2%) photo of the RNA samples of stress induced cells .....	66
Figure 3.32 Formaldehyde agarose gel (1.2%) photo of the dscDNA samples of stress induced cells .....	66
Figure 3.33 MA-plot of eight arrays plotted with a reference array .....	68
Figure 3.34 MA-plot of eight arrays plotted with a reference array .....	68
Figure 3.35 Smoothed histograms and box plots of unprocessed log scale probe intensities for eight arrays .....	69
Figure 3.36 Density plot and box plots of RMA processed log scale probe intensities of eight arrays .....	69
Figure 3.37 Scatter plots of average probe intensity (Log2) for Roche NimbleGen microarray chips hybridized with cDNA from heat shock, pH stress, oxidative stress and control cultures of <i>Tpv</i> cells .....	70
Figure 3.38 The volcano plot for the heat stress dataset in comparison to control .....	71
Figure 3.39 Scatter plot of average probe intensity (Log2) for Roche NimbleGen microarray chips hybridized with cDNA from heat shock induced cultures versus control of <i>Tpv</i> cells .....	72
Figure 3.40 The volcano plot for the pH stress dataset in comparison to control .....	77
Figure 3.41 Scatter plot of average probe intensity (Log2) for Roche NimbleGen microarray chips hybridized with cDNA from pH stress induced cultures versus control of <i>Tpv</i> cells .....	77
Figure 3.42 The volcano plot for the oxidative stress dataset in comparison to control .....	84
Figure 3.43 Scatter plot of average probe intensity (Log2) for Roche NimbleGen microarray chips hybridized with cDNA from oxidative stress induced cultures versus control of <i>Tpv</i> cells .....	84

Figure 3.44 The sequence of TVN0489 gene (531 bp).....	91
Figure 3.45 The sequence of TVN1145 gene (888 bp).....	91
Figure 3.46 Amplification of GrpE (TVN0489) cDNAs by RT-PCR .....	92
Figure 3.47 Aplification of sugar permease (TVN1145) cDNAs by RT-PCR .....	92
Figure 3.48 Real-time PCR amplification and melting curves for TVN0489 gene .....	94
Figure 3.49 Real-time PCR amplification and melting curves for TVN0489 gene .....	94
Figure 3.50 Relative mRNA expression of TVN0489 gene determined by quantitative real-time PCR analysis under heat shock at 65°C and 70°C .....	95
Figure 3.51 Real-time PCR amplification and melting curves for TVN0489 gene .....	96
Figure 3.52 Relative mRNA expression of TVN0489 gene determined by quantitative real-time PCR analysis under pH stress at pH 4.0.....	97
Figure 3.53 Real-time PCR amplification and melting curves for TVN0489 gene .....	98
Figure 3.54 Relative mRNA expression of TVN0489 gene determined by quantitative real-time PCR analysis under oxidative stress at 0.02 mM .....	99
Figure 3.55 Real-time PCR amplification and melting curves for TVN1145 gene .....	101
Figure 3.56 Real-time PCR amplification and melting curves for TVN1145 gene .....	101
Figure 3.57 Relative mRNA expression of TVN1145 gene determined by quantitative real-time PCR analysis under heat shock at 65°C and 70°C .....	102
Figure 3.58 Real-time PCR amplification and melting curves for TVN1145 gene .....	103
Figure 3.59 Relative mRNA expression of TVN1145 gene determined by quantitative real- time PCR analysis under pH stress at pH 4.0.....	104
Figure 3.60 Real-time PCR amplification and melting curves for TVN1145 gene .....	105
Figure 3.61 Relative mRNA expression of TVN1145 gene determined by quantitative real-time PCR analysis under oxidative stress at 0.02 mM.....	106
Figure 4.1 The overlap of resulting up and down regulated genes in Venn diagram .....	115
Figure 4.2 The heat map of mean gene expression values of 113 genes under three stress conditions after 1 h stress exposure with a hierarchical analysis .....	116
Figure B.1 PageRuler™ Prestained Protein Ladder, Fermentas.....	135
Figure B.2 Thermo Sceintific Gene Ruler 50bp DNA Ladder, Fermentas.....	135
Figure B.3 Thermo Scientific MassRuler Low Range DNA Ladder, Fermentas .....	136
Figure C.1 Real-time PCR amplification and melting curves for TVN0382 gene under heat-shock.....	137
Figure C.2 Real-time PCR amplification and melting curves for TVN0382 gene under pH stress.....	138
Figure C.3 Real-time PCR amplification and melting curves for TVN0382 gene under oxidative stress.....	139
Figure C.4 Real-time PCR amplification and melting curves for TVN0947 gene under heat shock .....	140
Figure C.5 Real-time PCR amplification and melting curves for TVN0947 gene under pH stress.....	141
Figure C.6 Real-time PCR amplification and melting curves for TVN0947 gene under oxidative stress.....	142
Figure C.7 Real-time PCR amplification and melting curves for TVN0489 gene under heat-shock (65°C) .....	143

Figure C.8 Real-time PCR amplification and melting curves for TVN0489 gene under heat-shock (70°C).....	144
Figure C.9 Real-time PCR amplification and melting curves for TVN0489 gene under pH stress.....	145
Figure C.10 Real-time PCR amplification and melting curves for TVN0489 gene under oxidative stress.....	146
Figure C.11 Real-time PCR amplification and melting curves for TVN1145 gene under heat-shock (65°C).....	147
Figure C.12 Real-time PCR amplification and melting curves for TVN1145 gene under heat-shock (70°C).....	148
Figure C.13 Real-time PCR amplification and melting curves for TVN1145 gene under pH stress.....	149
Figure C.14 Real-time PCR amplification and melting curves for TVN1145 gene under oxidative stress.....	150

## LIST OF ABBREVIATIONS

Cdc 48: Cell division control protein 48

Ct: Cycle threshold

HSP: Heat-Shock Protein

PAN: Proteasome Activating Nucleotidase

PCR: Polymerase Chain Reaction

RT-PCR: Reverse Transcriptase Polymerase Chain Reaction

qRT-PCR: Quantitative Reverse Transcriptase Polymerase Chain Reaction

T<sub>m</sub>: Melting temperature

Tvo: *Thermoplasma volcanium*

UPS: Ubiquitin-Proteasome System

VAT: VCP like ATPase from *Thermoplasma acidophilum*

VCP: Valosine Containing Protein



## CHAPTER 1

### INTRODUCTION

The discovery of the unique evolutionary history and biochemical properties of archaea allows it to be a separate domain in the three-domain system. They were first discovered by the study of Carl Woese who used the small subunit rRNA sequences to classify organisms [1]. Although archaea were taken as extremophilic oddities for years, now they have a universal importance. They offered a unique opportunity for scientists to figure out how less extreme organisms and cells can cope with conditions that would be normally destructive for them. This idea has been led to a driving force in biotechnology industry which aims to fortify the cells to enhance survival and recovery [2]. Moreover, deriving from their greater simplicity, archaea have become very valuable model organisms for understanding more complex systems in other domains of life [3]. The need to conduct fundamental research on the organisms appeared depending on these appealing features of this domain.

#### 1.1 Life in Extreme Conditions

As a simple rule of evolution, living organisms should adapt to their natural environment. By this way they can maintain cellular homeostasis and survive. Extreme environments like deep sea vents, submarine hydrothermal areas, and continental solfataras seem to define the limits of this simple rule [4]. Surprisingly, there are several bacteria and archaea found living in these harsh conditions which show extreme variations in heat, pH, salinity, cold, pressure and radiation. In terms of archaea, they were first thought to live in only harsh environments, but now it is known that they are found in a broad range of habitats like soils, oceans and marshlands. Hydrothermal vents and planktonic freshwaters show the highest diversity of archaea and are considered as promising habitats for discovery of new archaeal groups [5].

The organisms living above the physiological tolerance are named as extremophiles. The best known extremophiles are “thermophiles, psychrophiles, halophiles, piezophiles, acidophiles, alkaliphiles and radioresistants” [6].

The phile- suffix means ‘loving’ in Greek, so it indicates the love of the particular condition they live in. One of the most studied groups of these extremophiles is thermophiles. They live in temperature ranges between 45-80°C, while hyperthermophiles prefer temperatures 80°C or above. The maximum growth temperature revealed to date is 113°C for an archaeon *Pyrolobus fumarii* [7].

Only one of the extreme conditions would be surprising enough for their survival, but extremophiles also thrive in an environment which contains more than one extreme condition, such as thermoacidophiles. They survive in both acidic and hot environments. This brings the question into mind: how are these organisms able to not only deal with these harsh conditions, but also exploit them for their own good? Although the structural features vary depending upon the organism, the answer lies behind the adaptations of their cellular structures, unique physiology and metabolism which need the expression of unusual enzymes [7].

## **1.2 Benefits of Studying with Archaea**

Archaea serve as a mosaic of bacterial and eukaryal features which makes them a starting point for studies to reveal more complex systems in the other domains of life [8]. These studies were accelerated by the improvements in genetic tools and the availability of genome sequence data for many archaeal organisms. This offered an opportunity to discover novel pathways and their unique physiology properties. The idea of integrating these traits into organisms which do not thrive in extreme conditions has led to unique opportunities especially in the field of biotechnology [9].

There are also other research areas including biochemistry, phylogeny and physiology that archaeal species can provide crucial insights, too. Biochemistry studies help to understand their stability mechanisms at the molecular level and this paves the way for production of more robust biomolecules; phylogeny studies offer theories to reveal the link between archaea and eukarya in evolutionary level; and physiology studies serve as a Rosetta Stone to decode the complex language of mechanisms which is not present only archaea but all species [10].

Regardless of the research area, one should know that their findings should be evaluated at the level of the species they have studied with. Even closely related archaea groups that live in the same environment can differ in their properties as in the example of *Halobacterium salinarium* is UV resistant, while *Haloferax volcanii* is not [11]. In light of all these, the more we know about archaeal systems, the better we learn the equivalent systems in bacteria and eukaryotes [12].

## **1.3 Stress and Stress Response**

There is a fact that won't change regardless of where the organism lives. If a sudden change occurs in the organism's habitat, it suffers stress. This is also applicable for extremophilic organisms. A physical or chemical change in their harsh environments can disrupt their cellular functions and trigger a stress response. If it is a chemical change, it can be an increase or a decrease in pH, salinity or oxygen concentration while a physical change can be temperature elevation [2]. These stressors lead to protein denaturation, in other words protein unfolding [12]. Although protein denaturation is not the only consequence of stress, it should

be considered as a key component of stress response while the other is activation of stress genes. These genes take role in dealing with stress and support the cellular survival. The proteins encoded by these genes assist in folding and assembly processes of denatured or partially denatured proteins [2]. The most conserved groups of proteins which take role in stress response are named as heat shock proteins. Although they were named as heat shock proteins, they take role in all cells under normal physiological temperatures and growth conditions too. Their role as molecular ‘chaperones’ attracts a special interest in stress and stress response studies [13].

Stress factors disrupt protein native structure by causing them to unfold or misfold, which in turn lead to protein aggregation [12]. Aggregated proteins should be degraded immediately to maintain cellular homeostasis [14]. Otherwise, it can cause some drastic results. It is possible to make a list of human diseases which are linked to protein aggregation. Most of them fall under the category of neurodegenerative diseases (Alzheimer, Creutzfeldt-Jakob, Huntington, and Parkinson) but there are also some others like cystic fibrosis, prion disease, and cataract formation [15]. Although the list is even longer, it is better to focus on the main reason of these illnesses. They all share a common feature, which is directly related to partial unfolding of proteins and the interactions between hydrophobic surfaces of denatured proteins [15]. The newly forming peptide chain can interact with other intra- or inter-polypeptide domains, and result in misfolding and aggregation. To prevent this, chaperones should be active, and ensure the proper folding of the polypeptides [13].

When we consider protein denaturation as the main threat for the cell after being exposed to stress, protein folding/unfolding and degradation mechanisms come to the stage as threat eliminators. This elimination needs a cross-talk between the refolding and degradation machineries which are called chaperones and proteasomes, respectively [16]. Investigating these machineries in archaea will reveal hardly detectable mechanisms in bacteria and/or eukaryotes which are modified by evolution [17]. This will help to understand their complex tasks and unveil the strategies to deal with protein folding diseases.

#### **1.4 Proteasomes at a Glance**

Proteasomes are large proteases which possess energy-dependent proteolytic activity [18, 19]. They are found in all three domains of life [18, 20]. These enzymes are responsible for the degradation of various types of substrate proteins which can be grouped into two; short half-life proteins (newly-synthesized, misfolded or regulatory), and abnormal proteins (resulted from a mutation, stress or postsynthetic damage) [21, 22, 23]. By this way, proteasomes assure the quality control of the cellular proteins and perform their important tasks in transcription machinery, cell-cycle control, DNA repair, cell division, antigen presentation and signal transduction in eukaryotes [24, 19]. The roles of energy-dependent proteasomes in bacteria and archaea differ from eukarya and these roles are directly related to cell survival and stress response [25]. Therefore, necessity of the proteasome differs depending on the organism and the environmental condition. For eukarya and archaea, their

existence in the cell is ubiquitous, but for bacteria it is rare. While eukaryotes need proteasomes for their survival, they are not essential for archaea or bacteria [26].

Proteasome subunit composition varies among three domains of life. However, its multi-subunit/cylindrical structure is conserved in all species [26]. The cylinder has a central chamber which is buried in the inner face of the particle and has proteolytic activity [18]. Substrates should be transferred into this central cavity for degradation which brings the specificity to the process.

#### **1.4.1 The 20S Proteasome**

The 20S proteasome, also known as core particle (CP), indicates the proteolytically active component of the proteasomes [19]. The CP is responsible for the hydrolysis of substrate proteins. In higher organisms, its one additional role is in immunological responses [27, 20]. In eukaryotes the CP is found in the cytosol, nucleus and in interaction with endoplasmic reticulum and cytoskeleton. Although their placement in the cell remains to be established for prokaryotes, purified complexes suggest that they may be placed in the cytosol and loosely attached to cell membrane [23].

##### **1.4.1.1 Distribution and Subunit Composition of the 20S Proteasome**

The 20S proteasome was first identified by Dahlmann *et al.* in 1989 in an archaea, *Thermoplasma acidophilum*. Since then, it has been found in many other species. It is widely distributed in archaea and eukarya domains but not found in eubacteria except actinomycetes [19, 26, 25].

All 20S proteasomes are stacked into four heptameric rings of proteins which are classified into two main superfamilies as  $\alpha$  and  $\beta$  subunits of proteasomes [20]. Although this main structure is conserved, it appears the subunit complexity varies among organisms. Archaea generally have only one type of  $\alpha$  and  $\beta$  subunits with 14 identical active sites, but there are some other archaea species which breaks this rule, like *Haloferax volcanii* with one  $\beta$  and two  $\alpha$ -type subunits; or *Pyrococcus furiosus* with one type  $\alpha$  and two types of  $\beta$  subunits [26]. Therefore, it is not possible to talk about subunit uniformity among all archaea species.

In bacteria, proteasomes are very rare because they have other protease complexes like HslUV which is the simplest form of the proteasome and ClpAP that show functions similar to the proteasomes [20, 28]. The protease HslV is regulated by ATPase rings of HslU, and these form a simple 20S proteasome with two homo-oligomeric rings [29]. Actinomycete is the only known lineage of bacteria with a genuine 20S proteasome of the  $\alpha+\beta$  type [28]. 20S proteasome of actinomycete *Rhodococcus erythropolis* has two types of  $\alpha$  and  $\beta$  subunits [26]. In eukaryotes, the subunit structure of the 20S proteasome gets a bit more complex. The barrel-like structure of 20S proteasome is composed of seven different  $\alpha$ -subunits and seven

different  $\beta$ -subunits arranged in a precise order to form ring complexes with two fold symmetry [19, 18, 20].

#### 1.4.1.2 Structure of the 20S Proteasome

The quaternary structure of the 20S proteasome is highly conserved in all three domains of life. It has a barrel-like structure which is composed of four stacked heptameric rings. The outer rings are formed by  $\alpha$ -subunits and the inner rings are formed by  $\beta$ -subunits. Rings follow the order of  $\alpha 7\beta 7\beta 7\alpha 7$  from bottom up. As a result, two types of cavities form between these rings. These two cavities are named the antechamber (forechamber), which exists between  $\alpha$  and  $\beta$  rings, and the central chamber (main chamber), which exists between two  $\beta$  rings [19, 26, 20]. The function of the antechambers is unknown but it may serve as an area to keep the substrates in an unfolded state until they reach the proteolytically active site [23].

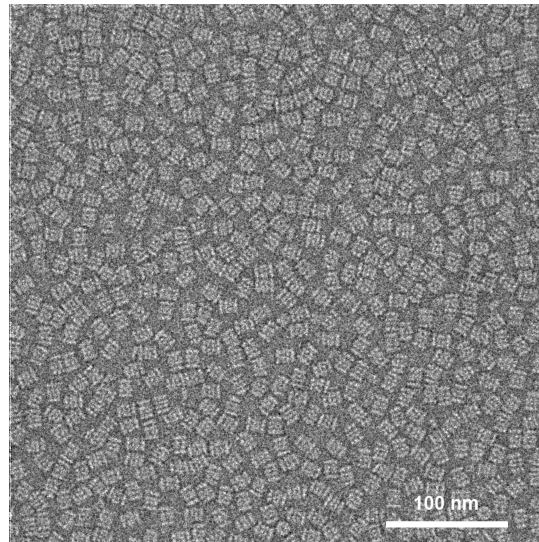


**Figure 1.1** ‘Transmission electron microscopy of the negatively stained recombinant *Tpv* 20S proteasome. The image shows end and side-views of the purified proteasome complexes. Samples were prepared and viewed on a CM12 Philips electron microscope.’ [30].

The whole complex has the total mass of 670-700 kDa, with approximately 12 nm in width and 15 nm in length. It has a pretty narrow opening (1.3 nm) formed by  $\alpha$  subunits. It limits the random access of proteins to pass through the channel. Activators are apparently needed to unfold proteins for access to the inner cavity of the cylindrical bundle [23]. The access to the proteolytic core is achieved by the gate opening of the 20S core particle. Gate formation differs depending on the organism. In eukaryotes the closed gate is formed by N-termini of  $\alpha$  subunits which have unique amino acid sequences that form an asymmetric network.

In archaea, this network is also formed by N-termini of  $\alpha$  subunits but it is less ordered and more flexible [31, 32]. This leads to diffusion of small substrates through  $\alpha$ -subunit N-termini with little hindrance. Therefore, the degradation of small peptides occurs in a higher level in archaea when compared to eukaryotes [31, 33].

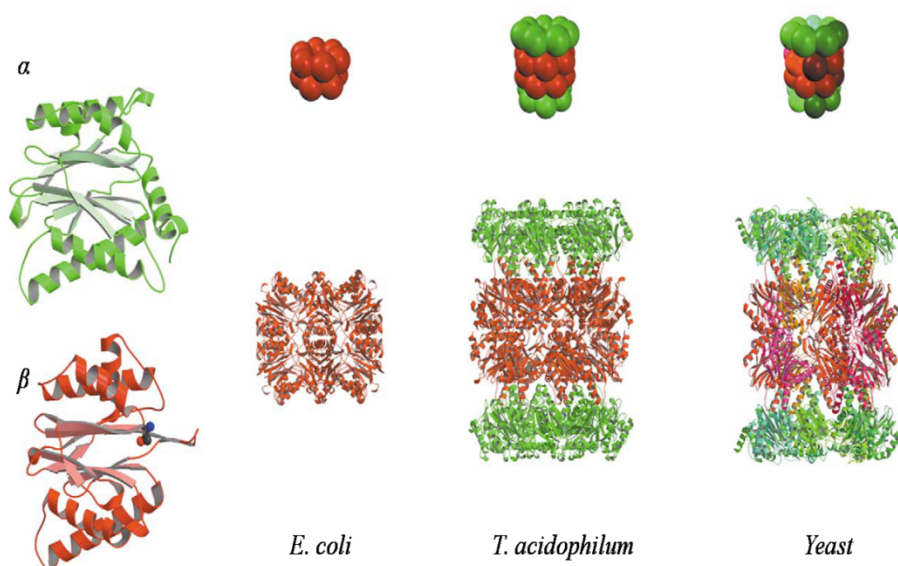


**Figure 1.2 Structure comparisons of the eubacterial, archaeal and eukaryotic 20S proteasome complexes.** The  $\alpha$ -subunits are indicated in green while active  $\beta$ -subunits in red [29].

While the N-termini of  $\alpha$  subunits take role in gate formation,  $\beta$  subunit N-termini serve as active sites of the core complex and are located at the inner face of the central chamber [19, 18]. The quantity of active sites is responsible for the peptide bond hydrolysis which varies from 6 to 14 depending on the organism [20]. In eukaryotes like yeast, 14 different  $\beta$  subunits ( $\beta 1$  to  $\beta 7$ ) are found in 20S proteasome structure and only three  $\beta$  subunits are catalytically active ( $\beta 1$ ,  $\beta 2$  and  $\beta 5$ ) in each  $\beta$  ring which results in six active sites in total [20, 26]. Also there are 7 different  $\alpha$  subunits ( $\alpha 1$  to  $\alpha 7$ ) in the structure of the each one of the 2  $\alpha$  rings of eukaryal 20S proteasome.

In higher eukaryotes complexity of the proteasome is further enhanced by formation of a new type of proteasome. When a cytokine  $\gamma$ -interferon induction occurs,  $\beta 1$ ,  $\beta 2$  and  $\beta 5$  subunits are replaced by alternative subunits:  $\beta 1i$ ,  $\beta 2i$  and  $\beta 5i$ . These proteasomes are called immunoproteasomes [29, 31].

One other form of proteasome is named thymoproteasome, which is formed when  $\beta 5$  is replaced by  $\beta 5t$ , and it is specific to the thymus [31]. Besides subunit composition, subunit expression also varies in different tissues and developmental stages [22]. In contrast to the eukaryotic ones, in most actinomycetes and archaea 20S core structure is more simple and both have  $\beta$ -type subunits with 14 identical active sites in the central chamber [34].

## 1.4.2 The 26S Proteasome

In eukaryotes, ATP-dependent 26S proteasome system is responsible for the degradation of more than 70-80% of intracellular proteins in the cytosol and nucleus [35, 21, and 36]. Although bacteria have at least five ATP-dependent proteases, 26S is the only ATP-dependent proteasome found in the nucleus and cytosol of eukaryotes up to now [37]. The density of proteasomes changes depending on cell type, tissue, organs, and protein turnover rate [22].

### 1.4.2.1 Structure of the 26S Proteasome

The 26S proteasome is a 1.5 MDa proteolytic machine [33] which is approximately 40 nm in length [18]. It has a “dumbbell” shape due to the complexes bound at each end of the 20S core particle. It is better to consider this massive structure as a hybrid between proteolytic machinery and ATP-dependent regulatory particles [39]. Therefore, it can be separated into two sub-particles as 670 kDa 20S core particle (CP) and 900 kDa 19S regulatory particle (AKA RP/PA700) [40, 29]. That is, 26S is formed when 20S core proteasome is capped by one or two 19S regulatory complexes [36].

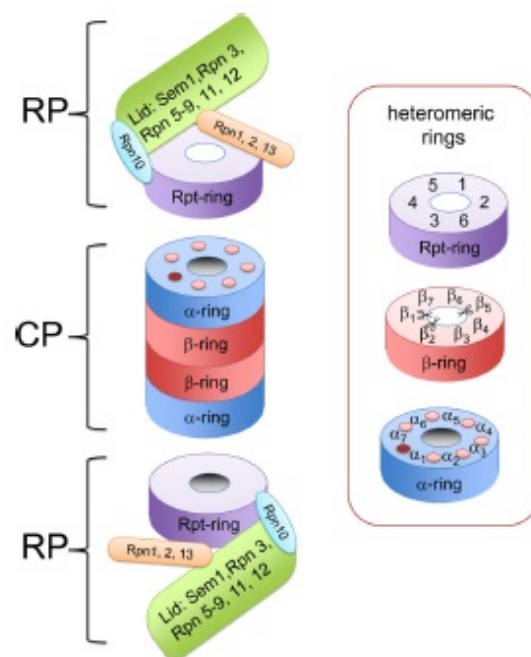


**Figure 1.3 The 26S proteasome composition.** It is composed of two regulatory particles and one core particle (CP). Regulatory particle (RP) is divided into two sub-complexes as the lid (green) and the base (purple). Rpt ring (purple) is composed of six, α (blue) and β (red) rings are seven subunits [41].

The CP is composed of 28 subunits which form 4 rings in total. Each ring consists of seven  $\alpha$  and  $\beta$ -type subunits and they are stacked in two fold symmetry to form a cylindrical structure [39]. Heteroheptameric  $\alpha$ -type subunits form the outer rings;  $\beta$ -type subunits form the inner rings. The proteolytically active  $\beta$ 1,  $\beta$ 2, and  $\beta$ 5 subunit activities are associated with caspase-like, trypsin-like, and chymotrypsin-like activity, respectively [21, 39]. While all these activities are observed for archaeal proteasomes, they differ in the activity level.

For many prokaryotes, only chymotrypsin-like activity is observed. However, there are also methanoarchaea species which have chymotrypsin and caspase-like activity at high levels. Trypsin-like activity has been only at low levels for archaeal proteasomes [23].

The RP, also called PA700, is composed of 19 subunits. It can be divided into two sub-complexes as the lid and the base. The base is the part which interacts with CP, and the lid stands distal to the core particle. The base has ten components and six of them are AAA+ ATPases, which are called as regulatory particle triple-A proteins (Rpt); Rpt1-Rpt6. They are key components of RP-CP complex formation. The remaining four components in base are regulatory particle non-ATPases (Rpn) and they are scaffolding proteins Rpn1 and Rpn 2, and ubiquitin receptors Rpn10 and Rpn13 [39, 21]. The lid is composed of nine non-ATPase subunits: Rpn3, Rpn5-Rpn9, Rpn12, Sem1 in yeast, and Rpn 11. Rpn 11 is responsible for the de-ubiquitination of the substrate proteins [38].

#### 1.4.2.2 The Ubiquitin-Proteasome System (UPS)

The ubiquitin-proteasome system (UPS) is the major proteolytic mechanism in the eukaryotic cytoplasm which takes part in life-span regulation of short-lived proteins, such as transcription factors, and degradation of folding-defective proteins which can lead toxic effects in the cell [42, 43]. By contrast with 20S proteasome in prokaryotes, eukaryotic 26S proteasome needs the ubiquitin chain to be attached to the substrate protein, so that it can recognize the substrate protein for degradation [18].

Ubiquitin is a small, 8.5 kDa, eukaryotic protein which covalently attached to a wide variety of proteins [18, 44]. It serves as a signal to regulate the function of covalently bound proteins and enables the rapid degradation of hundreds of substrate proteins by proteasome [45]. There is an enzymatic cascade that lies behind this type of degradation which includes the enzymes called, E1, E2, and E3. They are responsible for the ubiquitin attachment to the substrate protein. E1 takes role in ubiquitin activation, which is also called ubiquitin-activating enzyme. Then activated ubiquitin is transferred to ubiquitin-conjugating enzyme E2. And finally E3, ubiquitin-ligating enzyme, recruits the activated ubiquitin and transfers it to the substrate. Depending on the E3 enzyme type, this transfer can be from E2 enzyme to E3 and finally to substrate, or it can be directly from E2 enzyme to substrate protein [46]. To increase the specificity, numerous enzymes take place in the process which varies in diversity. Especially E2 and E3 enzyme (e.g 30 and 500 different species, respectively) show high diversity compared to E1 (e.g. 2 different species) [47].

Ubiquitination is an energy dependent process and needs a covalent attachment between the  $\epsilon$ -amino groups of Lys residue of substrate and carboxyl terminus of ubiquitin [25]. Just one ubiquitin attachment is not enough for targeting proteins to the proteasome. Therefore this process is repeated in a cycle until a ubiquitin chain forms. E4 enzyme is responsible for the chain formation; it adds ubiquitin to the previous ubiquitin which is bound to the substrate [42]. At least a chain of four ubiquitins is enough for targeting signal [46]. After recognition by the 26S proteasome, ubiquitins are recycled by de-ubiquitination process for later use.

The ubiquitin conjugated targeting system doesn't exist in prokaryotes. This system also doesn't include all degradation processes in eukaryotes. There is growing evidence for existence of ubiquitin-independent targeting in eukaryotic cells, and ornithine decarboxylase degradation stands as a well-studied example for this kind of proteolysis [25, 22].

#### **1.4.2.3 Multistep Mechanism of the 26S Proteasome**

Right before the protein degradation in the inner surface of the 20S core particle, the following steps should be met properly. First step is the recognition of the substrate which has a ubiquitin chain that serves as a targeting signal and then de-ubiquitination. Second step is the unfolding of the substrate since the 20S core particle is narrow and there is no other way to pass through the core complex. Third step is translocation of the unfolded protein to the proteolytically active complex [39].

The lid of the 19S regulatory particle is responsible for the first step of this multistep mechanism. The recognition of the substrate protein takes place in the lid particle by its components Rpn10 or Rpn13 [46, 42]. After recognition, de-ubiquitination is achieved by Rpn 11. By this way ubiquitins are recycled for later use. Second and third step take place in the base particle of the 19S complex. The functions of the base of the 19S particle are threefold: capturing substrate protein which has already been recognized by the lid particle, assisting protein unfolding, and translocating it into the core particle through interacting with  $\alpha$  subunits of the 20S gate [47]. The hetero-hexameric rings of AAA+ ATPase family members Rpt1-Rpt6 are responsible for these functions [38].

Protein degradation occurrence needs the CP gate opening to let the substrate access to the proteolytically active core. In the closed form of the CP, N terminal tails of  $\alpha$  subunits close the gate by serving as a plug [26, 39]. This plug should be disrupted to open the gate, and this is achieved by the docking of 19S regulatory particle onto 20S particle [31, 39]. The gate to the core particle channel opens directly onto the 19S particle, and regulatory particle guides substrates into this channel.

The channel is pretty narrow to prevent degradation of unfolded, cytosolic proteins. By this way, it also limits the degradation of even true substrates by requiring unfolding process as a prerequisite [39]. When substrate reaches the catalytic core, it is degraded and then released as short peptides of 8-11 amino acids in length [48].

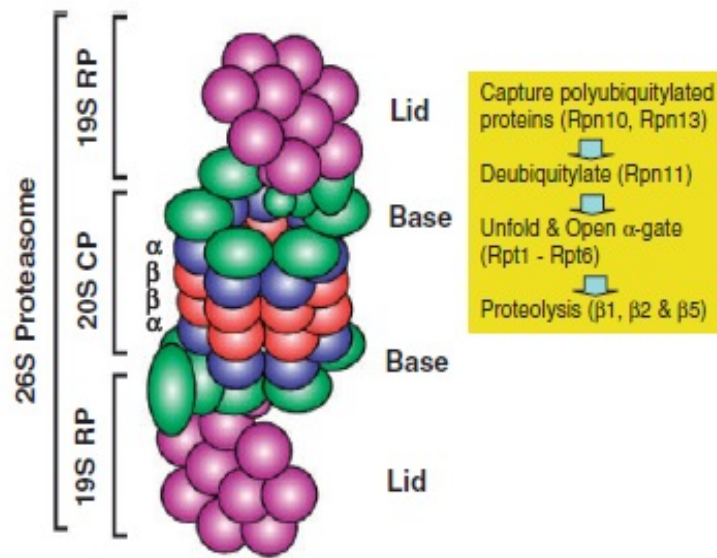


**Figure 1.4 Protein degradation process by the 26S proteasome.** After substrate protein is recognized, deubiquitylated and unfolded in the regulatory particle, it is translocated into 20S core particle for proteolysis by the active  $\beta$ 1,  $\beta$ 2 and  $\beta$ 5 subunits [47].

Although the proteolytic core of the 26S proteasome has been well studied; there is limited information about 19S regulatory subunits and their functions due to its structural complexity [38].

## 1.5 Proteasome Assisting Complexes

Self-compartmentalized proteases can catalyze the degradation of unfolded polypeptides or short peptides, alone. However they are unable to degrade most of the aggregated proteins which may form after a mutation or stress exposure. In such cases, proteasomes need the ATP hydrolysis to unfold and disaggregate substrate protein to facilitate its entry to proteolytic chamber for degradation. This type of assistance is provided by ATPase domains or complexes [23].

### 1.5.1 AAA+ Superfamily

AAA+ is a superfamily [23] which is found in all three domains of life and takes role in wide variety of processes in the cell [49] like protein degradation, cell-cycle control, biogenesis, vesicle transportation [3], spindle formation, microtubule disassembly, and membrane fusion [50]. Although they take role in several processes in the cell, their chaperone activity stands as a common duty in all those processes [51]. In the proteasomal system, they take role in recognition of ubiquitin conjugated substrates (from which enzymes remove ubiquitin) and unfolding of the proteins [33].

The AAA proteins have a defining feature of ATPase domain of about 220 amino acids. This domain is highly conserved and contains Walker A and Walker B type consensus motifs [52]. There is also one more sequence conservation area which is called the second region of homology (SRH). SRH motif distinguishes AAA+ family from other Walker-type ATPases [49]. Members of the AAA family can be grouped into two depending on the number of their domain possession. Group I has one AAA domain, and Group II has two AAA domains [50]. Group II is characterized by the N1-D1-D2 domain organization while N defines the substrate-binding region of AAA proteins [53].

AAA+ superfamily includes 19S regulatory particle of eukaryotes, eubacterial ClpX, ClpA, HslU, Lon, FtsH, ARC (ATPase ring-forming complex) of *Rhodococcus erythropolis*, and archaeal PAN (Proteasome activating nucleotidase) [25]. These proteins have the tendency of forming oligomeric, mostly hexameric rings which have a central pore. Same formation is observed for the ATPases p97 from eukaryotes, Cdc48 in yeast, and the valosine-containing protein like ATPase from *Thermoplasma acidophilum* (VAT). They all take role in disassembly or degradation processes of proteins [50].

#### 1.5.1.1 Archaeal PAN Complex

Ubiquitin proteins don't exist in archaea. Instead of 19S regulatory complex, archaeal proteasomes have a hexameric complex of the AAA+ family which shows its activity in an ATP dependent manner [33]. Although it is not possible to talk about one specific structure of this kind in all Archaea species, it is worth mentioning the system available in *Methanococcus jannaschii*. Evolutionarily, it is thought to be the ancestor of the 19S regulatory particle before protein degradation became dependent on ubiquitin signaling [33].

*Methanococcus jannaschii* genome sequencing study revealed a gene named as S4 which shows high sequence similarity to Rpt subunits of 19S regulatory particle of eukaryotes. The protein product of this gene was 50 kDa, and had a coiled coil N-terminal region which is a hallmark of proteasomal AAA ATPases. This protein was expressed in *E. coli* and purified as 650 kDa nucleotidase complex. When this complex was mixed with the *Thermoplasma acidophilum* proteasomes, the protein degradation increased up to 25-fold. As a result of this, the complex was named as PAN which stands for proteasome activating nucleotidase [26].

The 3D reconstruction study of PAN in the presence of ATP $\gamma$ S has shown that PAN has a two ring structure with a cavity in the center of the rings. The size of the internal cavity changed depending on the nucleotide binding. It suggested that the cavity gets bigger by nucleotide binding, and gets smaller when the substrate is translocated into the 20S core which can be considered a trap [54]. PAN-20S proteasome complex is responsible for the degradation of a wide variety of polypeptides in an ATP-dependent manner [36]. Sequence of events starts with ATP hydrolysis which is stimulated by substrate binding. This leads to protein unfolding, opening of axial gate and protein translocation to the 20S core particle [55]. This process is not applicable for small tetrapeptides which enter freely into 20S proteasome [36].

There are multiple steps which were observed in degradation of a globular protein by PAN-proteasome complex. PAN should associate with the 20S particle to open proteasome entry channel [52]. ATP binding to PAN is crucial for its association to proteasome, for gate opening and translocation of substrates [56]. It has been shown that PAN-20S association differs depending on the type of nucleotides while ATP and ATP $\gamma$ S enhance the interaction between 20S and PAN, ADP inhibits it. However, 20S-PAN complex formation is not stable in the presence of ATP when it is compared to ATP $\gamma$ S [57]. The crystal structure of the 20S-PAN has revealed that C-terminus HbYX (hydrophobic residue-tyrosine-X<sub>(any amino acid)</sub>) motif of PAN ATPases interacts with the 20S  $\alpha$  inter-subunit pockets and causes an 'induced-fit' conformational change for docking [58]. Thereby, it stabilizes open gate conformation of their N-terminal ends. The N-terminal domain of PAN is involved in substrate binding, and its AAA unfoldase module is responsible for the unfolding of the substrate. Then the substrate is translocated through the open gate into the 20S core particle for degradation [52]. This process reveals the fact PAN should experience several conformational changes upon ATP hydrolysis [52].

### 1.5.1.2 Eukaryotic Cdc48 / p97

PAN's simple structure and independency of ubiquitin conjugation offered several advantages to understand more complex or ATPase related proteasomal degradation systems [36]. However, it can't be attributed to all archaea. PAN homologs are absent in major archaeal lineages including *Thermoplasma* species [26]. This entailed the studies to find another protein that fulfills the functions of PAN. To address this question, eukaryal AAA ATPases which take role in protein degradation were referred to perform a systematic analysis to find out their homolog counterparts in different archaea.

Cdc48 was the first which was identified in yeast. It takes role in cell-cycle control [59]. Complete genome studies of 81 archaeal species showed that approximately 15% of archaea didn't contain PAN genes but they all had 20S proteasome genes and at least one Cdc48 gene [48, 60]. This means that Cdc48 is highly conserved and ATPase mediated proteasomal regulation is an essential function. Homologues of this protein were found in different organisms with different names, such as p97 in vertebrates, VCP (valosine containing protein) in mammals, TER94 in insects, CDC48 in *C. elegans* and VAT in archaea [61].

p97 is found in eukaryotic cells, especially in cytoplasm and nucleus. It is an AAA ATPase family member and has highly conserved domains. It is composed of six subunits where every single one has two ATPase domains, and they all form a homo-hexameric ring. It interacts with the substrates and promotes unfolding of the proteins [62].

Cdc48 and p97 are involved in several cellular activities. Cdc48 is crucial in cell division and fusion of endoplasmic reticulum membranes while p97 is important in rebuilding of golgi cisternae after mitosis [63]. Besides these, both of them facilitate ubiquitin dependent protein degradation in eukaryotes [26]. This information can be taken as a hint to investigate the proteasomal degradation system in archaea. Archaeal Cdc48 shares the same C terminal

HbYX motif with its eukaryal counterpart Cdc48 enzymes, PAN, and Rpt<sub>1-6</sub> subunits of the 19S regulatory particle [60]. All sequenced archaeal organisms up to now have at least one AAA protein which contains HbYX motif [48]. This motif takes role in the gate opening of 20S by docking into the pockets formed between  $\alpha$  subunits [47].

One study of recombinant Cdc48 has shown that Cdc48 can discriminate the native and non-native substrates. It prevented the aggregation of a protein after heat shock and bound heat denatured protein specifically in an ATP-independent manner. Furthermore a co-chaperone activity was also observed for Cdc48 [51]. Cdc48 seems to have two different mode of action. One is taking role in ubiquitin chain formation for substrate recognition, and the other is extracting ubiquitinated proteins from membranes or complex structures (e.g. chromatin) and sending them to proteasomes in the cytosol. Therefore, it works in a similar way to 19S caps [64].

There are two models offered for Cdc48 function in the cell. One of the models suggest that Cdc48 was working as an activator of 20S proteasome but when the eukaryal proteasomal degradation system evolved, 19S appeared as a particle that interacts with 20S directly, and Cdc48 pushed aside. It evolved to have other functions related to ubiquitin pathways. However, second model suggests that Cdc48 and 19S particle both have direct interactions with 20S core particle and takes role in translocation of the substrate [64].

Both of the models have their conflicts and need further investigation to be able to reach a conclusion. However, it is a fact that Cdc48 in eukaryotes and VAT protein in archaea have a tight relation based on their sequence homology and shared HbYX motifs.

### **1.5.1.3 *Thermoplasma* VAT Protein**

As was discussed earlier, PAN doesn't exist in *Thermoplasma* species, so its role is performed by another AAA ATPase family member. Three putative proteins, VAT, VAT2 and Lon2, were asserted to exert the role of PAN [65]. VAT2 and Lon2 were not well characterized but for VAT, chaperone like activity was reported [26]. While its eukaryotic homologues, Cdc48 and p97 take role in ER membrane fusion, golgi cisternae formation and ubiquitin dependent activities; VAT only function in protein quality control by interacting with thermosome or 20S proteasome due to lack of ER, golgi or ubiquitin in archaea [63]. This is supported by a recent study that VAT seems to be the only partner of 20S proteasome in ~15% of the archaea. Barthelme and Sauer showed a functional interaction between VAT and 20S proteasome which indicates that through binding to 20S proteasome, VAT induces gate opening, unfolds and translocates the substrate protein into the proteolytic chamber [60].

VAT from *Thermoplasma acidophilum* was first identified by Baumeister *et. al* in 1997 [66], and named as VCP like ATPase. VAT homohexamer complex is 500 kDa with a core structure of 15 nm in diameter, 7 nm in length and substrate binding N-domains are placed in the upper periphery of the core [49, 67, 63]. It is the archaeal member of Cdc48/p97 family and shows Mg<sup>+2</sup> dependent activity at an optimum temperature of 70°C [66]. It belongs to the

group II AAA proteins and composed of two ATPase domains; D1, D2 and one additional N-terminal domain [3]. N-terminal (VAT-N) has 185 residues and is thought to be involved in substrate recognition [50]. Although single AAA+ domain of PAN shows high sequence similarity to D1 and D2 domains of VAT, they differ from each other especially on their N domains [56].

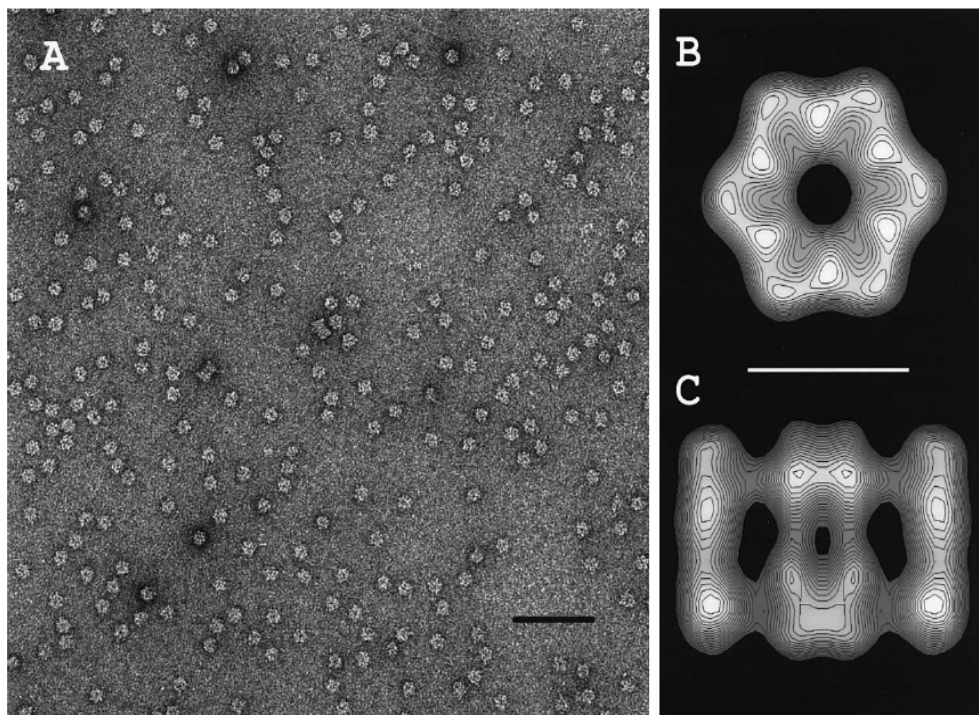


**Figure 1.5** Electron micrograph of negatively stained VAT protein particles are represented in (A). Top view (B) and side view (C) of single VAT particle is also depicted. (Scaling 100 nm for A and 10 nm for B and C) [66].

One of the structural studies with amino terminal domain of VAT (VAT-N) has been shown that it could bind polypeptides, prevent their aggregation and refold substrates [50]. It was reported that VAT requires  $Mg^{+2}$  for enzymatic activity and it can be modulated into two activity states by changing the  $Mg^{+2}$  concentrations. They are low activity mode (refolding) and high activity mode (unfolding) both state being ATP-dependent [3].

In mammalian p97/VCP protein, it has been shown that its N domain is directly related to ATP hydrolysis. It adapts two conformational changes while one is flexible and induces ATPase activity; other is locked down and decreases it [68].

It brings the question whether VAT N domain also has an activity in a similar fashion or not. It was suggested that a cleft of 3.5 nm in length forms on the surface of the N-domain and it shows chaperone activity by itself [50]. This region may take role in substrate recognition [25, 67].

In one study it has been shown that isolated VAT-N domain had an energy-independent chaperone activity and achieved folding of some substrates [3]. Another study has revealed that an N-domain deleted mutant of VAT (VAT $\Delta$ N) has shown 24-fold increased ATP hydrolysis and 250-fold enhanced unfolding activity compared to the wild type VAT [69]. All these results suggest that N-domain of VAT is not essential for ATP hydrolysis, but it controls ATPase activity by changing its flexibility and conformation according to the D1 ring [68]. That is, ATPase activity of VAT seems under control of N-domain [69].

## 1.6 Proteasome, PAN and VAT Involvement in Stress Response

Proteasome and chaperones are two important components of stress response mechanisms that protect cells from destructive effects of protein denaturation. Their increase in the cell right after stress exposure is a part of stress protection system to overcome the growth and environmental constraints.

In prokaryotes and eukaryotes, there are reports indicating a significant increase in the amount of proteasomes or chaperones when the cells are exposed to different types of stresses. Aiken *et. al.* proposed that under oxidative stress conditions, activities of the 26S proteasome is stimulated by unknown mechanisms for degrading mildly oxidized proteins. However, when oxidative insult persists, or acute oxidative stress is applied, proteasomes disassemble into 20S CPs and 19 RPs, leading the accumulation of ubiquitinated substrates. Following dissociation, free 20S proteasome are activated and oxidized proteins are degraded independently of ATP and ubiquitin [70]. CDC48 has also been essential to deal with the degradation of heat or oxidative stress damaged proteins in yeasts [71]. In *Thermoplasma acidophilum*, proteasome inhibition impaired thermotolerance when  $\beta$ -subunits of 20S proteasome in *T. acidophilum* irreversibly modified by an inhibitor (Z-L<sub>3</sub> VS). The cell growth was significantly arrest upon thermal stress but inhibition did not effect growth under normal conditions [72].

In another study with halophilic archaeon *Halobacterium*, it has been shown that PAN has a crucial role in temperature and salt stress response, and prevents harmful effects of such stressors on protein stability. A direct regulation was observed on the PAN-proteasome system to compensate for proteasome activity loss under stress. Active 20S particles increased and positive transcriptional regulation was observed for proteasome  $\alpha$  and  $\beta$  subunits [40].

Besides the key roles of PAN and VAT proteins in regulating proteasome function in archaea, the studies have shown that these regulatory complexes may function by themselves as molecular chaperones. Three types of chaperone-like activities have been revealed for PAN from *Methanococcus jannaschii* which differs depending on the type of the nucleotide bound which can prevent protein aggregation or promote protein unfolding or promote protein refolding. Among all three activities, only unfolding takes part in the stimulation of proteasomal degradation while the others occur independent from the proteasome [36, 25].

Activity of VAT in protein folding and unfolding also suggested a chaperone like function associated with this protein [50]. Collective transcriptional analysis of heat shock response in hyperthermophilic archaeon *Pyrococcus furiosus* using cDNA microarray revealed that thermosome (Hsp60), two VAT-related chaperones, heat shock protein (Hsp20), proteolysis and stabilization might act as a cooperative rescue strategy under thermal stress [73].

Proteomics analysis of *T. acidophilum* has indicated a high protein turnover-rate to high level expression of thermosome, VAT, DnaK, proteasome, elongation factors, translation, initiation factors and ribosomes. This can be due to production of large amounts of reactive oxygen species and H<sub>2</sub>O<sub>2</sub> in the cell [74]. In another study, in *Haloferax volcanii* strains when the genes encoding 20S proteasomal  $\alpha$ 1 subunit gene or PanA (one of the PAN encoding gene) were deleted, an increased sensitivity to hypo-osmotic stress and heat stress was observed [75].

Based on these studies, VAT protein presents a functional model for new studies on regulation of stress response in archaea. It also has a great potential to reveal the structural and functional mysteries of Cdc48/p97 family which takes role in many cellular processes. Therefore, the expression analysis of VAT gene under stress conditions would shed a light on functional mystery of Cdc48/p97 family and reveal VAT gene's position in archaic stress response.

## **1.7 A Study from a Specific Gene to a Genome Wide Analysis**

If we take genome to be a functioning machine, genes stand as the gears of it. The interaction of the teeth of the multiple gears resembles the genes' interaction. One's activity affects the other's action directly or indirectly. Thus, to be able to understand the whole genome, we need to know not only one gene's action but also others. Then we can draw conclusions more accurately for our research. Microarray technology seems to meet this desire and is used in many laboratories with a great enthusiasm.

### **1.7.1 Microarray Technology**

Microarray is a technique to measure the expression levels of large numbers of genes, or an entire genome, in a single experiment on a single chip [76]. Only a while ago, it was just a dream to be able to evaluate the transcripts for every gene simultaneously, but now it came true by this technology [77]. Depending on the application's quick and easy nature, it is widely preferred in many laboratories [10]. Referring to hybridization partners, a 'probe' is the tethered nucleic acid with known sequence or identity and a 'target' is the free nucleic acid sample whose identity and/or abundance are being detected. After its emergence in 1990s, it has changed a lot depending on advancements in technology. Nowadays, the most commonly used DNA microarrays are cDNA or oligonucleotide based DNA arrays [78]. The cDNA microarrays are fabricated by printing cDNAs (probes) using high-speed robotics

generally on glass slide which is coated by poly-lysine or poly-amine to enhance the DNA binding onto the slide.

At every step of printing, robotic arms' rectangular pins are loaded with cDNAs from different cDNA stocks and these PCR product clones are printed on the slide surface. After washing of the pins, the same practice is repeated with new sampling from remained cDNA stocks. However, oligonucleotide arrays are prepared in a different way than cDNA arrays. This time, oligonucleotides (probes) are synthesized directly on the array surface through 'in situ synthesis'. The chip is bathed in a solution containing the one of the four nucleotides which will be attached to the anchor or the partially constructed oligonucleotide chain on the chip. The light enables anchor-nucleotide attachment. While doing this, a set of photolithographic masks is used for light activation of the hydroxyl-protected deoxynucleotides. Synthesis of oligonucleotides is taken place in light-induced deprotecting and masking areas. Oligonucleotides are synthesized in parallel at all zones of the chip and synthesis continues with multiple baths, washes and masks until intended length of the sequence is reached [79].

There are several commercially available arrays from different companies like Affymetrix, Agilent, CombiMatrix and NimbleGen. They all have their unique printing methods for oligonucleotides while the logic lays behind the process remains the same. The platform we used, NimbleGen (Roche), has adopted the technology of Maskless Array Synthesizer (MAS) (Figure 1.6). It has two main differences from the traditional oligonucleotide synthesizing methods. NimbleGen uses glass slides instead of controlled pore glass supports and a digital micromirror device (DMD) which creates virtual masks instead of physical chromium masks. DMD is comprised of thousands of miniature aluminum mirrors which all individuals can be addressed directly by computer. By this way UV-light is reflected to the desired location through the mirror where the next nucleotide will be attached [80].

The general use of DNA microarray can be simplified as the comparison of mRNA transcripts of cells present in different tissues, cultures or experimental conditions. The amount of mRNA transcript indicates the expression level of a specific gene under selected circumstance. First of all total RNA should be extracted from the specimen, and mRNA should be isolated. The mRNA is then converted to cDNA by reverse transcription. cDNAs which are fluorescently labeled are the *targets*. The microarray consists of a solid support, mainly glass, silicon chips or nylon membrane. This support has identified and sequenced polynucleotides attached onto it, and that are called the *probes* [79]. Probes can be cDNAs printed on the solid support or oligonucleotides chemically synthesized and spotted on the surface as previously discussed [78]. The labeled targets are applied onto the probes on the array. The targets hybridize with probes which they have high sequence complementarities [79]. After a washing process of the unbound targets, the intensity of the fluorophores is compared with the control group of the experiment. This intensity measurement enables the estimation of the expression level of the corresponding cDNA transcript [81]. By this way, it is possible to define up-regulated or down-regulated genes, their interactions and pathways as a response to different experimental conditions [82].

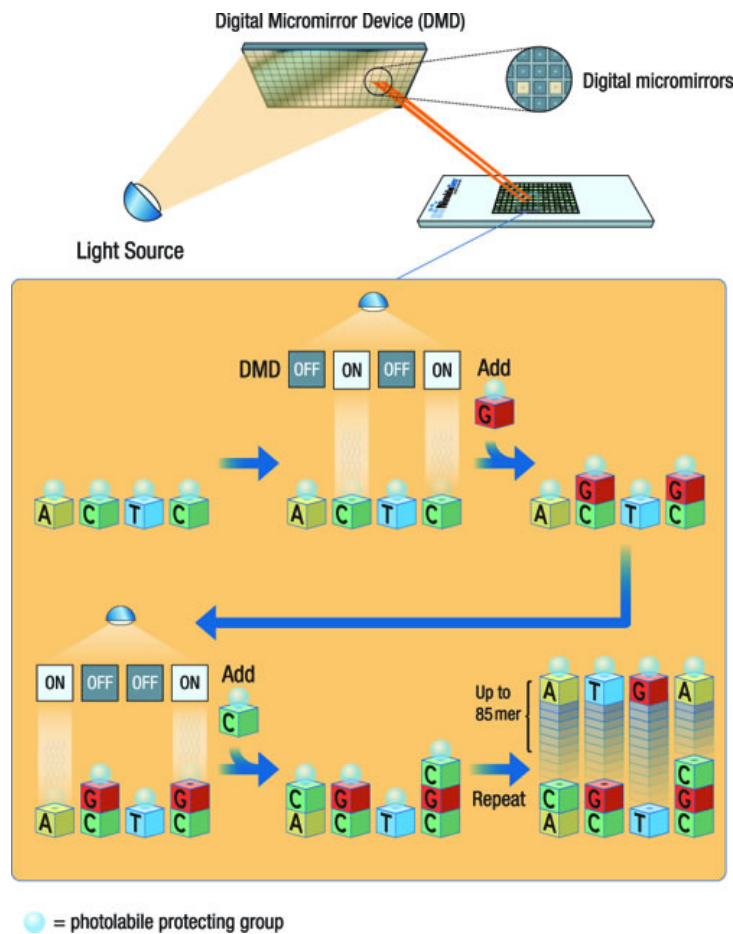


**Figure 1.6 The synthesis of microarrays using NimbleGen MAS technology [80].**

There are several publications based on microarray studies and they keep growing in the literature. While some use microarray technology as a single method to evaluate gene expression levels, others use it in conjunction with other techniques. In archaea, the most of microarray studies were gathered around the topics of stress response, tolerance to different stimuli and comparison of two different experimental conditions. For stress response, thermal stress is generally used as a parameter to observe the changes at transcriptional level of the organisms.

*Pyrococcus furiosus* heat shock response was investigated by targeted cDNA microarray and found that it responded to heat stress by a cooperative strategy of rescue which ended up differentiated gene expression of thermosome (Hsp60), small heat shock protein (Hsp20) and two VAT-related chaperones [73]. Cold adaptation response also was examined in the same organism by DNA microarray; results were compared with proteomic and metabolomic analysis and up or down regulated genes were revealed [83]. *Archaeoglobus fulgidus* heat shock response was studied by whole-genome DNA array and the results indicated decrease or increase in transcripts of the genes that take role in energy production, amino acid metabolism and signal transduction [84].

Global transcriptional analysis of *Sulfolobus solfataricus* using DNA microarray revealed a relation between specific TA (toxin-antitoxin) loci gene and thermal stress [85]. Another type of stress, oxidative stress response, was also investigated in hyperthermophilic archaea by microarrays. Whole genome transcriptional profiling of *Pyrococcus furiosus* by DNA microarray revealed that damage repair related genes were up regulated under peroxide stress [86]. Global transcriptional analysis of *Halobacterium salinarium* and comparison of active regulatory programs under various stresses helped to determine the processes which were specifically triggered by oxidative stress [87]. Oligonucleotide microarray was also used for investigation of oxidative stress in *Halobacterium salinarium* and a specific transcription factor was found to be required to deal with reactive oxygen species damage of hydrogen peroxide [88]. Whole genome microarray was employed to identify gamma irradiation tolerance in *Pyrococcus furiosus* and data analysis showed that a putative DNA-repair gene cluster was up-regulated [89]. Metal tolerance of *Thermococcus gammatolerans* was investigated using oligonucleotide microarray. The results revealed that redox homeostasis genes were constitutively expressed [90]. Growth under two different conditions was compared for *Methanosarcina mazei* with two different carbon and energy sources, acetate or methanol, using DNA arrays. It was found that similar pathways for both utilization of energy sources were functional while acetate seemed to regulate some additional genes' expression [91]. cDNA arrays were used for *Methanococcus maripaludis* to compare mRNA levels in a wild-type and one mutant strain of the organism. In total of the 1722 open reading frames encoded in the genome, 93% were probed by cDNA. Of these, 50 were over-expressed while 45 were under-expressed in the mutant compared to the wild-type [92]. And finally two different archaea, *Halobacterium salinarium* and *Haloferax volcanii*, were compared by using DNA microarrays to investigate differentially regulated genes at exponential and stationary phases of growth. No conservation assigned for the regulated genes between these two species, indicating both species have their own unique differential translational control for the regulation of gene expression [93].

The appealing features of the technique, such as obtaining the results in a short time, its relatively cheap price, flexibility to transform the information into other tools, and convenient nature of the array as being non-radioactive or toxic [94], stands as a driving force for the researchers to use microarray in their studies. However, there are also drawbacks which should be considered seriously when one decides to perform a microarray study. First of all, there are lots of variables during and after the experiment that must be optimized carefully. Quality of the probes [78] and RNA samples, reverse transcriptase enzyme efficiency, fluorescent dyes and their incorporation efficiencies should be considered carefully to decrease the possibility of the error [95]. However, in some cases error can occur at the manufacture step of the microarray chip [78] and therefore it is important to choose reliable platforms. Moreover, the question of how many replicates are required to detect changes still remains to be addressed [76].

Secondly, validation process of the microarray results can be problematic because microarray experiments produce massive amount of data [96]. Researchers use different statistical analysis software or procedures, but the results show variation in parallel to

changing methods and different platforms used [95]. Therefore, universal standards are required to produce consistent results that could be used within the scientific world [77].

The third problem is the need of an independent experiment to validate the expression levels of the genes. The same sample should be used in both microarray and in verification experiment to correlate the results. For such an approach, commonly used techniques are transcription PCR, real time PCR, northern blot, and *in situ* hybridization assay [97]. However, there might be some controversies about the reliability of these verification methods.

Overall, microarray experiment seems to have three check points: (i) the quality control of the experiment, (ii) the data validation, and (iii) the universality of the results [97]. When all these steps fulfilled with care, there is no doubt one might have an overall idea about the gene expression and their roles [78].

### **1.8 *Thermoplasma volcanium* as a Model Organism**

**Lineage:** Archaea; Euryarchaeota; Thermoplasmata; Thermoplasmatales; Thermoplasmataceae; Thermoplasma; *volcanium*

Species of the genus *Thermoplasma* do not possess a rigid cell wall; they are delimited by a plasma membrane [65]. *Thermoplasma volcanium* GSS 1 is a thermoacidophilic archaeon that thrives life at the pH range of 1-4, with an optimum pH 2.0.

The growth and temperature range between 33-67°C being optimal at 60°C [98]. It is unique among Archaea by adaptation to both aerobic and anaerobic environments [99]. It was first isolated from solfataric fields by Segerer *et al.* in 1988 [98] and its complete genomic sequence was determined in 1999 by Kawashima *et. al.* [100] which is composed of 1.584.804 bases with the GC content of 39.92%. They have irregular cell shape depending on the absence of the cell wall [101]. They have multiple flagella enable it high motility [102].

### **1.9 Aim of the Study**

This study involves two levels of analyses. First level of investigations involved time-course analysis of transcription profiles of two *Tpv* VAT genes by qRT-PCR. The second level investigations included transcriptome analysis of the *Tpv* exposed to three different stressors.

In the first level of our research, we aimed at analyze the differential expression of VAT genes (TVN0382 and TVN0947) which are VCP/Cdc48 homologues [19] in thermoacidophilic archaeon *Thermoplasma volcanium* GSS1 as a response to external stresses i.e. heat, pH and hydrogen peroxide to provide new insights to the role of VAT proteins in stress response.

Second level of our investigations included whole-genome transcriptome analysis to determine differentially expressed genes when *T. volcanium* GSS 1 cells were subjected to various environmental stressors with an intention of identifying critical stress responsive genes. To this end, microarray technology was used for expression profiling in response to heat, pH and hydrogen peroxide.



## CHAPTER 2

### MATERIALS AND METHODS

#### 2.1 Materials

##### 2.1.1 Chemicals, Enzymes and Kits

Glucose, NaOH, Sodium dodecyl sulfate,  $\text{KH}_2\text{PO}_4$ ,  $\text{MgSO}_4$ ,  $\text{CaCl}_2 \cdot 2\text{H}_2\text{O}$ ,  $(\text{NH}_4)_2\text{SO}_4$ , NaOAc, Tris-HCl, NaCl,  $\text{MgCl}_2$ , Acrylamide/Bis-acrylamide were purchased from Merck (Darmstadt, Germany). Yeast extract was from Difco (Detroit, USA). Hydrogen peroxide was from AppliChem (Darmstadt, Germany). Page Blue Protein Staining Solution was from Fermentas (Vilnius, Lithuania). Lysozyme,  $\beta$ -mercaptoethanol, ethanol, formaldehyde, formamide, agarose, EtBr, methanol, streptavidin, Tris, EDTA, Glycin, Glycerol, MOPS, Ammonium persulfate, TEMED, BSA, Tween-20, were purchased from Sigma Chemical Company (Missouri, USA). Molecular screening agarose (1%) and NBT/BCIP solution were purchased from Roche Diagnostics (Switzerland).

RNeasy Mini Kit and RNA All Prep Kit were purchased from QIAGEN Inc, Valencia, USA. FastStart DNA Master PLUS SYBR Green I Kit was purchased from Roche Diagnostics, Switzerland. Fermentas, RevertAid<sup>TM</sup> H Minus First Strand cDNA Synthesis Kit, The Light Cycler<sup>®</sup> using Biotin Protein Labeling Kit (ROCHE), Millipore Immobilon-P Transfer Membrane User Guide, cDNA Synthesis Invitrogen SuperScript<sup>®</sup> Double-Stranded cDNA Synthesis Kit.

##### 2.1.2 Buffers and Solutions

Composition of buffers and solutions used in this study are listed in Appendix A.

##### 2.1.3 Molecular Size Markers and Ladders

PageRuler<sup>TM</sup> Prestained Protein Ladder (Fermentas, Vilnius, Lithuania) was used as molecular weight standard for estimation of molecular weight of protein samples on SDS-Polyacrylamide gel. Gene Ruler 50bp DNA Ladder (Thermo Scientific) and MassRuler Low

Range DNA Ladder (ready-to-use) (Thermo Scientific) were used as standard size markers for DNA size determination on agarose gel. The ladder images were given in Appendix B.

## **2.2 Strain and Medium**

### **2.2.1 Archaeal Strain**

*Thermoplasma volcanium* (*Tpv*) GSS1 (strain type 4299) was used as the source organism in this study which was purchased from Deutsche Sammlung von Microorganismen und Zellkulturen (Braunschweig, Germany).

### **2.2.2 Growth and Maintenance**

For routine uses, *Tpv* GSS1 cells were grown in 50 ml liquid Volcanium medium (pH 2.7) [103] which was supplemented with glucose (0.5%, w/v) and yeast extract (0.1%, w/v) at 60°C without shaking. The culture was maintained by subculturing (10%, v/v) into fresh medium once a week.

## **2.3 Methods**

### **2.3.1 Growth of *T. volcanium* Cells for Transcription Induction under Stress**

*Tpv* cells were exposed to three different stress conditions (heat shock, pH and H<sub>2</sub>O<sub>2</sub>) prior to RNA isolation. The conditions were determined based on previous research in our laboratory whereby effects of various stressors on *Tpv* growth were examined.

For each one of the stress experiment, culture was prepared following the same protocol. Overnight cultures were prepared in a total volume of 50 ml supplemented with Volcanium medium in 250 ml flasks. Cultures were incubated 3 days until mid-log phase under optimal conditions (60°C, and pH 2.7). When the optical density at 600 nm (OD<sub>600</sub>) was reached to 0.5-0.7, cells were subcultured to 120 ml fresh medium in 500 ml flasks.

#### **2.3.1.1 Heat Stress**

The heat-induced changes in the target genes' expression at transcription level were examined by shifting the growth temperature to 65°C and 70°C, separately. The cultures used

as controls were continued to grow under optimal growth temperature (at 60°C). Samples from heat-shocked and control cultures were removed with 30 min intervals for 2 h.

### **2.3.1.2 pH Stress**

The pH stress was applied to mid-log cultures by increasing the pH of the growth medium to 3.5, 4.0, 4.5 and 5.0 by NaOH solution (0.5 N). The pH of the control culture was not changed. After pH adjustment, cultures were grown for 2 h at 60°C and meanwhile samples were taken with 30 min intervals for RNA isolation.

### **2.3.1.3 Oxidative Stress**

Oxidative stress was applied to mid-log cultures by addition of H<sub>2</sub>O<sub>2</sub> into final concentrations of 0.01 mM, 0.02 mM, 0.03 mM, and 0.05 mM, separately. Control culture was not supplemented with hydrogen peroxide. Following H<sub>2</sub>O<sub>2</sub> addition, samples were taken with 30 min intervals for 2 h as in other stress conditions.

## **2.3.2 RNA Isolation**

Total RNA isolation was performed by using RNeasy Mini Kit, QIAGEN Inc. (Valencia, USA), and RNA All Prep Kit, QIAGEN Inc. (Valencia, USA). Manufacturer's instructions were followed essentially with minor changes whenever needed for optimization.

### **2.3.2.1 RNeasy Mini Kit Protocol**

RNeasy Mini Kit protocol was followed for purification of total RNA to be used in RT-PCR. The lysate of the stress exposed cells was obtained by following RNeasy Mini Kit protocol. Culture aliquotes were mixed with RNAprotect Bacteria Reagent. After vortexing the mixture, it was incubated for 5 min at room temperature. Then the mixture was centrifuged at 5000xg by Sigma 3K30 Centrifuge (Germany). Supernatant was removed and 100 µl TE Buffer containing lysozyme was added into the pellet. After vortexing for 10 s, it was incubated at room temperature for 5 min.

Then 350 µl RLT Buffer which was supplemented with β-mercaptoethanol was added and vortexed. Finally 250 µl ethanol (96-100%) was added into mixture and mixed by pipetting. When the cell lysate became ready, it was applied into RNeasy Mini spin column placed in a collection tube and centrifuged by Micromax RF, ThermoIEC (USA) at 12000 rpm for 15 s. Supernatant was removed after centrifugation and Buffer RW1 was added into the column to wash the spin column membrane and centrifuged for a further 15 s at 12000 rpm. A new collection tube was placed under spin column and RPE Buffer was added and centrifuged for

15 s at 12000 rpm. Flow through was discarded and RPE Buffer was added into spin column once more for further centrifugation at 12000 rpm for 2 min this time. As a last step, the column placed into a new collection tube, RNase-free water was added directly to the column membrane and centrifuged for 1 min at 12000 rpm to elute the RNA.

### **2.3.2.2 RNA All Prep Kit Protocol**

RNA All Prep Kit protocol was performed to obtain protein and RNA simultaneously from the lysate. In this protocol three different columns were used; AllPrep spin column, Protein Cleanup spin column, and RNeasy spin column. For cell lysis, certain volume (5-10 ml) of cell cultures was centrifuged at 5000xg for 5 min. The pellet was then washed in *Tpv* medium and was dissolved in appropriate volume of APL Buffer and incubated for 5 min at room temperature. The lysate was applied into an AllPrep Spin column and centrifuged for 1 min at 12.000 rpm. After centrifugation, total protein collected in flow through while RNA remained bound to the column. RNA bound AllPrep spin column was placed into a new collection tube, and Buffer RLT was applied onto the column. It was centrifuged for 1 min at 12000 rpm. Ethanol (70%) was added into flow through and mixed by pipetting. Then the sample was applied into RNeasy spin column and centrifuged for 1 min at 12000 rpm. Flow through was discarded and RW1 Buffer was applied onto the column. This time it was centrifuged for 30 s at 12000 rpm. After that, column was washed for two times by APL Buffer application and centrifugation at 12000 rpm for 30 s. For removal of any residual of the buffer, column was centrifuged at full speed (13000 rpm) for 1 min. And as a final step, column placed in a new collection tube and RNase-free water was added directly to the spin column membrane and centrifuged for 1 min at 12000 rpm to elute the RNA.

After RNA isolation, the concentrations of the purified samples were determined by measuring the absorbance at 260 nm and 280 nm by UV-visible double beam spectrophotometer Shimadzu 1601 UV/Visible Spectrophotometer, Shimadzu Analytical Co. (Kyoto, Japan). Samples were kept at  $-80^{\circ}\text{C}$  for later use.

### **2.3.3 Agarose Gel Electrophoresis of Stress Exposed RNA Samples**

Since RNAs have the tendency of forming secondary or tertiary structures, electrophoresis of these samples were done under denaturing conditions. Formaldehyde and formamide were used as denaturants; also RNA samples were heat-denatured prior to electrophoresis. The components and the quantities of the formaldehyde agarose gel (1.2%) were listed in Appendix A.

For a 1.2% agarose gel, 0.48 g of agarose mixed with 4 ml 10XFA Buffer, and RNase-free water added up to 40 ml. Then the mixture was boiled and stirred to dissolve the agarose. After cooling, 720  $\mu\text{l}$  Formaldehyde and 5  $\mu\text{l}$  EtBr were added into the flask. The components of the gel were mixed by rotating the flask gently and poured into the gel tray

slowly to let to solidify at room temperature. After gel setting, 1XFA Buffer was poured onto the gel and left for about 1 h for equilibration.

RNA samples (5 µl) were mixed with 1.2 µl of 5XRNA, heat denatured at 65°C for 5 min, and then cooled on ice. After loading the samples, electrophoresis was performed at 70 mAmp by use of Bio-Rad Power Supply, 200/2.0 for about 2.5 h.

Finally the gel was removed from the electrophoresis tank to visualize and photograph the RNA bands by Vilber Lourmat Gel Imaging and Analysis System (Marne La Vallee Cedex 1, France).

### 2.3.4 Real-Time Reverse Transcription PCR (qRT-PCR)

To be able to evaluate the changes in gene expression after exposure of the *Tpv* cells to stress, qRT-PCR technique was used. First, specific mRNAs in total RNA samples were converted into cDNAs by reverse transcriptase, and then cDNAs were used as template in real-time PCR using gene specific primers.

#### 2.3.4.1 Reverse Transcription PCR

Reverse transcription was carried out based on the Fermentas, RevertAid™ H Minus First Strand cDNA Synthesis Kit's protocol. Gene specific reverse primers were designed and used in the experiment, and their sequences are given in Table 2.1. Prepared RNA/primer mixture; 0.1 ng-5 ng total RNA, and 15-20 pmol gene specific primer was added into sterile 0.2 ml PCR tubes. Double distilled sterile water added into mixture up to a total volume of 12 µl and mixed gently. The mixture incubated at 65°C for 5 min. Then sample tubes were placed on ice and 4 µl 5X reaction buffer, 1 µl RiboLock™ RNase inhibitor, 10 mM dNTP mix and 1 µl RevertAid™ H Minus M-MuLV Reverse Transcriptase were added. After mixing, tubes were placed in a conventional thermal cycler (Techgene, Techne Inc., NJ, USA) and incubated at 42°C for 60 min. The reaction was stopped by heating at 70°C for 5 min. The reverse transcription products (cDNAs) were kept on ice until use.

**Table 2.1 Gene specific reverse primers (RP) for cDNA synthesis.**

<b>RP-TVN0382</b>	5'- GCA ATG ACG CTG CCC TGA AAA GCT TGG -3'
<b>RP-TVN0947</b>	5'- CAC AGA TAC AGT CCC TGA TCC TG -3'
<b>RP-TVN0489</b>	5'- GGG TAT AAC CCC TTT GAA CTT CG -3'
<b>RP-TVN1145</b>	5'- GTC ATG GAT ATG CCA TTG ATG -3'

### 2.3.4.2 The Real Time PCR

The reverse transcription product cDNAs were used as templates on The Real Time PCR which was performed on the The Light Cycler® using FastStart DNA Master PLUS SYBR Green I kit (Roche Diagnostics, Switzerland). Gene specific reverse and forward primers were designed and used in the experiment, and their sequences are given in Table 2.2. Following components were added into capillaries in the indicated order: double distilled water (9 µl), gene-specific reverse (1 µl) and forward (1 µl) primers, master mix (4 µl) and cDNA samples (5 µl) to reach a total concentration of 20 µl. The control was prepared by adding water instead of template cDNA. The capillary tubes were closed and centrifuged to collect the liquid at the bottom. After all these processes, the qRT-PCR was performed in LightCycler® 1.5, Roche instrument. The capillaries were transferred into LightCycler® sample carousel which was placed into the LightCycler® instrument. Each sample was specified with name of the experimental condition in the folder. The  $2^{-\Delta\Delta C_t}$  method [104] was used to calculate fold differences.

The products of real time PCR were analyzed by agarose gel electrophoresis. The contents of the capillary tubes were supplemented with tracking dye and applied into wells of agarose gel. Roche, Molecular screening agarose (1%) was used for gel preparation and after electrophoresis for 1.5 h at 70 volts in 1XTAE running buffer, DNA fragments were visualized under UV light (Vilber Lourmat, Marne La Vallée Cedex 1, France) and photographs were taken by gel imaging and documenting system (Vilber Lourmat Gel Imaging and Analysis System, Marne La Vallée Cedex, France).

**Table 2.2 Gene specific forward (Fp) and reverse primers (Rp) for qRT-PCR.**

<b>Fp-TVN0382</b>	5'- AAA CTA CTG CAC GCA GGG ATA -3'
<b>Rp-TVN0382</b>	5'- CTC CTT TGC CTT ATC TTT ATG TCC -3'
<b>Fp-TVN0947</b>	5'- ACC ATG GGC AAA TCG GTA T -3'
<b>Rp-TVN0947</b>	5'- GTT GCA TCT GGG TTC TCT CG -3'
<b>Fp-TVN0489</b>	5'- ACA AGA AAT CTG AAG AAG AGA GCT G -3'
<b>Rp-TVN0489</b>	5'- CTG TTC AGC AAT GCT ACG GTA A -3'
<b>Fp-TVN1145</b>	5'- TTC TTG TGG CCT TTG ATG G -3'
<b>Rp-TVN1145</b>	5'- AAG GAC AAG AGG TAG CGT GAA C -3'

### 2.3.5 Detection of the VAT protein by Western Blot Analysis

Western Blotting/Hybridization studies were carried out using the total protein samples from *T. volcanium* cultures exposed to oxidative stress at 0.02 mM H<sub>2</sub>O<sub>2</sub>, heat shock at 65°C and 70°C, and pH stress at pH 4.0 for 60 min and 120 min. Control samples were prepared from *T. volcanium* cultures grown under optimum conditions.

### **2.3.5.1 Purification of Total Protein**

RNA All Prep Kit (QIAGEN) was used for total protein purification. Before beginning the process, the Protein Cleanup spin column was prepared by vortexing to resuspend the resin. The column cap was opened by a quarter turn and placed into 2 ml collection tube. It was centrifuged at 750xg (Micromase RF, ThermoIEC, USA) for 3 min. Then lysis buffer was applied onto it for equilibration, after vortexing gently, the column was centrifuged at 750xg for 3 min. Then the column was transferred into a clean microcentrifuge tube to be used for protein purification. The cell lysate was prepared as described before (*Section 2.3.2.2*) following the kit protocol. Lysate was applied onto AllPrep spin column and centrifuged for 1 min at 12000 rpm. Flow through pooled in a collection tube which contained total cell protein. Then the flow through was applied onto the center of slanted gel of the prepared Protein Cleanup spin column in a microcentrifuge tube. Then the column was centrifuged for 3 min at 250xg to collect total protein in the microcentrifuge tube which was kept at  $-20^{\circ}\text{C}$  for later use in downstream applications. Purified protein samples were quantitated by measuring the absorbance at 260 nm and 280 nm by UV-visible double beam spectrophotometer Shimadzu 1601 UV/Visible Spectrophotometer (Shimadzu Analytical Co., Kyoto, Japan) as described in the Kit protocol.

### **2.3.5.2 Biotin Labeling of the Antibody**

VCP monoclonal antibody (M15) (Abnova Corporation, Taiwan) was used for cross hybridization with *Tpv* VAT proteins. The labeling of the VCP antibody was performed by using Biotin Protein Labeling Kit (Roche). Antibody was dissolved in 250  $\mu\text{l}$  PBS solution and 8  $\mu\text{l}$  freshly prepared Biotin-7-NHS solution was added onto it. The mixture was incubated for 2 h at  $25^{\circ}\text{C}$  by gentle shaking. Then 5 ml blocking solution was applied onto the column, and then it was rinsed with 30 ml PBS solution. Biotin labeled VCP antibody was applied to the column. After collection of the flow through, the labeled antibody was eluted with 3.5 ml PBS solution. The presence of the antibody in the elutes was determined by measuring the absorbance at 280 nm using UV-visible double beam spectrophotometer (Shimadzu 1601 UV/Visible Spectrophotometer, Shimadzu Analytical Co., Kyoto, Japan). Biotin-labeled samples were kept at  $+4^{\circ}\text{C}$  for further use.

### **2.3.5.3 SDS Polyacrylamide Gel Electrophoresis of the Purified Total Protein**

SDS Polyacrylamide Gel Electrophoresis (SDS-PAGE) was performed with 12% polyacrylamide gel using Whatman Biometra (Göttingen, Germany) system. Equal volume of the 2X loading dye and the protein samples were mixed. The mixture was boiled for 5 min to denature the proteins, chilled on ice and then was loaded into wells. One well was loaded with PageRuler<sup>TM</sup> Prestained Protein Ladder (Fermentas UAB, Vilnius, Lithuania) as a molecular weight standard. Electrophoresis was carried out using Bio-Rad Power Supply, 200/2.0 at 100 V. The polyacrylamide gel with separated polypeptides was used in blotting

using a Semi-dry Blotter (BioRad). After blotting, the gel was stained with Page Blue Protein Staining Solution (Fermentas) to check the efficiency of blotting process. Gel photos were taken by an imaging system (Vilber Lourmat Gel Imaging and Analysis System, Marne La Vallée Cedex 1, France).

#### **2.3.5.4 Western Blotting**

Semi-dry transfer system was used for transferring of the protein samples from polyacrylamide gel (SDS-PAG) to Immobilon PVDF transfer membrane. Millipore Immobilon-P Transfer Membrane User Guide protocol was followed with minor changes in required steps for optimization. Required buffers were prepared freshly as 100 ml Anode I and, 200 ml of each Anode II and Cathode buffers. The polyacrylamide gel was removed from the glass cassettes and cut with a lancet to a dimension that includes all the protein sample lanes. A notch was made to a corner of the gel to orientate the samples in the right order. Then the gel was immersed in cathode buffer for 15 min. Meanwhile six pieces of Whatman 3MM filter papers were cut to the same dimensions as the gel to let the current forced to flow through the gel. Prepared filter papers were soaked in buffers in the order of 2 pieces filter papers in Anode I, 1 piece of filter paper in Anode II and 3 pieces of filter papers in Cathode at least 30 s. Then the membrane was cut to the same size of the gel and a notch was also made on a corner. Membrane was soaked in 100% methanol for 15 s. Then it was transferred into Milli-Q grade water for 2 min and finally it was soaked in Anode buffer II for 5 min. When the gel, filter papers and membrane got ready, BIO-RAD Trans Blot SD Semi Dry Transfer Cell was used as the transfer system. 2 pieces of filter papers, immersed in Anode buffer I, were placed onto the anode electrode plate of the BIO-RAD Trans Blot SD Semi Dry Transfer Cell system. Then the other filter paper soaked in Anode buffer II was placed on it. The membrane was placed on top of these and gel was placed on top of the membrane by orienting the notches in the same corner. Finally three pieces of filter papers that soaked in cathode buffer were placed on membrane. As a final step the cathode electrode plate was placed on top of the transfer stack assembly. Cathode and anode leads were connected to Bio-Rad Power Supply, 200/2.0. Current was calculated according to the gel dimensions. Transfer has occurred after 30 min.

#### **2.3.5.5 Immunodetection**

Blocking solution and antibody solution were prepared as described in the Millipore Immobilon-P Transfer Membrane User Guide. When the electro-transfer was completed, gel was stained and blotted membrane was immersed in 100% methanol for 10 s and then left on the filter paper for the methanol to evaporate for 15 min. The membrane was incubated in biotin labeled VCP mouse monoclonal antibody (M15), clone 2H5 which has human reactivity (Abnova Corporation, Taiwan) by agitation for 2 h on a shaker (Stuart Scientific, Drive Unit STR8, U.K.) and then was washed in 50 ml TBS for 10 min, twice. Thereafter the membrane was placed in tagged streptavidin (Streptavidin-AP) solution and incubated for 1

h on shaker. Then the membrane was washed with twice 50 ml TBS for 2 min. For chromogenic detection of the protein bands, the membrane was incubated in Roche NBT/BCIP (nitro-blue tetrazolium chloride/5-bromo-4-chloro-3-indolyphosphate p-toluidine salt) color development solution in the dark which formed an intense purple precipitate on the blot. Then the membrane blot was rinsed with Milli-Q grade water to stop the reaction, and dried on a filter paper. It was stored in the dark to prevent fading of the bands. Photos of the membrane were taken by a digital camera.

### 2.3.6 Microarray

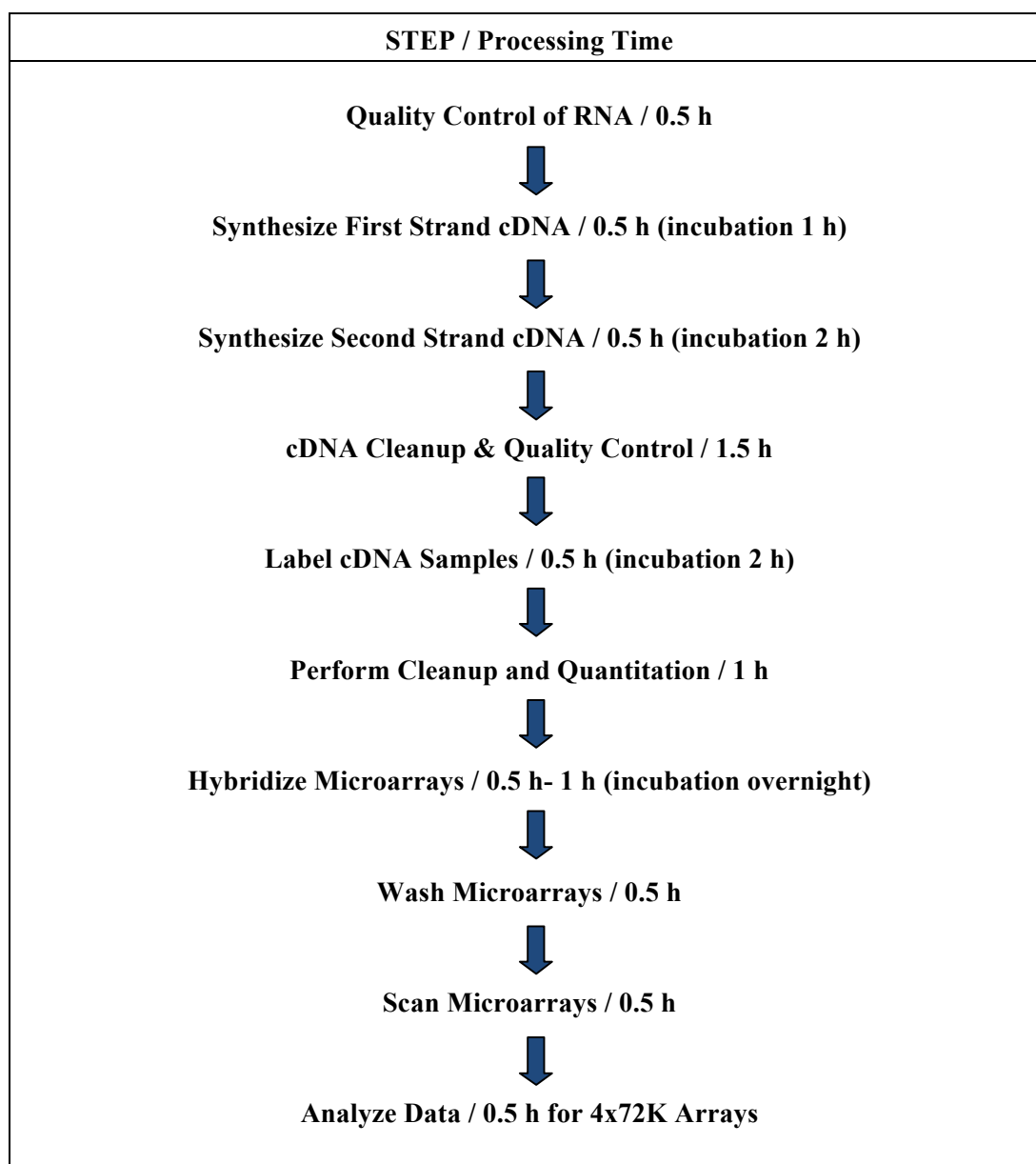
Four independent cultures of *Tpv* cells were grown to mid-log phase at optimum growth temperature 60°C and pH 2.7. Then the cultures were exposed to previously designed stress conditions: heat shock by temperature shift to 65°C, oxidative stress by adding 0.02 mM H<sub>2</sub>O<sub>2</sub>, and pH stress by a shift in pH to pH 4.0. The fourth culture was set aside without any stress exposure and used as control. The genome-wide transcription profiling of stressed exposed cells were examined by Roche NimbleGen custom designed 4x72K format expression array. The workflow for NimbleGen gene expression array is given in Table 2.3. The microarray covered all 1501 transcripts using 8 probes per transcript. 2 technical replicates were tested in the experiments.

Quality control of RNA and double stranded cDNA synthesis steps of the experiment were performed in our laboratory. Total RNA was isolated from the 1 h stress exposed cultures by RNAeasy MiniKit, QIAGEN. Isolated samples were used to synthesize double stranded cDNAs. For ds cDNA synthesis Invitrogen SuperScript® Double-Stranded cDNA Synthesis Kit was used. Random hexamer primer (100 pmol/μl) and RNA were mixed in DEPC water and heated to 70°C for 10 min by thermal cycler Techgene, Techne Inc. (NJ, USA). After chilling on ice for 5 min, 5X First-Strand Reaction buffer, 0.1 M DTT and 10 mM dNTP mix were added onto the content of the first mixture. After mixing gently and collecting the content by centrifugation, it was placed into thermal cycler again at 45°C for 2 min. Then SuperScript II RT enzyme was added into the tube, total volume reached to 20 μl and this mixture was incubated at 45°C for 1 h. When the incubation was over, tube was taken onto ice to terminate the reaction. For second strand synthesis, 5X 2<sup>nd</sup> strand synthesis buffer, 10 mM dNTP mix, 2<sup>nd</sup> strand enzyme blend (DNA Ligase, DNA Polymerase and RNase H) and DEPC-treated water were added onto the newly synthesized first strand cDNA sample tube. After mixing all the contents by pipetting up and down, it was incubated for 2 h at 16°C. After that 2 μl of T4 DNA Polymerase was added and incubated for further 5 min at 16°C. Each ds cDNA sample was quantitated by PICOPET01, Picodrop (U.K.) and checked if they met the required concentration (≥100 ng/μl) for the following steps of the experiment.

Remaining steps included the labeling of the cDNA samples, the hybridization, the scanning of the one-color NimbleGen arrays and the data extraction were carried out by Genmar Diagnostic Company (TR). The labeling cDNA samples were performed by NimbleGen One-Color DNA labeling kit and samples were labeled by Cy-3. Then the samples were prepared for hybridization. A hybridization solution master mix was prepared and added to

each sample in appropriate volumes. Then the samples were loaded into 4x72K arrays and samples were hybridized to arrays at 42°C for 16-20 hours. When it was over, washing and drying steps were performed to obtain high quality data. Finally NimbleGen arrays were scanned in 5µm resolution. Raw intensity signals were processed by Genmar Laboratories (TR), and resultant data were normalized. For analysis of the extracted data, we used DNASTAR ArrayStar Software.

**Table 2.3 Flow chart for NimbleGen gene expression array.**



## CHAPTER 3

### RESULTS

#### 3.1 RNA Isolation, Concentration and Quality Check

RNA was isolated from stress exposed cell cultures in four different time intervals, 30', 60', 90' and 120' as described in *Section 2.3.2*. For the quality check of the samples and to make estimation about RNA yields, RNA samples were run in a denaturing agarose gel. Agarose gel electrophoresis results of representative RNA samples isolated under heat stress at 65°C and 70°C, oxidative stress in the presence of 0.02 mM H<sub>2</sub>O<sub>2</sub> and pH stress at pH 4.0 between 30' and 120' are shown in the Figures 3.1, 3.2 and 3.3. The samples were loaded in the same volume but not in equal concentrations.

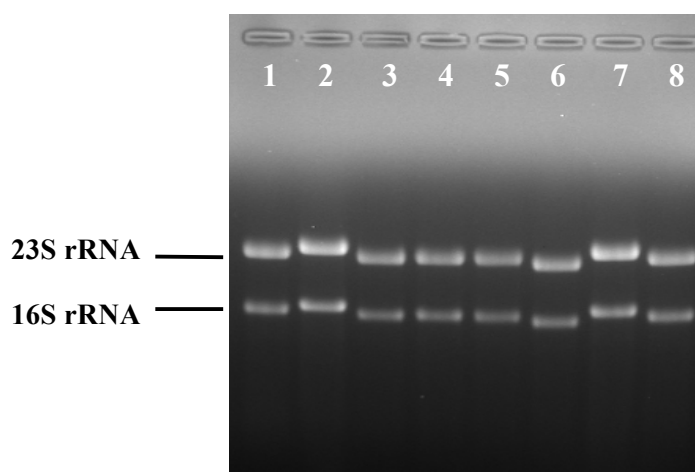


**Figure 3.1 Gel electrophoresis of RNA samples isolated from *Tpv* cells under heat shock.** Lanes 2, 3, 4, 5: RNA from heat shocked samples at 65 °C for 30', 60', 90', and 120', respectively. Lanes 1, 6, 7, and 8: RNA from heat shocked samples at 70 °C for 30', 60', 90', and 120', respectively.

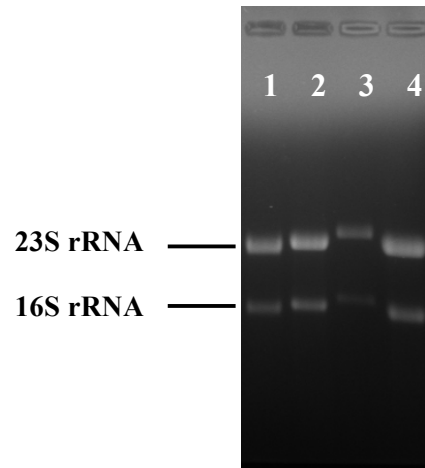


**Figure 3.2 Gel electrophoresis of RNA samples isolated from *Tpv* cells under pH stress.** Lanes 1, 2, 3, and 4: RNA from cultures exposed to pH 4.0 for 30', 60', 90', and 120', respectively.

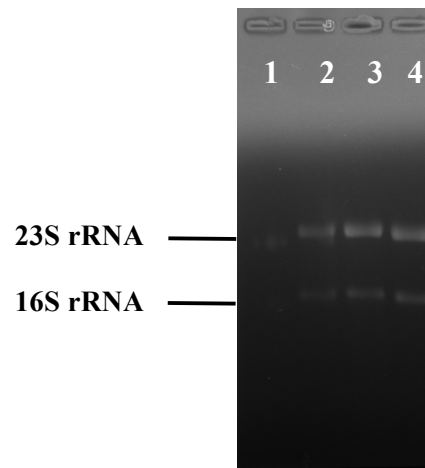


**Figure 3.3 Gel electrophoresis of RNA samples isolated from *Tpv* cells under oxidative stress.** Lanes 1, 2, 3, and 4: RNA from cultures exposed to 0.02 mM H<sub>2</sub>O<sub>2</sub> for 30', 60', 90', and 120', respectively.

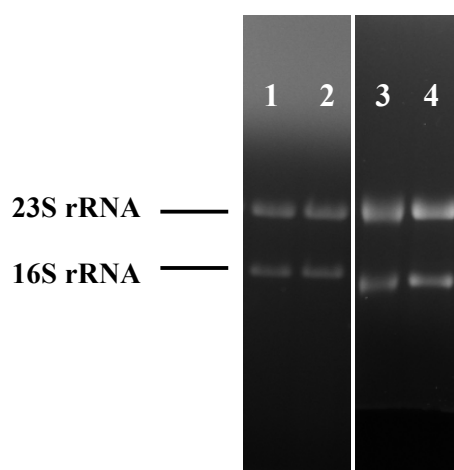


**Figure 3.4 Gel electrophoresis of control RNA samples isolated from *Tpv* cells under optimum conditions.** Lanes 1, 2, 3, and 4: RNA isolated from cultures grown at pH 2.7 and 60°C at 30<sup>th</sup>, 60<sup>th</sup>, 90<sup>th</sup>, and 120<sup>th</sup> minutes following stress application to the test cultures, respectively.

The quality of RNA samples based on gel electrophoresis results was quite satisfactory since distinct 23S and 16S rRNA bands were observed without any degradation for all RNA samples. RNA concentration was determined by OD<sub>260</sub> measurements according to the equation: OD<sub>260</sub> = 40 µg/ml RNA. The RNA yields of samples isolated from heat and pH stressed cultures seemed to be close to each other at all time points and average RNA concentration was 0.7 µg/µl ±0.07. However, the RNA concentrations of the samples from control and oxidative stress exposed cultures were relatively low, being approximately 0.6 µg/µl ±0.03. The purity of the RNA samples was also checked by the ratio of A<sub>260</sub>/A<sub>280</sub> (Table 3.1).

The ratio of absorbance at 260 nm and 280 nm (A<sub>260</sub>/A<sub>280</sub>) should be between 1.9 and 2.3, for pure RNA, but for our RNA samples calculated A<sub>260</sub>/A<sub>280</sub> ratio was around 1.4. This can be due to dilution of RNA samples in RNase-free water instead of 10 mM Tris.Cl, pH 7.5, for absorbance measurements.

**Table 3.1 Concentrations of the RNA samples and  $A_{260}/A_{280}$  ratio.**

Stress	Minute	$A_{260}$	$A_{280}$	$A_{260}/A_{280}$	Concentration ( $\mu\text{g}/\mu\text{l}$ )
<b>65°C (Heat shock stress)</b>	<b>30</b>	0.122	0.086	1.41	0.751
	<b>60</b>	0.115	0.084	1.36	0.708
	<b>90</b>	0.141	0.096	1.46	0.868
	<b>120</b>	0.107	0.078	1.37	0.659
<b>70°C (Heat shock stress)</b>	<b>30</b>	0.116	0.084	1.38	0.714
	<b>60</b>	0.121	0.088	1.37	0.745
	<b>90</b>	0.118	0.085	1.38	0.726
	<b>120</b>	0.114	0.084	1.35	0.702
<b>pH 4.0 (pH stress)</b>	<b>30</b>	0.115	0.085	1.35	0.708
	<b>60</b>	0.118	0.086	1.37	0.726
	<b>90</b>	0.088	0.071	1.23	0.542
	<b>120</b>	0.131	0.094	1.39	0.806
<b>0.02 mM (Oxidative stress)</b>	<b>30</b>	0.097	0.069	1.40	0.597
	<b>60</b>	0.105	0.073	1.43	0.646
	<b>90</b>	0.102	0.073	1.39	0.628
	<b>120</b>	0.109	0.074	1.47	0.671
<b>Control</b>	<b>30</b>	0.093	0.065	1.43	0.572
	<b>60</b>	0.093	0.065	1.43	0.572
	<b>90</b>	0.099	0.069	1.43	0.609
	<b>120</b>	0.099	0.069	1.43	0.609

### 3.2 Reverse Transcription and Quantitative Real-Time PCR for Expression Analysis of TVN0382

We have used quantitative real time PCR (qRT-PCR) technique to investigate differential expression of VAT gene, TVN0382, under stress conditions relative to optimum conditions. The mRNAs of VAT gene in the total cellular RNA were converted into single-stranded cDNAs by reverse transcription. Then they were used as templates in qRT-PCR experiments. TVN0382 gene specific forward primer sequence, complementary of reverse primer sequence and the amplified PCR product (60 bp) are depicted in the TVN0382 gene sequence (1128 bp) in Figure 3.5. Agarose gel photographs of qRT-PCR products yielded 60 bp amplicons for TVN0382 as expected from the positions of the amplification primers (Figure 3.6).

```

>gi|13540831:372394-373521 Thermoplasma volcanium GSS1 chromosome,
complete genome

ATGAGTGATGATGTTTCAGAATAAGATTGAAAAAGCCACAAAACTACTGCACGCAGGGATAAAAAGAA
GAGGAAAATGGACATAAAAGATAAAGCAAAGGAGTACTATCTTGTGGCTTACAGGGTAATGTTAGAA
GCTGCAAACGACTCTCCATCGGATCTTAAGAAGAAAAGACTTGATCAATGTGCTTTAATATTTAAAT
GCCTACAAACGCGTTAGTGGAGAAAGGACAGACTTCACAGTGAAAAAACAAAATGATGATGAAATA
GTAGAAGGTGAGGCTCTACTAGAAGAGATAGGAATAGAAAAACCAGAGATACCAAAAGTAACCTTT
GAAGATGTTGACAGGTCTAGATGACGTTAAAAATGAGATATTAGGAAAAATTATTTACCCAATGAAA
TTTAAGGAATTATCGCAGGAATATAATATACAATTCGGAGGCGGAATGTTATTGTACGGTCCGCCA
GGCACTGGAAAAACCTTTATTGTTAAGGCTATAGCCAACGAGGTAAAGGCCAGATTTATCAACGTA
AATCCTTCCACACTCTACAGTGAATGGTTTGGTGTTTTTGAAAAGAATATATCCAAGCTTTTCAGG
GCAGCGTCATTGCTATCTCCAGCAATAATATTCTTTGATGAGATAGATGCTTTGGTGCCAAAGAGA
GACACCTCCAATTCAGATGCTGCAAAGAGAGGAGTTGCACAGCTTTTGAATGAGGTTGGTGGTATA
AATTCTCAGAAGAACAATAATATATTCATCATCGCAGCAACAACAATCCCTGGGAAGTAGATGAG
GCCATGCTTAGGCCAGGTCGCTTCGATATAAAGATATACGTGCCACCTCCAGACATAGTCGCTAGA
AAGAAAATATTTTCAGCTTAATCTAGCGAAAATTAACAGGTAGGAAACGTAGACTACGATCTGCTG
GCAGAGGAGACAGAAGGATACAGTGGTGCAGATATAGAGTTCATATGCAAAAAGGCAGCTCAGAAT
GTATTCATGGAAGCGGTGAAAACAGGGAAGAGCAGACCAGTTGAAACGAGGGACGTCATAGACGTT
ATAGGAAGCATCAAACCTTCCATTGATTATGAACTGCTGGAAAAATATTCAAAGTATGGTTCGCT
TTTTAG

```

**Figure 3.5 The sequence of TVN0382 gene (1128 bp).** The underlined region of the gene defined by the gene specific forward (red) and reverse primers (blue), indicates the amplified sequences by RT-PCR (60 bp).

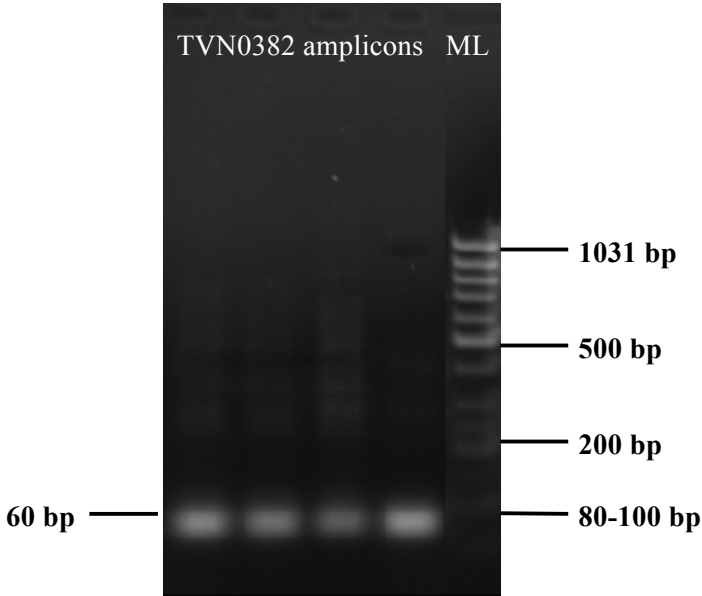


**Figure 3.6 Agarose gel electrophoresis of cDNA samples of VAT gene, TVN0382.** The size of the amplified TVN0382 cDNA by RT-PCR was about 60 bp. ML: MassRuler Low Range DNA Ladder, Thermo Scientific).

### 3.2.1 Time-Course Differential Expression of TVN0382 Gene under Heat Stress

In a real-time PCR, Ct (Threshold cycle) is defined as the number of cycles needed for the fluorescent signal to cross the threshold line (background level). The Ct value is inversely proportional to the initial amount of the mRNA sample. That is, the lower the Ct value, the higher the initial amount of specific mRNA is.

Based on Ct values of tests and controls, it can be suggested that TVN0382 gene expression was induced during heat shock at 65°C for 120 min (Table 3.2).

A unique, single peak was obtained by melting analysis and the melting temperature (T<sub>m</sub>) was 81.61°C ±0.5, implying specific amplification of the TVN0382 gene's cDNAs. Negative control in Figure 3.8 didn't yield any amplification or melting peak indicating absence of non-specific amplification. The real-time PCR absolute quantification analyses and T<sub>m</sub> curves of TVN0382 cDNA samples for 65°C heat shock experiments are given in the Appendix C. Figure 3.7 shows the results of 30 min 65°C heat-shock experiment.

Transcription of TVN0382 gene was induced by heat-shock at 70°C for 2 h, as revealed by lower Ct values of the tests as compared to that of controls (Table 3.2).

Melting curve analysis for these qRT-PCR experiments verified the specific amplification of TVN0382 gene's cDNAs and average T<sub>m</sub> was 82.5°C ±0.4. Representative RT-PCR absolute quantification analyses and T<sub>m</sub> curves of TVN0382 cDNA samples for 70°C heat shock experiments are given in the Appendix C. Figure 3.8 shows the results of 30 min 70°C heat-shock experiment.

**Table 3.2 Representative Ct values and mean value of at least three melting temperatures from heat shock experiments for TVN0382 gene.**

Stress	Time (min)	Ct values		Melting Temperature (± STD)
		Test	Control	
65°C	30	12.84	17.14	81.97°C (± 0.7)
	60	14.72	15.19	82.13°C (± 1.4)
	90	12.04	13.62	81.06°C (± 0.07)
	120	12.60	12.75	81.28°C (± 0.21)
70°C	30	14.41	17.14	82.49°C (± 0.1)
	60	13.79	15.08	81.99°C (± 0.3)
	90	18.55	19.06	82.74°C (± 0.6)
	120	18.66	19.06	82.90°C (± 0.3)

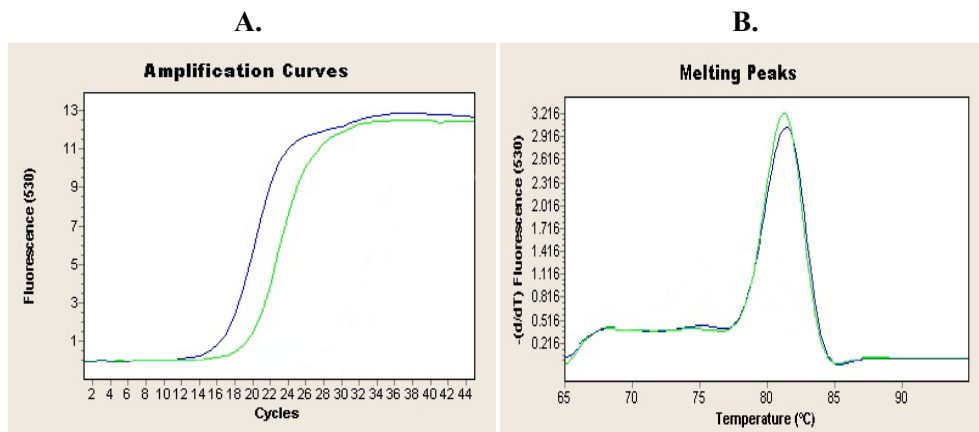


**Figure 3.7 Real-time PCR amplification and melting curves for TVN0382 gene.** RNA samples were isolated from cultures exposed to heat stress at 65°C for 30' used for reverse transcription. **A.** Amplification curves (blue—test, green—control) **B.** Melting curves (blue—test, green—control).

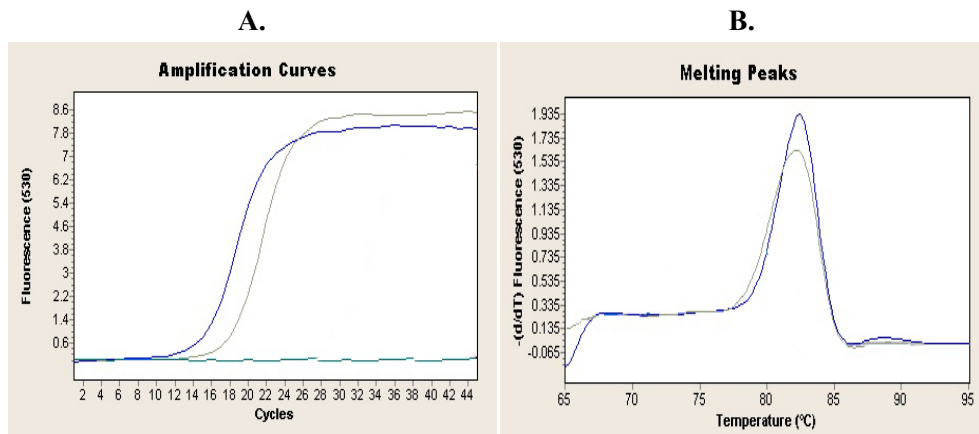


**Figure 3.8 Real-time PCR amplification and melting curves for TVN0382 gene.** RNA samples were isolated from cultures exposed to heat stress at 70°C for 30' used for reverse transcription. **A.** Amplification curves (blue—test, grey—control, green—negative control) **B.** Melting curves (blue—test, grey—control).

### 3.2.2 Fold Difference Analysis of Time Course Expression of TVN0382 Gene under Heat Shock

The qRT-PCR data was analyzed by a relative quantification method to find out fold differences between expression levels of the tests and controls. For the calculation of the relative expression of the stress exposed genes' PCR efficiency and threshold cycle number (Ct) for the test and control genes are required. An on-line program was used for calculation of the PCR efficiencies. The Ct values for the experiments are given in the Table 3.2. The equation used to calculate the fold-changes is given below:

$$\Delta Ct = Ct_{(control)} - Ct_{(test)}$$

$$(\text{Average PCR}_{\text{Efficiency}})^{\Delta Ct} = \text{Fold change} \quad (3.1)$$

To study modulation of the expression of TVN0382 gene at 65°C and 70°C, we have measured the expressions relative to control (60°C) over 120 min. The fold differences were calculated for each stress conditions for all time intervals and they were represented as the mean of at least three independent experiments (Table 3.3). The related data points are plotted in a chart and depicted by bars (Figure 3.9).

The results have shown that mRNA levels of TVN0382 gene significantly increased (about fivefold) after exposure to heat shock at 65°C for 30 min. However prolonged exposure to 65°C for 2 h did not changed expression of the TVN0382 gene. The TVN0382 gene expression was up regulated for 1 h following heat stress at 70°C, and then expression level decreased almost up to level of control mRNA (Figure 3.9).

**Table 3.3 Fold difference of TVN0382 gene expression under heat shock.** The results are the means of at least three independent qRT-PCR experiments.

Stress	Time (min)	Fold Difference ( $\pm$ STD)
65°C	30	5.56 $\pm$ 0.282
	60	1.356 $\pm$ 0.08
	90	1.778 $\pm$ 0.14
	120	1.047 $\pm$ 0.03
70°C	30	2.93 $\pm$ 0.001
	60	1.774 $\pm$ 0.6
	90	1.307 $\pm$ 0.4
	120	1.263 $\pm$ 0.2

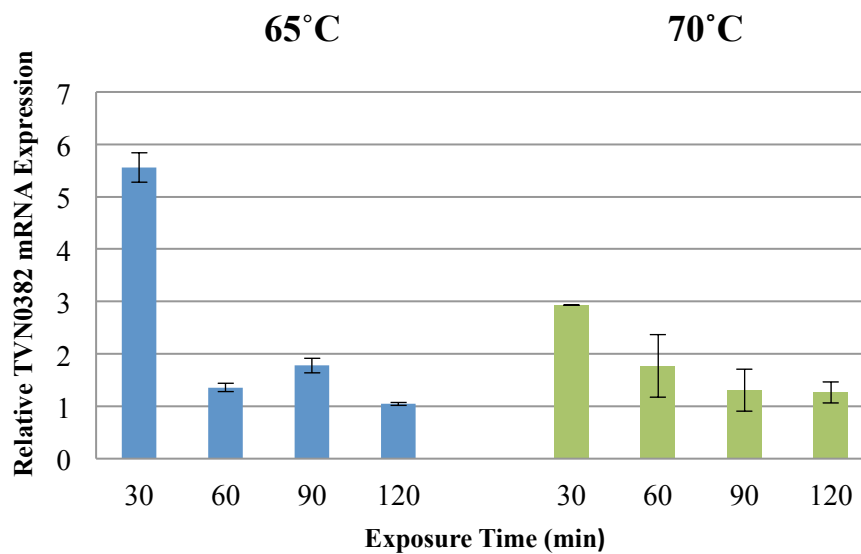


**Figure 3.9** Relative mRNA expression of TVN0382 gene determined by quantitative real-time PCR analysis under heat shock at 65°C and 70°C. Expressions are shown as fold-increase or decrease relative to the control (60°C) level (1-fold) TVN0382 gene expression. The values are means of at least 3 replicates.

### 3.2.3 Time-Course Differential Expression of TVN0382 Gene under pH Stress

The pH stress was maintained by increasing the pH of the mid-log *Tpv* cultures to pH between 3.6 and pH 5.0 as described in the *Section 2.3.1.2*. For the control culture, initial pH, pH 2.7, which is the optimum pH for *Tpv* was not changed during 2 h while stress being applied to test cultures.

During stress at pH 3.6 and pH 4.0 for 2 h, TVN0382 gene expression was up-regulated as indicated by lower Ct values compared to that of control. Due to similar Ct values of tests and controls, stress at pH 4.5 did not cause a detectable alteration in the expression of TVN0382 gene. However stress at pH 5.0 caused down-regulation of TVN0382 gene expression as revealed by higher Ct values of the tests than that of the control (Table 3.4). Representative RT-PCR absolute quantitative analyses and Tm curves of TVN0382 cDNA samples for pH stress experiments are given in the Appendix C. Figure 3.10 and 3.11 show the results of stress at pH 4.0 (30 min) and pH 5.0 (90 min).

The melting curves analysis showed that all amplified cDNAs of TVN0382 in RT-PCR experiments of pH stress produced single-peak and average melting temperature was 82.56°C ±0.4, implying specific amplification of TVN0382 cDNA (Figures 3.10 and 3.11).

**Table 3.4 Representative Ct values and mean value of at least three melting temperatures from pH stress experiments for TVN0382 gene.**

Stress	Time (min)	Ct values		Melting Temperature ( $\pm$ STD)
		Test	Control	
pH 3.6	30	20.12	20.31	83.12°C ( $\pm$ 0.03)
	60	19.72	20.31	83.16°C ( $\pm$ 0.2)
	90	20.7	20.31	82.58°C ( $\pm$ 0.1)
	120	18.41	17.17	83.13°C ( $\pm$ 0.04)
pH 4.0	30	13.53	15.68	82.83°C ( $\pm$ 0.1)
	60	17.23	18.58	82.35°C ( $\pm$ 0.3)
	90	22.16	22.79	83.26°C ( $\pm$ 0.6)
	120	22.3	22.79	83.37°C ( $\pm$ 0.3)
pH 4.5	30	29.11	28.14	81.94°C ( $\pm$ 0.3)
	60	16.05	14.91	82.29°C ( $\pm$ 0.2)
	90	33.99	32.76	82.67°C ( $\pm$ 0.3)
	120	37.54	40.01	82.19°C ( $\pm$ 0.02)
pH 5.0	30	16.33	16.17	82.04°C ( $\pm$ 0.04)
	60	19.69	19.87	82°C ( $\pm$ 0.01)
	90	16.28	15.39	82.05°C ( $\pm$ 0.25)
	120	18.73	18.02	82.10°C ( $\pm$ 0.1)

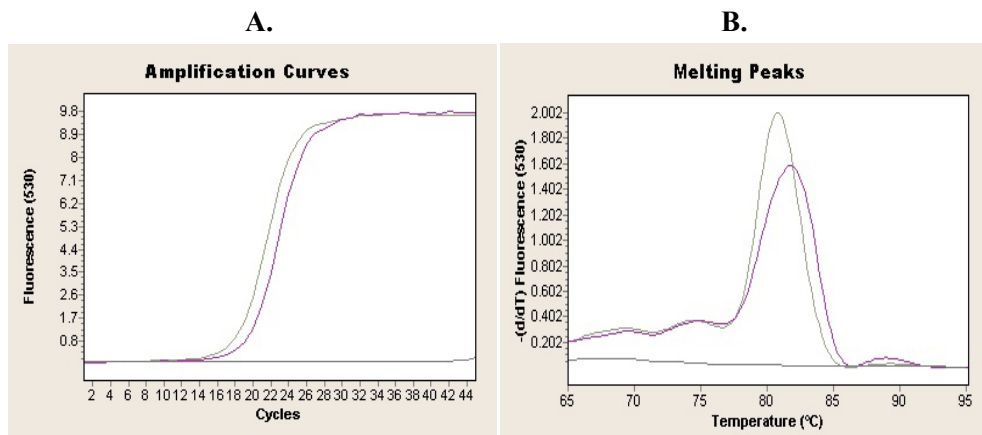


**Figure 3.10 Real-time PCR amplification and melting curves for TVN0382 gene.** RNA samples were isolated from cultures exposed to pH stress at pH 4.0 for 30' used for reverse transcription. **A.** Amplification curves (grey—test, purple—control, dark grey—negative control) **B.** Melting curves (grey—test, purple—control, dark grey—negative control).

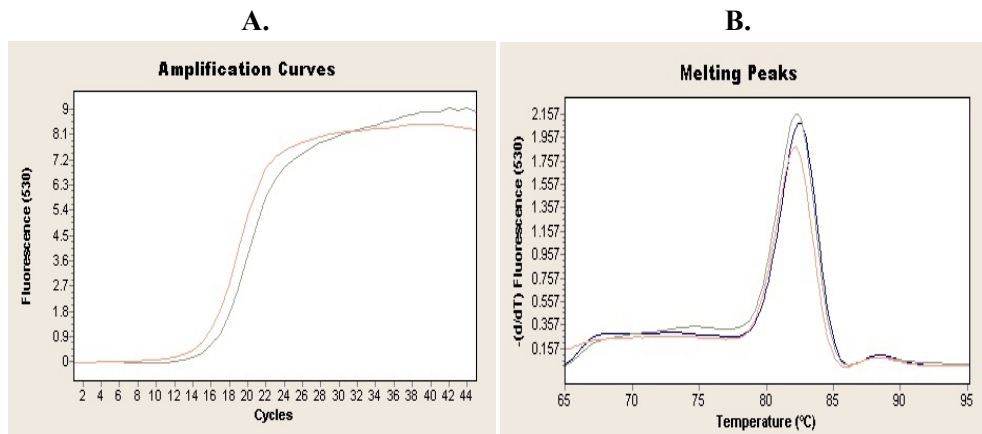


**Figure 3.11 Real-time PCR amplification and melting curves for TVN0382 gene.** RNA samples were isolated from cultures exposed to pH stress at pH 5.0 for 90' used for reverse transcription. **A.** Amplification curves (grey—test, pink—control) **B.** Melting curves (grey—test, pink—control).

### 3.2.4 Fold Difference Analysis of Time-Course Expression of TVN0382 Gene under pH Stress

The changes in the expression of TVN0382 gene at four different pH stresses (pH 3.6, pH 4.0, pH 4.5 and pH 5.0) were analyzed relative to control (pH 2.7) over 120 min. The fold differences were calculated and represented as the mean of at least three independent experiments (Table 3.5). The related data points are plotted in a chart and depicted by bars (Figure 3.12).

The fold difference analysis have shown that TVN0382 gene expression increased at pH 3.6 about 1.4 fold for 1 h, then stabilized almost at the level of the control mRNA up to 2 h. At pH 4.0 there was up-regulation (2-fold) during 2 h stress but at pH 4.5 and pH 5.0, the gene expression either decreased or did not change as compared to control.

**Table 3.5 Fold difference of TVN0382 gene expression under pH stress.** The results are the means of at least three independent qRT-PCR experiments.

Stress	Time (min)	Fold Difference ( $\pm$ STD)
pH 3.6	30	1.262 $\pm$ 0.5
	60	1.428 $\pm$ 0.3
	90	0.755 $\pm$ 0.04
	120	0.812 $\pm$ 0.001
pH 4.0	30	2.007 $\pm$ 0.2
	60	1.457 $\pm$ 0.2
	90	1.6 $\pm$ 0.08
	120	1.604 $\pm$ 0.2
pH 4.5	30	0.795 $\pm$ 0.3
	60	0.630 $\pm$ 0.2
	90	0.809 $\pm$ 0.05
	120	0.821 $\pm$ 0.2
pH 5.0	30	1.092 $\pm$ 0.2
	60	1.170 $\pm$ 0.07
	90	0.665 $\pm$ 0.02
	120	0.507 $\pm$ 0.0007

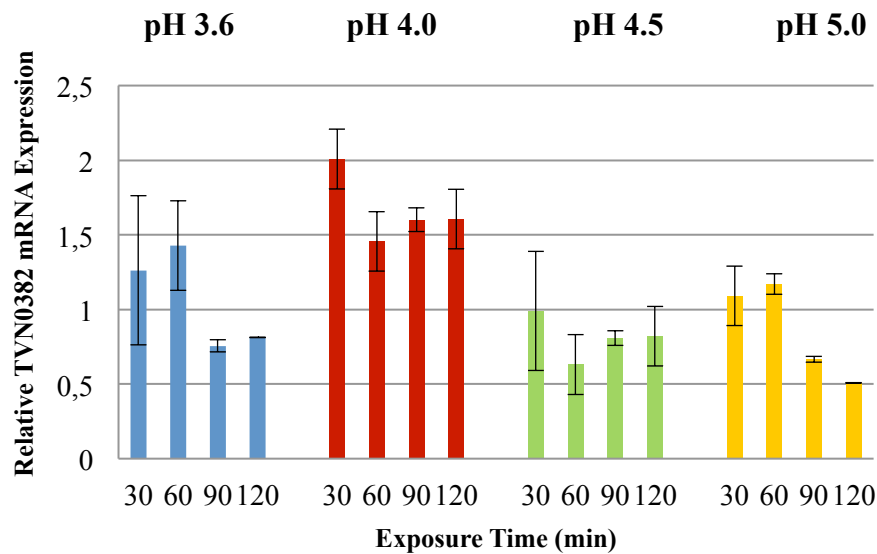


**Figure 3.12** Relative mRNA expression of TVN0382 gene determined by quantitative real-time PCR analysis under pH stress at pH 3.6, 4.0, 4.5 and 5.0. Expressions are shown as fold-increase or decrease relative to the control (pH 2.7) level (1-fold) TVN0382 gene expression. The values are means of at least 3 replicates.

### 3.2.5 Time-Course Differential Expression of TVN0382 Gene under Oxidative Stress

The effect of oxidative stress was analyzed by exposure of the *TPV* cultures to H<sub>2</sub>O<sub>2</sub> at varying concentrations, and analyzing the expression of TVN0382 gene by qRT-PCR. At 0.01 mM H<sub>2</sub>O<sub>2</sub> concentration TVN0382 gene expression should not change significantly compared to control. At 0.02 mM H<sub>2</sub>O<sub>2</sub> concentration as can be predicted from lower Ct values of tests than that of controls TVN0382 gene was up-regulated and the highest expression should be at 90 min. Although there was some increase in the expression during first 1 h of 0.03 mM H<sub>2</sub>O<sub>2</sub> exposure, no detectable change is expected following 1 h. Due to relatively higher Ct values of tests at 0.05 mM H<sub>2</sub>O<sub>2</sub> for 2 h, TVN0382 gene expression probably was down-regulated (Table 3.6).

The melting curve analysis showed that all amplified TVN0382 cDNAs produced single-peak and average 82.25°C ±0.5 implying specific amplification of the cDNA. Representative amplification curves and melting curves for qRT-PCR experiments for oxidative stress imposed by 0.01-0.05 mM H<sub>2</sub>O<sub>2</sub> are given in Appendix C.

Figure 3.13 and 3.14 show the results of stress at 0.02 mM (60 min) and at 0.05 mM (90 min) H<sub>2</sub>O<sub>2</sub>, respectively.

**Table 3.6 Representative Ct values and mean value of at least three melting temperatures from oxidative stress experiments for TVN0382 gene.**

Stress	Time (min)	Ct values		Melting Temperature (± STD)
		Test	Control	
0.01 mM	30	14.76	14.86	81.88°C (± 0.01)
	60	14.75	14.86	81.11°C (± 0.01)
	90	16.11	15.66	81.36°C (± 0.3)
	120	15.32	14.57	81.85°C (± 0.9)
0.02 mM	30	18.59	19.45	82.01°C (± 0.4)
	60	17.76	18.79	82.42°C (± 0.1)
	90	27.77	29.75	82.22°C (± 0.1)
	120	18.41	18.74	82.33°C (± 0.2)
0.03 mM	30	14.89	15.5	82.61°C (± 0.1)
	60	15.29	15.5	82.7°C (± 0.1)
	90	14.97	14.62	82.89°C (± 0.4)
	120	16.06	15.5	82.48°C (± 0.2)
0.05 mM	30	16.95	16.06	82.61°C (± 0.3)
	60	17.01	16.06	82.68°C (± 0.2)
	90	16.58	16.28	82.37°C (± 0.02)
	120	17.08	16.28	82.62°C (± 0.5)

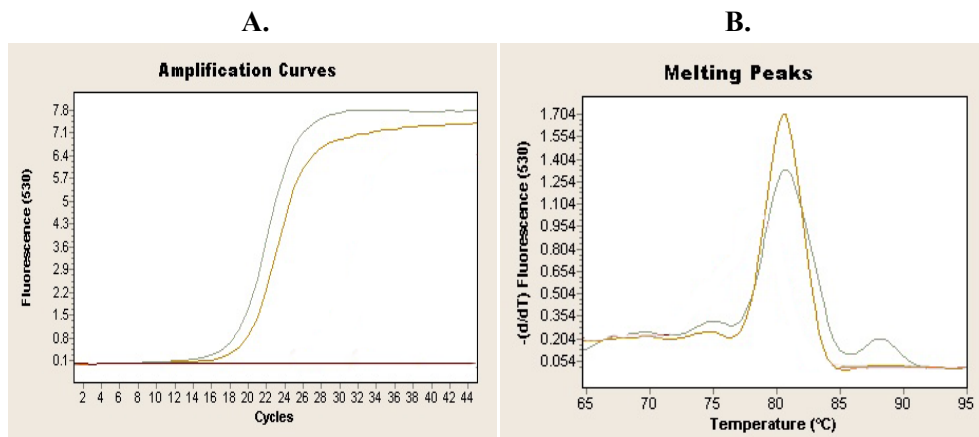


**Figure 3.13 Real-time PCR amplification and melting curves for TVN0382 gene.** RNA samples were isolated from cultures exposed to oxidative stress at 0.02 mM for 60' used for reverse transcription. **A.** Amplification curves (grey—test, light brown—control, dark red—negative control) **B.** Melting curves (grey—test, light brown—control).

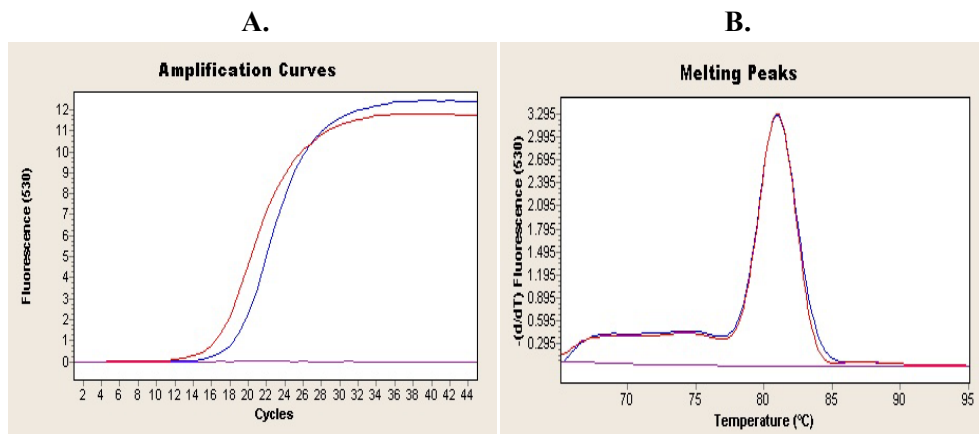


**Figure 3.14 Real-time PCR amplification and melting curves for TVN0382 gene.** RNA samples were isolated from cultures exposed to oxidative stress at 0.05 mM for 90' used for reverse transcription. **A.** Amplification curves (blue—test, red—control, purple—negative control) **B.** Melting curves (blue—test, red—control).

### 3.2.6 Fold Difference Analysis of Time Course Expression of TVN0382 Gene under Oxidative Stress

The calculated fold differences were represented as the mean of at least three independent experiments (Table 3.7). The related data points are plotted in a chart and depicted by bars (Figure 3.15).

Fold difference analysis showed that oxidative stress which was achieved by exposure of the cultures to H<sub>2</sub>O<sub>2</sub> at a concentration of 0.02 mM, the highest increase (about fourfold at 90 min) in the TVN0382 gene transcription was obtained. At 0.01 mM H<sub>2</sub>O<sub>2</sub> concentration, expression of the gene almost did not change as compared to control. At 0.03 mM H<sub>2</sub>O<sub>2</sub> concentration for initial 1 h, there was a slight increase in the gene's expression but afterwards the expression gradually decreased below the control expression level. The increased H<sub>2</sub>O<sub>2</sub> concentration (0.05 mM) caused a constant down-regulation of TVN0382 gene transcription for 2 h.

**Table 3.7 Fold difference of TVN0382 gene expression under oxidative stress.** The results are the mean of at least three independent experiments.

Stress	Time (min)	Fold Difference ( $\pm$ STD)
0.01 mM	30	1.035 $\pm$ 0.001
	60	1.038 $\pm$ 0.001
	90	0.836 $\pm$ 0.001
	120	0.746 $\pm$ 0.03
0.02 mM	30	1.19 $\pm$ 0.4
	60	1.511 $\pm$ 0.4
	90	3.78 $\pm$ 0.6
	120	1.45 $\pm$ 0.6
0.03 mM	30	1.34 $\pm$ 0.001
	60	1.106 $\pm$ 0.001
	90	0.763 $\pm$ 0.2
	120	0.568 $\pm$ 0.3
0.05 mM	30	0.676 $\pm$ 0.1
	60	0.598 $\pm$ 0.01
	90	0.799 $\pm$ 0.1
	120	0.621 $\pm$ 0.1

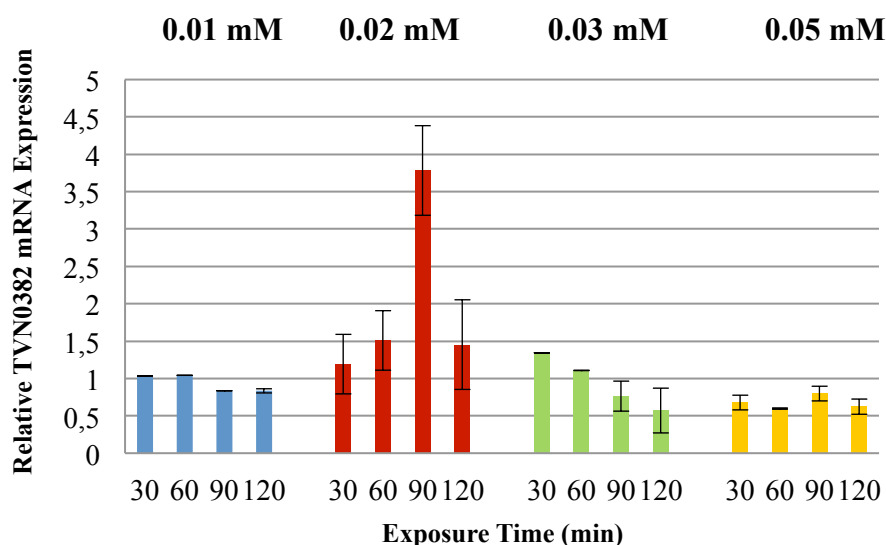


**Figure 3.15** Relative mRNA expression of TVN0382 gene determined by quantitative real-time PCR analysis under oxidative stress at 0.01 mM, 0.02 mM, 0.03 mM and 0.05 mM. Expressions are shown as fold-increase or decrease relative to the control level (1-fold) TVN0382 gene expression. The values are means of at least 3 replicates.

### 3.3 Reverse Transcription and Quantitative Real-Time PCR for Expression Analysis of TVN0947

The Real-Time PCR was performed to investigate differential expression of VAT 2 gene, TVN0947, under stress conditions relative to control. The mRNAs of VAT 2 gene in the total RNA isolated from control and stress exposed *Tpv* culture samples were converted into single-stranded cDNAs by reverse transcription. Then they were used as templates in Quantitative Real-Time PCR (qRT-PCR) experiments.

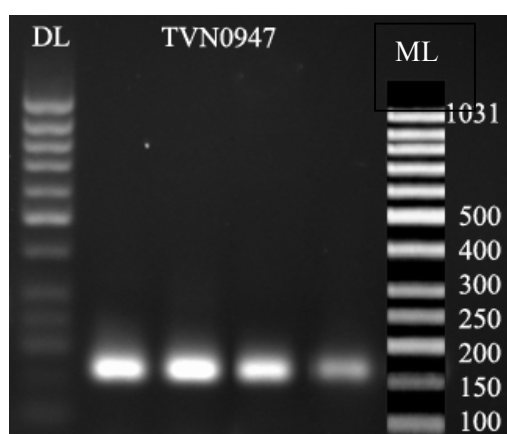


**Figure 3.16** Agarose gel electrophoresis of cDNA samples of VAT gene, TVN0947. The size of the amplified TVN0947 cDNA by RT-PCR was about 177 bp. DL: Fermentas Gene Ruler™ 50 bp DNA Ladder. ML: MassRuler Low Range DNA Ladder, Thermo Scientific).

Agarose gel photographs of qRT-PCR products yielded 177 bp amplicons of TVN0947 gene (Figure 3.16). The positions of forward and reverse primers used in RT-PCR and the amplified TVN0947 gene sequences (177 bp) are shown in the Figure 3.17.

```

>gi|13540831:996521-998758 Thermoplasma volcanium GSS1 chromosome,
complete genome

ATGGATAACAGCAGCGGTATAATACTCAGGGTTGCCGAGGCCAACTCAACAGATCCAGGCATGTCT
AGGGTTAGGCTTGATGAATCGTCTAGGCGCCTGCTCGATGCCGAGATCGGCGATGTAGTAGAGATC
GAGAAGGCCAGAAAACTGTAGGCAGGGTATACAGGGCCAGGCCGGAGGACGAGAACAAGGGGATA
GTAAGGATAGACAGTGTAAATGAGGAATAACTGCGGCGCTTCCATAGGGGATAAGGTAAGGGTCAGA
AAAGTAAGGACAGAGATAGCCAAGAAAAGTAACGCTTGCAACCATAATACGTAAAGATCAACGCTTA
AAATTTGGCGAAGGCATAGAGGAATACGTCCAAAGGGCGCTTATAAGAAGGCCAATGCTCGAACAG
GACAACATAAGCGTCCCAGGTTTAAACGCTTGCAAGCCAAACCGGACTTTTATTTAAGGTTGTAAAA
ACTATGCCTGGCAAGGTACCAGTTGAAATCGGAGAAGAGACAAAGATAGAGATAAGGGAGGAACCT
GCCTCTGAAGTATTGGAGGAGGTATCTAGGGTTAGTTATGAAGATATAGGAGGTCTCTCAGAACAG
CTGGGCAAGATCAGGGAGATGATCGAGCTTCCATTAAGCATCCTGAACTATTGAAAGGCTGGGC
ATTACACCTCCAAAGGGTGTATACTATATGGGCCCTCCTGGAACCTGGAAAAACCCCTTATTGCTAGA
GCTGTTGCAAAATGAATCTGGGGCCAATTTCTGTCCATAAACGGACCGGAGATAATGAGTAAGTAC
TATGGGCAGAGCGAGCAAAAGCTGAGAGAGATATTCTCAAAGGCAGAAGAAACAGCCCCATCTATA
ATATTCATAGATGAAATAGATTTCGATTGCACCCAAGAGGGAAAGAGGTACAGGGGGAGGTCGAAAGA
AGAGTAGTTGCACAACCTCCTTACTTTGATGGACGGTATGAAGGAACGCGGTCACGTAATAGTCATA
GGTGAACCAACAGGATAGACGCAGTGGATCCAGCGCTGAGAAGGCCAGGAAGGTTGACAGAGAG
ATCGAAATAGGAGTTCCAGACCGCAATGGCAGAAAAGGAAATCTTAATGATACATACCAGAAACATG
CCTCTAGGCATGGACGAGGAGCAGAAAAACAAGTTCCCTTGAGGAAATGGCTGACTACACCTATGGA
TTTGTAGGAGCTGATCTTGCCGCCCTCGTAAGGGAGAGTGCAATGAACGCCCTAAGGAGGTATCTA
CCGAAATCGACCTAGATAAGCCGATACCTACAGAAAATATTGGAAAAAATGGTTGTTACTGAAGAA
GACTTTAAGAATGCATTGAAGAACATTGAACCAAGCAGCCTCAGAGAGGTAATGGTCGAAGTGCCT
AACGTACACTGGGATGACATAGGCGGTCTCGAAGATGTTAAGAGGGAGGTAAGGAAACTGTAGAA
TTGCCGCTTCTAAAGCCAGATGTGTTTAAAGAGATTAGGAATAAGGCCGTCGAAAGGTTTCTTGTTA
TACGGTCCGCCCCGAGTTGGAAAAGACGCTGTTGGCCAAGGCGGTTGCCACAGAGAGCAACGCTAAC
TTTATATCTATTAAGGGCCCCGAGGTATTAAGCAAGTGGGTAGGAGAGAGCGAGAAGGCTATAAGG
GAAATATTCAAGAAAGCAAAGCAAGTCGCCCTGCTATAGTATTCTCGATGAAATAGATTCTATA
GCGCCAAGGAGAGGTACGACAAGCGACTCAGGCGTCACTGAAAGGATAGTTAATCAACTCCTAACA
TCGCTCGATGGCATAGAGGTTATGAACGGAGTTGTAGCCATTGGGGCCACGAATAGGCCGGATATA
ATGGATCCAGCACTGCTTAGGGCTGGAAGATTTGATAAACTTATCTACATACCGCCACCGGACAAG
GACGCACGCCTCAGCATATTAAGGTACATACCAAAAAATATGCCGCTCGCGCCGGATGTGATCTG
GACAGCATTGCCCAAAGGACAGAGGGCTACGTGGGTGCAGACCTTGAGAACCCTATGCAGGGAAGCA
GGTATGAATGCCTATCGAGAGAACCAGATGCAACTCAGGTTTCACAGAAGAAGCTTTATTGATGCC
CTTAAGACTATAAGGCCATCCATAGATGAAGAAGTAATAAAGTTCTACAAGAGCATCAGCGAAACC
ATGGGCAAATCGGTATCGGAAAAGAGGAAGGAGCTTCAGGATCAGGGACTGTATCTGTGA

```

**Figure 3.17 The sequence of TVN0947 gene (2238 bp).** The underlined region of the gene defined by the gene specific forward (red) and reverse primers (blue), indicates the amplified sequence by RT-PCR (177 bp).

### 3.3.1 Time-Course Differential Expression of TVN0947 Gene under Heat Stress

Depending on Ct values of tests and controls (Table 3.8), it can be suggested that TVN0947 gene expression was induced during heat shock at 65°C for 120 min (Table 3.8) and the induction of the gene's expression was at the highest level at 60 min.

Transcription of TVN0947 gene was induced mainly by heat-shock at 70°C for 60 min, as revealed by lower Ct values of the tests as compared to that of controls (Table 3.8), and then was sustained almost at level of control expression during the last 1 h.

Melting curve analysis for these qRT-PCR experiments verified the specific amplification of TVN0947 gene's cDNAs. The average T<sub>m</sub> value was 80.74°C ±0.07. Representative results for RT-PCR absolute quantification analyses of TVN0947 cDNA samples from 65°C and 70°C heat shock experiments are given in the Appendix C. Figures 3.18 and 3.19 show RT-PCR amplification curves of 65°C and 70°C heat-shock experiments for 30 min.

**Table 3.8 Representative Ct values and mean value of at least three melting temperatures from heat shock experiments for TVN0947 gene.**

Stress	Time (min)	Ct values		Melting Temperature (± STD)
		Test	Control	
65°C	30	12.59	14.05	80.77°C (± 0.3)
	60	12.28	14.05	80.71°C (± 0.4)
	90	12.97	14.27	80.81°C (± 0.4)
	120	13.75	14.93	80.64°C (± 0.5)
70°C	30	14.54	16.70	80.91°C (± 0.4)
	60	14.41	15.29	80.52°C (± 0.06)
	90	14.1	14.11	80.32°C (± 0.2)
	120	12.84	13.58	81.25°C (± 0.4)

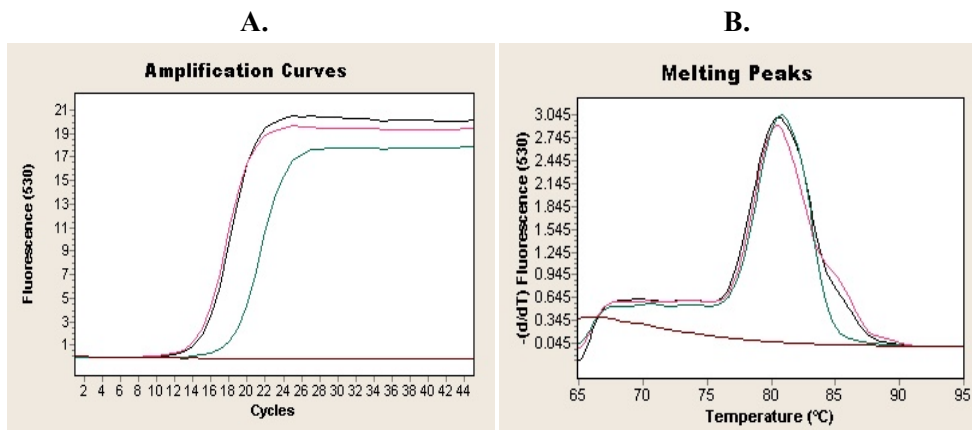


**Figure 3.18 Real-time PCR amplification curves for TVN0947 gene.** RNA samples were isolated from cultures exposed to heat stress at 65°C for 30' and 60' used for reverse transcription. **A.** Amplification curves (black—30', pink—60', green—control, dark red—negative control) **B.** Melting curves (black—30', pink—60', green—control, dark red—negative control)

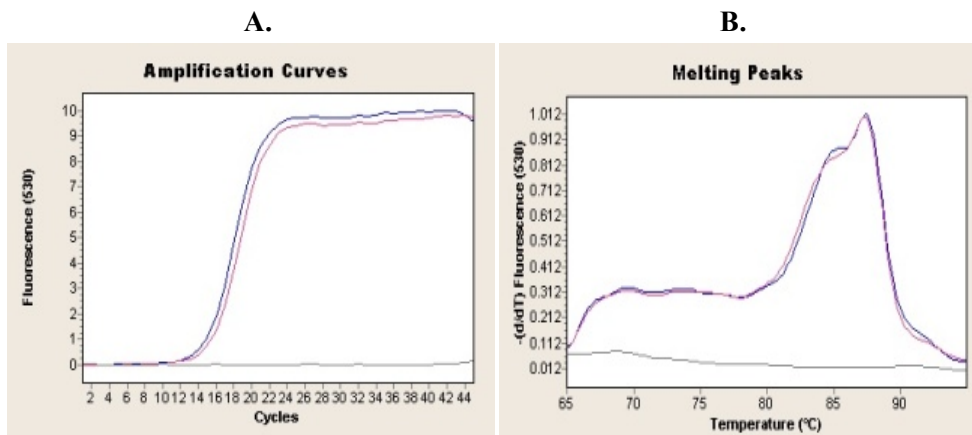


**Figure 3.19 Real-time PCR amplification curves for TVN0947 gene.** RNA samples were isolated from cultures exposed to heat stress at 70°C for 30' used for reverse transcription. **A.** Amplification curves (blue—test, purple—control, grey—negative control) **B.** Melting curves (blue—test, purple—control, grey—negative control)

### 3.3.2 Fold Difference Analysis of Time Course Expression of TVN0947 Gene under Heat Shock

Fold difference analysis indicated that TVN0947 gene expression enhanced 3-4 fold under 65°C heat stress, as compared to expression under optimum conditions. The gene expression was not effected from heat-shock at 70°C for 90 min. There was only a 1.5-fold increase in mRNA content after 120 min.

The calculated fold differences were represented as the mean of at least two independent experiments (Table 3.9). The related data points are plotted in a chart and depicted by bars (Figure 3.20).

**Table 3.9 Fold difference of TVN0947 gene expression under heat shock.** The results are the means of at least 3 independent qRT-PCR experiments.

Stress	Time (min)	Fold Difference ( $\pm$ STD)
65°C	30	2.447 $\pm$ 0.01
	60	2.959 $\pm$ 0.01
	90	2.451 $\pm$ 0.01
	120	2.125 $\pm$ 0.02
70°C	30	3.105 $\pm$ 1.5
	60	1.209 $\pm$ 0.3
	90	1.041 $\pm$ 0.05
	120	1.484 $\pm$ 0.4

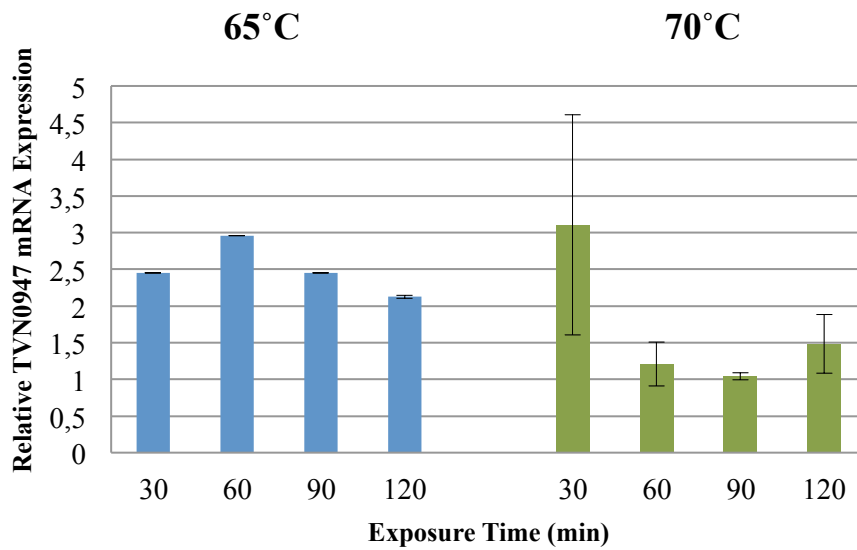


**Figure 3.20** Relative mRNA expression of TVN0947 gene determined quantitative real-time PCR analysis under heat shock at 65°C and 70°C. Expressions are shown as fold-increase or decrease relative to the control (60°C) level (1-fold) TVN0947 gene expression. The values are means of at least 3 replicates.

### 3.3.3 Time-Course Differential Expression of TVN0947 Gene under pH Stress

According to test and control Ct values, TVN0947 gene expression should be up-regulated for 60 min under stress at pH 4.0, but then reduced to almost control level at 120'. The TVN0947 gene expression did not change at pH 3.6 for 2 h compared to control. However, at higher pH values (pH 4.5 and pH 5.0) the gene expression was down-regulated during 2 h stress exposure.

The melting curve analysis showed that all amplified TVN0947 cDNAs produced single-peak and average melting temperature was  $82.61^{\circ}\text{C} \pm 2$  implying specific amplification of the cDNA. Representative amplification and melting curves for qRT-PCR experiments of stress at pH 4.0 and pH 5.0 are given in the Appendix C. The RT-PCR amplification curves for pH 4.0 (30 min) and pH 5.0 (120 min) are given in Figures 3.21 and 3.22.

**Table 3.10 Representative Ct values and mean value of at least three melting temperatures from pH stress experiments for TVN0947 gene.**

Stress	Time (min)	Ct values		Melting Temperature (± STD)
		Test	Control	
pH 3.6	30	13.3	13.2	80.31°C (± 0.01)
	60	13.53	13.2	81.99°C (± 0.01)
	90	13.84	13.46	80.65°C (± 0.48)
	120	13.48	13.46	80.17°C (± 0.2)
pH 4.0	30	13.46	12.94	84.9°C (± 0.3)
	60	13.12	12.94	84.81°C (± 0.4)
	90	12.60	12.94	84.76°C (± 0.2)
	120	12.32	12.98	84.49°C (± 0.4)
pH 4.5	30	15.72	14.61	80.76°C (± 0.01)
	60	16.33	14.61	80.82°C (± 0.01)
	90	15.21	13.81	80.93°C (± 0.01)
	120	15.08	13.81	80.75°C (± 0.01)
pH 5.0	30	14.84	13.94	84.51°C (± 0.05)
	60	15.95	14.83	84.04°C (± 0.01)
	90	16.98	14.83	84.73°C (± 0.3)
	120	14.62	13.94	84.21°C (± 0.3)

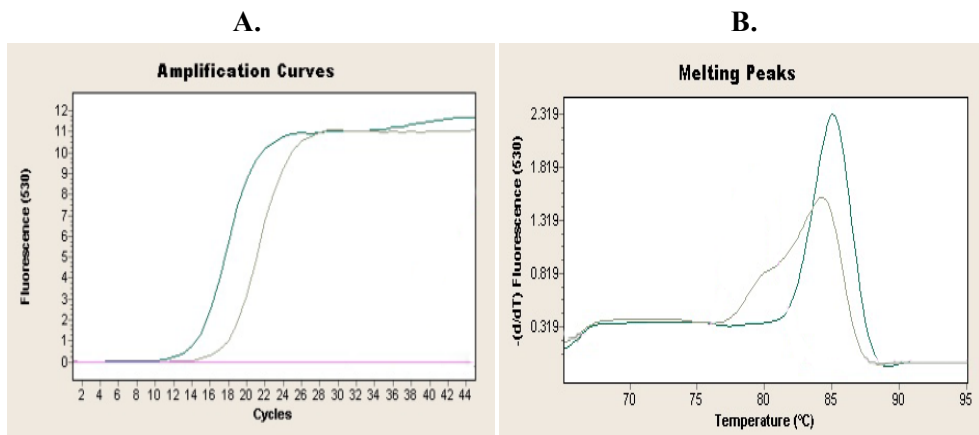


**Figure 3.21 Real-time PCR amplification and melting curves for TVN0947 gene.** RNA samples were isolated from cultures exposed to pH stress at pH 4.0 for 30' used for reverse transcription. **A.** Amplification curves (green—test, grey—control, pink—negative control) **B.** Melting curves (green—test, grey—control).

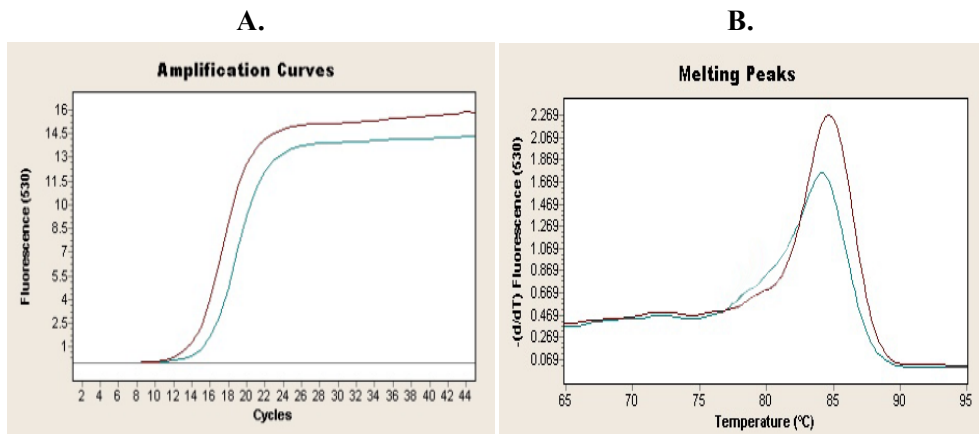


**Figure 3.22 Real-time PCR amplification and melting curves for TVN0947 gene.** RNA samples were isolated from cultures exposed to pH stress at pH 5.0 for 120' used for reverse transcription. **A.** Amplification curves (green—test, dark red—control, grey—negative control) **B.** Melting curves (green—test, dark red—control).

### 3.3.4 Fold Difference Analysis of Time Course Expression of TVN0947 Gene under pH Stress

The changes in the expression of TVN0947 gene at four different pH stresses (pH 3.6, pH 4.0, pH 4.5 and pH 5.0) were analyzed relative to control (pH 2.7) over 120 min.

The fold difference analysis has shown that TVN0947 gene expression was down regulated at pH 3.6, pH 4.5 and pH 5.0 for 2 h. When the culture pH was shifted to pH 4.0, expression was slightly increased at 30 min, but then gradually increased up to 1.4-fold at 120 min relative to control expression level. The most significant effect was observed after 90 min post exposure to pH 5.0 when the transcription level was about one third of the control expression level. The fold differences were calculated and represented as the mean of at least three independent experiments (Table 3.11). The related data points are plotted in a chart and depicted by bars (Figure 3.23).

**Table 3.11 Fold difference of TVN0947 gene expression under pH stress.** The results are the means of at least three independent qRT-PCR experiments.

Stress	Time (min)	Fold Difference ( $\pm$ STD)
pH 3.6	30	0.93 $\pm$ 0.01
	60	0.787 $\pm$ 0.01
	90	0.778 $\pm$ 0.01
	120	0.987 $\pm$ 0.01
pH 4.0	30	0.746 $\pm$ 0.01
	60	0.904 $\pm$ 0.01
	90	1.211 $\pm$ 0.01
	120	1.389 $\pm$ 0.01
pH 4.5	30	0.532 $\pm$ 0.01
	60	0.376 $\pm$ 0.01
	90	0.711 $\pm$ 0.01
	120	0.765 $\pm$ 0.01
pH 5.0	30	0.747 $\pm$ 0.3
	60	0.602 $\pm$ 0.09
	90	0.393 $\pm$ 0.02
	120	0.376 $\pm$ 0.03

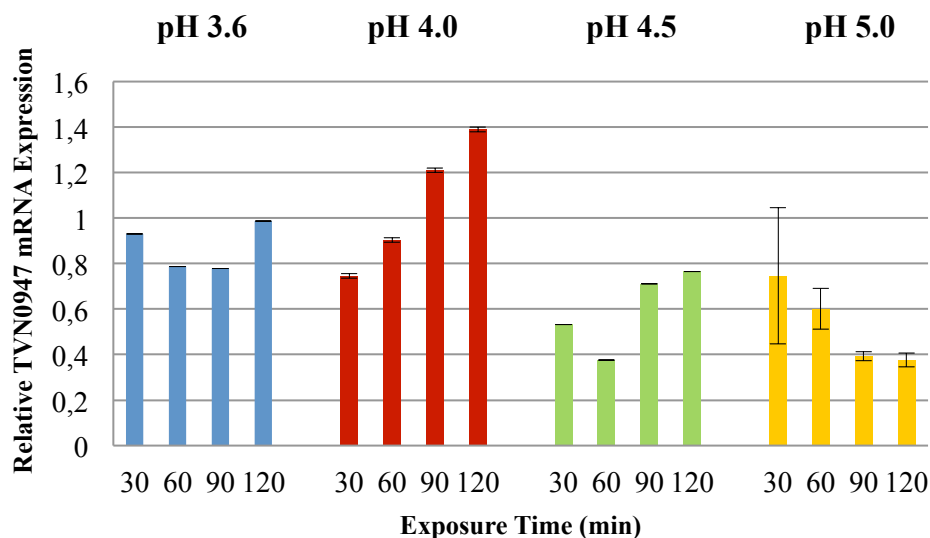


**Figure 3.23** Relative mRNA expression of TVN0947 gene was determined by quantitative real-time PCR analysis under pH stress at pH 3.6, 4.0, 4.5 and 5.0. Expressions are shown as fold-increase or decrease relative to the control (pH 2.7) level (1-fold) TVN0947 gene expression. The values are means of at least 3 replicates.

### 3.3.5 Time-Course Differential Expression of TVN0947 Gene under Oxidative Stress

Quantitative real time PCR experiments were repeated at least three times for each one of the oxidative stress conditions. Figures 3.24 and 3.25 show the RT-PCR amplification and melting curves for TVN0947 gene expression after 0.02 mM H<sub>2</sub>O<sub>2</sub> (60 min) and 0.03 mM H<sub>2</sub>O<sub>2</sub> (60 min) amplification.

Based on the relatively lower Ct values of the tests during exposure to H<sub>2</sub>O<sub>2</sub> at 0.01, and 0.02 mM concentrations, it is expected that TVN0947 gene expression can be slightly accelerated by 90 min. At higher concentrations of H<sub>2</sub>O<sub>2</sub> (0.03 mM and 0.05 mM), TVN0947 gene expression levels may be declined or unchanged at 120 min post exposure to stress (Table 3.12).

The melting curve analysis for qRT-PCR experiments of oxidative stress showed that all amplified cDNAs of TVN0947 produced single-peak and average melting temperature was 82.48°C ±1.9 implying specific amplification of the TVN0947 cDNA. Representative amplification and melting curves of the TVN0947 cDNA samples of oxidative stress experiments were given in Appendix C. Figure 3.24 and 3.25 show RT-PCR amplification and melting curves for TVN0947 gene expression after 0.02 mM and 0.03 mM H<sub>2</sub>O<sub>2</sub> applications, respectively for 60 min.

**Table 3.12 Representative Ct values and mean value of at least three melting temperatures of oxidative stress experiments for TVN0947 gene.**

Stress	Time (min)	Ct values		Melting Temperature (± STD)
		Test	Control	
0.01 mM	30	14.68	14.91	83.61°C (± 0.01)
	60	14.16	14.91	83.96°C (± 0.01)
	90	12.99	13.43	84.22°C (± 0.01)
	120	13.91	13.43	84.54°C (± 0.01)
0.02 mM	30	17.85	17.03	84.18°C (± 0.01)
	60	14.15	15.3	85.02°C (± 0.01)
	90	13.84	12.52	83.96°C (± 0.01)
	120	15.99	16.3	83.92°C (± 0.01)
0.03 mM	30	15.79	16.74	80.63°C (± 0.01)
	60	13	13.6	80.96°C (± 0.01)
	90	13.82	13.6	80.60°C (± 0.4)
	120	12.13	11.91	81°C (± 0.01)
0.05 mM	30	18.19	17.3	80.79°C (± 0.6)
	60	14.88	13.11	80.39°C (± 0.2)
	90	14.25	13.11	81.56°C (± 1.9)
	120	15.02	14.64	80.51°C (± 0.5)

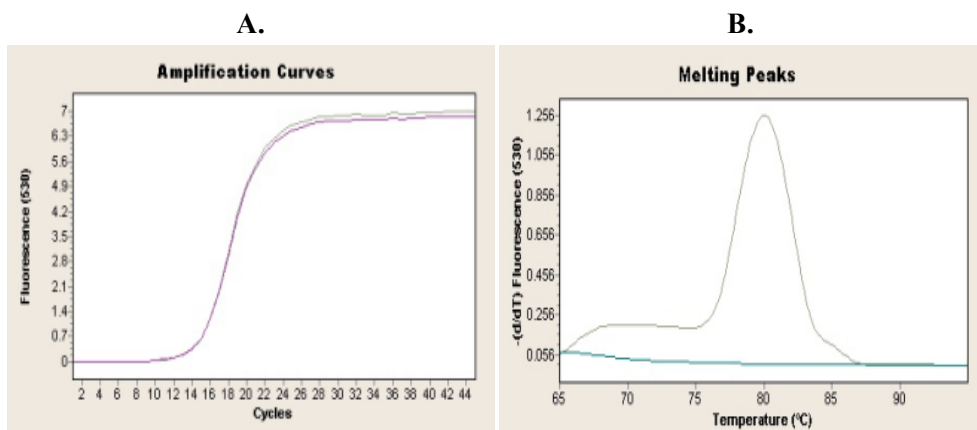


**Figure 3.24 Real-time PCR amplification and melting curves for TVN0947 gene.** RNA samples were isolated from cultures exposed to oxidative stress at 0.02 mM for 60' used for reverse transcription. **A.** Amplification curves (grey—test, purple—control) **B.** Melting curves (grey—test, green—negative control).

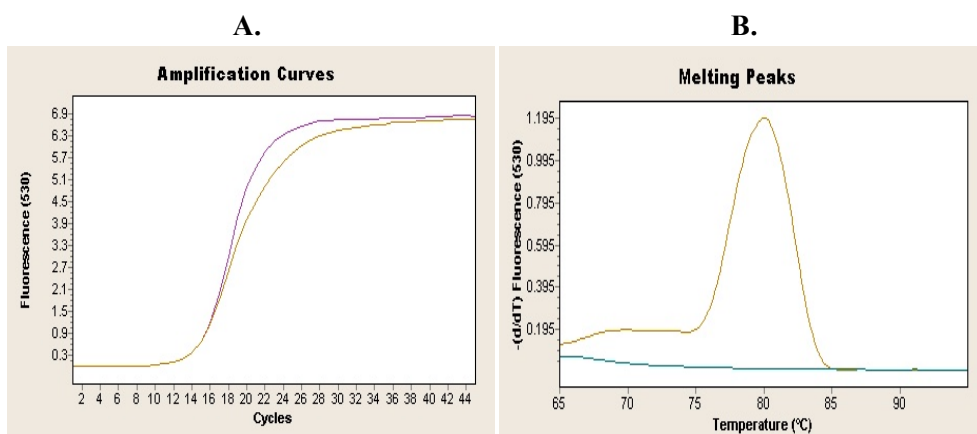


**Figure 3.25 Real-time PCR amplification and melting curves for TVN0947 gene.** RNA samples were isolated from cultures exposed to oxidative stress at 0.03 mM for 60' used for reverse transcription. **A.** Amplification curves (light brown—test, purple—control) **B.** Melting curves (light brown—test, green—negative control).

### 3.3.6 Fold Difference Analysis of Time Course Expression of TVN0947 Gene under Oxidative Stress

According to fold-analysis, TVN0947 gene transcription induced at most approximately 1.6 fold at 60 min and 30 min under oxidative stress maintained by H<sub>2</sub>O<sub>2</sub> at 0.02 mM and 0.03 mM concentrations, respectively. Under the same conditions, the gene's expression did not change at other time points for 120 min. At 0.01 mM H<sub>2</sub>O<sub>2</sub> concentration, TVN0947 transcription was gradually enhanced up to 1 h (about 1.5-fold), but then decreased almost to control expression level at 90 min and even below at 120 min. At 0.05 mM H<sub>2</sub>O<sub>2</sub>, TVN0947 gene transcription was almost constantly down-regulated for 2 h.

The mean value of fold differences of at least two independent experiments were calculated (Table 3.13) and they were plotted as bar graphs (Figure 3.26).

**Table 3.13 Fold difference of TVN0947 gene expression under oxidative stress.** The results are the means of at least three independent qRT-PCR experiments.

Stress	Time (min)	Fold Difference ( $\pm$ STD)
0.01 mM	30	1.125 $\pm$ 0.01
	60	1.49 $\pm$ 0.01
	90	1.297 $\pm$ 0.01
	120	0.747 $\pm$ 0.01
0.02 mM	30	0.702 $\pm$ 0.1
	60	1.336 $\pm$ 0.4
	90	1.04 $\pm$ 0.1
	120	1.248 $\pm$ 0.3
0.03 mM	30	1.588 $\pm$ 0.01
	60	1.1 $\pm$ 0.01
	90	0.955 $\pm$ 0.01
	120	0.944 $\pm$ 0.05
0.05 mM	30	0.575 $\pm$ 0.1
	60	0.503 $\pm$ 0.06
	90	0.898 $\pm$ 0.3
	120	0.412 $\pm$ 0.05

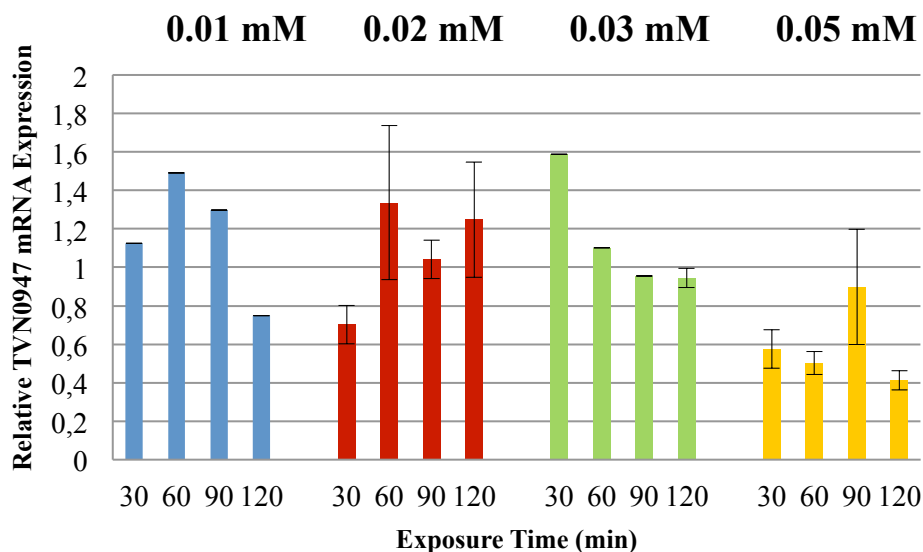


**Figure 3.26** Relative mRNA expression of TVN0947 gene determined by quantitative real-time PCR analysis under oxidative stress at 0.01 mM, 0.02 mM, 0.03 mM and 0.05 mM. Expressions are shown as fold-increase or decrease relative to the control level (1-fold) TVN0947 gene expression. The values are means of at least 3 replicates.

### 3.4 Expression Analysis of VAT Genes at Translation Level under Stress Conditions by Western Blot Hybridization Assay

The expression levels of VAT protein under four different stress conditions (heat shock at 65°C and 70°C, pH stress at pH 4.0 and oxidative stress imposed by 0.02 mM H<sub>2</sub>O<sub>2</sub>) at 60 min and at 120 min post exposure were determined relative to the protein's expression under optimal conditions, by Western blot/hybridization technique. Immunodetection was performed using a commercially available VCP mouse monoclonal antibody (M15), clone 2H5 which has human reactivity (Abnova Corporation, Taiwan) with an expectation of a cross hybridization with *Tpv* VAT proteins, from stress exposed *Tpv* cells. As already mentioned, we have studied two VAT genes, TVN0382 (VAT 1) and TVN0947 (VAT 2), both are the members of the AAA+ superfamily involved in cell division. The sequence homology between VAT genes and human VCP, clone 2H5 peptide is shown in the Figures 3.27 and 3.28.

In the experiments, Human VCP partial ORF recombinant protein with GST-tag at N-terminal (35.64 kDa) (Abnova Corporation, Taiwan) was used as positive control. The positive control showed that the reaction between VCP antibody and human VCP protein was specific, and unique hybridization band (at 35.64 kDa position) was observed after immunodetection (Figures 3.29 and 3.30).

```

TVN0382 MSDDVQNKIEKATKLLHAGIKKEENGHKDKAKEYYLVAYRVMLEAANDSPSDLKKKRLDQCALIINAY
VCP -----
TVN0382 RVSGERTDFTVKKQNDDEIVEGEALLEEIGIEKPEIPKVTFFEDVAGLDDVKNEILGKIIYPMKFKELS
VCP -----
TVN0382 QEYNIQFGGGMLLYGPPGTGKTFIVKAIANEVKARFINVNPSTLYSEWFGVFEKNISKLFRAASLLSP
VCP -----
TVN0382 AIIFFDEIDALVPKRDTSNSDAAKRGVAQLLNEVGGINSQKNKNIFIIAATNPNWEVDEAMLRPGRFD
VCP -----
TVN0382 IKIYVPPPDIVARKKIFQLNLAKIKQVGNVDYDLAEEETEGYSGADIEFICKAAQNVFMEAVKTKGS
VCP -----IHTKNMKLADDVDLEQVANETHGHVGADLAALCSEALQAIRKKM-----
: . :*: :*: : :*:*: * :*: :*: :*: :*: :*: :*: :*: :*: :*:
TVN0382 RPVETRDVIDVIGSIKPSIDYELLEKYSKYGSFAF-----
VCP -----DLIDLEDETIDAEVMNSLAVTMDDFRWALSQSNPSALRETVVEVP
*:* . :* *::: . :*

```

Figure 3.27 Clustel Q (1.1.0) multiple sequence alignment of subject TVN0382 versus object partial VCP protein.

```

TVN0947 MDNSSGIILRVAEANSTDPGMSRVRLDESSRRLDAEIGDVVEIEKARKTVGRVYRARPEDENKGIVRI
VCP -----
TVN0947 DSVMRNCGASIGDKVRVRKVRTEIAKKVTLAPIIRKDQRLKFGEGIEEYVQRALIRRPMLQDNISVP
VCP -----
TVN0947 GLTLAGQTGLLFKVVKTPMGKVPVEIGEETKIEIREEPASEVLEEVSRVSYEDIGGLSEQLGKIREMIE
VCP -----
TVN0947 LPLKHPELFEERLGITPPKGVILYGGPPGTGKTLIARAVANESGANFLSINGPEIMSKEYGQSEQKLRIF
VCP -----
TVN0947 SKAETAPSIIFFIDEIDSIAPKREEVQGEVERRVVAQLLTLMDGMKERGHVIVIGATNRIDAVDPALRR
VCP -----
TVN0947 PGRFDREIEIGVPDRNGRKEILMIHTRNMPGMDDEEQKNKFLEEMADYTYGFVGADLAALVRESAMNAL
VCP -----IHTKNMKLADD-----VDLEQVANETHGHVGADLAALCSEALQAI
*:*: * * * * * * * * * * * * * * * * * * * * * * * * * * * * * * * * * * *
TVN0947 RRYLPEIDLK-PIPTEILEKMOVTEEDFKNALKNIEPSSLREVMVEVPNVHDDIGGLEDVKREVKET
VCP -----RKKMDLIDLEDETIDAEVMNSLAVTMDDFRWALSQSNPSALRETVVEVP-----
: : **: . * :*: :*: :*: :*: :*: :*: :*: :*: :*: :*: :*: :*: :*: :*: :*:
TVN0947 VELPLLKPDVFKRLGIRPSKGFLLYGGPPGVGKTLAKAVATESNANFISIKGPEVLSKWVGESEKAIRE
VCP -----
TVN0947 IFKKAKQVAPAIVFLDEIDSIAPRRGTTSDSGVTERIVNQLLTSLDGIEVMNGVVAIGATNRPDMDPA
VCP -----
TVN0947 LLRAGRFDKLIYIPPPKDARLSILKVHTKNMPLAPDVLDSIAQRTEGYVGADLENLCREAGMNAYRE
VCP -----
TVN0947 NPDATQVSQKNFIDALKTIRPSIDEEVIKFKYSISETMGKSVSEKRKELQDQGLYL
VCP -----

```

Figure 3.28 Clustel Q (1.1.0) multiple sequence alignment of subject TVN0947 versus object partial VCP protein.

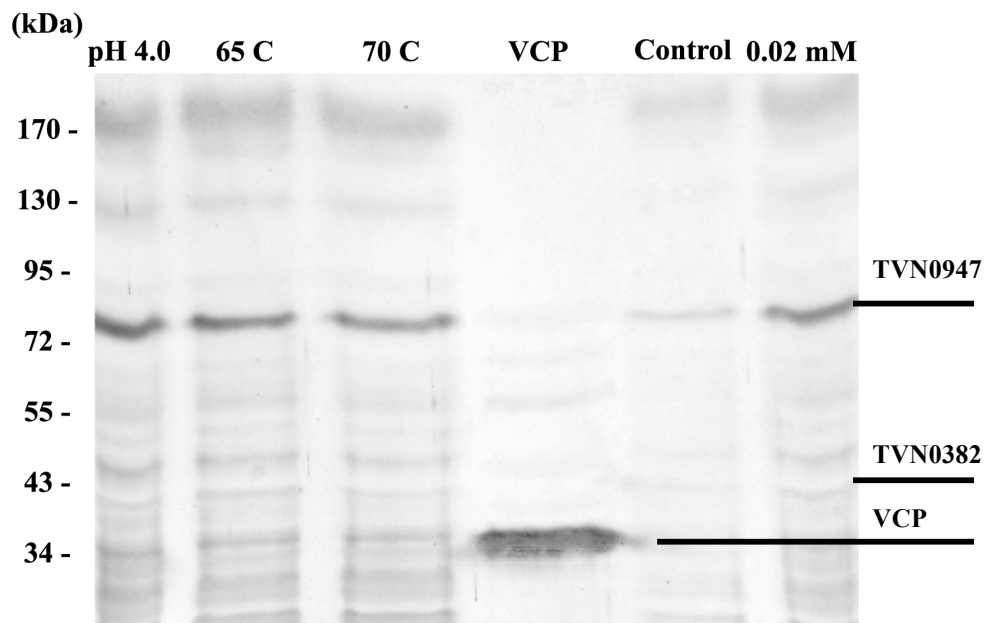


**Figure 3.29** Western blot hybridization analyses of *Tpv* protein extracts from control and stress exposed cultures for 60 min. Expression of VAT 1 (TVN0382), and VAT 2 (TVN0947) proteins were examined by cross-reaction with human VCP antibody. Human VCP was used as the positive control.

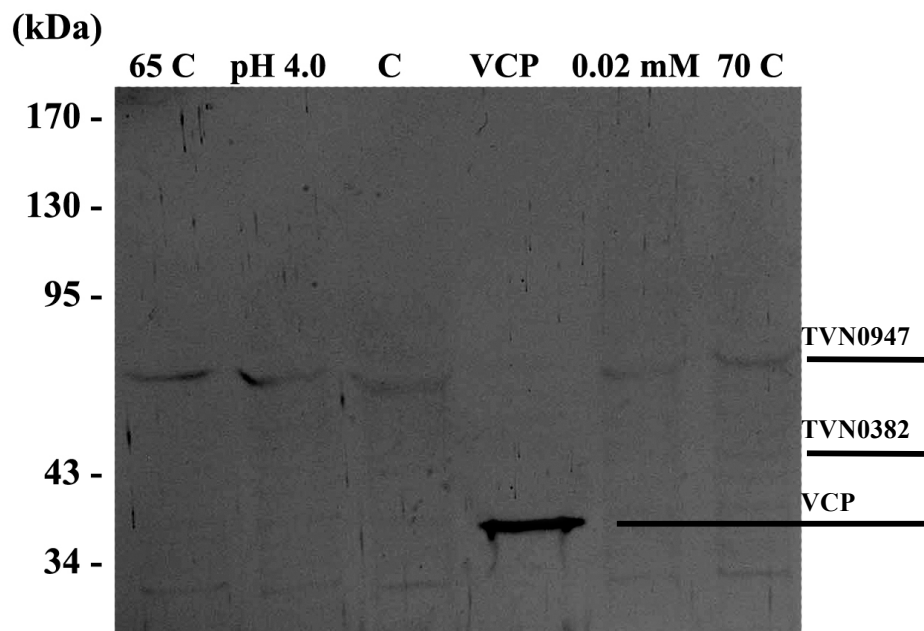


**Figure 3.30** Western blot hybridization analyses of *Tpv* protein extracts from control and stress exposed cultures for 120 min. Expression of VAT 1 (TVN0382) and VAT 2 (TVN0947) proteins were examined by cross-reaction with human VCP antibody. Human VCP was used as the positive control.

It is clear from the Figures 3.29 and 3.30 that the VCP antibody could detect TVN0947 and TVN0382 proteins, as the hybridization bands appeared at the positions possibly corresponding to their known molecular weights, i.e. 83.01 kDa and 42.01 kDa, respectively. Cross hybridization of human VCP antibody with the TVN0382 gene produced weaker bands than the TVN0947. Based on sequence alignment results, TVN0382 has 34% sequence overlap with the VCP protein sequence while TVN0947 has 83% sequence overlap. This may explain the signal intensity difference between the bands of the two VAT proteins.

When the band intensities compared, it is quite evident that the highest amount of TVN0947 protein level could be achieved by heat induction at 65°C for 120 min. Hybridization signals for pH 4.0, 70°C heat and 0.02 mM H<sub>2</sub>O<sub>2</sub> related stresses were more than that of the control. The signals for TVN0382 protein were too weak to make a conclusive comparison.

### 3.5 Whole Genome Microarray Analysis of *Thermoplasma volcanium* GSS 1 Response to Heat shock, pH and Oxidative Stress

#### 3.5.1 RNA Isolation of Stress Induced Cells for Microarray Study

We have investigated genome-wide transcriptional response of *T. volcanium* to heat shock (at 65°C), 0.02 mM H<sub>2</sub>O<sub>2</sub> and pH stress (at pH 4.0), by using NimbleGen oligo expression microarray platform. All experiments were run as two technical replicates. Tpv cultures grown to mid-log phase were exposed to these stressors for 1 h and then RNA was isolated as described in the Materials and Methods section. The total RNA concentrations of the samples determined using UV/visible spectrophotometer verified the required quantity of RNA samples (Table 3.14). RNA concentrations were also estimated using a Picodrop spectrometer (Table 3.15). RNA quality was assessed by visualization on agarose formaldehyde gel (Figure 3.31). These results showed that quantity and quality of the RNA samples were suitable to perform cDNA synthesis.

**Table 3.14 Concentrations of the RNA samples.** Concentrations were calculated by the equation given by NimbleGen protocol; RNA concentration = 40 µg/ml x A<sub>260</sub> x Dilution Factor. Dilution factor was 40%.

Stress condition	A <sub>260</sub>	Concentration (µg/µl)
65°C	0.168	0.94
0.02 mM	0.123	0.69
pH 4.0	0.135	0.76
Control	0.244	1.37

The quality and quantity of the double stranded cDNAs were independently assessed by agarose gel electrophoresis and Bioanalyzer (Agilent) to verify all samples meet the desired qualification for the microarray experiment. As can be seen in the Table 3.15, the

concentrations of all ds cDNAs were  $\geq 100$  ng/nl, as required. Figure 3.32 shows agarose gel electrophoresis results of dscDNA samples.

**Table 3.15 Concentrations of the double stranded cDNA samples.** Concentrations were given as the mean of five independent measurements.

Stress condition	Picodrop measurement (ng/ $\mu$ l)	A <sub>260</sub> / A <sub>280</sub>
0.02 mM	785.96	2
pH 4.0	837.82	2
65°C	808.06	2
Control	801.66	2

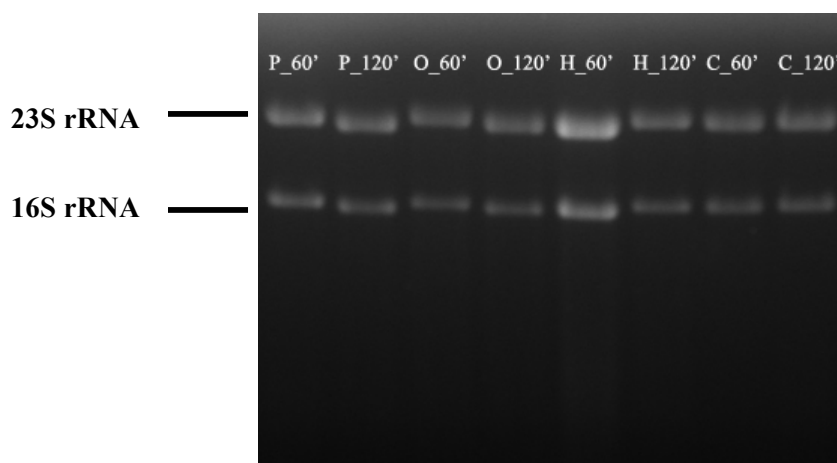


**Figure 3.31 Formaldehyde agarose gel (1.2%) photo of the RNA samples of stress induced cells.** P indicates pH 4.0, O indicates Oxidative stress 0.02 mM, H indicates Heat shock at 65°C and C indicates Control.

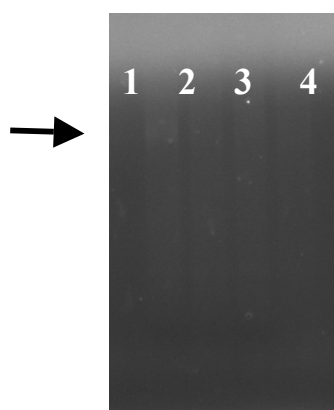


**Figure 3.32 Agarose gel (1.2%) photograph of the dscDNA samples of stress induced cells.** Lanes 1, 2, 3, and 4 represent the samples of heat-shock at 65°C, oxidative stress 0.02 mM, control, and pH 4.0, respectively.

The labeling of the cDNA samples with Cy3, then hybridization, array scanning, primary data collection and analysis (to align grids and evaluate spot quality) were carried out by Genmar Diagnostics, (TR). Data from NimbleGen array was analyzed in our laboratory using DNASTar ArrayStar Software.

### 3.5.2 Quality Assessment of Microarray Data and Normalization

Normalization is the process of reducing unwanted variation either within or between arrays. It may use information from multiple chips. Non-biological factors can contribute to the variability of data. In order to reliably compare data from multiple probe arrays, differences of non-biological origin must be minimized. Therefore normalization is a tool to reduce background noise to see the real data.

Normalization of the microarray data was carried out by Genmar Diagnostics, (TR). Data was also double-checked by HGM Bioinformatics, (TR) by generating MA plots, histogram and box plots using R-Bioconductor Package. MA plots are useful tools to decide if the data needs normalization and test if normalization worked.

Global normalization method (Lowess) was applied to the data. MA plots were created for each replicate and they were compared with a reference array. By this way it was aimed to check array qualities, individually [105].  $M$ , on the  $y$  axis represents the log fold change and  $A$  on the  $x$  axis represents the average log intensity. When Lowess curve differs from the  $M=0$  axis, it indicates an intensity level difference between each array (or zero line) and reference array means the data should be normalized. After normalization, Lowess line (red line on the diagram) is expected to be close to the horizontal line at  $M=0$  [106]. As can be seen in the Figure 3.33, arrays were needed to be normalized depending on differences between shapes and center of distributions. RMA (Robust Multi-Array Average expression measure) was performed for the normalization process. Hereby, the data was manipulated to make different arrays comparable (Figure 3.34) [106].

The *histograms* and *box-plots* were also used as diagnostics plots to see raw-probe intensity differences between arrays [106] or to examine the homogeneity of the arrays [105]. When the arrays are homogeneous, the boxes are expected to be at the same width and  $y$  axis position for box-plot method. After normalization the median values are similar across the arrays and the distributions across the replicates are similar. This indicates that data is not problematic and normalization has been appropriate. Density estimate plots give an idea about signal distribution across a chip. They are represented as a histogram and expected to show similar distribution for each array after normalization which is typical for reasonable experiments. Density-plots and box-plots were generated before and after normalization can be seen in Figures 3.35 and 3.36, respectively.

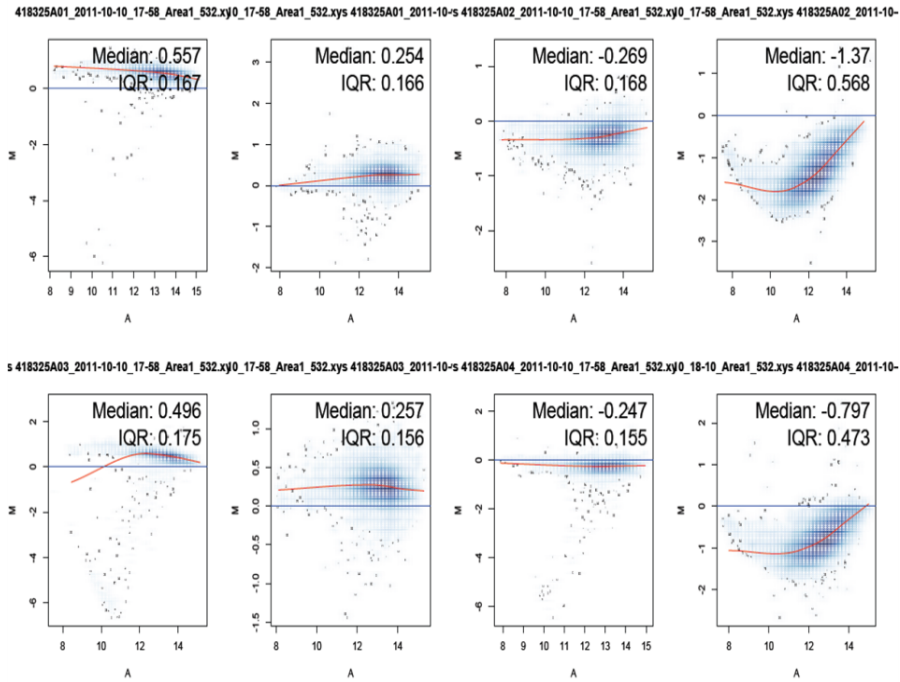


**Figure 3.33** MA-plot of eight arrays plotted with a reference array. Inter-quartile range (IQR) and median of the M values were given in the plots. Lowess curves (red line) differ from the M=0 axis before normalization.

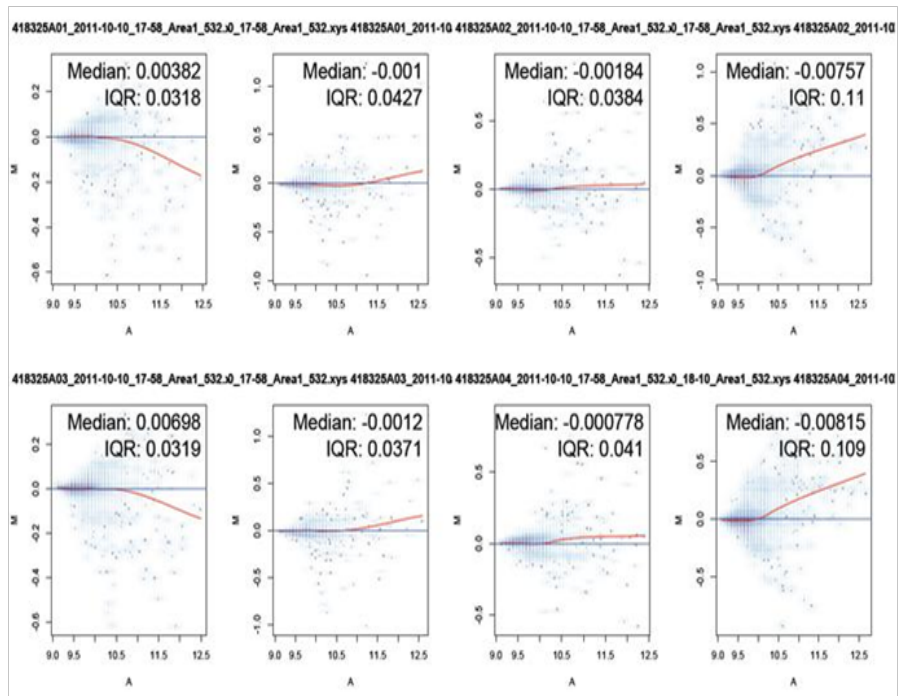


**Figure 3.34** MA-plot of eight arrays plotted with a reference array. Inter-quartile range (IQR) and median of the M values were given in the plots. Lowess curves (red line) close to the horizontal line of M=0 axis after normalization.

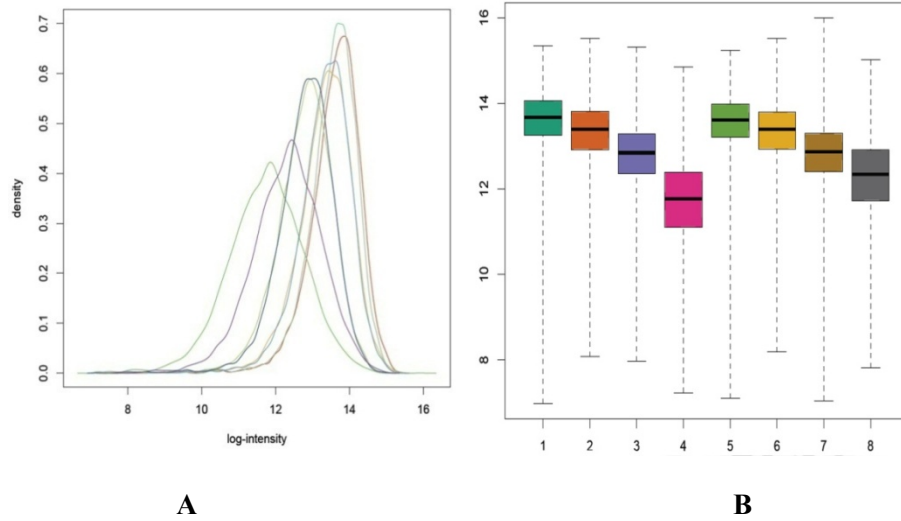


**Figure 3.35** A) Smoothed histograms of raw log-scale intensities. B) Box-plots of unprocessed log scale probe intensities for eight arrays.

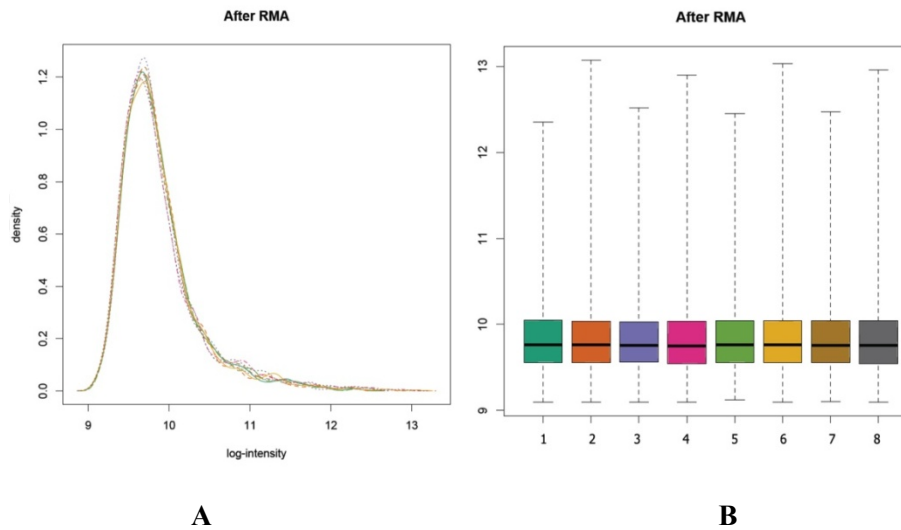


**Figure 3.36** A) Density plot of log scale intensities after RMA. B) Box-plots of RMA processed log scale probe intensities of eight arrays.

The compliance of the two replicates was checked in our laboratory by aligning two replicates in scatter plots using DNASTar ArrayStar Software (Figure 3.37).

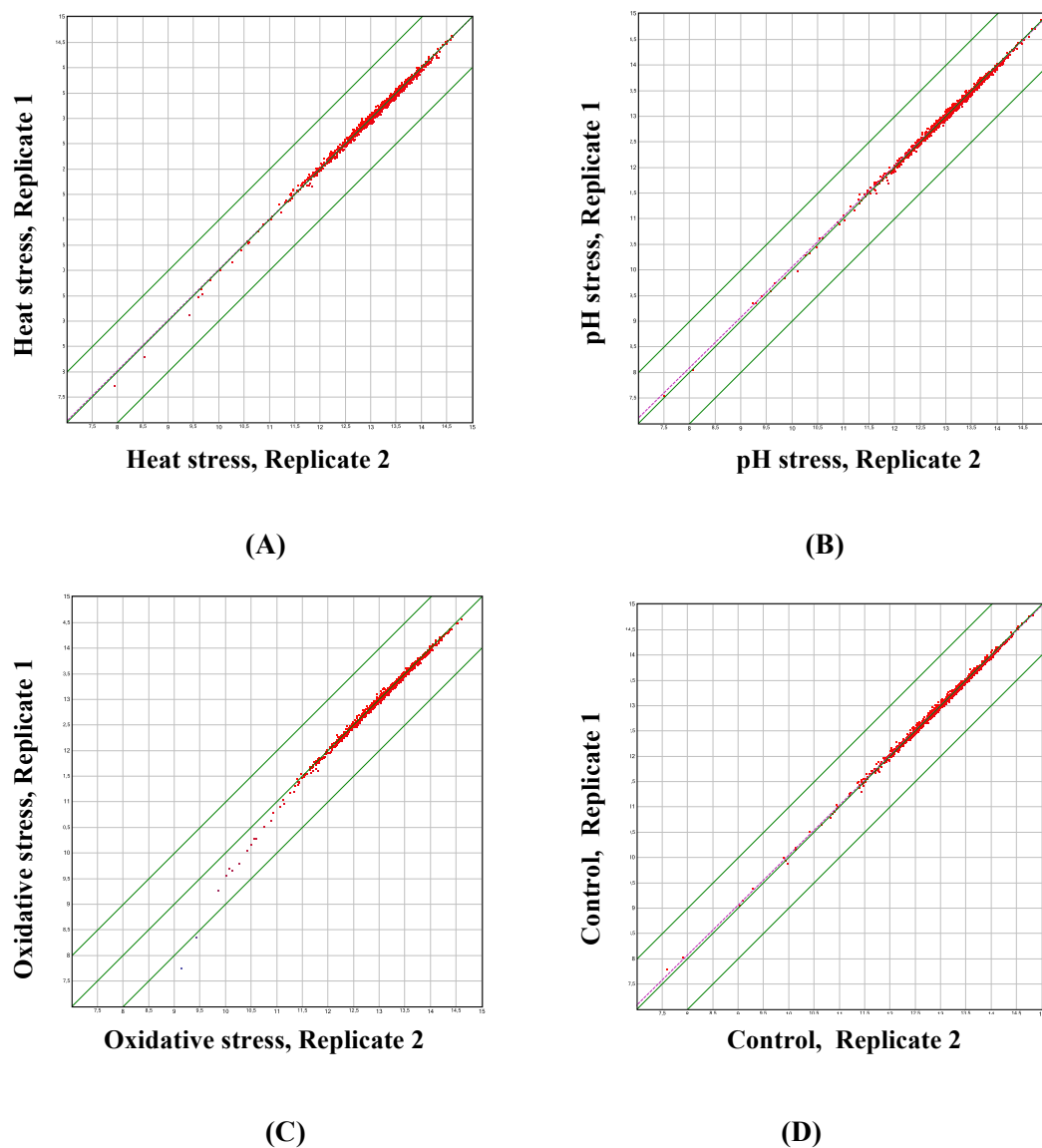


**Figure 3.37** Scatter plots of average probe intensity (Log<sub>2</sub>) for Roche NimbleGen microarray chips hybridized with cDNA from heat shock, pH stress, oxidative stress and control cultures of *Tpv* cells. Plots were generated by the alignments replicate 1 versus replicate 2. Probes corresponding to genes up-regulated and down regulated are plotted in red. Linear regression is indicated in magenta (A\_R<sup>2</sup>=0.9956, B\_R<sup>2</sup>=0.9966, C\_R<sup>2</sup>=0.9912, D\_R<sup>2</sup>=0.9978); green lines indicate threshold of fold change >2.

### 3.5.3 Microarray Data Analysis

#### 3.5.3.1 Heat Stress

Changes in *T. volcanium* gene expression were evaluated by analysis of expression arrays from NimbleGen. DNASTar ArrayStar Software and Bioconductor R Software were used for statistical data analysis. Results indicated that the expression of 181 transcripts out of 1501 annotated *Tpv* ORFs included on the array significantly changed by at least 1.2 fold at 60 min post exposure to heat stress at 65°C. The majority of the genes (103) were down regulated and 78 genes were up-regulated (Table 3.16). Volcano plots, where the magnitude of the gene expression ratio is displayed on the *x*-axis and the significance of the difference in expression between heat-shock and control groups on the *y*-axis, are shown in Figure 3.38. Scatter plot of the genes is also represented in Figure 3.39.

**Table 3.16 Number of genes differentially expressed in total of 1501 genes under heat-shock.** They have represented as up and down regulated genes in comparison mode to control.

FOLD CHANGE	HEAT STRESS (65°C)		TOTAL
	UP	DOWN	
1.2-fold	78	103	181
1.5-fold	—	9	9

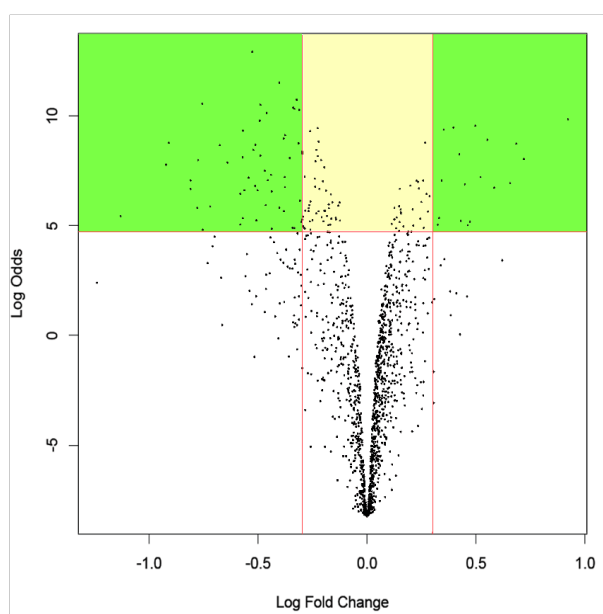
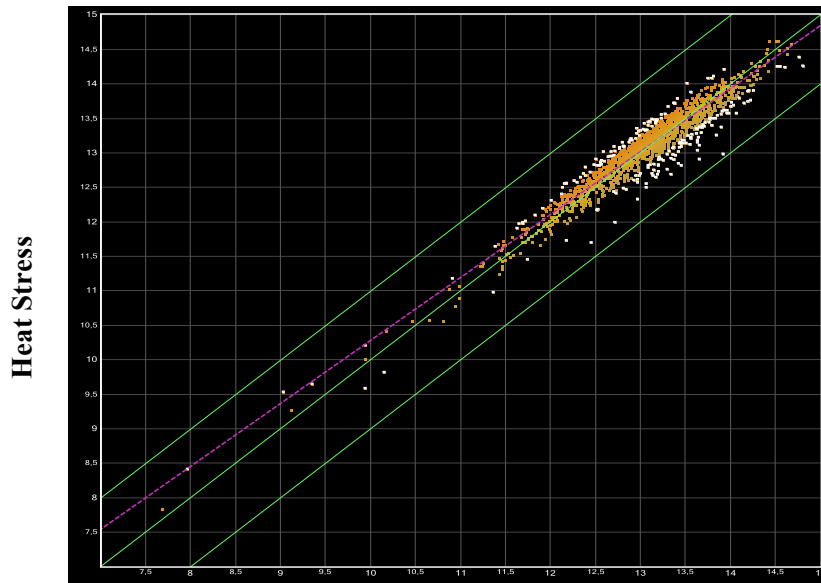


**Figure 3.38 The volcano plot for the heat stress dataset in comparison to control.** Under the filter of log-fold change  $\geq 0.3$  or  $\leq -0.3$  and logOdds  $\geq 4.6$ , genes are located in the upper left corner of plot are significantly down-regulated, while in the upper right corner are significantly up-regulated.



**Control**

**Figure 3.39** Scatter plot of average probe intensity (Log<sub>2</sub>) for Roche NimbleGen microarray chips hybridized with cDNA from heat shock induced cultures versus control of *Tpv* cells. Probes corresponding to genes up-regulated and down regulated to 1.2 fold are plotted in white. Linear regression is indicated in magenta ( $R^2=0.9279$ ): green lines indicate threshold of fold change  $>2$ .

Only genes with at least 1.2 fold differences ( $\log_2$  ratios  $\geq 0.3$  or  $\leq -0.3$ ) and  $\log$ Odds  $\geq 4.6$  were considered differentially expressed. When categorized by function, the differentially expressed genes were broadly dispersed across a variety of cellular functions. The most frequently affected categories with increased or decreased abundance of mRNA were ‘heat shock’ related proteins, ‘transport proteins’, ‘translation and transcription proteins’, proteins of ‘energy production and conversion’, proteins of ‘inorganic ion transport and metabolism’ and ‘hypothetical proteins’. In addition, genes involved in protein biogenesis, including molecular chaperone GrpE (heat shock protein), signal peptidase I, thioredoxin genes and oxidative damage repair enzyme (NTP pyrophosphohydrolase) gene and nucleic acid binding protein gene were up-regulated (Table 3.17). The Hsp70 (DnaK, DnaJ, GrpE) system acts early in protein biogenesis to avoid aggregation of nascent polypeptides during translation or immediately thereafter. Our results indicated that genes encoding GroEL/ES ( $\alpha$  and  $\beta$  thermosome) subunits were not responsive to heat-shock after 60 min of heat-shock treatment at 65°C. This result may suggest that a mechanism based on Hsp70 played important role in heat stress response in *T. volcanium* under experimental condition. Microarray analysis revealed 1.5 fold or greater changes in probe intensity for 9 genes at 99% confidence for the transcripts from heat-shocked samples.

**Table 3.17 Differentially expressed genes of *Tpv* cells under heat shock.**

COG category / Gene	Log <sub>2</sub> Heat-shock ratio
<b>Amino acid transport and metabolism</b>	
<i>TVN0496</i> aspartate aminotransferase	-1,371
<i>TVN1423</i> amino acid transporter	1,308
<i>TVN0939</i> amino acid transporter	-1,277
<i>TVN0911</i> amino acid transporter	1,247
<i>TVN1492</i> glutamine synthetase	-1,226
<i>TVN0715</i> threonine efflux protein	1,222
<b>Carbohydrate transport and metabolism</b>	
<i>TVN0685</i> Beta-galactosidase	-1,456
<i>TVN1145</i> sugar permease	1,447
<i>TVN0436</i> major facilitator superfamily permease	-1,374
<i>TVN1144</i> ABC-type sugar transporter, permease component	1,301
<i>TVN1143</i> sugar-binding protein	1,288
<i>TVN0894</i> sugar transport permease	1,268
<i>TVN0219</i> multidrug efflux permease	1,256
<i>TVN0138</i> multidrug efflux permease	1,223
<i>TVN0666</i> putative transaldolase	-1,223
<i>TVN0668</i> transketolase	-1,218
<b>Lipid transport and metabolism</b>	
<i>TVN0130</i> hypothetical protein	-1,428
<i>TVN0131</i> acetyl-CoA acetyltransferase	-1,339
<i>TVN0122</i> Acyl-coenzyme A synthetase	1,250
<i>TVN1150</i> Acyl-coenzyme A synthetase	1,245
<i>TVN1301</i> hypothetical protein	1,212
<b>Intracellular trafficking and secretion</b>	
<i>TVN0348</i> preprotein translocase SecY	-1,367
<i>TVN0319</i> preprotein translocase subunit SecE	1,234
<i>TVN0065</i> MarC family integral membrane protein	1,219
<i>TVN0221</i> Signal peptidase I	1,207
<b>Cell motility</b>	
<i>TVN1426</i> flagellin	1,286
<i>TVN0609</i> flagellar protein E	-1,225
<b>Posttranslational modification, protein turnover, chaperones</b>	
<i>TVN0663</i> proteasome protease subunit beta	-1,215
<i>TVN0304</i> proteasome subunit alpha	1,116
<i>TVN0487</i> chaperone protein DnaJ	1,027
<i>TVN0488</i> molecular chaperone DnaK	1,131
<i>TVN0489</i> molecular chaperone GrpE (heat shock protein)	1,236
<i>TVN0202</i> glutaredoxin	-1,282
<i>TVN0418</i> putative deoxyhypusine synthase	1,264
<i>TVN0777</i> thioredoxin	1,245
<i>TVN0304</i> proteasome subunit alpha	-1,243
<i>TVN0710</i> hypothetical protein	1,228
<i>TVN1128</i> chaperonin GroEL	1,051
<i>TVN0507</i> chaperonin GroEL	1,072
<i>TVN0531</i> prefoldin subunit alpha	-1,274
<i>TVN1213</i> prefoldin subunit beta	-1,203

**Table 3.17 (continued).**

COG category / Gene	Log <sub>2</sub> Heat-shock ratio
<b>Posttranslational modification, protein turnover, chaperones <i>cont.</i></b>	
<i>TVN0382</i> ATPase of the AAA+ class involved in cell division	1,048
<i>TVN0947</i> ATPase of the AAA+ class involved in cell division	1,044
<i>TVN1401</i> stress induced protein	-1,098
<i>TVN0984</i> molecular chaperone (sHsp, hsp20- related)	-1,563
<i>TVN1011</i> heat shock protein HtpX	1,209
<i>TVN0775</i> molecular chaperone (sHsp, hsp20- related)	1,046
<b>Replication, recombination and repair</b>	
<i>TVN1236</i> single-stranded DNA-binding protein	-1,895
<i>TVN1413</i> adenine-specific DNA methylase	-1,422
<i>TVN0110</i> hypothetical protein	-1,333
<i>TVN0842</i> transposase	-1,332
<i>TVN1464</i> adenine specific DNA methylase	-1,284
<i>TVN0843</i> hypothetical protein	-1,278
<i>TVN0781</i> bifunctional methylated DNA-protein cysteine methyltransferase/deoxyinosine 3'endonuclease	1,274
<i>TVN0160</i> nucleoid DNA-binding protein (HB-related)	-1,265
<i>TVN1209</i> single-stranded DNA-specific exonuclease	-1,250
<i>TVN0693</i> hypothetical protein	-1,239
<i>TVN0114</i> hypothetical protein	1,208
<b>Signal transduction mechanism</b>	
<i>TVN0646</i> nucleotide-binding protein (UspA-related)	-1,241
<b>Multifunctional</b>	
<i>TVN0994</i> ferredoxin subunit of tungsten formylmethanofuran dehydrogenase	-1,532
<i>TVN1377</i> hypothetical protein	-1,318
<i>TVN1197</i> benzoylformate decarboxylase	1,293
<i>TVN0802</i> carbamoyl phosphate synthase small subunit	-1,255
<i>TVN0758</i> cell division control protein 6	-1,247
<b>General function prediction only</b>	
<i>TVN0769</i> acetyltransferase	-1,621
<i>TVN0166</i> ABC transporter permease	-1,505
<i>TVN0410</i> hypothetical protein	-1,354
<i>TVN0932</i> Fe-S oxidoreductase	-1,275
<i>TVN0280</i> phosphoglycolate phosphatase	1,273
<i>TVN0120</i> hypothetical protein	1,255
<i>TVN1376</i> solute-binding protein	-1,254
<i>TVN0816</i> NAD(FAD)-dependent dehydrogenase	-1,252
<i>TVN0008</i> hypothetical protein	-1,225
<i>TVN1496</i> DMT family permease	1,223
<i>TVN0851</i> nucleic acid-binding protein	1,217
<i>TVN0132</i> nucleic-acid-binding protein	-1,211
<i>TVN1096</i> ATPase	1,210
<i>TVN0798</i> Zn-dependent protease	-1,205
<b>Energy production and conversion</b>	
<i>TVN0993</i> geranylgeranyl reductase	-1,520
<i>TVN0768</i> malate oxidoreductase (malic enzyme)	-1,407

**Table 3.17 (continued).**

COG category / Gene	Log <sub>2</sub> Heat-shock ratio
<b>Energy production and conversion cont.</b>	
<i>TVN1395</i> Fe-S oxidoreductase	-1,340
<i>TVN0119</i> ferredoxin	-1,320
<i>TVN1313</i> Fe-S oxidoreductase	-1,238
<i>TVN1279</i> ferredoxin-like protein	1,229
<i>TVN0840</i> glycerol-3-phosphate dehydrogenase	-1,229
<i>TVN1378</i> Fe-S oxidoreductase	-1,224
<i>TVN0049</i> V-type ATP synthase subunit E	-1,223
<i>TVN0506</i> tRNA-modifying enzyme	-1,206
<b>Cell cycle control, mitosis and meiosis</b>	
<i>TVN0027</i> Cell division protein FtsZ	-1,232
<b>Cell wall/membrane biogenesis</b>	
<i>TVN0876</i> Cell wall biosynthesis glycoyltransferase	1,343
<b>Coenzyme transport and metabolism</b>	
<i>TVN0918</i> Precorrin-2 methylase	-1,203
<b>Defense mechanism</b>	
<i>TVN0165</i> ATP-type multidrug transport system, ATPase component	-1,291
<b>Inorganic ion transport and metabolism</b>	
<i>TVN0061</i> superoxide dismutase	-1,338
<i>TVN1365</i> major facilitator superfamily permease	1,314
<i>TVN0285</i> arsenite transport permease	1,305
<i>TVN0404</i> Ca <sup>2+</sup> /Na <sup>+</sup> antiporter	1,278
<i>TVN0063</i> phosphate permease	1,256
<i>TVN1056</i> arsenite transporting ATPase	-1,170
<b>Nucleotide transport and metabolism</b>	
<i>TVN0452</i> nucleoside diphosphate kinase	-1,277
<i>TVN1166</i> secreted endonuclease distantly related to Holliday junction resolvase	1,230
<i>TVN0268</i> phosphoribosylformylglycinamide synthase I	-1,225
<i>TVN0033</i> CTP synthetase	-1,222
<i>TVN0349</i> adenylate kinase	-1,218
<i>TVN1258</i> NTP pyrophosphohydrolase (mutT-related oxidative damage repair enzyme)	1,200
<b>Transcription</b>	
<i>TVN0295</i> transcription regulator	-1,590
<i>TVN1137</i> DNA-directed RNA polymerase subunit N	-1,314
<i>TVN0356</i> small nuclear ribonucleoprotein	-1,305
<i>TVN1188</i> transcription regulator	-1,281
<i>TVN1089</i> transcription initiation factor IIB	-1,276
<i>TVN1179</i> transcription elongation factor NusA-like protein	-1,270
<i>TVN1437</i> RNA-binding protein snRNP	-1,264
<i>TVN1075</i> small nuclear ribonucleoprotein (snRNP)-like protein	-1,255
<i>TVN1443</i> transcription antitermination protein NusG	-1,254
<b>Translation</b>	
<i>TVN0010</i> 50S ribosomal protein L31e	-1,782
<i>TVN0009</i> 50S ribosomal protein L39e	-1,654
<i>TVN1077</i> exosome complex RNA-binding protein Csl4	-1,496
<i>TVN1135</i> 50S ribosomal protein L13P	-1,456

**Table 3.17 (continued).**

COG category / Gene	Log <sub>2</sub> Heat-shock ratio
<b>Translation cont.</b>	
<i>TVN1208</i> 30S ribosomal protein S15P	-1,432
<i>TVN1136</i> 30S ribosomal protein S9P	-1,414
<i>TVN0412</i> translation initiation factor IF-2 subunit alpha	-1,405
<i>TVN0411</i> H/ACA RNA-protein complex component Nop10p	-1,377
<i>TVN0007</i> 30S ribosomal protein S19e	-1,367
<i>TVN0414</i> 50S ribosomal protein L44e	-1,347
<i>TVN0346</i> 50S ribosomal protein L30P	-1,317
<i>TVN0420</i> 50S ribosomal protein L12P	-1,312
<i>TVN0340</i> 30S ribosomal protein S8P	-1,278
<i>TVN0347</i> 50S ribosomal protein L15P	-1,275
<i>TVN0355</i> 50S ribosomal protein L37e	-1,265
<i>TVN0647</i> 30S ribosomal protein S17e	-1,248
<i>TVN0399</i> 30S ribosomal protein S2	-1,241
<i>TVN0563</i> 30S ribosomal protein S4P	-1,248
<i>TVN0337</i> 30S ribosomal protein S4e	-1,148
<i>TVN0342</i> 50S ribosomal protein L32e	-1,239
<i>TVN0437</i> RNA processing exonuclease	-1,221
<i>TVN0332</i> translation initiation factor Sui1	-1,219
<i>TVN1388</i> glycyl-tRNA synthetase	-1,210
<i>TVN0066</i> 2'-5' RNA ligase	1,209
<i>TVN0307</i> exosome complex exonuclease Rrp41	-1,206

### 3.5.3.2 pH Stress

*Thermoplasma volcanium* is a thermoacidophilic archaeon which normally grows in the pH range 2.0-2.7, aerobically. In the microarray study we addressed the question of what proteins are induced at the acidic limit for growth (pH 4.0). The transcriptional response to acidic external pH above the optimum pH, was evaluated by microarray at 60 min post exposure to pH stress. The full list of genes each showed an expression ratio of at least 1.2-fold ( $\log_2=0.3$ ) is presented in the Table 3.19. Our results show that genes out of 282 ORFs were differentially expressed at pH 4.0 and most of these genes were down-regulated (56%) (Table 3.18). The volcano plot identifying genes which are transcribed significantly different between control and pH stressed *Tpv* cells are shown in the Figure 3.40. The scatter plot of the genes is given in Figure 3.41.

**Table 3.18 Number of genes differentially expressed in total of 1501 genes under pH stress.** They have represented as up and down regulated genes in comparison mode to control.

FOLD CHANGE	pH STRESS (pH 4.0)		TOTAL
	UP	DOWN	
<b>1.2-fold</b>	125	157	282
<b>1.5-fold</b>	—	15	15

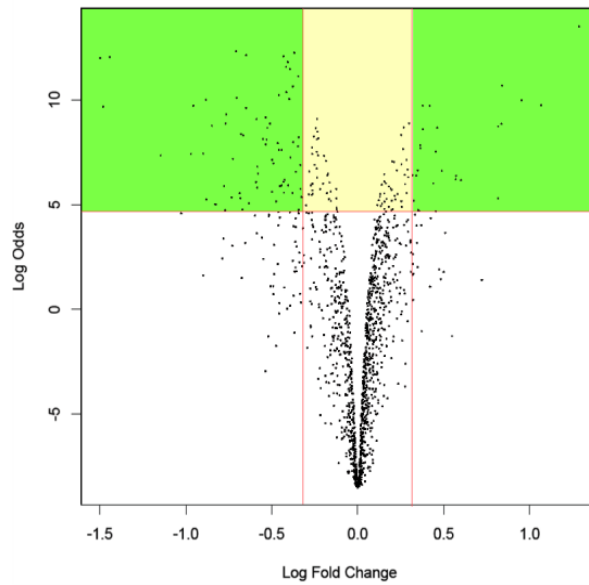


**Figure 3.40** The volcano plot for the pH stress dataset in comparison to control. Under the filter of log-fold change  $\geq 0.3$  or  $\leq -0.3$  and logOdds  $\geq 4.6$ , genes are located in the upper left corner of plot are significantly down-regulated, while in the upper right corner are significantly up-regulated.

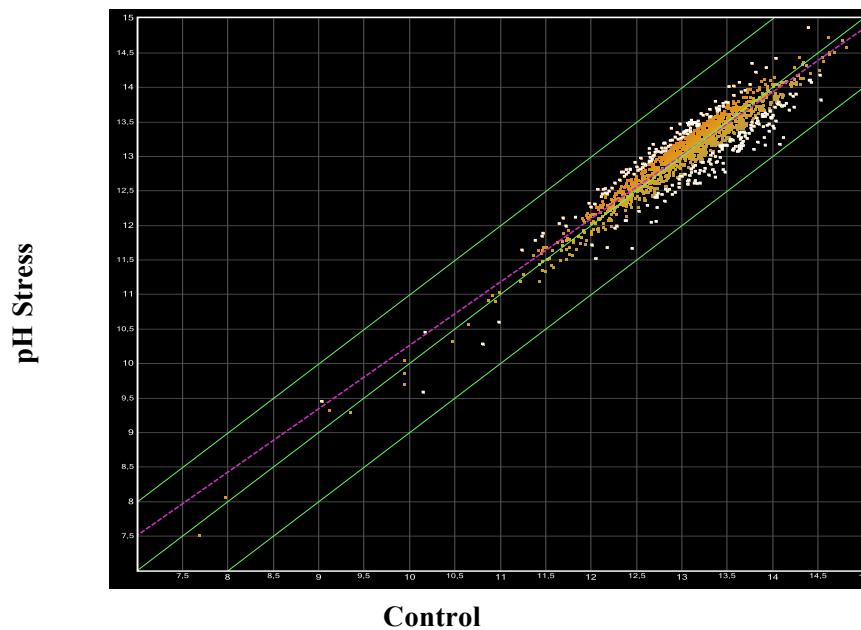


**Figure 3.41** Scatter plot of average probe intensity (Log2) for Roche NimbleGen microarray chips hybridized with cDNA from pH stress induced cultures versus control of *Tpv* cells. Probes corresponding to genes up-regulated and down regulated to 1.2 fold are plotted in white. Linear regression is indicated in magenta ( $R^2=0.9041$ ): green lines indicate threshold of fold change  $>2$ .

**Table 3.19 Differentially expressed genes of *Tpv* cells under pH stress.**

COG category / Gene	Log <sub>2</sub> pH ratio
<b>Amino acid transport and metabolism</b>	
<i>TVN0939</i> amino acid transporter	-1,489
<i>TVN1036</i> amino acid transporter	1,397
<i>TVN0759</i> glutamate dehydrogenase	-1,340
<i>TVN1238</i> amino acid transporter	1,335
<i>TVN0439</i> asparagine synthase	1,315
<i>TVN0911</i> amino acid transporter	1,298
<i>TVN1262</i> amino acid transporter	1,288
<i>TVN1423</i> amino acid transporter	1,269
<i>TVN0071</i> threonine synthase	-1,262
<i>TVN0496</i> aspartate aminotransferase	-1,261
<i>TVN1336</i> aspartate ammonia-lyase	-1,246
<b>Carbohydrate transport and metabolism</b>	
<i>TVN1145</i> sugar permease	1,444
<i>TVN0894</i> sugar transport permease	1,353
<i>TVN0219</i> multidrug efflux permease	1,347
<i>TVN0685</i> transcription regulator	-1,342
<i>TVN0138</i> multidrug efflux permease	1,327
<i>TVN1143</i> sugar-binding protein	1,308
<i>TVN0524</i> multidrug efflux permease	1,296
<i>TVN0907</i> major facilitator superfamily permease	1,277
<i>TVN1263</i> multidrug efflux permease	1,271
<i>TVN1425</i> multidrug efflux permease	1,263
<i>TVN1060</i> major facilitator superfamily permease	1,260
<i>TVN0594</i> major facilitator superfamily permease	1,258
<i>TVN0176</i> major facilitator superfamily permease	1,235
<i>TVN1163</i> multidrug efflux permease	1,234
<i>TVN0436</i> major facilitator superfamily permease	-1,229
<i>TVN1158</i> cofactor-independent phosphoglycerate mutase	1,212
<i>TVN1043</i> major facilitator superfamily permease	1,207
<b>Lipid transport and metabolism</b>	
<i>TVN1150</i> Acyl-coenzyme A synthetase	1,356
<i>TVN1269</i> isovaleryl-CoA dehydrogenase	1,353
<i>TVN0122</i> Acyl-coenzyme A synthetase	1,298
<i>TVN0131</i> acetyl-CoA acetyltransferase	-1,297
<i>TVN1260</i> acetyl-CoA acetyltransferase	1,294
<i>TVN1268</i> Acyl-coenzyme A synthetase	1,238
<i>TVN0130</i> hypothetical protein	-1,226
<b>Intracellular trafficking and secretion</b>	
<i>TVN0371</i> Sec-independent protein secretion pathway component	-1,374
<i>TVN0065</i> MarC family integral membrane protein	1,277
<i>TVN1444</i> protein translocase subunit Sss1	-1,229
<i>TVN0221</i> Signal peptidase I	1,216
<i>TVN0348</i> preprotein translocase SecY	-1,206
<b>Cell motility</b>	
<i>TVN1426</i> flagellin	1,363
<i>TVN0608</i> flagellar protein C	-1,273
<i>TVN0609</i> flagellar protein E	-1,234

**Table 3.19 (continued).**

COG category / Gene	Log <sub>2</sub> pH ratio
<b>Coenzyme transport and metabolism</b>	
<i>TVN1270</i> molybdopterin-guanine dinucleotide biosynthesis protein	1,343
<i>TVN0918</i> precorrin-2 methylase	-1,309
<i>TVN0495</i> cobalamin synthase	-1,216
<i>TVN1428</i> GTP:adenosylcobinamide-phosphate guanylyltransferase	1,214
<b>Cell wall/membrane biogenesis</b>	
<i>TVN0876</i> cell wall biosynthesis glycosyltransferase	1,348
<b>Energy production and conversion</b>	
<i>TVN1279</i> ferredoxin-like protein	-1,572
<i>TVN1280</i> electron transfer flavoprotein subunit beta	-1,509
<i>TVN0083</i> cytochrome bd-type quinol oxidase, subunit 1	-1,507
<i>TVN1115</i> NADH dehydrogenase subunit B	-1,457
<i>TVN1278</i> dehydrogenase (flavoprotein)	-1,446
<i>TVN0846</i> 2-oxoacid--ferredoxin oxidoreductase, alpha subunit	-1,428
<i>TVN1116</i> NADH dehydrogenase subunit A	-1,419
<i>TVN0847</i> 2-oxoglutarate ferredoxin oxidoreductase subunit beta	-1,412
<i>TVN1109</i> NADH dehydrogenase subunit J	-1,398
<i>TVN0768</i> malate oxidoreductase (malic enzyme)	-1,383
<i>TVN1334</i> 2-oxoacid ferredoxin oxidoreductase subunit beta	-1,351
<i>TVN1114</i> NADH dehydrogenase subunit C	-1,338
<i>TVN1335</i> 2-oxoacid--ferredoxin oxidoreductase, alpha subunit	-1,330
<i>TVN1281</i> electron transfer flavoprotein subunit alpha	-1,325
<i>TVN0119</i> ferredoxin	-1,295
<i>TVN0049</i> V-type ATP synthase subunit E	-1,293
<i>TVN1111</i> NADH dehydrogenase subunit I	-1,263
<i>TVN1108</i> NADH dehydrogenase subunit K	-1,258
<i>TVN1113</i> NADH dehydrogenase subunit D	-1,238
<i>TVN0052</i> V-type ATP synthase subunit A	-1,231
<i>TVN1104</i> NADH dehydrogenase subunit N	-1,231
<i>TVN1457</i> Ni,Fe-hydrogenase III small subunit	1,224
<i>TVN0245</i> hypothetical protein	1,223
<i>TVN0576</i> indolepyruvate oxidoreductase subunit beta	1,217
<i>TVN1110</i> NADH dehydrogenase subunit J	-1,216
<i>TVN1284</i> alcohol dehydrogenase IV	1,206
<b>Nucleotide transport and metabolism</b>	
<i>TVN0371</i> nucleoside diphosphate kinase	-1,374
<i>TVN0065</i> phosphoribosylcarboxyaminoimidazole carboxylase catalytic subunit	1,277
<i>TVN1444</i> phosphoribosylformylglycinamide synthase I	-1,229
<i>TVN0221</i> secreted endonuclease distantly related to Holliday junction resolvase	1,216
<i>TVN0348</i> NTP pyrophosphohydrolase (mutT-related oxidative damage repair enzyme)	-1,206
<b>Inorganic ion transport and metabolism</b>	
<i>TVN1240</i> cation transport ATPase	-1,502
<i>TVN1048</i> ABC-type Fe <sup>3+</sup> -siderophores transporter, solute-binding component	1,320
<i>TVN0404</i> Ca <sup>2+</sup> /Na <sup>+</sup> antiporter	1,285

**Table 3.19 (continued).**

COG category / Gene	Log <sub>2</sub> pH ratio
<b>Inorganic ion transport and metabolism <i>cont.</i></b>	
<i>TVN0063</i> phosphate permease	1,275
<i>TVN0285</i> arsenite transport permease	1,275
<i>TVN1365</i> major facilitator superfamily permease	1,272
<i>TVN0292</i> Fe <sup>2+</sup> uptake regulation protein	-1,216
<i>TVN1056</i> Arsenite transporting ATPase	-1,197
<b>Posttranslational modification, protein turnover, chaperones</b>	
<i>TVN1248</i> transcription regulator	-1,797
<i>TVN0984</i> molecular chaperone (small heat shock protein, hsp20-related)	-1,642
<i>TVN1391</i> Iron-regulated ABC transporter ATPase subunit	1,443
<i>TVN1390</i> membrane component of an uncharacterized iron-regulated ABC-type transporter	1,414
<i>TVN0710</i> hypothetical protein	1,350
<i>TVN0489</i> molecular chaperone GrpE (heat shock protein)	-1,403
<i>TVN1389</i> membrane component of an uncharacterized iron-regulated ABC-type transporter	1,296
<i>TVN0488</i> molecular chaperone DnaK	-1,261
<i>TVN0487</i> chaperone protein DnaJ	-1,187
<i>TVN0507</i> chaperonin GroEL	-1,187
<i>TVN1128</i> Chaperonin GroEL	-1,230
<i>TVN0418</i> putative deoxyhypusine synthase	1,262
<i>TVN0531</i> prefoldin subunit alpha	-1,152
<i>TVN0663</i> proteasome protease subunit beta	-1,185
<i>TVN0304</i> proteasome subunit alpha	1,107
<i>TVN1213</i> prefoldin subunit beta	-1,241
<i>TVN1128</i> chaperonin GroEL	-1,223
<i>TVN0492</i> membrane-bound serine protease	1,212
<i>TVN0775</i> molecular chaperone (sHsp, hsp-20 related)	1,077
<i>TVN1011</i> Heat shock protein HtpX	1,189
<i>TVN1401</i> stress-induced protein	-1,031
<i>TVN0947</i> ATPase of the AAA+ class involved in cell division	1,052
<i>TVN0382</i> ATPase of the AAA+ class involved in cell division	1,026
<b>Replication, recombination and repair</b>	
<i>TVN1236</i> single-stranded DNA-binding protein	-1,675
<i>TVN0109</i> hypothetical protein	-1,410
<i>TVN0110</i> hypothetical protein	-1,394
<i>TVN1413</i> adenine-specific DNA methylase	-1,374
<i>TVN0263</i> integrase/recombinase	1,353
<i>TVN1409</i> IS5 inactivated transposase	1,333
<i>TVN0781</i> bifunctional methylated DNA-protein cysteine methyltransferase/deoxyinosine 3'endonuclease	1,305
<i>TVN1464</i> adenine specific DNA methylase	-1,209
<i>TVN0739</i> DNA helicase II	-1,204
<i>TVN1209</i> single-stranded DNA-specific exonuclease	-1,200
<b>Signal transduction mechanism</b>	
<i>TVN0646</i> nucleotide-binding protein (UspA-related)	-1,418
<i>TVN0820</i> GAF domain-containing protein	1,287
<i>TVN0662</i> CBS domain-containing protein	-1,225

**Table 3.19 (continued).**

COG category / Gene	Log <sub>2</sub> pH ratio
<b>Multifunctional</b>	
<i>TVN1198</i> 2-hydroxyacid dehydrogenase	1,315
<i>TVN1377</i> hypothetical protein	-1,310
<i>TVN1197</i> benzoylformate decarboxylase	1,300
<i>TVN1300</i> Na <sup>+</sup> /panthothenate symporter permease	1,292
<i>TVN1059</i> 3-oxoacyl-[acyl-carrier-protein] reductase	1,281
<i>TVN0303</i> phosphate ABC transporter permease	1,276
<i>TVN1357</i> imidazolonepropionase	1,214
<i>TVN0402</i> transcription regulator	-1,209
<b>General function prediction only</b>	
<i>TVN1432</i> NAD(FAD)-dependent dehydrogenase	-1,861
<i>TVN0769</i> acetyltransferase	-1,570
<i>TVN0410</i> hypothetical protein	-1,429
<i>TVN0505</i> nucleoside-diphosphate sugar epimerase	1,412
<i>TVN0008</i> hypothetical protein	-1,358
<i>TVN0120</i> hypothetical protein	1,334
<i>TVN1212</i> hypothetical protein	-1,331
<i>TVN0743</i> CoA-binding protein	1,319
<i>TVN0112</i> HD superfamily hydrolase	-1,311
<i>TVN0652</i> hypothetical protein	-1,283
<i>TVN0068</i> nucleic-acid-binding protein	1,282
<i>TVN0719</i> hypothetical protein	1,274
<i>TVN1259</i> nucleic-acid-binding protein	1,268
<i>TVN0914</i> metal-dependent hydrolase	1,258
<i>TVN1074</i> methyltransferase	1,256
<i>TVN0115</i> hypothetical protein	1,254
<i>TVN0851</i> nucleic acid-binding protein	1,248
<i>TVN0645</i> helicase (Lhr-related)	-1,245
<i>TVN0243</i> hypothetical protein	1,237
<i>TVN1481</i> ATPase	1,224
<i>TVN0858</i> metal-dependent hydrolase	1,216
<i>TVN0215</i> hypothetical protein	1,200
<b>Transcription</b>	
<i>TVN0983</i> transcription regulator	-1,559
<i>TVN0295</i> transcription regulator	-1,449
<i>TVN1137</i> DNA-directed RNA polymerase subunit N	-1,369
<i>TVN1075</i> small nuclear ribonucleoprotein (snRNP)-like protein	-1,329
<i>TVN1337</i> transcription regulator	-1,307
<i>TVN1089</i> transcription initiation factor IIB	-1,295
<i>TVN0356</i> small nuclear ribonucleoprotein	-1,280
<i>TVN1437</i> RNA-binding protein snRNP	-1,270
<i>TVN1179</i> transcription elongation factor NusA-like protein	-1,266
<i>TVN1435</i> DNA-directed RNA polymerase subunit L	-1,236
<i>TVN1408</i> transcription regulator	-1,222
<i>TVN0565</i> DNA-directed RNA polymerase subunit D	-1,216
<i>TVN0983</i> transcription regulator	-1,559
<i>TVN0295</i> transcription regulator	-1,449

**Table 3.19 (continued).**

COG category / Gene	Log <sub>2</sub> pH ratio
<b>Translation</b>	
<i>TVN0010</i> 50S ribosomal protein L31e	-1,770
<i>TVN0412</i> translation initiation factor IF-2 subunit alpha	-1,608
<i>TVN1208</i> 30S ribosomal protein S15P	-1,492
<i>TVN0411</i> H/ACA RNA-protein complex component Nop10p	-1,488
<i>TVN1136</i> 30S ribosomal protein S9P	-1,470
<i>TVN0563</i> 30S ribosomal protein S4P	-1,255
<i>TVN0325</i> 50S ribosomal protein L4P	-1,464
<i>TVN0340</i> 30S ribosomal protein S8P	-1,464
<i>TVN0420</i> 50S ribosomal protein L12P	-1,464
<i>TVN0346</i> 50S ribosomal protein L30P	-1,462
<i>TVN1135</i> 50S ribosomal protein L13P	-1,441
<i>TVN0326</i> 50S ribosomal protein L23P	-1,420
<i>TVN0414</i> 50S ribosomal protein L44e	-1,410
<i>TVN0337</i> 30S ribosomal protein S4e	-1,222
<i>TVN0338</i> 50S ribosomal protein L5P	-1,405
<i>TVN0009</i> 50S ribosomal protein L39e	-1,398
<i>TVN0647</i> 30S ribosomal protein S17e	-1,394
<i>TVN0328</i> 30S ribosomal protein S19P	-1,387
<i>TVN0332</i> translation initiation factor Sui1	-1,383
<i>TVN0339</i> 30S ribosomal protein S14P	-1,383
<i>TVN0347</i> 50S ribosomal protein L15P	-1,381
<i>TVN0355</i> 50S ribosomal protein L37e	-1,375
<i>TVN1077</i> exosome complex RNA-binding protein Csl4	-1,362
<i>TVN0342</i> 50S ribosomal protein L32e	-1,342
<i>TVN0829</i> isoleucyl-tRNA synthetase	-1,334
<i>TVN0343</i> 50S ribosomal protein L19e	-1,331
<i>TVN0564</i> 30S ribosomal protein S11P	-1,330
<i>TVN0353</i> Nop56p-related protein (ribosomal biogenesis)	1,328
<i>TVN0007</i> 30S ribosomal protein S19e	-1,321
<i>TVN0066</i> 2'-5' RNA ligase	1,301
<i>TVN0329</i> 50S ribosomal protein L22P	-1,288
<i>TVN0423</i> 50S ribosomal protein L11P	-1,282
<i>TVN0399</i> 30S ribosomal protein S2	-1,274
<i>TVN1275</i> 30S ribosomal protein S6e	-1,274
<i>TVN0341</i> 50S ribosomal protein L6P	-1,267
<i>TVN0330</i> 30S ribosomal protein S3P	-1,265
<i>TVN0451</i> 50S ribosomal protein L24e	-1,262
<i>TVN0334</i> 30S ribosomal protein S17P	-1,256
<i>TVN1274</i> translation initiation factor IF-2 subunit gamma	-1,256
<i>TVN0413</i> 30S ribosomal protein S27e	-1,255
<i>TVN0563</i> 30S ribosomal protein S4P	-1,255
<i>TVN0336</i> 50S ribosomal protein L24P	-1,252
<i>TVN1134</i> 50S ribosomal protein L18e	-1,247
<i>TVN0267</i> 50S ribosomal protein L40e	-1,246
<i>TVN0324</i> 50S ribosomal protein L3P	-1,244
<i>TVN0270</i> RNA methylase	1,232
<i>TVN0333</i> ribonuclease P protein component 1	-1,231
<i>TVN0331</i> 50S ribosomal protein L29P	-1,226
<i>TVN0337</i> 30S ribosomal protein S4e	-1,222
<i>TVN0449</i> 50S ribosomal protein L7Ae	-1,214

The genes most strongly regulated by pH are summarized in the Table 3.19. These genes showed 1.2-fold or greater changes in probe intensity at 99%. The major functional categories for genes of particular interest in this group are; post translational modification, protein turnover, chaperones, energy production and conversion, translation, carbohydrate transport and metabolism, inorganic ion and amino acid transport and metabolism. ‘Extracellular’ pH exposure mainly leads to the functions that take place in the membrane. Therefore, it is not surprising that several membrane proteins mainly various transport proteins showed pH dependant expression.

Membrane bound systems for proton and electron transport were also regulated by change in the external pH e.g. NAD(FAD)-dependant dehydrogenase, electron transfer flavoprotein, ferredoxin oxidoreductases, cytochrome quinol oxidase which export H<sup>+</sup> were down-regulated.

### 3.5.3.3 Oxidative Stress

The H<sub>2</sub>O<sub>2</sub> induced (0.02 mM) oxidative stress response at transcriptional level for 60 min was investigated in *T. volcanium* by microarray. The results showed that a total of 277 genes were differentially regulated by oxidative stress that showed a fold difference ≥1.2 fold (Table 3.20). Among the genes responsive to H<sub>2</sub>O<sub>2</sub>, 153 genes were down-regulated and 124 genes were up-regulated. The volcano plot and scatter plot showing genes that were considered as differentially expressed are given in Figures 3.42 and 3.43.

**Table 3.20 Number of genes differentially expressed in total of 1501 genes under oxidative stress.** They have represented as up and down regulated genes in comparison mode to control.

FOLD CHANGE	OXIDATIVE STRESS (0.02 mM)		TOTAL
	UP	DOWN	
<b>1.2-fold</b>	124	153	277
<b>1.5-fold</b>	3	19	22

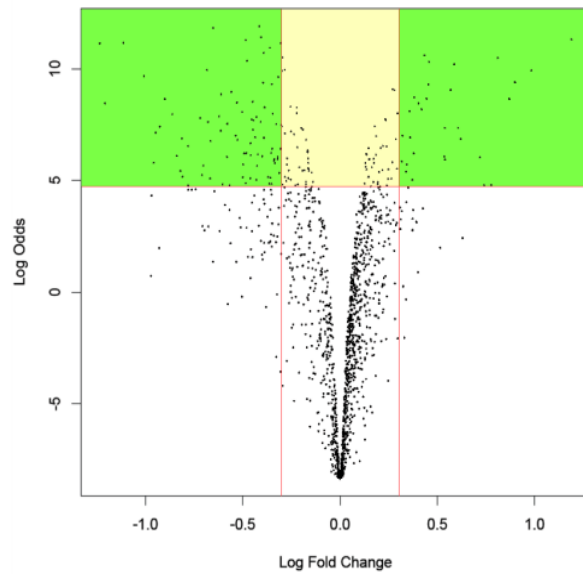


**Figure 3.42** The volcano plot for the oxidative stress dataset in comparison to control. Under the filter of log-fold change  $\geq 0.3$  or  $\leq -0.3$  and logOdds  $\geq 4.6$ , genes are located in the upper left corner of plot are significantly down-regulated, while in the upper right corner are significantly up-regulated.

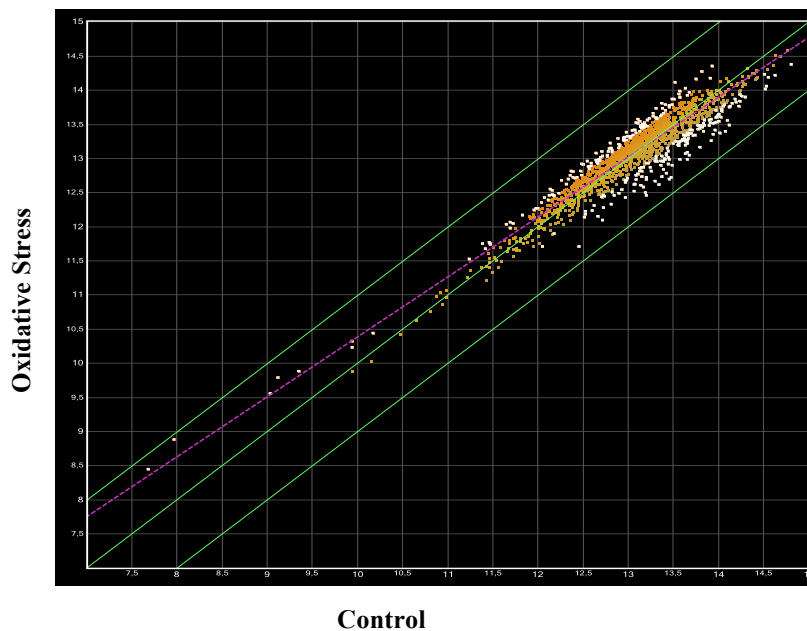


**Figure 3.43** Scatter plots of average probe intensity (Log<sub>2</sub>) for Roche NimbleGen microarray chips hybridized with cDNA from oxidative stress induced cultures versus control of *Tpv* cells. Probes corresponding to genes up-regulated and down regulated to 1.2 fold are plotted in white. Linear regression is indicated in magenta ( $R^2=0.901$ ); green lines indicate threshold of fold change  $>2$ .

**Table 3.21 Differentially expressed genes of *Tpv* cells under oxidative stress.**

COG category / Gene	Log <sub>2</sub> Oxidative ratio
<b>Amino acid transport and metabolism</b>	
<i>TVN0071</i> threonine synthase	-1,397
<i>TVN0496</i> aspartate aminotransferase	-1,353
<i>TVN1332</i> ABC-type peptide transport system, solute-binding component	-1,336
<i>TVN1423</i> amino acid transporter	1,304
<i>TVN0911</i> amino acid transporter	1,303
<i>TVN0759</i> glutamate dehydrogenase	-1,278
<i>TVN1262</i> amino acid transporter	1,273
<i>TVN0439</i> asparagine synthase	1,235
<i>TVN1036</i> amino acid transporter	1,227
<i>TVN1025</i> N-(5'-phosphoribosyl)anthranilate isomerase	1,218
<i>TVN0800</i> aminopeptidase N	-1,205
<b>Carbohydrate transport and metabolism</b>	
<i>TVN1145</i> sugar permease	1,528
<i>TVN0685</i> transcription regulator	-1,456
<i>TVN0138</i> multidrug efflux permease	1,395
<i>TVN0219</i> multidrug efflux permease	1,364
<i>TVN1143</i> sugar-binding protein	1,357
<i>TVN0894</i> sugar transport permease	1,338
<i>TVN1425</i> multidrug efflux permease	1,294
<i>TVN1060</i> major facilitator superfamily permease	1,282
<i>TVN0907</i> major facilitator superfamily permease	1,276
<i>TVN0436</i> major facilitator superfamily permease	-1,276
<i>TVN1144</i> ABC-type sugar transporter, permease component	1,272
<i>TVN0594</i> major facilitator superfamily permease	1,269
<i>TVN0524</i> multidrug efflux permease	1,249
<i>TVN1263</i> multidrug efflux permease	1,235
<i>TVN0250</i> major facilitator superfamily permease	1,234
<i>TVN0176</i> major facilitator superfamily permease	1,230
<i>TVN0485</i> DNA-directed RNA polymerase subunit E"	-1,208
<b>Lipid transport and metabolism</b>	
<i>TVN1269</i> isovaleryl-CoA dehydrogenase	1,346
<i>TVN1150</i> Acyl-coenzyme A synthetase	1,303
<i>TVN0131</i> acetyl-CoA acetyltransferase	-1,265
<i>TVN0122</i> Acyl-coenzyme A synthetase	1,246
<i>TVN1305</i> Acyl-CoA dehydrogenase	-1,237
<i>TVN0772</i> methylmalonyl-CoA mutase, alpha subunit	-1,235
<i>TVN1268</i> Acyl-coenzyme A synthetase	1,230
<i>TVN0130</i> hypothetical protein	-1,219
<i>TVN0782</i> mevalonate pyrophosphate decarboxylase	1,218
<b>Cell cycle control, mitosis and meiosis</b>	
<i>TVN0027</i> Cell division protein FtsZ	-1,200
<b>Cell motility</b>	
<i>TVN1426</i> flagellin	1,407
<i>TVN0609</i> flagellar protein E	-1,484
<i>TVN0608</i> flagellar protein C	-1,519

**Table 3.21 (continued).**

COG category / Gene	Log <sub>2</sub> Oxidative ratio
<b>Cell wall/membrane biogenesis</b>	
<i>TVN0529</i> dTDP-glucose pyrophosphorylase	1,250
<b>Coenzyme transport and metabolism</b>	
<i>TVN0918</i> precorrin-2 methylase	-1,341
<i>TVN1270</i> molybdopterin-guanine dinucleotide biosynthesis protein	1,331
<i>TVN0924</i> siroheme synthase	-1,309
<i>TVN1428</i> GTP:adenosylcobinamide-phosphate guanylyltransferase	1,255
<i>TVN0923</i> uroporphyrinogen-III methylase	-1,213
<i>TVN1095</i> 6-pyruvoyl-tetrahydropterin synthase	1,200
<b>Intracellular trafficking and secretion</b>	
<i>TVN0371</i> Sec-independent protein secretion pathway component	-1,348
<i>TVN0065</i> MarC family integral membrane protein	1,274
<i>TVN0221</i> Signal peptidase	1,233
<i>TVN0348</i> preprotein translocase SecY	-1,227
<b>Energy production and conversion</b>	
<i>TVN0119</i> ferredoxin	-1,553
<i>TVN0083</i> cytochrome bd-type quinol oxidase, subunit 1	-1,541
<i>TVN1115</i> NADH dehydrogenase subunit B	-1,362
<i>TVN0768</i> malate oxidoreductase (malic enzyme)	-1,344
<i>TVN0273</i> succinyl-CoA synthetase subunit alpha	-1,315
<i>TVN0846</i> 2-oxoacid--ferredoxin oxidoreductase, alpha subunit	-1,314
<i>TVN1383</i> electron transfer flavoprotein subunit beta	-1,298
<i>TVN0993</i> geranylgeranyl reductase	-1,290
<i>TVN1313</i> Fe-S oxidoreductase	-1,288
<i>TVN1114</i> NADH dehydrogenase subunit C	-1,284
<i>TVN1280</i> electron transfer flavoprotein subunit beta	-1,281
<i>TVN1335</i> 2-oxoacid--ferredoxin oxidoreductase, alpha subunit	-1,281
<i>TVN1334</i> 2-oxoacid ferredoxin oxidoreductase subunit beta	-1,278
<i>TVN1279</i> ferredoxin-like protein	-1,275
<i>TVN0049</i> V-type ATP synthase subunit E	-1,271
<i>TVN1281</i> electron transfer flavoprotein subunit alpha	-1,271
<i>TVN0245</i> hypothetical protein	1,264
<i>TVN1109</i> NADH dehydrogenase subunit J	-1,260
<i>TVN0847</i> 2-oxoglutarate ferredoxin oxidoreductase subunit beta	-1,254
<i>TVN0052</i> V-type ATP synthase subunit A	-1,242
<i>TVN0732</i> cytochrome bd-type quinol oxidase, subunit 1	-1,234
<i>TVN1116</i> NADH dehydrogenase subunit A	-1,232
<i>TVN1395</i> Fe-S oxidoreductase	-1,228
<i>TVN0274</i> succinyl-CoA synthetase subunit beta	-1,211
<b>Inorganic ion transport and metabolism</b>	
<i>TVN0404</i> Ca <sup>2+</sup> /Na <sup>+</sup> antiporter	1,373
<i>TVN1240</i> cation transport ATPase	-1,361
<i>TVN0063</i> phosphate permease	1,344
<i>TVN1365</i> major facilitator superfamily permease	1,331
<i>TVN0285</i> arsenite transport permease	1,319
<i>TVN0061</i> superoxide dismutase	-1,280

**Table 3.21 (continued).**

COG category / Gene	Log <sub>2</sub> Oxidative ratio
<b>Inorganic ion transport and metabolism <i>cont.</i></b>	
<i>TVN1048</i> ABC-type Fe <sup>3+</sup> -siderophores transporter, solute-binding component	1,250
<i>TVN0292</i> Fe <sup>2+</sup> uptake regulation protein	-1,208
<i>TVN1056</i> Arsenite transporting ATPase	-1,167
<b>General function prediction only</b>	
<i>TVN1432</i> NAD(FAD)-dependent dehydrogenase	-1,628
<i>TVN0769</i> acetyltransferase	-1,569
<i>TVN0166</i> ABC transporter permease	-1,341
<i>TVN1496</i> DMT family permease	1,336
<i>TVN1212</i> hypothetical protein	-1,306
<i>TVN0427</i> hypothetical protein	1,295
<i>TVN0505</i> nucleoside-diphosphate sugar epimerase	1,279
<i>TVN0120</i> hypothetical protein	1,275
<i>TVN0652</i> hypothetical protein	-1,264
<i>TVN0851</i> nucleic acid-binding protein	1,249
<i>TVN0068</i> nucleic-acid-binding protein	1,248
<i>TVN0914</i> metal-dependent hydrolase	1,228
<i>TVN0798</i> Zn-dependent protease	-1,228
<i>TVN0719</i> hypothetical protein	1,223
<i>TVN0549</i> hypothetical protein	1,218
<b>Multifunctional</b>	
<i>TVN0994</i> ferredoxin subunit of tungsten formylmethanofuran dehydrogenase	-1,454
<i>TVN1197</i> benzoylformate decarboxylase	1,363
<i>TVN0758</i> cell division control protein 6	-1,353
<i>TVN1198</i> 2-hydroxyacid dehydrogenase	1,319
<i>TVN1377</i> hypothetical protein	-1,294
<i>TVN1329</i> ABC-type peptide transport system, ATPase component	-1,288
<i>TVN1357</i> imidazolonepropionase	1,218
<i>TVN1013</i> hypothetical protein	1,212
<b>Nucleotide transport and metabolism</b>	
<i>TVN0452</i> nucleoside diphosphate kinase	-1,293
<i>TVN1258</i> NTP pyrophosphohydrolase (mutT-related oxidative damage repair enzyme)	1,233
<i>TVN1297</i> phosphoribosylcarboxyaminoimidazole carboxylase catalytic subunit	1,215
<b>Posttranslational modification, protein turnover, chaperones</b>	
<i>TVN0984</i> molecular chaperone (small heat shock protein, hsp20-related)	-1,703
<i>TVN1248</i> transcription regulator	-1,534
<i>TVN0489</i> molecular chaperone GrpE (heat shock protein)	-1,335
<i>TVN0710</i> hypothetical protein	1,311
<i>TVN1099</i> putative peroxiredoxin	-1,304
<i>TVN0202</i> glutaredoxin	-1,295
<i>TVN0418</i> putative deoxyhypusine synthase	1,278
<i>TVN1391</i> Iron-regulated ABC transporter ATPase subunit	-1,275

**Table 3.21 (continued).**

COG category / Gene	Log <sub>2</sub> Oxidative ratio
<b>Posttranslational modification, protein turnover, chaperones cont.</b>	
<i>TVN1213</i> prefoldin subunit beta	-1,231
<i>TVN0382</i> ATPase of the AAA+ class involved in cell division	-1,001
<i>TVN0947</i> ATPase of the AAA+ class involved in cell division	-1,042
<i>TVN1401</i> Stress-induced protein	-1,028
<i>TVN0507</i> chaperonin GroEL	-1,194
<i>TVN1128</i> chaperonin GroEL	-1,178
<i>TVN0487</i> Chaperone protein DnaJ	-1,109
<i>TVN0488</i> molecular chaperone DnaK	-1,159
<i>TVN0304</i> Proteasome subunit alpha	-1,129
<i>TVN0663</i> Proteasome protease subunit beta	-1,090
<i>TVN0531</i> Prefoldin subunit alpha	-1,201
<i>TVN1011</i> Heat shock protein HtpX	1,203
<i>TVN0775</i> molecular chaperone (small heat shock protein, hsp20-related)	1,038
<b>Replication, recombination and repair</b>	
<i>TVN0160</i> nucleoid DNA-binding protein (HB-related)	-1,657
<i>TVN1236</i> single-stranded DNA-binding protein	-1,597
<i>TVN1413</i> adenine-specific DNA methylase	-1,372
<i>TVN0781</i> bifunctional methylated DNA-protein cysteine methyltransferase/deoxyinosine 3'endonuclease	1,341
<i>TVN0842</i> transposase	-1,288
<i>TVN0263</i> integrase/recombinase	1,277
<i>TVN0843</i> hypothetical protein	-1,263
<i>TVN0971</i> endonuclease IV	-1,245
<i>TVN0114</i> hypothetical protein	1,243
<i>TVN0108</i> hypothetical protein	1,240
<i>TVN0804</i> endonuclease III	1,238
<i>TVN0110</i> hypothetical protein	-1,236
<i>TVN0739</i> DNA helicase II	-1,233
<i>TVN0133</i> ribonuclease HII	1,228
<i>TVN0156</i> DNA primase	-1,225
<i>TVN1045</i> DNA polymerase I	1,217
<i>TVN1464</i> adenine specific DNA methylase	-1,215
<i>TVN1409</i> IS5 inactivated transposase	1,201
<b>Signal transduction mechanism</b>	
<i>TVN0646</i> nucleotide-binding protein (UspA-related)	-1,325
<i>TVN1098</i> ATPase	-1,307
<i>TVN0820</i> GAF domain-containing protein	1,266
<b>Transcription</b>	
<i>TVN0295</i> transcription regulator	-1,631
<i>TVN0983</i> transcription regulator	-1,442
<i>TVN1137</i> DNA-directed RNA polymerase subunit N	-1,418
<i>TVN1075</i> small nuclear ribonucleoprotein (snRNP)-like protein	-1,359
<i>TVN0356</i> small nuclear ribonucleoprotein	-1,312
<i>TVN1089</i> transcription initiation factor IIB	-1,281
<i>TVN1392</i> transcription regulator	-1,228

**Table 3.21 (continued).**

COG category / Gene	Log <sub>2</sub> Oxidative ratio
<b>Transcription cont.</b>	
<i>TVN1337</i> transcription regulator	-1,221
<b>Translation</b>	
<i>TVN0010</i> 50S ribosomal protein L31e	-1,727
<i>TVN1135</i> 50S ribosomal protein L13P	-1,608
<i>TVN0007</i> 30S ribosomal protein S19e	-1,594
<i>TVN0337</i> 30S ribosomal protein S4e	-1,153
<i>TVN1077</i> exosome complex RNA-binding protein Csl4	-1,579
<i>TVN0420</i> 50S ribosomal protein L12P	-1,570
<i>TVN0412</i> translation initiation factor IF-2 subunit alpha	-1,562
<i>TVN1136</i> 30S ribosomal protein S9P	-1,537
<i>TVN0009</i> 50S ribosomal protein L39e	-1,535
<i>TVN1208</i> 30S ribosomal protein S15P	-1,504
<i>TVN0423</i> 50S ribosomal protein L11P	-1,461
<i>TVN0939</i> amino acid transporter	-1,441
<i>TVN0414</i> 50S ribosomal protein L44e	-1,439
<i>TVN0411</i> H/ACA RNA-protein complex component Nop10p	-1,420
<i>TVN0355</i> 50S ribosomal protein L37e	-1,409
<i>TVN0346</i> 50S ribosomal protein L30P	-1,389
<i>TVN0829</i> isoleucyl-tRNA synthetase	-1,389
<i>TVN0340</i> 30S ribosomal protein S8P	-1,377
<i>TVN0326</i> 50S ribosomal protein L23P	-1,366
<i>TVN0066</i> 2'-5' RNA ligase	1,356
<i>TVN0659</i> asparagine synthetase A	-1,351
<i>TVN0325</i> 50S ribosomal protein L4P	-1,349
<i>TVN0647</i> 30S ribosomal protein S17e	-1,343
<i>TVN0353</i> Nop56p-related protein (ribosomal biogenesis)	1,332
<i>TVN1134</i> 50S ribosomal protein L18e	-1,330
<i>TVN0422</i> 50S ribosomal protein L1P	-1,324
<i>TVN0339</i> 30S ribosomal protein S14P	-1,318
<i>TVN0332</i> translation initiation factor Sui1	-1,317
<i>TVN0563</i> 30S ribosomal protein S4P	-1,305
<i>TVN0564</i> 30S ribosomal protein S11P	-1,305
<i>TVN0270</i> RNA methylase	1,297
<i>TVN0338</i> hypothetical protein	-1,297
<i>TVN1275</i> 30S ribosomal protein S6e	-1,287
<i>TVN0342</i> 50S ribosomal protein L32e	-1,277
<i>TVN0347</i> 50S ribosomal protein L15P	-1,274
<i>TVN0330</i> 30S ribosomal protein S3P	-1,266
<i>TVN0413</i> 30S ribosomal protein S27e	-1,264
<i>TVN0399</i> 30S ribosomal protein S2	-1,259
<i>TVN0343</i> 50S ribosomal protein L19e	-1,258
<i>TVN0328</i> 30S ribosomal protein S19P	-1,247
<i>TVN0421</i> acidic ribosomal protein P0	-1,238
<i>TVN0312</i> 50S ribosomal protein L21e	-1,230
<i>TVN0329</i> 50S ribosomal protein L22P	-1,224
<i>TVN1274</i> translation initiation factor IF-2 subunit gamma	-1,209
<i>TVN0324</i> 50S ribosomal protein L3P	-1,206

Functional analysis showed that the most down-regulated genes were those involved in housekeeping functions (Table 3.21). The top category down-regulated genes by oxidative stress were genes involved in translation, ribosomal structure suggesting that when exposed to oxidative stress overall protein biosynthesis was slowed-down. Other categories which were down-regulated by H<sub>2</sub>O<sub>2</sub> exposure included genes involved in energy production and conversion, amino acid transport and metabolism, and posttranslational modification.

Under oxidative stress conditions proteins with high homology to proteins having a suggested function in TCA cycle were down-regulated. These included NAD(FAD)-dependant dehydrogenase, ferredoxin, Fe-S reductase, cytochrome bd-type quinol oxidase. A protein similar to a member of the major facilitator permease family was also up-regulated. This sugar permease may be up-regulated to provide substrate for central metabolic pathways.

### **3.6 Validation of Microarray Results Using Real-Time Quantitative PCR**

Among the genes identified by microarray analysis, sugar permease gene which was up-regulated under heat shock, pH stress and oxidative stress, and molecular chaperone GrpE (heat shock protein) gene which was only up-regulated during heat shock were selected for further analysis by qRT-PCR. Sugar permease protein is a component of putative multiple sugar transport system which contains ABC transport system permeases and ATP-binding proteins. Molecular chaperone GrpE is a part of a molecular chaperone machine composed of Hsp70 (DnaK), Hsp40 (DnaJ) and GrpE, assists in folding of proteins. The distribution of components or the sequence length of the genes of this machine varies throughout domains, archaea, bacteria and eukarya [2].

Quantitative real time PCR technique was used to investigate differential expression of GrpE gene (TVN0489) and sugar permease gene (TVN1145), under stress conditions that 65°C and 70°C heat-shock, pH 4.0 and 0.02 mM H<sub>2</sub>O<sub>2</sub> induced oxidative stress. The mRNAs of GrpE and sugar permease genes in the total RNA were converted into single-stranded cDNAs by reverse transcription as described in the Materials and Methods. Then they were used as templates in Quantitative Real-Time PCR (qRT-PCR) experiments. The gene specific forward and reverse primers sequences and the amplified PCR products for TVN0489 (531 bp) and TVN1145 (888 bp) genes are depicted in the gene sequences given in Figures 3.44 and 3.45. Both genes yielded 60 bp amplicons. Agarose gel photograph of qRT-PCR products for TVN0489 and TVN1145 are represented in Figure 3.46 and 3.47.

```

>gi|13540831:c473843-473313 Thermoplasma volcanium GSS1
chromosome, complete genome

ATGTATTCACCTTCGTCATCAAATTACATTAAGGATCCTATAAGCACTGAAATAATAAAGTCAAAG
ACAAGAAATCTGAAGAAGAGAGCTGAAGAAGCCATACTTTACCGTAGCATTGCTGAACAGTCCAGC
AGAAAATTAGCTGAGATTTTCAGAAGCATATAAACATAAGCTCGCCGATATGGAGAATTATCTTAAA
ATAAAAAGACAGGGAAACTGAAATTATCAGAAAAAATGCCAATGAGAGTCTTATTAAGGACTTTCTC
CCAGTGATAGATTCAATGGATGCTGCGATCCAAGCAGAAAAAGATAACAACCTAATCAGAATAAGG
GATCAGATGCTCAGTATACTCTCAAATATGGTCTCCAACCCATAAAAGCCGAGGGAGAAAAATTT
GATCCCTACCTGCATGAAGCTATCGGAATGACTCAGGATGGCGAAGATGGCAAAATCAAATACGAA
GTTCAAAGGGGTTATACCCTTAATAACAGTGTATTGAGGACATCTAAGGTAATTGTTGTTAAAAGG
TGA

```

**Figure 3.44 The sequence of TVN0489 gene (531 bp).** The underlined region of the gene defined by the gene specific forward (red) and reverse primers (blue), indicates the amplified sequences by RT-PCR (60 bp).

```

>gi|13540831:1197134-1198021 Thermoplasma volcanium GSS1
chromosome, complete genome

ATGTTAAGCACAGGTAAGAAAGTTTATGCTAGACCAAAAAGATCGATGAGGCCGCTGTTGAAAAAA
ACCATAATTTACGTACTGTCTATAGTTTTGGCAATGATCTACCTCCTCCCGTTTTATTGGACTGTA
ATTAAGCGTTCAGAAACAGTATCTTTGCAAATTTTCCCAAACCTAAATCCGCTCAGTGAGACA
AGCCTATCCTACTTTCTGGCAAATCTTAGGACAGTTTGGAGTTTTGGAGACTTTCTCTCTGGTAT
TTTAATAGCGTATTCGTATCGGCTTGCGTCGTTGCTGGCAGTGTATTCGTTGGCATGTTATCGGGA
TACGCGTTTTGCGAAACTGAAGTTTCCGGGTAGGAACGTATTATTTTATGCTGTTCTTGCAACTTTG
ATGATCCCATTCCCCGTAATATCTATAGCATCTTATGTATTTATGCTAGACCTAATTGGCTAAGC
ACGTATCAGGGTCTTATTCTTCTCAGATAGCTTCTGCGCTGGATGTTTTTATTATGAGGCAGTAT
TTTCTCACGATACCTGAGGAAATGGAACCTGCAGCTAAAATTGATGGTTTTGAGGCCTTGGCAAATT
TTCTTTTCTATAGATCTGCCAATGCAAAGCCAGCAATAGCTGCTGCTACGATATTTTCGTTTATA
GGTTCATGGAATAATTTCTTGTGGCCTTTGATGGAAGTTCACAGCCTCAACATGTTACAGCTACCT
CTTGTCCCTTAACTTCTTTAAGGGTGCAAACGGGACGCAAATATACTGGAATCAGATGATGACCGTC
AATATACTAACAATGATTCCAACCTATAGCTATATTCGTGGCATTTCGAGCGATATTTTCATCAATGGC
ATATCCATGACTTTTTCTGATGGGAGGTAA

```

**Figure 3.45 The sequence of TVN1145 gene (888 bp).** The underlined region of the gene defined by the gene specific forward (red) and reverse primers (blue), indicates the amplified sequences by RT-PCR (60 bp).

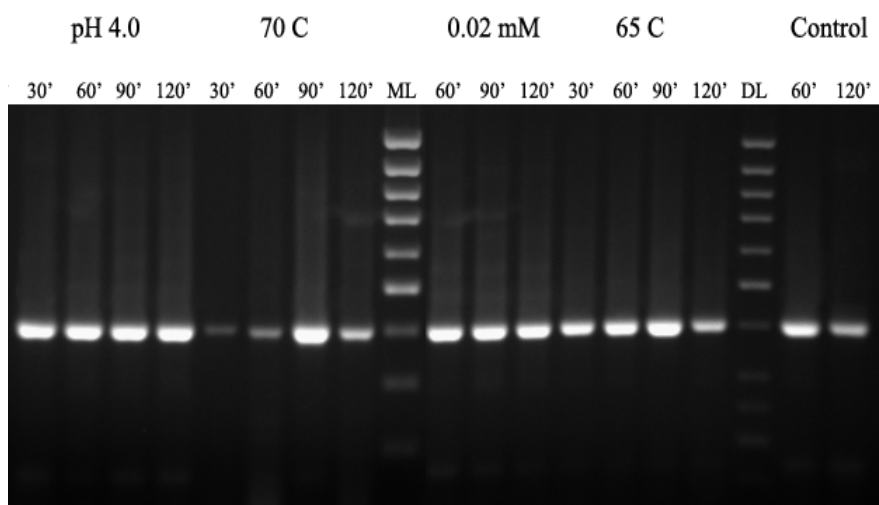


**Figure 3.46 Amplification of GrpE (TVN0489) cDNAs by RT-PCR.** The PCR amplicons were analyzed by 1% agarose gel electrophoresis. ML is MassRuler Low Range DNA Ladder, ready-to-use (Thermo Scientific, Fermentas) and DL is GeneRuler 50bp DNA Ladder (Thermo Scientific, Fermentas).

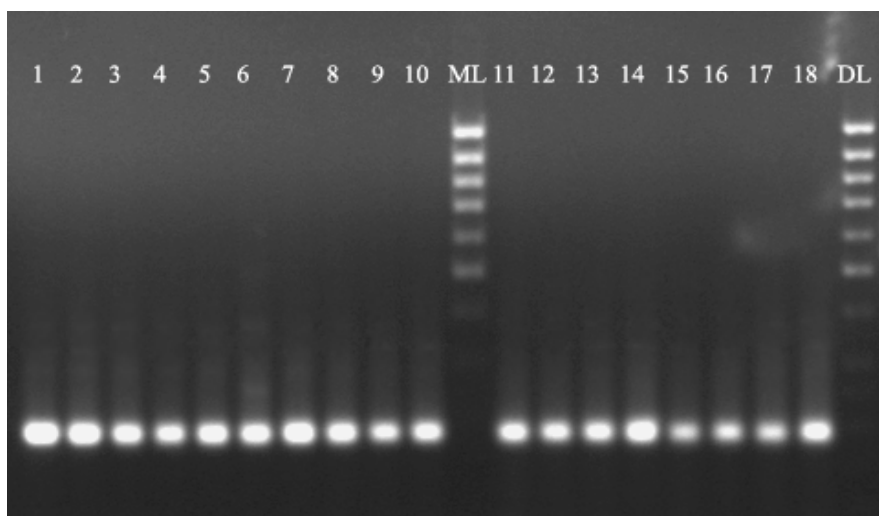


**Figure 3.47 Amplification of sugar permease (TVN1145) cDNAs by RT-PCR.** The PCR amplicons were analyzed by 1% agarose gel electrophoresis. Lanes 1–4 are 70°C heat shock samples of 30', 60', 90' and 120', respectively. Lanes 5–8 are 65°C heat shock samples of 30', 60', 90' and 120', respectively. Lanes 9 and 10 are Control 60' and 120'. Lanes 11, 12 are pH 4.0 stress samples of 30', and 60', 13 is Control 60' and 14 is pH 4.0 stress sample of 120'. Lanes 15, 16, 17, 18 are 0.02 mM H<sub>2</sub>O<sub>2</sub> stress samples of 30', 60', 90' and 120', respectively. ML is MassRuler Low Range DNA Ladder, ready-to-use (Thermo Scientific, Fermentas) and DL is GeneRuler 50bp DNA Ladder (Thermo Scientific, Fermentas).

### 3.7 Reverse Transcription and Quantitative Real-Time PCR for Expression Analysis of TVN0489

#### 3.7.1 Time-Course Differential Expression of TVN0489 Gene under Heat Stress

Transcription of molecular chaperone GrpE (TVN0489) gene was investigated by quantitative real time PCR after 65°C and 70°C heat shock. The experiments were repeated two times. The melting curve analysis showed that all amplified cDNAs of TVN0489 in RT-PCR experiments of heat stress produced single-peak and average melting temperature was 82.04°C ±0.02 for 65°C and 82.06°C ±0.07 for 70°C heat shock (Table 3.22). Negative control neither yielded any amplification nor a melting curve indicating that there was not any contamination in the amplifications (Figures 3.48 and 3.49).

As can be expected from lower Ct values of test samples of heat stress at 65°C for all time points compared to control Ct values, TVN0489 gene transcription should be up-regulated during 2 h stress. The highest expression level may be reached at 60 min of the heat stress.

Up regulation of TVN0489 gene seems maintained during 2 h heat-stress application at 70°C due to lower Ct values of the tests relative to control. The time point 60 min shows the lowest Ct value may be indicating the highest expression level of TVN0489 gene under this stress conditions. Amplification and melting curves for TVN0489 gene expression analysis under heat stress by qRT-PCR are given in the Appendix C.

**Table 3.22 Representative Ct values and mean value of at least two melting temperatures from heat shock experiments for TVN0489 gene.**

Stress	Time (min)	Ct values		Melting Temperature (± STD)
		Test	Control	
65°C	30	13.49	15.02	82.05°C (± 0.6)
	60	12.09	15.02	82.06°C (± 0.7)
	90	12.08	14.48	82.06°C (± 0.5)
	120	13.88	16.28	82.01°C (± 0.6)
70°C	30	12.34	15.02	82.15°C (± 0.6)
	60	11.67	15.02	82.02°C (± 0.5)
	90	12.08	14.63	81.99°C (± 0.5)
	120	11.71	14.63	82.08°C (± 0.5)

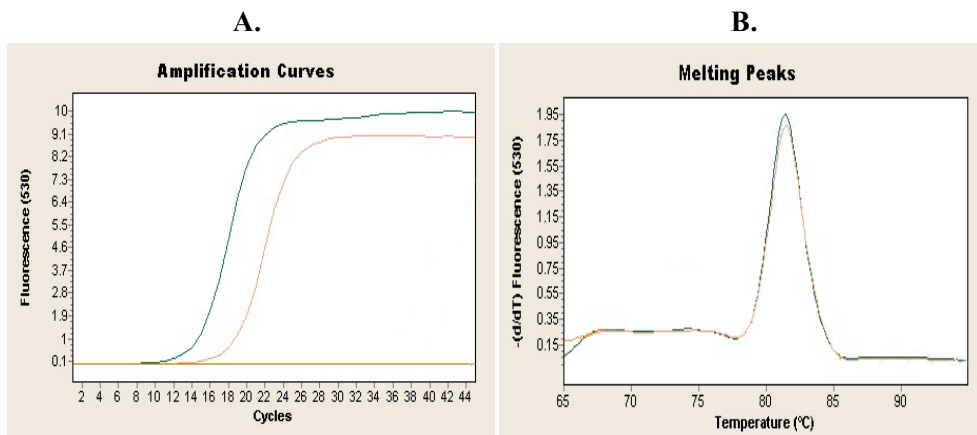


**Figure 3.48 Real-time PCR amplification and melting curves for TVN0489 gene.** RNA samples were isolated from cultures exposed to heat stress at 65°C for 60' used for reverse transcription. **A.** Amplification curves (green—test, light pink—control, light brown—negative control) **B.** Melting curves (green—test, light pink—control).

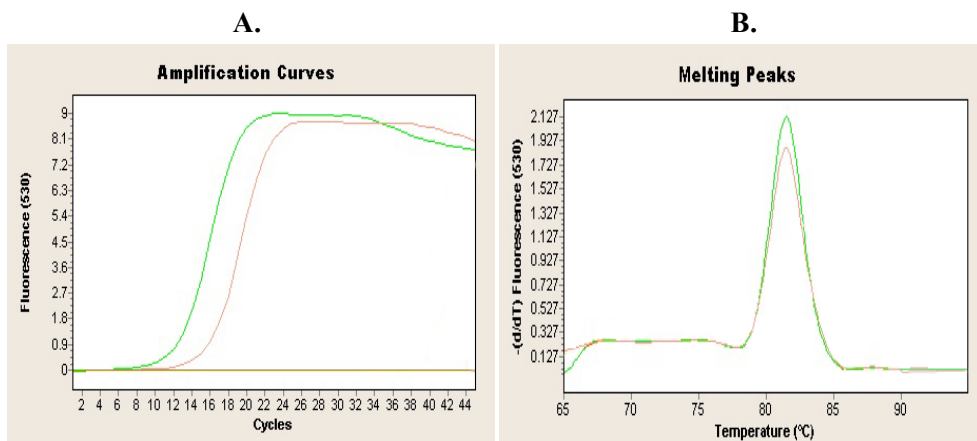


**Figure 3.49 Real-time PCR amplification and melting curves for TVN0489 gene.** RNA samples were isolated from cultures exposed to heat stress at 70°C for 60' used for reverse transcription. **A.** Amplification curves (green—test, light pink—control, light brown—negative control) **B.** Melting curves (green—test, light pink—control).

### 3.7.2 Fold Difference Analysis of Time Course Expression of TVN0489 Gene under Heat Shock

The fold difference analysis results were comparable with the results deduced from evaluation of the test Ct values as compared to control Cts. The TVN0489 gene expression gradually increased from 2-fold (at 30 min) to about 4-fold (at 90 min) during heat shock at 65°C. However, expression level started to decline by 120 min. The expression of TVN0489 gene was up-regulated by heat shock at 70°C for 2 h and the highest expression level was reached at 60 min (about 6-fold).

**Table 3.23 Fold difference of TVN0489 gene expression under heat shock.** The results are the means of at least two independent qRT-PCR experiments.

Stress	Time (min)	Fold Difference ( $\pm$ STD)
65 °C	30	2.216 $\pm$ 0.5
	60	3.966 $\pm$ 0.5
	90	3.805 $\pm$ 0.7
	120	3.623 $\pm$ 0.03
70 °C	30	3.33 $\pm$ 1.2
	60	5.725 $\pm$ 1.2
	90	3.669 $\pm$ 1.2
	120	4.18 $\pm$ 0.78

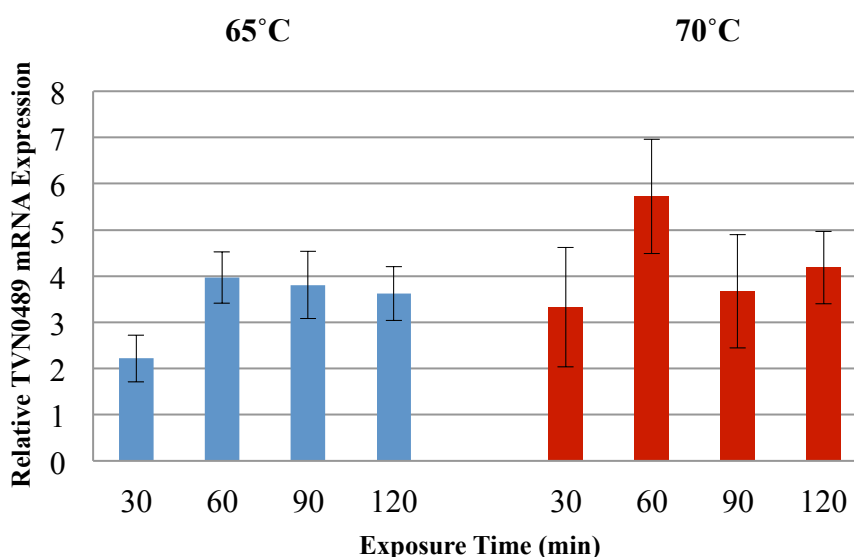


**Figure 3.50 Relative mRNA expression of TVN0489 gene determined by quantitative real-time PCR analysis under heat shock at 65°C, and 70°C.** Expressions are shown as fold-increase or decrease relative to the control level (1-fold) TVN0489 gene expression. The values are means of at least 2 replicates.

The mean values of fold differences of at least two independent experiments were given in Table 3.23 and their bar graph is given in Figure 3.50.

### 3.7.3 Time-Course Differential Expression of TVN0489 Gene under pH Stress

Due to higher Ct values compared to control Ct values for the qRT-PCR experiments of the pH stress (at pH 4.0), TVN0489 gene expression might be induced during 2 h stress exposure (Table 3.24). The amplification and melting curves of the RT-PCR experiments are given in the Appendix C. Specific amplification of the TVN0489 cDNA in these RT-PCR experiments was verified by melting curve analysis and average  $T_m$  was found  $82.37^\circ\text{C} \pm 0.1$ . Figure 3.51 shows the RT-PCR amplification melting curves for stress at pH 4.0 (60 min).

**Table 3.24 Representative Ct values and mean value of at least two melting temperatures from pH stress experiments for TVN0489 gene.**

Stress	Time (min)	Ct values		Melting Temperature ( $\pm$ STD)
		Test	Control	
pH 4.0	30	16.7	18.04	$82.75^\circ\text{C} (\pm 0.01)$
	60	16.62	18.04	$82.86^\circ\text{C} (\pm 0.01)$
	90	16.95	17.98	$82.82^\circ\text{C} (\pm 0.01)$
	120	16.12	17.98	$82.87^\circ\text{C} (\pm 0.01)$

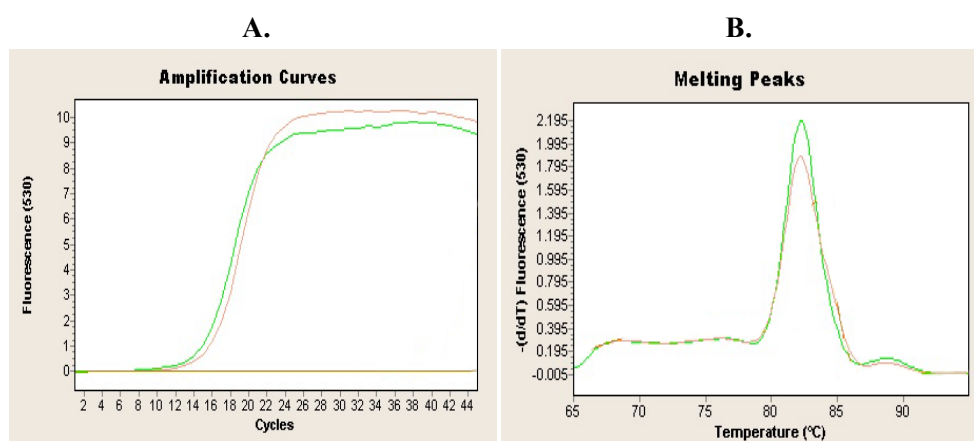


**Figure 3.51 Real-time PCR amplification and melting curves for TVN0489 gene.** RNA samples were isolated from cultures exposed to pH stress at pH 4.0 for 60' used for reverse transcription. **A.** Amplification curves (green—test, pink—control, light brown—negative control) **B.** Melting curves (green—test, pink—control).

### 3.7.4 Fold Difference Analysis of Time Course Expression of TVN0489 Gene under pH Stress

The fold difference analysis of TVN0489 gene also indicated up-regulation of TVN0489 gene under stress at pH 4.0 and the highest transcription level was reached at 60 min (1.5-fold). This result was consistent with the estimations from Ct values of tests and control.

The mean values of at least 2 independent experiments were given in Table 3.25 and related diagram is shown in Figure 3.52.

**Table 3.25 Fold difference of TVN0489 gene expression under pH stress.** The results are the means of at least two independent qRT-PCR experiments.

Stress	Time (min)	Fold Difference ( $\pm$ STD)
pH 4.0	30	1.376 $\pm$ 0.01
	60	1.541 $\pm$ 0.02
	90	0.961 $\pm$ 0.08
	120	1.272 $\pm$ 0.02

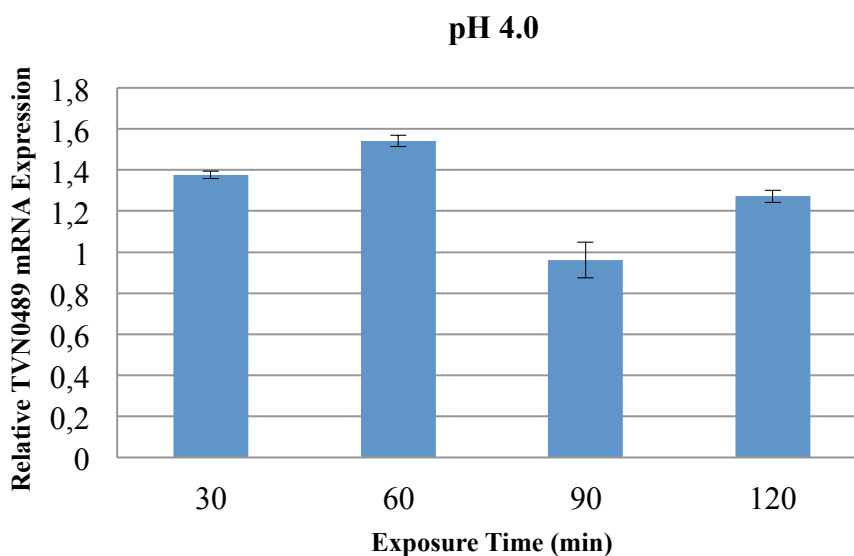


**Figure 3.52 Relative mRNA expression of TVN0489 gene determined by quantitative real-time PCR analysis under pH stress at pH 4.0.** Expressions are shown as fold-increase or decrease relative to the control level (1-fold) TVN0489 gene expression. The values are means of at least 2 replicates.

### 3.7.5 Time-Course Differential Expression of TVN0489 Gene under Oxidative Stress

TVN0489 gene expression possibly induced under oxidative stress imposed by exposure to H<sub>2</sub>O<sub>2</sub> (at 0.02 mM) since Ct values of the tests was lower than control Ct values for 2 h. Expression level was the highest following 120 min H<sub>2</sub>O<sub>2</sub> exposure (Table 3.26).

Melting curve analysis for these qRT-PCR experiments verified the specific amplification of TVN0489 gene's cDNAs and average T<sub>m</sub> was 82.49°C ±0.07 at 0.02 mM H<sub>2</sub>O<sub>2</sub>. RT-PCR absolute quantification and melting analyses of TVN0382 cDNA samples from 0.02 mM H<sub>2</sub>O<sub>2</sub> experiments are given in the Appendix C. Figure 3.53 shows the RT-PCR amplification and melting curves for oxidative stress imposed by 0.02 mM H<sub>2</sub>O<sub>2</sub> (60 min).

**Table 3.26 Representative Ct values and mean value of at least two melting temperatures from oxidative stress experiments for TVN0489 gene.**

Stress	Time (min)	Ct values		Melting Temperature (± STD)
		Test	Control	
0.02 mM	30	18.56	18.97	82.5°C (± 0.01)
	60	22.83	23.03	82.59°C (± 0.01)
	90	14.63	14.94	82.43°C (± 0.01)
	120	13.97	14.94	82.44°C (± 0.01)

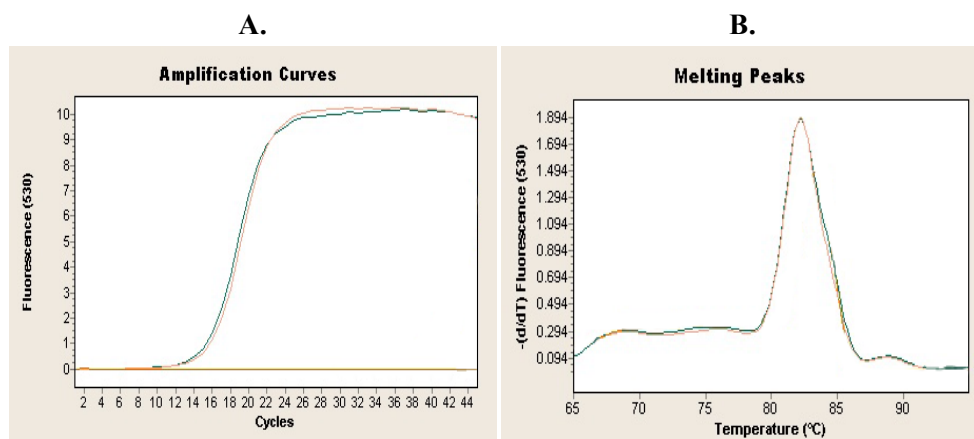


**Figure 3.53 Real-time PCR amplification and melting curves for TVN0489 gene.** RNA samples were isolated from cultures exposed to oxidative stress at 0.02 mM for 60' used for reverse transcription. **A.** Amplification curves (green—test, light pink—control, light brown—negative control) **B.** Melting curves (green—test, light pink—control).

### 3.7.6 Fold Difference Analysis of Time Course Expression of TVN0489 Gene under Oxidative Stress

The changes in the expression of TVN0489 gene at 0.02 mM H<sub>2</sub>O<sub>2</sub> stress were analyzed relative to control over 120 min. The fold differences were calculated and represented as the mean of at least two independent experiments (Table 3.27). The related data points are plotted in a chart and depicted by bars (Figure 3.54).

The fold-difference analysis has indicated that TVN0489 gene expression did not show any significant changes during 90 min, but increased 1.5-fold at 120 min. These results are consistent with the results deduced from analysis of the Ct values.

**Table 3.27 Fold difference of TVN0489 gene expression under oxidative stress.** The results are the means of at least two independent qRT-PCR experiments.

Stress	Time (min)	Fold Difference ( $\pm$ STD)
0.02 mM	30	1.002 $\pm$ 0.2
	60	1.148 $\pm$ 0.09
	90	1.13 $\pm$ 0.05
	120	1.544 $\pm$ 0.163

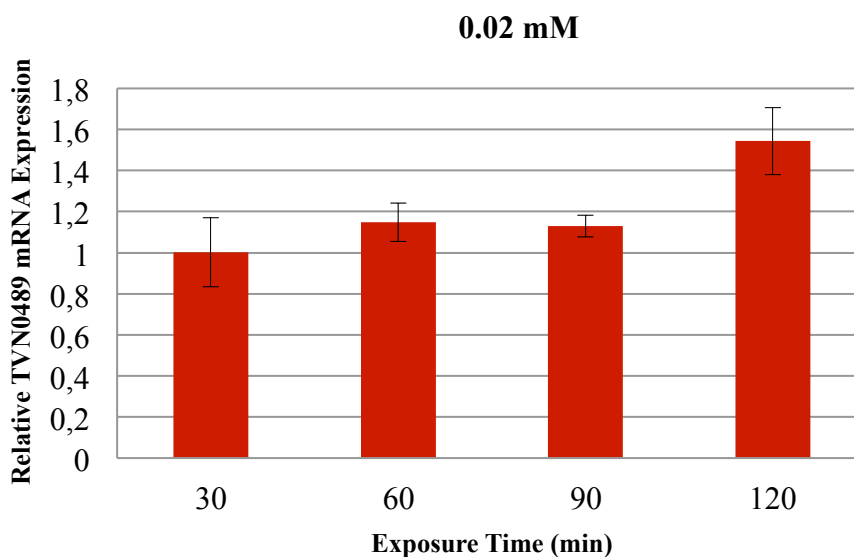


**Figure 3.54 Relative mRNA expression of TVN0489 gene determined by quantitative real-time PCR analysis under oxidative stress at 0.02 mM.** Expressions are shown as fold-increase or decrease relative to the control level (1-fold) TVN0489 gene expression. The values are means of at least 2 replicates.

### 3.8 Reverse Transcription and Quantitative Real-Time PCR for Expression Analysis of TVN1145

#### 3.8.1 Time-Course Differential Expression of TVN1145 Gene under Heat Stress

Since the test Ct values relative to control Ct values were lower for 65°C heat stress experiments, transcription of the TVN1145 gene should be up-regulated for 2 h. The test Ct values of 70°C heat stress experiments were also lower than control Ct values. This may indicate that TVN1145 gene was up-regulated during 2 h with the highest rate at 30 min (Table 3.28).

Specific amplification of the TVN1145 gene was verified by melting curve analysis. The average melting temperature was 82.65°C ±0.05 for 65°C and 82.68°C ±0.06 for 70°C heat-stress.

RT-PCR absolute quantification and melting analysis of TVN1145 cDNAs from 65°C and 70°C heat-shock experiments are given in the Appendix C. Figures 3.55 and 3.56 show the RT-PCR amplification and melting curves for heat stress at 65°C (30 min) and 70°C (30 min), respectively.

**Table 3.28 Representative Ct values and mean value of at least two melting temperatures from heat shock experiments for TVN1145 gene.**

Stress	Time (min)	Ct values		Melting Temperature (± STD)
		Test	Control	
65 °C	30	16.67	17.82	82.71°C (± 0.01)
	60	15.97	17.82	82.6°C (± 0.01)
	90	15.91	17.72	82.69°C (± 0.01)
	120	16.44	17.72	82.63°C (± 0.01)
70 °C	30	15.75	17.82	82.76°C (± 0.01)
	60	16.51	17.82	82.7°C (± 0.01)
	90	15.87	17.72	81.61°C (± 0.01)
	120	16.19	17.72	82.65°C (± 0.01)

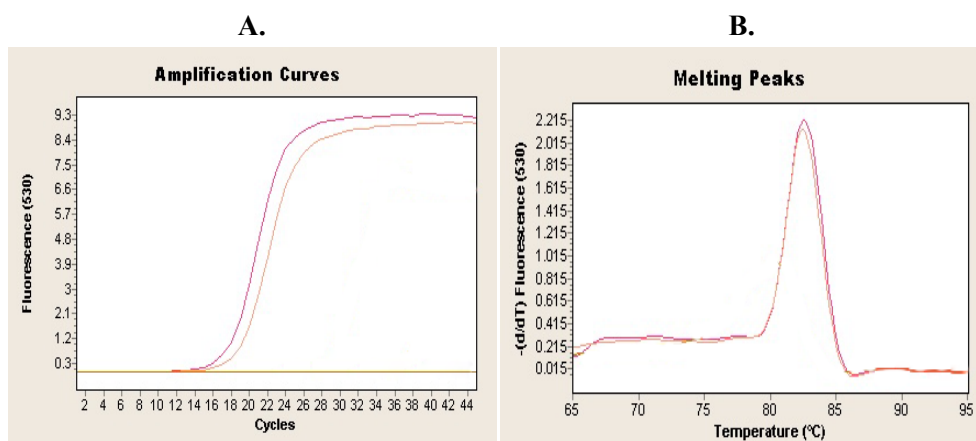


**Figure 3.55 Real-time PCR amplification and melting curves for TVN1145 gene.** RNA samples were isolated from cultures exposed to heat shock at 65°C for 30' used for reverse transcription. **A.** Amplification curves (pink—test, light pink—control, light brown—negative control) **B.** Melting curves (pink—test, light pink—control).

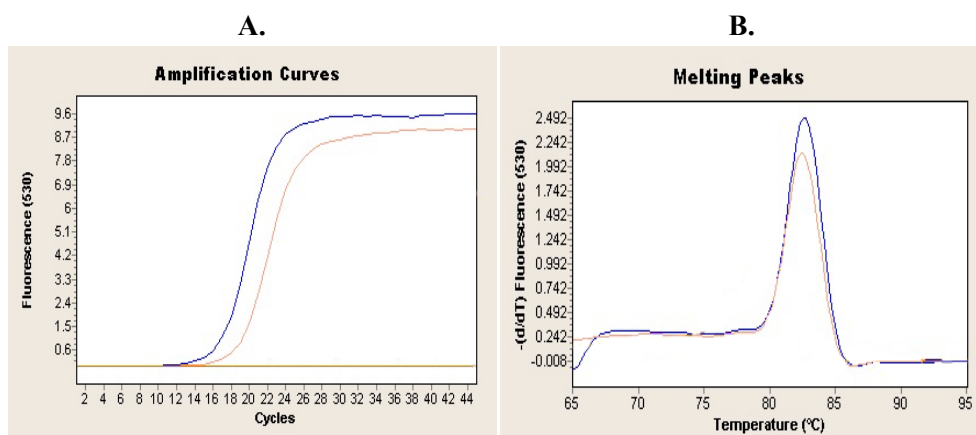


**Figure 3.56 Real-time PCR amplification and melting curves for TVN1145 gene.** RNA samples were isolated from cultures exposed to heat shock at 70°C for 30' used for reverse transcription. **A.** Amplification curves (blue—test, light pink—control, light brown—negative control) **B.** Melting curves (blue—test, light pink—control).

### 3.8.2 Fold Difference Analysis of Time Course Expression of TVN1145 Gene under Heat Shock

According to fold analysis, TVN1145 gene transcription was induced after heat shock 65°C for 120 min. The highest expression (2.6-fold) was reached at 90 min. The fold difference analysis of TVN1145 gene also indicated up-regulation under heat stress at 70°C for 2 h. The

TVN1145 gene expression was induced at most about 3-fold at most 30 min following stress exposure.

The calculated fold differences were represented as the mean of at least two independent experiments (Table 3.29). The related data points are plotted in a chart and depicted by bars (Figure 3.57).

**Table 3.29 Fold difference of TVN1145 gene expression under heat shock.** The results are the means of at least two independent qRT-PCR experiments.

Stress	Time (min)	Fold Difference ( $\pm$ STD)
65 °C	30	1.95 $\pm$ 0.07
	60	2.515 $\pm$ 0.3
	90	2.63 $\pm$ 0.3
	120	2.01 $\pm$ 0.1
70 °C	30	2.99 $\pm$ 0.3
	60	1.96 $\pm$ 0.1
	90	2.62 $\pm$ 0.3
	120	2.54 $\pm$ 0.2

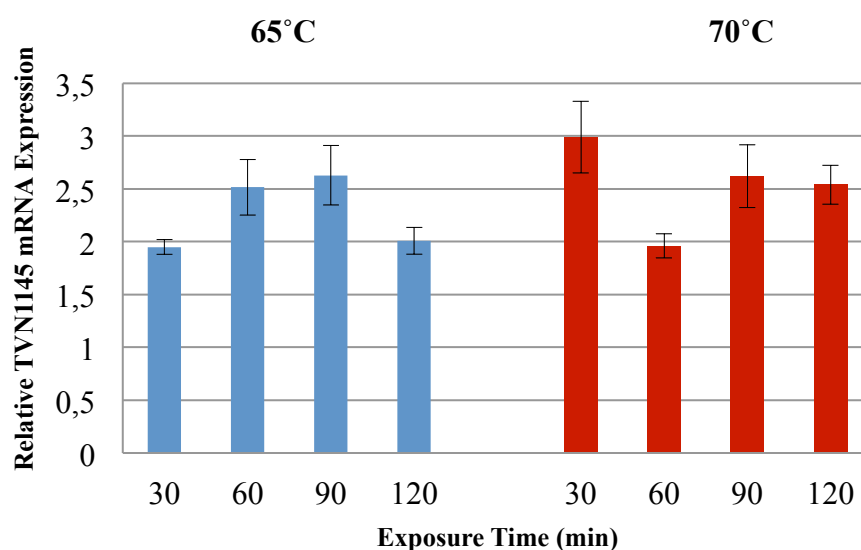


**Figure 3.57 Relative mRNA expression of TVN1145 gene determined by quantitative real-time PCR analysis under heat shock at 65°C and 70°C.** Expressions are shown as fold-increase or decrease relative to the control level (1-fold) TVN1145 gene expression. The values are means of at least 2 replicates.

### 3.8.3 Time-Course Differential Expression of TVN1145 Gene under pH Stress

Transcription of TVN1145 gene was induced by pH stress at pH 4.0 for 1 h, as revealed by lower test Ct values as compared to that of controls. The gene expression seems to be higher during first 1 h of stress exposure due to higher Ct test values than the control Ct values (Table 3.30).

Melting curve analysis for these qRT-PCR experiments verified the specific amplification of TVN1145 gene's cDNAs and average  $T_m$  was  $82.82^\circ\text{C} \pm 0.05$  under pH stress at pH 4.0. RT-PCR absolute quantification and melting analyses of TVN1145 cDNA samples from pH stress at pH 4.0 experiments are given in the Appendix C. Figure 3.58 shows the RT-PCR amplification and melting curves for TVN1145 gene for pH stress at pH 4.0 (60 min).

**Table 3.30 Representative Ct values and mean value of at least two melting temperatures from pH stress experiments for TVN1145 gene.**

Stress	Time (min)	Ct values		Melting Temperature ( $\pm$ STD)
		Test	Control	
pH 4.0	30	16.7	18.04	$82.75^\circ\text{C} (\pm 0.01)$
	60	16.62	18.04	$82.86^\circ\text{C} (\pm 0.01)$
	90	16.95	17.98	$82.82^\circ\text{C} (\pm 0.01)$
	120	16.12	17.98	$82.87^\circ\text{C} (\pm 0.01)$

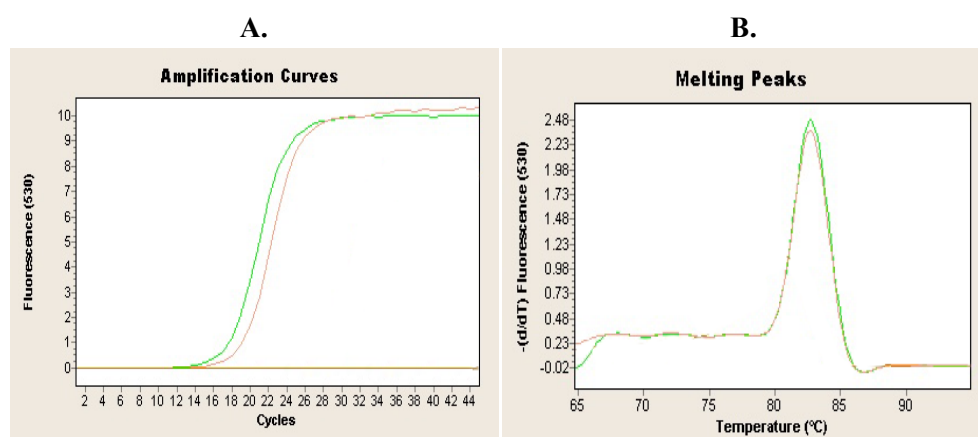


**Figure 3.58 Real-time PCR amplification and melting curves for TVN1145 gene.** RNA samples were isolated from cultures exposed to pH stress at pH 4.0 for 60' used for reverse transcription. **A.** Amplification curves (green—test, pink—control, light brown—negative control) **B.** Melting curves (green—test, pink—control).

### 3.8.4 Fold Difference Analysis of Time Course Expression of TVN1145 Gene under pH Stress

The fold difference analysis have shown that TVN1145 gene expression was up-regulated during pH stress at pH 4.0 for 2 h and the gene expression level reached the highest (about 2.7-fold) after 2 h.

The calculated fold differences were represented as the mean of at least two independent experiments (Table 3.31). The related data points are plotted in a chart and depicted by bars (Figure 3.59).

**Table 3.31 Fold difference of TVN1145 gene expression under pH stress.** The results are the means of at least two independent qRT-PCR experiments.

Stress	Time (min)	Fold Difference ( $\pm$ STD)
pH 4.0	30	1.92 $\pm$ 0.3
	60	2.03 $\pm$ 0.3
	90	1.715 $\pm$ 0.2
	120	2.74 $\pm$ 0.6

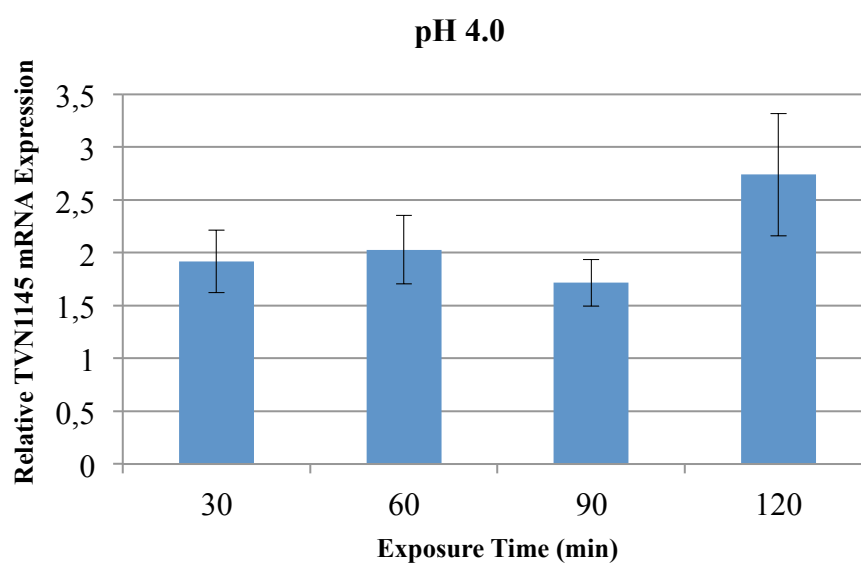


**Figure 3.59 Relative mRNA expression of TVN1145 gene determined by quantitative real-time PCR analysis under pH stress at pH 4.0.** Expressions are shown as fold-increase or decrease relative to the control level (1-fold) TVN1145 gene expression. The values are means of at least 2 replicates.

### 3.8.5 Time-Course Differential Expression of TVN1145 Gene under Oxidative Stress

Due to higher test Ct values compared to that of control values for the qRT-PCR experiments, TVN1145 gene expression might be induced during 60 min oxidative stress. However expression level may be decreased there after to the control expression level (Table 3.32). The melting analysis showed that all amplified TVN0947 cDNAs produced single-peak and average melting temperature was  $82.88^{\circ}\text{C} \pm 0.05$  was implying specific amplification of the TVN1145 cDNAs. Amplification and melting curves for qRT-PCR experiments of oxidative stress at 0.02 mM  $\text{H}_2\text{O}_2$  are given in Appendix C. Figure 3.60 shows the RT-PCR amplification and melting curves for TVN1145 gene for oxidative stress at 0.02 mM  $\text{H}_2\text{O}_2$  (60 min).

**Table 3.32 Representative Ct values and mean value of at least two melting temperatures from oxidative stress experiments for TVN1145 gene.**

Stress	Time (min)	Ct values		Melting Temperature ( $\pm$ STD)
		Test	Control	
0.02 mM	30	17.08	18.04	$82.87^{\circ}\text{C} (\pm 0.01)$
	60	16.69	18.04	$82.88^{\circ}\text{C} (\pm 0.01)$
	90	17.21	17.98	$82.86^{\circ}\text{C} (\pm 0.01)$
	120	17.03	17.98	$82.93^{\circ}\text{C} (\pm 0.01)$

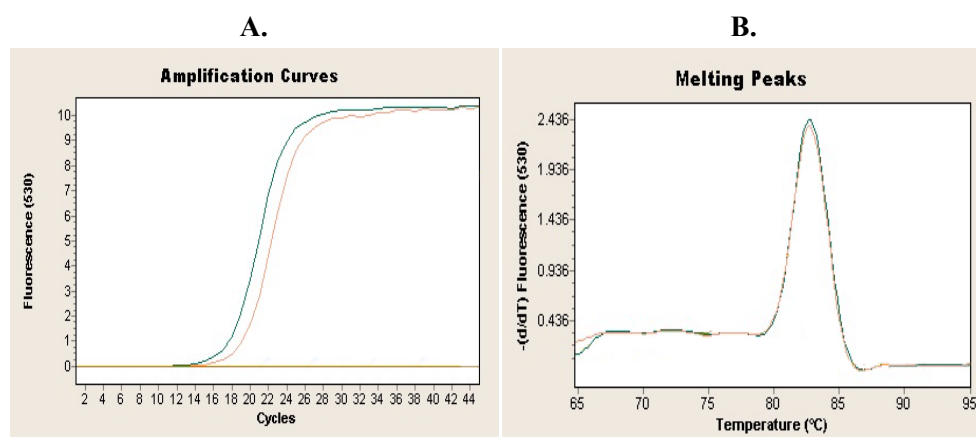


**Figure 3.60 Real-time PCR amplification and melting curves for TVN1145 gene.** RNA samples were isolated from cultures exposed to oxidative stress at 0.02 mM for 60' used for reverse transcription. **A.** Amplification curves (green—test, light pink—control, light brown—negative control) **B.** Melting curves (green—test, light pink—control).

### 3.8.6 Fold Difference Analysis of Time Course Expression of TVN1145 Gene under Oxidative Stress

Fold difference analyses showed that oxidative stress which was achieved by exposure of the cultures to H<sub>2</sub>O<sub>2</sub> at a concentration of 0.02 mM induced expression of TVN1145 gene for 2 h. An increase of about 2-fold was obtained after 60 min being the highest transcription under this condition.

The calculated fold differences were represented as the mean of at least two independent experiments (Table 3.33). The related data points are plotted in a chart and depicted by bars (Figure 3.61).

**Table 3.33** Fold difference of TVN1145 gene expression under oxidative stress. The results are the means of at least two independent qRT-PCR experiments.

Stress	Time (min)	Fold Difference ( $\pm$ STD)
0.02 mM	30	1.6 $\pm$ 0.2
	60	2.08 $\pm$ 0.3
	90	1.53 $\pm$ 0.1
	120	1.635 $\pm$ 0.2

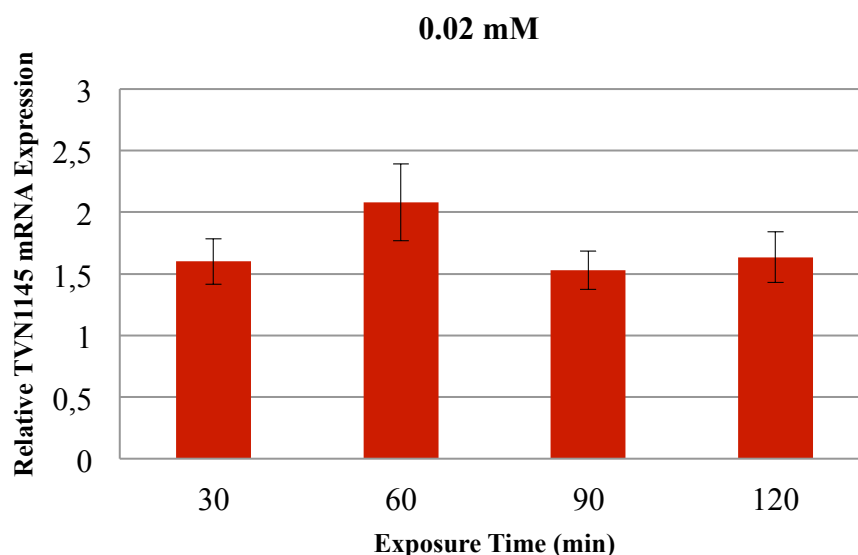


**Figure 3.61** Relative mRNA expression of TVN1145 gene determined by quantitative real-time PCR analysis under oxidative stress at 0.02 mM. Expressions are shown as fold-increase or decrease relative to the control level (1-fold) TVN1145 gene expression. The values are means of at least 2 replicates.

## CHAPTER 4

### DISCUSSION

To date, still very little is known about the genes, proteins and molecules underlying the mechanisms responsible for stress response in archaea. For a comprehensive investigation of anti-stress mechanism and strategies adopted to respond rapid environmental changes, we have chosen thermoacidophilic archaeon *Thermoplasma volcanium* GSS 1 (*Tpv*) as the model organism.

It has often been hypothesized that proteasome associated ATPases, as well as the ATPase components of the bacterial ATP-dependent proteases (ClpAP, Lon, and FtsH) function as molecular chaperones that prevent protein aggregation and promote refolding of denatured proteins. Benaroudj and Goldberg (2000) have shown that the proteasome activating nucleotidase (PAN) from the archaeon *M. jannaschii* that is homologous to ATPases in the eukaryotic 26S proteasome may function as a molecular chaperone and reduces aggregation of denatured proteins and enhances their refolding [36].

In the first part of this thesis project, differential expression of the two VAT proteins (TVN0382 and TVN0947) that fulfill the functions of PAN in *Thermoplasma* species, was investigated in confronting external stresses; heat shock, pH and oxidative stress. The VAT genes are homologues of VCP/Cdc48 gene that takes part in ubiquitin dependent proteasomal degradation in eukaryotes and a plausible function for VAT protein in protein degradation in association with the 20S proteasome was suggested [19, 49]. Besides this, Golbik *et al.* has shown that VAT has chaperone-like activities, protein folding and unfolding [3].

To specify how crucial VAT proteins are in stress response of *Tpv*, we investigated differential expression of VAT genes by qRT-PCR technique and fold difference analysis for each stress conditions. The calculated average fold differences for each stress condition indicated a maximum in expression level under heat stress for TVN0382 and TVN0947 genes. The qRT-PCR data analysis demonstrated that VAT genes were highly induced after a thermal shift from 60°C to 65°C (up to 5.5-fold for TVN0382 and 2.9 for TVN0947). Although TVN0947 gene expression was up-regulated throughout the heat-shock at 65°C for 2 h, TVN0382 gene expression was rapidly increased in the early stages of heat-shock response (initial 30 min). Similarly heat stress at 70°C induced expression of both VAT genes (about 3-fold) for 30 min post-exposure to heat-shock. The rapid increase in VAT transcripts after 30 min or 1 h following heat stress may be caused by their low translation levels under optimum conditions. The decrease in transcription rates after 60 min heat shock

at 65°C and 70°C to the rate of control may indicate a balance reached to deal with heat shock.

VAT is known to be the only partner of 20S proteasome in ~15% of the archaea, and it induces gate opening of 20S proteasome, enables the substrate protein unfolding and translocating into the proteolytic chamber of 20S for proteasomal degradation [60]. It was somewhat surprising that *Haloferax volcanii* cells harboring deletions in the PanA gene displayed enhanced thermotolerance [75]. In contrast to this result, it has been shown that close relative of *Tpv*, *Thermoplasma acidophilum*, was dependant on 20S proteasome activity to survive under heat stress while its existence was not crucial under normal conditions for the survival of the cell [72]. This points a possible correlation between the increase of VAT genes' expression and enhanced proteasomal activity to degrade denatured proteins under heat stress. Thus, we may suggest a rescue strategy in *Tpv* cells similar to that of another hyperthermophilic archaea *Pyrococcus furiosus*, which deals with increased temperature by increasing gene expression levels of small heat shock protein (Hsp20), thermosome (Hsp60), and two VAT related chaperones [73].

Nevertheless, VAT genes' expressions were either did not change or down-regulated under the pH stress conditions we tested, except pH 4.0. The TVN0382 gene expression induced only between 1.5 and 2-fold as compared to control for 2 h after pH stress application. TVN0947 gene expression gradually but slowly increased up to 1.4-fold at 120 min post exposure to pH 4.0. Previous study which was conducted in our laboratory has shown that *Tpv* proteasomal 20S  $\alpha$  and  $\beta$  subunit genes were up-regulated remarkably high (6-10 fold) (*data is not shown*) under pH stress at pH 4.0. All together these results might indicate that at pH 4.0 up-regulation of the VAT-20S proteasome complex genes should be a critical part of stress response network in *Tpv*. Increased protein turn-over rate may indicate rapid removal of the damaged proteins.

The acidophiles cytoplasmic pH is generally more alkaline than their environment. For example, *Thermoplasma acidophilum* has an internal pH near 5.5-6.5 while it thrives at pH 2.0; *Sulfolobus solfataricus* has cytoplasmic pH ~6.5 while it grows at pH 2.0-4.0 [107]. This is enabled by the prevention of passive influx of protons from the environment. Archaeal membranes are highly impermeable to protons which are translocated by water but their membranes also have decreased influx of water. However, the pH shift to 4.5 or to 5.0 should have an adverse effect on regulation of the pH homeostasis in *Tpv* cells, since cell growth rates were significantly reduced (previous observation in our laboratory). This might lead to a global transcriptional down-regulation and may explain the lower transcription rates of the VAT genes relative to control transcription under these conditions.

The TVN0947 gene expression although slightly increased at low H<sub>2</sub>O<sub>2</sub> concentration (i.e., 0.01 mM), at higher H<sub>2</sub>O<sub>2</sub> concentrations either did not change (at 0.02 mM and 0.03 mM H<sub>2</sub>O<sub>2</sub>) or down-regulated (at 0.05 mM H<sub>2</sub>O<sub>2</sub>). The TVN0382 gene transcription seemed to be more sensitive to oxidative stress. Its expression although was not effected at low H<sub>2</sub>O<sub>2</sub> concentration (i.e., 0.01 mM), its transcription induced about 4-fold at 90 min post exposure

to 0.02 mM H<sub>2</sub>O<sub>2</sub>. At higher H<sub>2</sub>O<sub>2</sub> concentrations the genes transcription either did not change (i.e., 0.03 mM H<sub>2</sub>O<sub>2</sub>) or down regulated (at 0.05 mM H<sub>2</sub>O<sub>2</sub>).

Our results indicate that regulation of VAT genes transcription is H<sub>2</sub>O<sub>2</sub> dose-dependant. There is a model suggested by Aiken *et. al.* that 26S proteasome dissociates into 19S particle and 20S particle to liberate 20S particle for increasing the ATP/ubiquitin independent degradation of oxidized proteins when oxidative stress is persistent [70]. Based on this finding, VAT expression may no longer needed for the degradation of oxidized proteins after a prolonged H<sub>2</sub>O<sub>2</sub> application and 20S proteasome alone may undertake defense task.

Intensity comparisons from the Western hybridization on VAT proteins, TVN0382 and TVN0947, for selected time points 60' and 120', were consistent with the differential expression patterns observed in the qRT-PCR results. VAT proteins were cross-hybridized with human reactive VCP antibody which had sequence overlap of 34% with TVN0382 and 83% with TVN0947. Weak bands obtained from TVN0382 protein due to lower homology with the human VAT peptide sequence. The TVN0947 protein has yielded bands in immunodetection at higher intensities than control after 60' stress exposure than 120' stress exposure for selected stressors, which is 0.02 mM H<sub>2</sub>O<sub>2</sub> for oxidative stress, pH 4.0 for pH stress, 65°C and 70°C heat-shock. The good agreement between qRT-PCR results and Western Blotting/Hybridization analysis for the selected stress conditions indicate that increased TVN0947 gene expression occurs both at transcription and translation levels.

In the second part of this study, we have investigated the global transcriptional response of *Tpv* cells under external stresses, oxidative stress at 0.02 mM H<sub>2</sub>O<sub>2</sub>, pH stress at pH 4.0 and heat shock at 65°C after 60 min by using expression microarrays. Following the stress exposure, we have observed changes in mRNA levels of the 1501 total *Tpv* transcripts approximately 14% under heat shock, and 20% under oxidative and pH stress. The down-regulated genes were more abundant than the up-regulated genes and under all stress categories.

The genes that showed corrected intensity ratios of approximately 1.2-fold induction or repression ( $\log_{2}FC \geq 0.3$ ) were grouped in two categories. Up-regulated genes were mainly associated with carbohydrate transport and those of unknown function while the down-regulated genes were dominated by the genes having function in energy production and conversion, transcription and translation. The down-regulated genes related to 30S and 50S ribosomal protein genes, ribosome structure and protein synthesis may indicate that overall protein synthesis was slowed down under the stress conditions. Repression of protein synthesis may serve as a global adaptive response to protect cells from destructive effects of toxic agents and ensure the conservation of the other crucial checkpoints which are needed for survival [108].

Several enzymes were affected by heat shock, oxidative stress and pH stress. Notably, expressions of permeases, dehydrogenases, transferases, and oxidoreductases were repressed or induced during exposure to these stressors. This indicates principle regulations in *Tpv* cells which comprise the energy and central metabolic pathways, and transport through the cell membrane under stress conditions [109].

**Heat shock regulation.** When *Tpv* growth temperature was shifted from 60°C to 65°C, approximately 12% of the genome responded (78 ↑ / 103 ↓ in total 181 genes) with  $\geq 1.2$ -fold differences within 1 h. It is well known that a temperature up-shift mainly causes the up-regulation of a group of proteins, called heat shock proteins (Hsps) which manage the correct folding and assembly of polypeptides and also the proteases that enable degradation of irreversibly unfolded proteins [110]. Our global gene expression analysis in *Tpv* cells has shown that not only proteases (TVN0424, TVN0492, TVN0616, TVN0818, TVN0895, TVN0291, TVN0254, TVN0316, TVN0322 and TVN0304) but also heat shock proteins (TVN0507, TVN1128, TVN0487, TVN0488, TVN0489, TVN0775, TVN0382 and TVN0947) were up-regulated as response to heat-shock. This indicates a critical role for proteases and heat-shock proteins for defense of the *Tpv* cells against heat stress. Other proteins with functions in stress response such as inorganic ion transport and metabolism, replication, recombination and repair mechanisms were up-regulated. However, the expression levels of many of these proteins were below 1.2-fold except that of molecular chaperone GrpE (TVN0489) (1.312-fold). This slight increase in stress associated genes' expression might be explained by the temperature and duration of the applied heat-shock. The time dependency of gene expression as a response to heat-shock has been observed in hyperthermophilic archaeon *Pyrococcus furiosus*. Transcription level of AAA+ ATPase gene increased by a factor of 25 after 30 min and decreased to a factor of 11 and 13 after 60 and 90 min, respectively [111]. Similarly, heat shock related genes of *Tpv* might be induced at higher levels rapidly following heat exposure, then may be decreased and reached to a steady state after 60 min. Transient increase in gene expression is a known characteristic of heat shock response. For example, in a phytopathogen *Xylella fastidiosa* induced transcript levels of chaperone and protease related genes decreased after 45 min exposure to heat stress [110]. The molecular chaperone GrpE which is a component of Hsp70 system responded after temperature shift by 1.3-fold up-regulation indicating a possible role for this chaperone in heat-shock response for *Tpv*. Our results showed that, the thermosome subunits were not induced at sufficient levels may be due to their higher level expression under normal conditions. This is consistent with previous reports on heat-shock response of hyperthermophilic archaea *Sulfolobus shibatae* and *Sulfolobus solfataricus* [112, 113]. ATP-independent chaperones, prefoldins (TVN0351 and TVN1213), were down regulated ( $>1.2$ -fold) which is consistent with the previous works with *P. furiosus* [73] and *Archaeoglobus fulgidus* [84]. The Hsp20-like small heat shock protein and two other molecular chaperones, VAT proteins, were strongly induced in *P. furiosus* after heat shock [73]. However, only a slight increase was observed for VAT genes (TVN0382\_1.048-fold, TVN0947\_1.047-fold) and for Hsp20 related molecular chaperone (TVN0775\_1.046-fold) in our study. The proteasome  $\beta$ -subunit (1.339-fold) gene was down regulated while  $\alpha$ -subunit gene showed some up-regulation (1.116-fold) in contrast to induced expression of  $\beta$ -subunits and repressed  $\alpha$ -subunit expression of *P. furiosus* [73]. Although ATP-dependent proteases were not detected as heat-shock responsive, signal peptidase I (TVN0221) was among the induced enzymes of *Tpv*. Heat shock protein X (Htp X) a peptidase which has been implicated elsewhere in surface protein expression (a membrane bound metalloprotease in *E.coli*) was induced 1.2-fold in *Tpv* at 60 min after heat shock. HtpX is also induced in *A. fulgidus* (2-fold after 30 min) and in *P. furiosus* upon temperature up-shift [73, 84].

During heat shock, 57% of the heat induced genes were down-regulated while 43% were up-regulated in total of 181 genes by the fold change threshold of  $\geq 1.2$ . A set of down-regulated proteins fell into categories of transcription and translation predicted by cluster of orthogonal genes (COG). During heat-shock we observed down regulation of genes encoding several 50S and 30S ribosomal proteins and genes encoding glycyl-tRNA synthetase and translation initiation factor. Similarly a number of genes encoding transcription factors, RNA polymerase subunit N and some other transcription proteins were down-regulated. Overall, these results indicate a general shut-down of transcription and protein synthesis under heat-stress in parallel to previous reports [110]. According to decreased transcription, genes encoding exosome (involved in mRNA polyadenylation and degradation) was strongly repressed. In our microarray analysis, we observed significant changes in the transcription level of genes related to energy production and conversion. This can be explained by global reduction in cells under heat-shock. On the other hand, induction of genes of amino acid metabolism, lipid metabolism and carbohydrate metabolism points out how crucial is metabolic adaptation to thermal stress as was also observed in *A. fulgidus* [84]. Especially in relation to carbohydrate metabolism, the increased levels of sugar permease (1.410-fold), sugar-binding protein (1.288-fold) and sugar transport permease (1.268-up) indicates an increased demand in ATP during heat stress to maintain energy balance of the cell [73]. In addition, temperature up-shift favored expression of several transport proteins. Proteins of lipid transport and metabolism and proteins associated with membrane biogenesis and cell motility. Differential expression of these genes is probably involved in extracytoplasmic stress response.

Among differentially expressed genes, 56 of the total 181 heat responsive genes were classified as hypothetical proteins by NCBI Protein cluster and 14 of another cluster of genes were not assigned a function in COG category. Many of the hypothetical proteins have shown altered gene expression out of total 56 genes, 36 of them up-regulated while 20 were down-regulated. To be able to reveal the comprehensive heat-shock response regulation in *Tpv* cells, those hypothetical proteins remains to be characterized in structure and function.

***Oxidative stress regulation.*** When the oxygenic photosynthesis evolved about 2.4 billion years ago, it led to formation of protective mechanisms in the cell to prevent the damage of DNA, lipids and proteins by reactive oxygen species (ROS), like hydrogen peroxide and superoxide anion. This prevention was enabled by the synthesis of superoxide dismutase (SOD), catalase, alkyl hydroperoxide reductase (Ahp), therodoxin and glutaredoxin proteins, and glutathione molecule [114].

We have exposed *Tpv* cells to oxidative stress by 0.02 mM H<sub>2</sub>O<sub>2</sub> application into cultures for 60 min. Then the changed mRNA levels were investigated by microarray. 55% of the total 277 genes by the fold change threshold of 1.2 fold ( $\geq 0.3$ ) were down regulated and 45% was up-regulated. As was observed in heat stress, oxidative stress also resulted in down-regulation of genes grouped under ‘energy production and conversion’, ‘transcription and translation’ while ‘carbohydrate transport and metabolism’ related genes were up-regulated. Down regulated genes in those pathways seems to be ‘on hold’ till the cells were detoxified [115].

Our results showed that the genes involved in main detoxification systems related to oxidative stress including ferredoxins, peroxiredoxins, superoxide dismutases, alkyl hydroperoxidases or glutaredoxins [114, 86, 87, 70] were not significantly affected. A large group of genes (26%) were assigned hypothetical proteins and 27 genes were annotated with an unknown function among total 227 responsive transcripts.

Thioredoxin (Trx) plays role in cell defense against oxidative stress in a hyperthermophilic archaea *Pyrococcus horikoshii* and in an aerobic hyperthermophilic archaeon *Aeropyrum pernix* to maintain redox homeostasis [114]. Another study with *Lactobacillus plantarum* has also shown that thioredoxin overproduction improves the tolerance to oxidative stress [115]. One other small protein Glutaredoxin (Grx) also plays a role in cell defense against oxidative stress. Trxs and thioredoxin reductases were found to be widespread in all phylogenetic branches and suggested to be crucial to maintain the cellular homeostasis of an anaerobic bacterium *Bacteroides fragilis* by playing a role in redox system [116]. Superoxide dismutase (SOD) was found in all archaeal complete genome sequences and this enzyme believed to be a key component detoxification system of the cell against oxidative stress [114, 86, 87]. Another gene, putative peroxiredoxin which is also termed alkyl hydroperoxidase, known to catalyze the reduction of hydrogen peroxide to water also takes role in detoxifying ROS [114]. What is intriguing about the expression of these genes in our study was they were slightly induced or down-regulated in response to H<sub>2</sub>O<sub>2</sub> exposure for 1h. The Trx (1.137-fold) was induced while Grx (1.295-fold) was repressed after 60 min oxidative stress. SOD (TVN0061), thioredoxin reductase (TVN1129) and putative peroxiredoxin (TVN1099) were down-regulated 1.304-fold, 1.136-fold and 1.304-fold, respectively. However, another thioredoxin reductase gene (TVN0470) was up-regulated 1.234-fold. Peroxiredoxins exert their role in cells by reducing and detoxifying hydrogen peroxide, peroxy nitrite and various organic hydroperoxides [114]. In our study, different types of peroxiredoxins have shown up-regulation at low levels (TVN0222\_1.110-fold, TVN0286\_1.103-fold and TVN0419\_1.030-fold). On the other hand, expression of the NTP pyrophosphohydrolase gene, that encodes MutT-related oxidative damage repair enzyme was enhanced >1.2-fold (1.233-fold) and may have a critical role in oxidative stress response of the *Tpv* cells [117]. Ferredoxins are iron-sulfur proteins that mediate a wide-range of electron transfer reactions. Down-regulation of ferredoxin in response to H<sub>2</sub>O<sub>2</sub> suggests that this protein is involved in maintaining intracellular redox potentials. Several genes encoding a multi-drug efflux pump was up-regulated up to 1.9-fold. Involvements of cation efflux pumps in resistance against oxidative stress were previously reported for *Methanosarcina barkeri* and obligate anaerob *Bacteroides fragilis* [114, 116].

The lack of consistency in induction or repression of the gene expressions at the same time up to a significant level may depend on the existence of multiple, and overlapping pathways to detoxify reactive oxygen species where the gene expression or regulation differ in time [114]. Therefore still it is worth to study time and concentration dependent H<sub>2</sub>O<sub>2</sub> effect on *Tpv* gene expression to reveal possible involvement of putative antioxidant genes (i.e., superoxide dismutase (TVN0061), putative peroxiredoxin (TVN1099), thioredoxin reductases (TVN1129, TVN0470), thioredoxin (TVN0777), peroxiredoxins (TVN0222, TVN0286, and TVN0419), and glutaredoxin (TVN0202) ) in cellular defense to oxidative

stress. *P. furiosus* transcriptional response has occurred after 30 min of H<sub>2</sub>O<sub>2</sub> exposure up to threefold and 62 ORFs were up-regulated. However, the level of differentially expressed genes decreased to 30 and 10 ORFs after 1h and 2h, respectively [86]. This indicates the importance of time-course investigation of the oxidative stress.

Except TVN0775 (Hsp20 related sHsp) (1.038-fold) and TVN1011, Heat shock protein HtpX (1.203-fold), all heat-shock proteins were down-regulated (most of them  $\geq 1.2$ -fold). This may suggest that anti-stress mechanisms employed by *Tpv* cells to defeat the heat-shock and oxidative stress differ from each other.

Other than the oxidative stress related genes mentioned above, the regulation of oxidative stress response indicates a tight relationship with ABC-type transporters, multidrug efflux permeases and general metabolism genes which reveals a complex system that manage oxidative stress response in *Tpv* cells. By its unique nature adapting to both aerobic and anaerobic environments, *Tpv* might developed alternative pathways with interesting features to protect the cells from the destructive effects of ROS. Therefore, investigation of hypothetical proteins' function can be helpful to fully appreciate the stress regulation of *Tpv* cells under hydrogen peroxide.

**pH stress regulation.** *Tpv* normally grows in the pH range (pH 2.0 to pH 2.7) and is faced with the problem of maintaining its cytosolic pH close to neutrality. To maintain the balance, *Tpv* generates a pH gradient which is dependent on proton extrusion across the membrane. We have examined the influence of pH up-shift (from pH 2.7 to 4.0) on gene expression of *Tpv* cells by microarray analysis. More genes were repressed than were induced in response to pH up-shift. Of the 282 genes differentially expressed by  $\geq 1.2$ -fold by pH stress, 56% of them were identified down-regulated and 44% were up-regulated 60 min after pH change. About 26% of differentially expressed genes were hypothetical proteins and the others were related to amino acid, carbohydrate and lipid transport and metabolisms; energy production and conversion; nucleotide transport and metabolism; replication, recombination and repair; signal transduction; transcription and translation. Transcription and translation related genes were highly repressed indicating a general inhibition of the protein synthesis. Genes belonging to carbohydrate and amino acid transport and metabolism however were all together induced as a response to pH stress.

To the best of our knowledge, there is no report on gene regulation by pH stress in thermoacidophilic archaea till now. However there are studies in bacteria demonstrated that cells adapt to pH changes by regulations in proton transport and membrane permeability. Metabolic switch also serves as a strategy to generate acidic or neutral end-products to maintain the pH homeostasis of the cell [107]. More elaborated version of these strategies for alkaline stress is employed by bacteria can be grouped into four: (1) metabolic acid production, (2) cell wall modification, (3) ATP synthase induction, and (4) increased expression/activity of cation/proton antiporters [118].

The gene expression trend in *Tpv* in response to pH stress has revealed some notable genes related to membrane proteins, sugar and amino acid transporters, cell motility, ATP synthases, cation transport, and antiporters which may have roles in maintaining cellular pH

homeostasis. Especially antiporters are crucial to maintain pH homeostasis which has been shown in *Bacillus subtilis* exposed to alkaline stress.  $\text{Na}^+$  ( $\text{K}^+$ )/ $\text{H}^+$  antiporter that was encoded by *tetA(L)* gene was up-regulated in the cells after pH up-shift [119]. It has been suggested antiporters had to be equipped by sensors to be activated under alkaline up-shifts to maintain pH homeostasis. Failure in activation or shut-off of the antiporters would lead cytoplasmic alkalization or over-acidification and energy depletion, respectively [118]. The  $\text{Ca}^{2+}/\text{Na}^+$  antiporter (TVN0404) was the only antiporter up-regulated by a factor of 1.3-fold according to our microarray data. The same gene was induced 1.4-fold by oxidative stress as well. There were also other genes belonged to the group of inorganic ion transport and metabolism that showed parallel regulation with oxidative stress such as cation transport ATPase (TVN1240) and  $\text{Fe}^{2+}$  uptake regulation protein (TVN0292) which were repressed in both conditions while phosphate permease (TVN0063), major facilitator superfamily permease (TVN1365), arsenite transport permease (TVN0285), and ABC type  $\text{Fe}^{3+}$  siderophores transporter (TVN1048) were induced. The similarity in gene expression profiles for oxidative stress and pH stress was observed for an anaerobic gram negative bacteria *Shewanella oneidensis* [96]. Our results also showed a similarity in differential gene expression profiles of *Tpv* under oxidative stress and pH stress [120].

Heat-shock proteins; chaperonin GroEL, molecular chaperone DnaK, DnaJ and GrpE, prefoldin subunit  $\alpha$  and  $\beta$ , an Hsp 20 related small heat-shock protein were down-regulated under pH stress. Therefore it is not possible to assign a critical role for heat-shock proteins in pH stress response. Three proteases (membrane bound serine protease, and signal peptidase I) together with heat shock protein HtpX were up-regulated. Increased expression of DNA binding proteins upon pH-upshift may be consistent with their role in maintaining negative supercoiling of DNA during pH stress.

Two of the genes belonging to cell motility group, flagellar protein C and E (TVN0608, TVN0609, respectively) were down-regulated after pH stress; however flagellin (TVN1426) was up-regulated by a factor of 1.4-fold. A microarray study conducted in sea water with *E. coli*, has shown that genes related to cell motility were induced by an pH up-shift indicating the organism intended to search for a new niche for survival [118]. In contrast to this, *Tpv* cells' cell motility related genes were down-regulated. This complies with the repression of energy production and conversion related genes. *Tpv* cells seemed to shut-off energy production after prolonged alkaline stress and down-regulated the genes related to cell-motility which would be energy-expensive [118, 120, 121]. We have observed the induction of cell wall biosynthesis glycosyltransferase gene (TVN0876) after alkaline stress up to 1.3-fold which may suggest a modification on the cell wall to regulate proton permeability or repair the damage introduced by external NaOH application similar to *S. oneidensis* [96, 118]. Even the gene induction level was low, when the underestimation of the gene expressions by microarray technique considered, it may have a significant psychological effect in *Tpv* cells to regulate membrane permeability. Also, there were a large number of hypothetical proteins functions of which are not known but expressions are responsive to changes in external pH in this study.

**Comparison of transcriptional response to heat-shock, pH and oxidative stress.** The closest pair clusters of gene expression profiles for three stress conditions indicated that oxidative stress and pH stress profiles are more similar, than heat shock profile. Large number of oxidative stress gene inducible by H<sub>2</sub>O<sub>2</sub> also showed significant pH dependent expression, which indicates a strong connection between pH stress and oxidative stress. The number of overlapping pH dependent and oxidative stress induced genes (total 105 genes) were more than the number of overlapping heat shock-oxidative stress regulated genes (29 genes) and the number of overlapping heat shock-pH stress regulated genes (9 genes) (Figure 4.1).

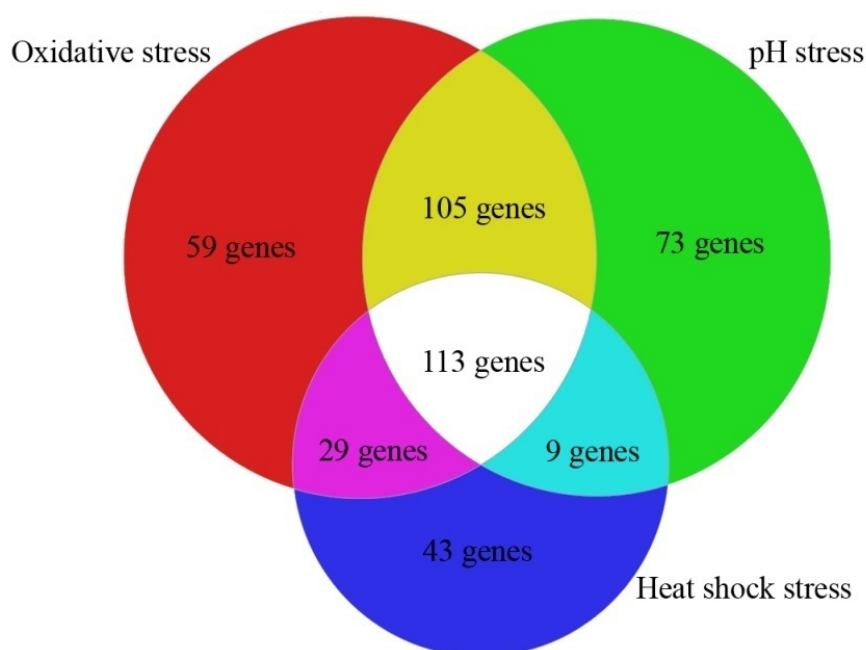


**Figure 4.1 The overlap of resulting up and down regulated genes in Venn diagram.** Within the Venn diagrams, circles represent the main effects of the stressors; oxidative stress (red), pH stress (green) and heat stress (blue). Each compartment represents the number of transcripts that are at  $\geq 1.2$  fold. Control is set as the baseline.

The Venn diagram showed that expressions of 113 genes were commonly affected under three stress conditions. Heat map of mean gene expression values of the 113 genes generated by hierarchical clustering is shown in Figure 4.2. The similarities or differences in gene expression profiles can be also recognized in this map.

When the functional categories of the 113 genes examined, it was found that in general the translation related genes and the genes for transcription and RNA biogenesis were shut-down. Multiple genes associated with efflux pumps and membrane-bound transporters (e.g. transporters of inorganic ion, lipid, amino acid, co-enzyme, carbohydrate) were up-regulated. This may indicate the significance of extracellular defense under three stress conditions.

Increased expression level of DNA repair proteins and nucleic acid binding proteins imply also critical roles for the related genes against stress.

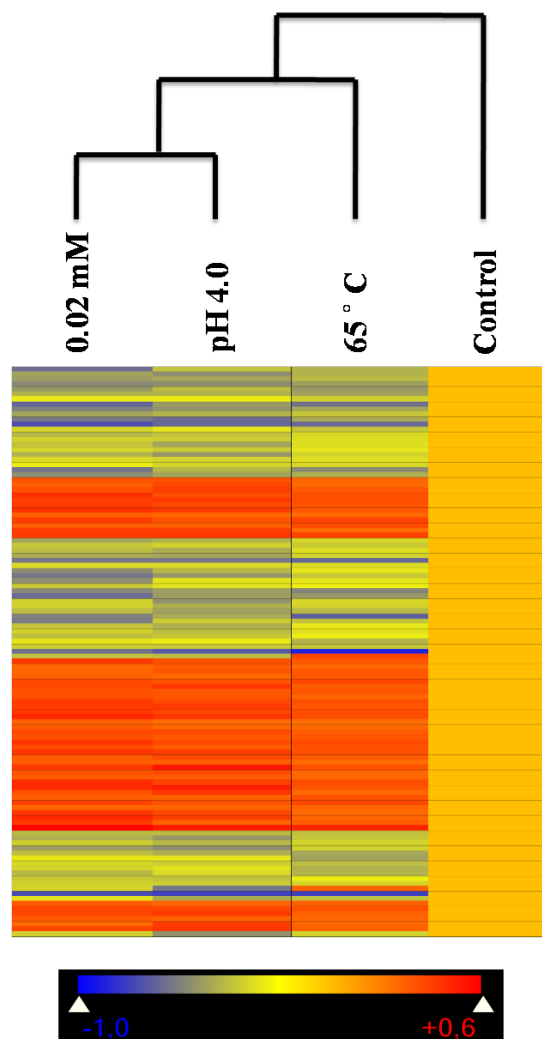


**Figure 4.2** The heat map of mean gene expression values of 113 genes under three stress conditions after 1 h stress exposure with a hierarchical analysis.

**Validation of microarray results using qRT-PCR.** Among the stress responsive genes identified by microarray study, the sugar permease gene which was up-regulated in three stress conditions and GrpE (molecular chaperone) gene which was induced only under heat stress were selected for further analysis by qRT-PCR.

The qRT-PCR experiments were performed under the same stress conditions applied for microarray studies. According to the qRT-PCR results sugar permease gene expression was induced under heat-shock at 65°C (2.5-fold), pH 4.0 (2-fold) and 0.02 mM H<sub>2</sub>O<sub>2</sub> (2-fold) induced stress. This result is consistent with the microarray data that revealed accelerated expression of the sugar permease gene by heat-shock (1.5-fold), pH stress (1.4-fold) and

oxidative stress (1.5-fold). According to qRT-PCR analysis, the GrpE gene transcription was induced under three stress conditions (heat-shock 4-fold, pH stress 1.4 fold, oxidative stress 1.2-fold). Microarray results also indicated increased transcription of the GrpE gene under heat-shock (1.2-fold), but down regulation of the gene under pH and oxidative stress (about 1.3- fold). Two VAT genes, TVN0382 and TVN0947, found to be up regulated under heat stress (1.048-fold and 1.044-fold respectively) and pH stress (1.026-fold and 1.052-fold, respectively), but down regulated under oxidative stress (1.001-fold and 1.042-fold, respectively) by microarray analysis. However, our qRT-PCR results showed that TVN0382 gene expression was induced under three stress conditions (1.4-fold by heat shock, 1.5-fold by pH stress and 1.5-fold by oxidative stress) and TVN0947 gene expression was up-regulated under heat stress (3-fold) and oxidative stress (1.5-fold) but slightly down-regulated (0.9-fold) by pH up-shift. Although these results points to a general agreement between microarray and qRT-PCR results, some contrasting outcomes might be obtained especially when the fold estimations of microarray analysis were insignificant (*i.e.*, <1.2-fold).



## CHAPTER 5

### CONCLUSION

The study presents a comprehensive investigation of two chaperone related VAT genes (TVN0382 and TVN0947), and the global transcriptional response of *Tpv* cells challenged by heat-, pH- and, oxidative-stress. The qRT-PCR data analysis demonstrated that VAT genes were highly induced after a thermal shift from 60°C to 65°C (up to 5.5-fold for TVN0382 and 2.9 for TVN0947). Although TVN0947 gene expression was up-regulated throughout the heat-shock at 65°C for 2 h, TVN0382 gene expression was rapidly increased in the early stages of heat-shock response (initial 30 min). Similarly heat stress at 70°C induced expression of both VAT genes (about 3-fold) for 30 min post-exposure to heat-shock.

The VAT genes' expressions were either did not change or down-regulated under the pH stress conditions we tested, except pH 4.0. The TVN0382 gene expression induced only between 1.5 and 2-fold as compared to control for 2 h after pH stress application. The TVN0947 gene expression decreased gradually but slowly increased up to 1.5 -fold at 120 min post exposure to pH 4.0. Previous study which was conducted in our laboratory has shown that *Tpv* proteasomal 20S  $\alpha$  and  $\beta$  subunit genes were up-regulated (*data is not shown*) under pH stress at pH 4.0. All together these results might indicate that at pH 4.0 up-regulation of the VAT-20S proteasome complex genes should be a critical part of stress response network in *T. volcanium* cells.

Our results indicate that regulation of VAT genes transcription is H<sub>2</sub>O<sub>2</sub> dose-dependant. The TVN0947 gene expression although slightly increased at low H<sub>2</sub>O<sub>2</sub> concentration (i.e., 0.01 mM), at higher H<sub>2</sub>O<sub>2</sub> concentrations either did not change (at 0.02 mM and 0.03 mM H<sub>2</sub>O<sub>2</sub>) or down-regulated (at 0.05 mM H<sub>2</sub>O<sub>2</sub>). The TVN0382 gene transcription seemed to be more sensitive to oxidative stress. Its expression although was not effected at low H<sub>2</sub>O<sub>2</sub> concentration (i.e., 0.01 mM), its transcription induced about 4-fold at 90 min post exposure to 0.02 mM H<sub>2</sub>O<sub>2</sub>.

There was a good agreement between qRT-PCR results and Western Blotting/Hybridization analysis for the selected stress conditions indicating that increased TVN0947 gene expression occurs both at transcription and translation levels.

The microarray analysis showed that, mRNA levels of total 1501 *Tpv* transcripts have changed approximately 14% under heat-shock, and 20% under oxidative and pH stresses. Gene expression profiles revealed a possible connection or similarity between pH stress response and oxidative stress response by the overlap of the genes regulated under these

conditions. However, their expression profiles were different than heat-shock regulated gene expression profile which may indicate a unique strategy for *Tpv* cells to deal with heat stress. Despite the fact that there were stress-specific genes regulated for each stress conditions; up-regulation of gene clusters related to carbohydrate transport and metabolism and down-regulation of transcription and translation related proteins under all stress conditions seemed to be general characteristic of responses against three stressors. This may indicate the repression of overall protein synthesis to prevent error prone protein synthesis and the activation of carbohydrate metabolism to meet the energy need of the cells during stress. Heat stress response was characterized by the induction of heat-shock related stress genes and proteases. Oxidative stress response resulted in changes in gene expression levels of detoxification system related redoxin species. However, the regulation of the well known oxidative stress genes was not consistent. Some of them were up-regulated while the others were down-regulated. This pointed out the existence of multiple and overlapping pathways where the genes' expressions differ in time and level. And finally pH stress response has revealed the importance of regulation of transporters and antiporters in the cell to maintain the pH homeostasis of the cell. Moreover a few cell membrane and cell motility related gene regulations were observed when the cell confronted with pH stress and other stresses, which may imply a critical role for the extracytoplasmic defense.

## REFERENCES

1. Woese RC, Fox EG (1977) Phylogenetic structure of the prokaryotic domain: The primary Kingdoms. *Proc Natl Acad Sci USA* 74: 5088-5090
2. Macario AJ, Lange M, Ahring BK, Conway de Macario E (1999) Stress genes and proteins in the archaea. *Microbiol Mol Biol Rev* 63:923-967
3. Golbik R, Lupas AN, Koretke KK, Baumeister W, Peters J (1999) The Janus face of archaeal Cdc48/p97 homologue VAT: protein folding versus unfolding. *Biol Chem* 380:1049-1062
4. Kumar S, Nussinov R (2001) How do thermophilic proteins deal with heat? *Cell Mol Life Sci* 58:1216-1233
5. Auguet JC, Barberan A, Casamayor EO (2010) Global ecological patterns in uncultured Archaea. *ISME J* 4:182-190
6. Ambily Nath IV, Loka Bharathi PA (2011) Diversity in transcripts and translational pattern of stress proteins in marine extremophiles. *Extremophiles* 15:129-153
7. Sterner R, Liebl W (2001) Thermophilic adaptation of proteins. *Crit Rev Biochem Mol Biol* 36:39-106
8. Jarrell KF, Walters AD, Bochiwal C, Borgia JM, Dickinson T, Chong JP (2011) Major players on the microbial stage: why archaea are important. *Microbiology* 157:919-936
9. Auernik KS, Cooper CR, Kelly RM (2008) Life in hot acid: pathway analyses in extremely thermoacidophilic archaea. *Curr Opin Biotechnol* 19:445-453
10. Walther J, Sierocinski P, Oost van der J (2010) Hot transcriptomics. *Archaea* 897585:1-14
11. Leigh JA, Albers SV, Atomi H, Allers T (2011) Model organisms for genetics in the domain Archaea: methanogens, halophiles, Thermococcales and Sulfolobales. *FEMS Microbiol Rev* 35:577-608

12. Macario AJ, Malz M, Conway de Macario E (2004) Evolution of assisted protein folding: the distribution of the main chaperoning systems within the phylogenetic domain archaea. *Front Biosci* 9:1318-1332
13. Georgopoulos C, Welch WJ (1993) Role of the major heat shock proteins as molecular chaperones. *Annu Rev Cell Biol* 9:601-634
14. Medalia N, Sharon M, Martinez-Arias R, Mihalache O, Robinson CV, Medalia O, Zwickle P (2006) Functional and structural characterization of the *Methanosarcina mazei* proteasome and PAN complexes. *J Struct Biol* 156:84-92
15. Clark JI, Muchowski PJ (2000) Small heat-shock proteins and their potential role in human disease. *Curr Opin Struct Biol* 10:52-59
16. Dantuma PN, Lindsten K (2010) Stressing the ubiquitin-proteasome system. *Cardiovasc Res* 85:263-271
17. Macario AJ, Conway de Macario E (1999) The archaeal molecular chaperone machine: peculiarities and paradoxes. *Genetics* 152:1277-1283
18. Rechsteiner M (2005) Proteasomes: *Encyclopedia of Molecular Cell Biology and Molecular Medicine*. 2nd Edition Weinheim, DE: Wiley-VCH Verlag GmbH&Co
19. Maupin-Furlow JA, Gil MA, Karadzic IM, Kirkland PA, Reuter CJ (2004) Proteasomes: perspectives from the Archaea. *Front Biosci* 9:1743-1758
20. Maupin-Furlow JA, Kaczowka SJ, Reuter CJ, Zuobi-Hasona K, Gil MA (2003) Archaeal proteasomes: potential in metabolic engineering. *Metab Eng* 5:151-163
21. Grimm S, Höhn A, Grune T (2012) Oxidative protein damage and the proteasome. *Amino Acids* 42:23-38
22. Coux O, Tanaka K, Goldberg AL (1996) Structure and function of the 20S and 26S proteasomes. *Annu Rev Biochem* 65:801-847
23. Maupin-Furlow JA, Wilson HL, Kaczowka SJ, Ou MS (2000) Proteasomes in the archaea: from the structure to function. *Front Biosci* 5:837-865
24. Lupas AN, Martin J (2002) AAA proteins. *Curr Opin Struct Biol* 12:46-53
25. Blum P (2001) *Archaea: Ancient Microbes, Extreme Environments and the Origin of Life*. Waltham, USA: Academic Press

26. Zwickl P, Seemüller E, Kapelari B, Baumeister W (2001) The proteasome: a supramolecular assembly designed for controlled proteolysis. *59*:187-222
27. Kopp F, Hendil KB, Dahlmann B, Kristensen P, Sobek A, Uerkvitz W (1997) Subunit arrangement in the human 20S proteasome. *Proc Natl Acad Sci USA* *94*:2939-2944
28. Li D, Li H, Wang T, Pan H, Lin G, Li H (2010) Structural basis for the assembly and gate closure mechanisms of the *Mycobacterium tuberculosis* 20S proteasome. *EMBO J* *29*:2037-2047
29. Groll M, Clausen T (2003) Molecular shredders: how proteasomes fulfill their role. *Curr Opin Struct Biol* *13*:665-673
30. Kocabiyik S, Ozdemir I, Zwickl P, Ozdogan S (2010) Molecular cloning and co-expression of *Thermoplasma volcanium* proteasome subunit genes. *Protein Expr Purif* *73*:223-230
31. Stadtmueller BM, Hill CP (2011) Proteasome activators. *Mol Cell* *41*:8-19
32. Cheng Y, (2009) Toward an atomic model of the 26S proteasome. *Curr Opin Struct Biol* *19*:203-208
33. Mayer RJ, Ciechanover AJ, Rechsteiner M (2006) *Protein Degradation: The Ubiquitin-Proteasome System*. Weinheim, DE: Wiley-VCH Verlag GmbH&Co,
34. Kaczowka SJ, Maupin-Furlow JA (2003) Subunit topology of two 20S proteasomes from *Haloflexax volcanii*. *J Bacteriol* *185*:165-174
35. Chamieh H, Guetta D, Franzetti B (2008) The two PAN ATPases from Halobacterium display N-terminal heterogeneity and form labile complexes with the 20S proteasome. *Biochem J* *411*:387-397
36. Benaroudj N, Goldberg AL (2000) PAN, the proteasome-activating nucleotidase from archaeobacteria, is a protein-unfolding molecular chaperone. *Nat Cell Biol* *2*:833-839
37. Mayer RJ, Ciechanover AJ, Rechsteiner M (2005) *Protein Degradation: Ubiquitin and The Chemistry of Life*. Weinheim, DE: Wiley-VCH GmbH&Co
38. Lander GC, Estrin E, Matyskiela ME, Bashore C, Nogales E, Martin A (2012) Complete subunit architecture of the proteasome regulatory particle. *Nature* *482*:186-191
39. Finley D (2009) Recognition and processing of ubiquitin-protein conjugates by the proteasome. *Annu Rev Biochem* *78*:477-513

40. Chamieh H, Marty V, Gueatta D, Perollier A, Franzetti B (2012) Stress regulation of the PAN-proteasome system in the extreme halophilic archaeon Halobacterium. *Extremophiles* 16:215-225
41. Bedford L, Paine S, Sheppard PW, Mayer RJ, Roeflofs J (2010) Assembly, structure, and function of the 26S proteasome. *Trends Cell Biol* 20:391-401
42. Jung T, Catalgol B, Grune T (2009) The proteasomal system. *Mol Aspects Med* 30:191-296
43. Hipp MS, Bersuker K, Kopito RR (2012) Live-cell imaging of ubiquitin-proteasome system function. *Methods Mol Biol* 832:463-472
44. Kish-Trier E, Hill CP (2013) Structural Biology of the Proteasome. *Annu Rev Biophys* 42:1.1-1.21
45. Finley D, Ulrich HD, Sommer T, Kaiser P (2012) The Ubiquitin-Proteasome system *Saccharomyces cerevisiae*. *Genetics* 192:319-360
46. Schrader EK, Harstad KG, Matouschek A (2009) Targeting proteins for degradation. *Nat Chem Biol* 5:815-822
47. Tanaka K (2009) The proteasome: overview of structure and functions. *Proc Jpn Acad Ser B Phys Biol Sci* 85:12-36
48. Forouzan D, Ammelburg M, Hobel CF, Ströh LJ, Sessler N, Martin J, Lupas AN (2012) The archaeal proteasome is regulated by a network of AAA ATPases. *J Biol Chem* 287:39254-39262
49. Rockel B, Walz J, Hegerl R, Peters J, Typke D, Baumeister W (1999) Structure of VAT, a CDC48/p97 ATPase homologue from the archaeon *Thermoplasma acidophilum* as studied by electron tomography. *FEBS Letter* 451:27-32
50. Coles M, Direcks T, Liermann J, Gröger A, Rockel B, Baumeister W, Koretke KK, Lupas A, Peters J, Kessler H (1999) The solution structure of VAT-N reveals a missing link in the evolution of complex enzymes from a simple  $\beta\alpha\beta$  element. *Current Biology* 9:1158-1168
51. Thoms S (2002) Cdc48 can distinguish between native and non-native proteins in the absence of cofactors. *FEBS Lett* 520:107-110
52. Horwitz AA, Navon A, Groll M, Smith DM, Reis C, Goldberg AL (2007) ATP-induced structural transitions in PAN, the proteasome-regulatory ATPase complex in Archaea. *J Biol Chem* 282:22921-22929

53. Rockel B, Guckenberger R, Gross H, Tittmann P, Baumeister W (2000) Rotary and unidirectional metal shadowing of VAT: localization of the substrate-binding domain. *J Struct Biol* 132:162-168
54. Medalia N, Beer A, Zwickl P, Mihalache O, Beck M, Medalia O, Navon A (2009) Architecture and molecular mechanism of PAN, the archaeal proteasome regulatory ATPase. *J Biol Chem* 284:22952-22960
55. Benaroudj N, Zwickl P, Seemüller E, Baumeister W, Goldberg AL (2003) ATP hydrolysis by the proteasome regulatory complex PAN serves multiple functions in protein degradation. *Mol Cell* 11:69-78
56. Striebel F, Kress W, Weber-Ban E (2009) Controlled destruction: AAA+ ATPases in protein degradation from bacteria to eukaryotes. *Curr Opin Struct Biol* 19:209-217
57. Smith DM, Kafri G, Cheng Y, Ng D, Walz T, Goldberg AL (2005) ATP binding to PAN or the 26S ATPases causes association with the 20S proteasome, gate opening, and translocation of unfolded proteins. *Mol Cell* 20:687-698
58. Yu Y, Smith DM, Kim HM, Rodrigues V, Goldberg AL, Cheng Y (2010) Interactions of PAN's C-termini with archaeal 20S proteasome and implications for the eukaryotic proteasome-ATPase interactions. *J Biol Chem* 285:692-702
59. Mayer RJ, Ciechanover AJ, Rechsteiner M (2006) *Protein Degradation: Cell Biology of the Ubiquitin-Proteasome System*. Weinheim, DE: Wiley-VCH Verlag GmbH&Co
60. Barthelme D, Sauer RT (2012) Identification of the Cdc48-20S proteasome as an ancient AAA+ proteolytic machine. *Science* 337:843-846
61. Franz A (2012) Role of the ubiquitin selective CDC-48 UFD-1/NPL-4 Chaperone in DNA Replication. Unpublished doctoral dissertation, University of Köln, Köln, Germany
62. Beskow A, Grimberg KB, Bott LC, Salomons FA, Dantuma NP, Young P (2009) A conserved unfoldase activity for the p97 AAA-ATPase in proteasomal degradation. *J Mol Biol* 394:732-746
63. Rockel B, Jakana J, Chiu W, Baumeister W (2002) Electron cryo-microscopy of VAT, the archaeal p97/CDC48 homologue from *Thermoplasma acidophilum*. *J Mol Biol* 17:673-381
64. Matouschek A, Finley D (2012) An ancient portal to proteolysis. *Science* 337:813-814

65. Ruepp A, Graml W, Santos-Martinez ML, Koretke KK, Volker C, Mewes HW, Frishman D, Stocker S, Lupas AN, Baumeister W (2000) The genome sequence of the thermoacidophilic scavenger *Thermoplasma acidophilum*. *Nature* 407:508-513
66. Pamnani V, Tamure T, Lupas A, Peters J, Cejka Z, Ashraf W, Baumeister W (1997) Cloning, sequencing and expression of VAT, a CDC48/p97 ATPase homologue from the archaeon *Thermoplasma acidophilum*. *FEBS Lett* 404:263-268
67. Ruepp A, Rockel B, Gutsche I, Baumeister W, Lupas AN (2001) The Chaperones of the archaeon *Thermoplasma acidophilum*. *J Struct Biol* 135:126-138
68. Niwa H, Ewens CA, Tsang C, Yeung HO, Zhang X, Freemont PS (2012) The role of the N-domain in the ATPase activity of the mammalian AAA ATPase p97/VCP. *J Biol Chem* 287:8561-8570
69. Gerega A, Rockel B, Peters J, Tamura T, Baumeister W, Zwickl P (2005) VAT, the *Thermoplasma* homolog of mammalian p97/VCP, is an N-domain regulated protein unfoldase. *J Biol Chem* 280:42856-42862
70. Aike CT, Kaake RM, Wang X, Huang L (2011) Oxidative stress-mediated regulation of proteasome complexes. *Mol Cell Proteomics* 10:R110.006924
71. Medicherla B, Goldberg AL (2008) Heat shock and oxygen radicals stimulate ubiquitin-dependent degradation mainly of newly synthesized proteins. *J Cell Biol* 182:663-673
72. Ruepp A, Eckerskorn C, Bogyo M, Baumeister W (1998) Proteasome function is dispensable under normal but not under heat shock conditions in *Thermoplasma acidophilum*. *FEBS Lett* 425:87-90
73. Shockley KR, Ward DE, Chhabra SR, Connors SB, Montero CI, Kelly RM (2003) Heat Shock response by the hyperthermophilic archaeon *Pyrococcus furiosus*. *Appl Environ Microbiol* 69:2365-2371
74. Sun N, Beck F, Knispel RW, Siedler F, Scheffer B, Nickell S, Baumeister W, Nagy I (2007) Proteomics analysis of *Thermoplasma acidophilum* with a focus on protein complexes. *Mol Cell Proteomics* 6:492-502
75. Zhou G, Kowalczyk D, Humbard MA, Rohatgi S, Maupin-Furlow JA (2008) Proteasomal components required for cell growth and stress responses in the haloarchaeon *Haloferax volcanii*. *J Bacteriol* 190:8096-8105
76. Pan W, Lin J, Le CT (2002) How many replicates of arrays are required to detect gene expression changes in microarray experiments? A mixture model approach. *Genome Biol* 3:reserach0022

77. Bassett DE Jr, Eisen MB, Boguski MS (1999) Gene expression informatics-it's all in your mine. *Nat Genet* 21:51-55
78. Kothapalli R, Yoder SJ, Mane S, Loughran TP (2002) Microarray results: how accurate are they? *BMC Bioinformatics* 3:22
79. Simon RM, McShane LM, Wright GW, Korn EL, Radmacher MD, Zhao Y (2004) *Design and Analysis of DNA Microarray Investigations*. USA: Springer
80. <http://www.nimblegen.com/company/technology/index.html> (last visited on 04/05/2013)
81. Derisi J (2001) Overview of nucleic acid arrays. *Curr Protoc Mol Biol* 49:22.1.1-22.1.7
82. Papatheodorou I, Sergot M, Randall M, Stewart GR, Robertson BD (2004) Visualization of microarray results to assist interpretation. *Tuberculosis* 84:275-281
83. Trauger SA, Kalisak E, Kalisiak J, Morita H, Weinberg MV, Menon AL, Poole FL, Adams MW, Siuzdak G (2008) Correlating the transcriptome, proteome and metabolome in the environmental adaptation of a hyperthermophile. *J Proteome Res* 7:1027-1035
84. Rohlin L, Trent JD, Salmon K, Kim U, Gunsalus RP, Liao JC (2005) Heat shock response of *Archaeoglobus fulgidus*. *J Bacteriol* 187:6046-6057
85. Cooper CR, Daugherty AJ, Tachdjian S, Blum PH, Kelly RM (2009) Role of vapBC toxin-antitoxin loci in the thermal stress response of *Sulfolobus solfataricus*. *Biochem Soc Trans* 37:123-126
86. Strand KR, Sun C, Li T, Jenny FE, Schut GJ, Adams MW (2010) Oxidative stress protection and the repair response to hydrogen peroxide in the hyperthermophilic archaeon *Pyrococcus furiosus* and in related species. *Arch Microbiol* 192:447-459
87. Kaur A, Van PT, Busch CR, Robinson CK, Pan M, Pang WL, Reiss DJ, DiRuggiero J, Baliga NS (2010) Coordination of frontline defense mechanisms under severe oxidative stress. *Mol Syst* 6:393
88. Sharma K, Gillum N, Boyd JL, Schmid A (2012) The RosR transcription factor is required for gene expression dynamics in response to extreme oxidative stress in a hypersaline-adapted archaeon. *BMC Genomics* 13:351
89. Williams E, Lowe TM, Savas J, DiRuggiero J (2007) Microarray analysis of the hyperthermophilic archaeon *Pyrococcus furiosus* exposed to gamma irradiation. *Extremophiles* 11:19-29

90. Lagorce A, Fourçans A, Dutertre M, Bouyssiere B, Zivanovic Y et. al. (2012) Genome-Wide Transcriptional Response of the Archaeon *Thermococcus gammatolerans* to cadmium. Plos ONE 7:e41935
91. Hovey R, Lentjes S, Ehrenreich A, Salmon K, Saba K, Gottschalk G, Gunsalus RP, Deppenmeier U (2005) DNA microarray analysis of *Methanosarcina mazei* Gö1 reveals adaptation to different methanogenic substrates. Mol Genet Genomics 273:225-239
92. Xia Q, Hendrickson EL, Zhang Y, Wang T, Taub F, Moore BC, Porat I, Whitman WB, Hackett M, Leigh JA (2006) Quantitative proteomics of the archaeon *Methanococcus marisaludis* validated by microarray analysis and real time PCR. Mol Cell Proteomics 5:868-881
93. Lange C, Zaigler A, Hammelmann M, Twellmeyer J, Raddatz G, Schuster SC, Oesterhelt D, Soppa J (2007) Genome-wide analysis of growth phase-dependent translational and transcriptional regulation in halophilic archaea. BMC Genomics 8:415
94. Duggan DJ, Bittner M, Chen Y, Meltzer P, Trent JM (1999) Expression profiling using cDNA microarrays. Nat Genet 21:10-14
95. Morey JS, Ryan JC, Van Dolah FM (2006) Microarray validation: factors influencing correlation between oligonucleotide microarrays and real-time PCR. Biol Preced Online 8:175-193
96. Leaphart AB, Thompson DK, Huang K, Alm E, Wan XF, Arkin A, Brown SD, Wu L, Yan T, Liu X, Wickham GS, Zhou J (2006) Transcriptome profiling of *Shewanella oneidensis* gene expression following exposure to acidic and alkaline pH. J Bacteriol 188:1633-1642
97. Chuaqui RF, Bonner RF, Best CJ, Gillespie JW, Flaig MJ, Hewitt SM, Phillips JL, Krizman DB, Tangrea MA, Ahram M, Linehan WM, Knezevic V, Emmert-Buck MR (2002) Post-analysis follow-up and validation of microarray experiments. Nat Genet 32:509-514
98. Segerer A, Langworthy TA, Stetter KO (1988) *Thermoplasma acidophilum* and *Thermoplasma volcanium* sp. nov. from solfataras fields. Syst Appl Microbiol 10:161-171
99. Kawashima T, Amano N, Koike H, Makino S, Higuchi S, Kawashima-Ohya Y, Watanabe K, Yamazaki M, Kanehori K, Kawamoto T, Nunoshiro T, Yamamoto Y, Aramaki H, Makino K, Suzuki M (2000) Archaeal adaptation to higher temperatures revealed by genomic sequence of *Thermoplasma volcanium*. Proc Natl Acad Sci USA 97:14257-14262

100. Kawashima T, Yamamoto Y, Aramaki H, Nunoshiro T, Kawamoto T, Watanabe K, Yamazaki M, Kanehori K, Amano N, Ohya Y, Makino K, Suzuki M (1999) Determination of the complete genomic DNA sequence of *Thermoplasma volcanium* GSS 1. *Proc Japan Acad* 75:213-218
101. Siddiqui KS, Thomas T (2008) Protein adaptation in extremophiles. Nova Science Publishers
102. Faguy DM, Bayley DP, Kostyukova AS, Thomas NA, Jarrell KF (1996) Isolation and characterization of flagella and flagellin proteins from the *Thermoacidophilic* archaea, *Thermoplasma volcanium* and *Sulfolobus shibatae*. *J Bacteriol* 178:902-905
103. Robb FT, Place AR (1995) Archaea: A laboratory manual. New York, ABD: Cold Spring Harbor Laboratory Press
104. Livak KJ, Schmittgen TD (2001) Analysis of relative gene expression data using real-time quantitative PCR and the 2(-Delta Delta C(T)) Method. *Methods* 25:402-408
105. Rustici G, Kauffmann A (2009) Microarray data analysis with Bioconductor. EMBL-EBI Tutorial:1-14
106. Gentleman R, Carey V, Huber W, Irizarry R, Dudoit S (2005) Bioinformatics and Computational Biology Solutions Using R and Bioconductor. USA: Springer
107. Slonczewski JL, Fujisawa M, Dopson M, Krulwich TA (2009) Cytoplasmic pH measurement and homeostasis in bacteria and archaea. *Adv Microb Physiol* 55:1-79
108. Sheikh MS, Fornace Jr AJ (1999) Regulation of translation initiation following stress. *Nature* 18: 6121-6128
109. Peeters E, Charlier D (2010) The Lrp family of transcription regulators in archaea. *Archaea* 2010:750457
110. Koide T, Vencio RZN, Gomes SL (2006) Global gene expression analysis of the heat shock response in the phytopathogen *Xylella fastidiosa*. *J Bacteriol* 188:5821-5830
111. Vierke G, Engelmann A, Hebbeln C, Thomm M (2003) A novel archaeal transcriptional regulator of heat shock response. *J Biol Chem* 3:18-26
112. Kagawa HK, Yaoi T, Brocchieri L, McMillan RA, Alton T, Trent JD (2003) The composition, structure and stability of a group II chaperonin are temperature regulated in a hyperthermophilic archaeon. *Mol Microbiol* 48:143-156

113. Tachdjian S, Kelly RM (2006) Dynamic Metabolic Adjustments and Genome Plasticity are implicated in the heat shock response of the extremely thermoacidophilic archaeon *Sulfolobus solfataricus*. *J Bacteriol* 188:4553-4559
114. Pedone E, Bartolucci S, Fiorentino G (2004) Sensing and adapting to environmental stress: the archaeal tactic. *Front Biosci* 1:2909-2926
115. Serrano LM, Molenaar D, Wels M, Teusink B, Bron AP, Vos de WM, Smid EJ (2007) Thioredoxin reductase is a key factor in the oxidative stress response of *Lactobacillus plantarum* WCFS1. *Microb Cell Fact* 6:29
116. Rocha ER, Tzianabos AO, Smith CJ (2007) Thioredoxin reductase is essential for thiol/disulfide redox control and oxidative stress survival of the anaerobe *Bacteroides fragilis*. *J Bacteriol* 189:8015-8023
117. Lu LD, Sun Q, Fan XY, Zhong Y, Yao YF, Zhao GP (2010) Mycobacterial MazG is a novel NTP pyrophosphohydrolase involved in oxidative stress response. *J Biol Chem* 285:28076-28085
118. Padan E, Bibi E, Ito M, Krulwich TA (2005) Alkaline pH homeostasis in bacteria: new insights. *Biochem Biophys Acta* 1717:67-88
119. Wiegert T, Homuth G, Versteeg S, Schumann W (2001) Alkaline shock induces the *Bacillus subtilis* sigma (W) regulon. *Mol Microbiol* 41:59-71
120. Maurer LM, Yohannes E, Bondurant SS, Radmacher M, Slonczewski JL (2005) pH regulates genes for flagellar motility, catabolism and oxidative stress in *Escherichia coli* K-12. *J Bacteriol* 187:304-319
121. Stolyar S, He Q, Joachimiak MP, He Z, Yang Z, Borglin SE, Huang K, Joyner D, Alm E, Hazen TC, Zhou J, Wall JD, Arkin AP, Stahl DA (2007) Response of *Desulfovibrio vulgaris* to alkaline stress. *J Bacteriol* 189:8944-8952

## APPENDIX A

### BUFFERS AND SOLUTIONS

MOPS (M.W. 209.3 g/lt/M) .....	20.93 g
50 mM NaOAc (M.W. 82.039 g/lt/M) .....	2.050 g
10 mM EDTA (M.W. 372.24 g/lt/M) .....	1.861 g
Adjust pH with NaOH.	

#### **5XRNA Loading Buffer (5 ml)**

Saturated bromophenol blue solution.....	8 $\mu$ l
500 mM EDTA (pH 8.0).....	40 $\mu$ l
Glycerol (100%).....	1 ml
Autoclave the mixture at 121°C for 20 minutes. Then add;	
12.3 M Formaldehyde (37%).....	360 $\mu$ l
Formamide.....	1.542 ml
10XFA Gel buffer.....	2 ml
RNase-free water.....	to 5 ml

#### **1XFA Equilibration Buffer (1000 ml)**

10XFA Gel buffer.....	100 ml
Formaldehyde.....	20 ml
RNase-free water.....	880 ml

### **Formaldehyde (FA) Agarose Gel (1.2%)**

Agarose.....	0.48 g
10XFA Buffer.....	4 ml
RNase free water.....	to 40 ml
Stir and heat at 150°C. Let it cool down. Right before pouring into tank, add;	
Formaldehyde.....	720 µl
EtBr.....	5 µl

### **SDS Running Buffer (500 ml) (pH 8.7)**

Tris.....	3.02 g
Glycin.....	14.4 g
SDS.....	1 g

No adjustment for pH.

### **SDS Gel Preparation**

	<b><u>Separating Gel (12%)</u></b>	<b><u>Stacking Gel (5%)</u></b>
ddH <sub>2</sub> O.....	1.2 ml.....	870 µl
Acrylamide/Bis-acrylamide.....	2.4 ml.....	330 µl
Tris, pH 8.9.....	1.2 ml (1.88 M).....	400 µl (0.625 M)
SDS (0.5%).....	1.2 ml.....	400 µl
Ammonium persulfate (10%).....	30 µl.....	10 µl
TEMED.....	5 µl.....	3 µl

### **Buffers for Semi-dry Transfer of Proteins**

#### **Anode Buffer I (100 ml) (pH 10.4)**

Tris.....	3.63 g
Methanol (100%).....	10 ml

#### **Anode Buffer II (200 ml) (pH 10.4)**

Tris.....	0.61 g
Methanol (100%).....	20 ml

#### **Cathode Buffer II (200 ml) (pH 9.4)**

Tris.....	0.61 g
Glycine.....	0.375 g
Methanol (100%).....	20 ml

No adjustment for pH. Concentrations were finalized by adding distilled water.

### **Immunodetection**

Blocking solution for diluting antibody;

BSA (Bovine Serum Albumin).....	1% (w/v)
Tween-20.....	0.05%

### **Staining Solution**

200 µl of NBT/ BCIP stock solution was applied to 10 ml 0.1 M Tris-HCl, pH 9.5 (20°C), 0.1 M NaCl, 0.05 M MgCl<sub>2</sub>.



## APPENDIX B

### LADDER IMAGES

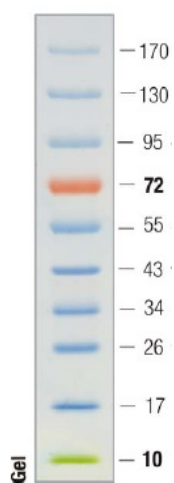


**Figure B.1** PageRuler™ Prestained Protein Ladder, Fermentas

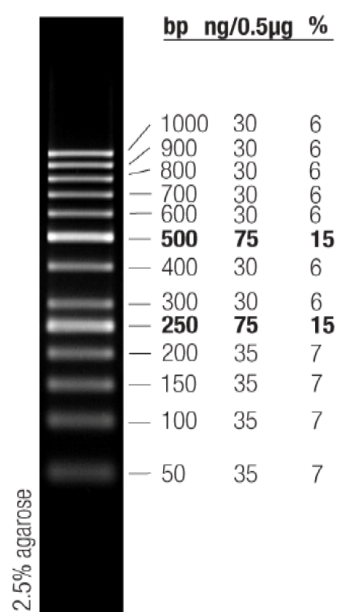


**Figure B. 2** Thermo Scientific Gene Ruler 50bp DNA Ladder, Fermentas

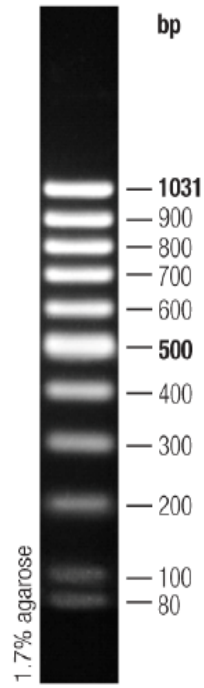


**Figure B.3** Thermo Scientific MassRuler Low Range DNA Ladder, Fermentas

## APPENDIX C

### AMPLIFICATION AND MELTING CURVES

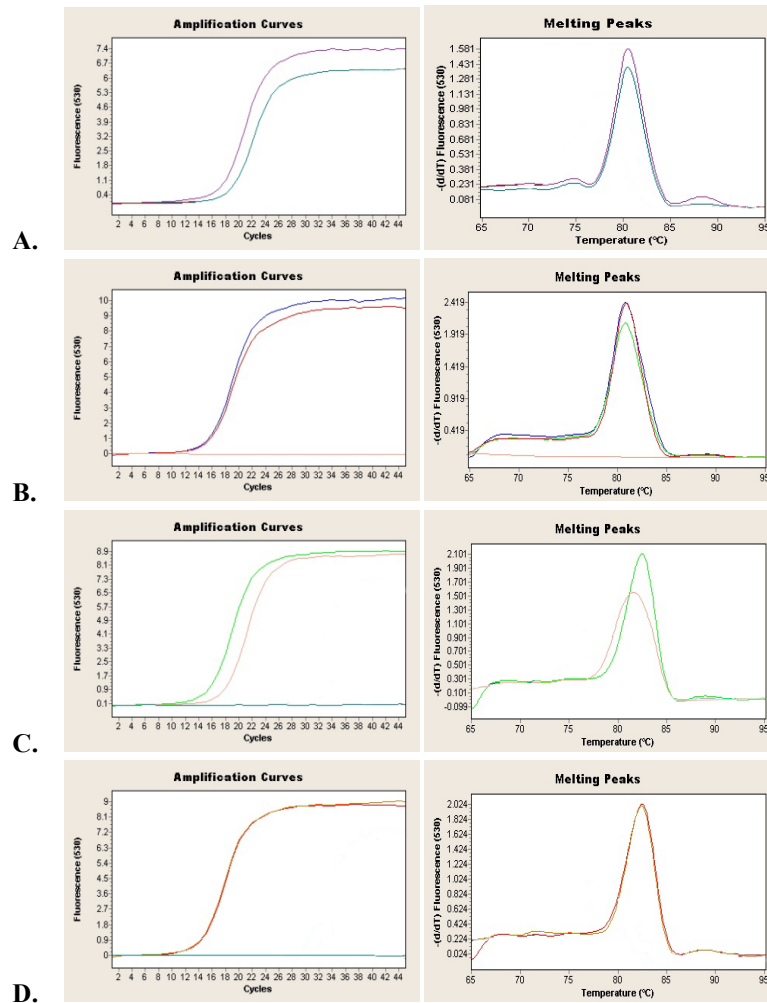


**Figure C.1 Real-time PCR amplification and melting curves for TVN0382 gene under heat-shock** **A.** Heat stress at 65°C for 90'. Amplification curves (purple—test, green—control), Melting curves (purple—test, green—control). **B.** Heat stress at 65°C for 120'. Amplification curves (blue—test, red—control, pink—negative control), Melting curves (blue—test, red—control, pink—negative control). **C.** Heat stress at 70°C for 60'. Amplification curves (light green—test, pink—control, green—negative control), Melting curves (light green—test, pink—control). **D.** Heat stress at 70°C for 120'. Amplification curves (red—test, brown—control, green—negative control), Melting curves (red—test, brown—control).

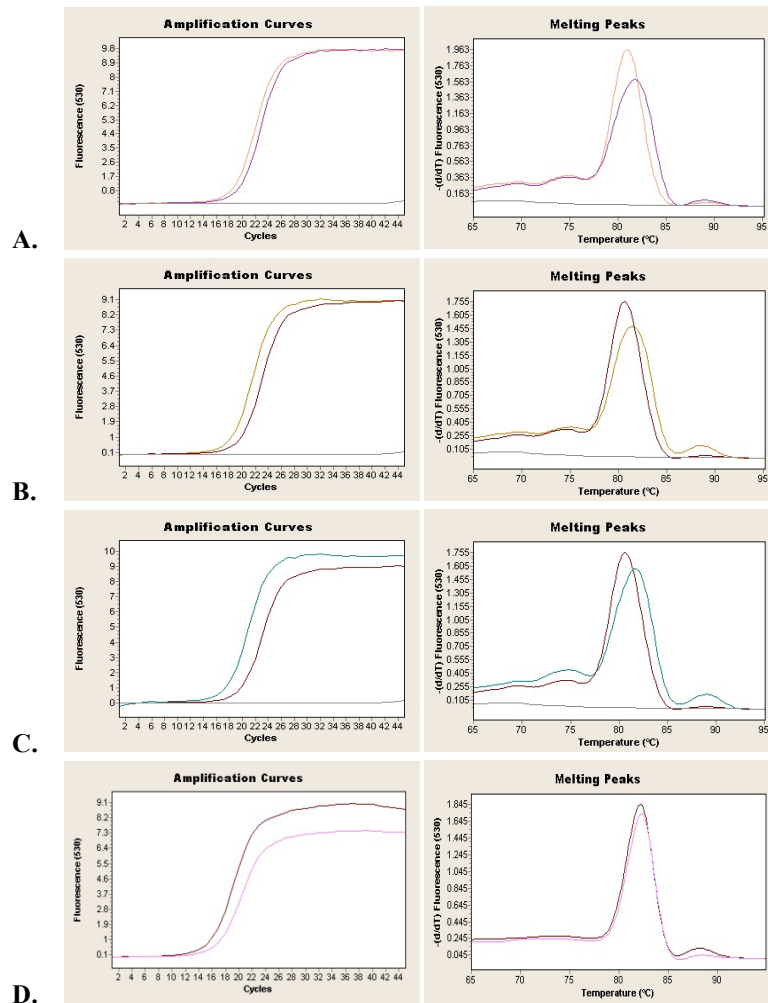


**Figure C.2 Real-time PCR amplification and melting curves for TVN0382 gene under pH stress.** **A.** pH stress at pH 4.0 for 60'. Amplification curves (pink—test, purple—control, grey—negative control), Melting curves (pink—test, purple—control, grey—negative control). **B.** pH stress at pH 4.0 for 90'. Amplification curves (light brown—test, dark red—control, grey—negative control), Melting curves (light brown—test, dark red—control, grey—negative control). **C.** pH stress at pH 4.0 for 120'. Amplification curves (green—test, dark red—control, grey—negative control), Melting curves (green—test, dark red—control, grey—negative control). **D.** pH stress at pH 5.0 for 120'. Amplification curves (brown—test, pink—control), Melting curves (brown—test, pink—control).

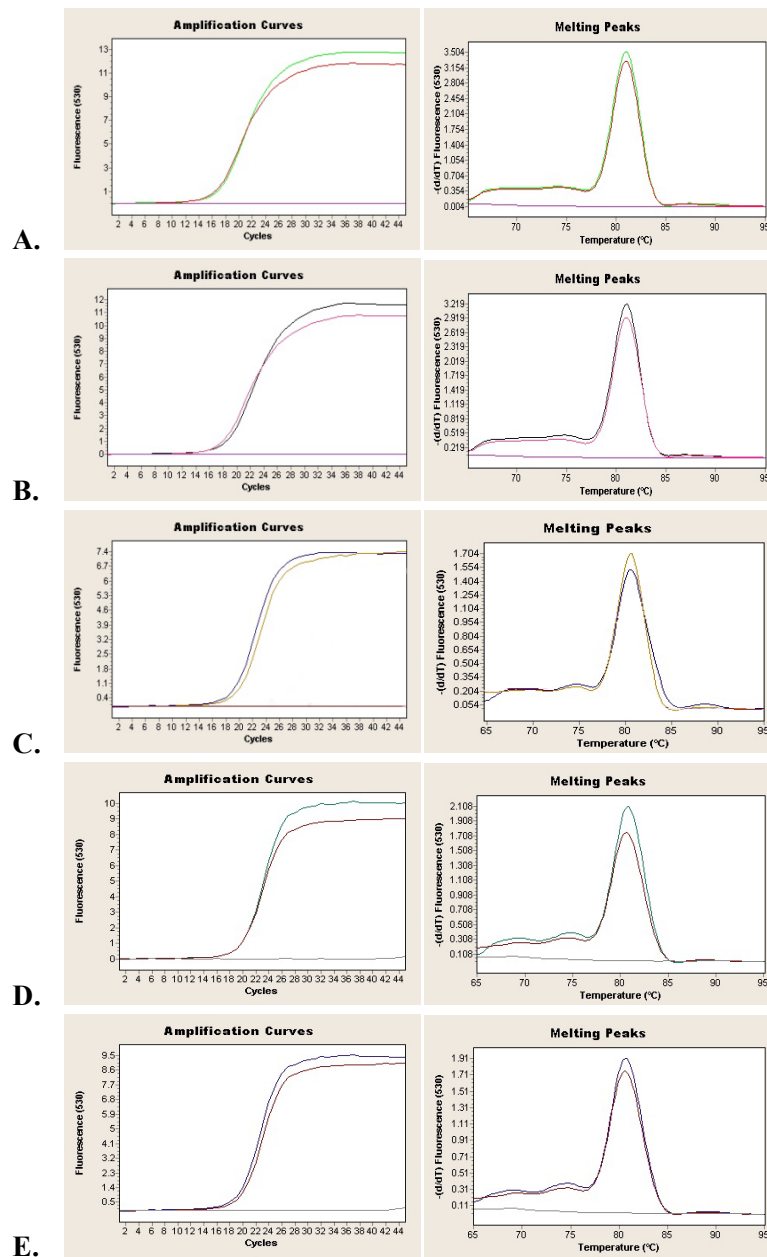


**Figure C.3 Real-time PCR amplification and melting curves for TVN0382 gene under oxidative stress.** **A.** Oxidative stress at 0.01 mM for 90'. Amplification curves (green—test, red—control, purple—negative control), Melting curves (green—test, red—control). **B.** Oxidative stress at 0.01 mM for 120'. Amplification curves (black—test, pink—control, purple—negative control), Melting curves (black—test, pink—control, purple—negative control). **C.** Oxidative stress at 0.02 mM for 30'. Amplification curves (dark blue—test, light brown—control, dark red—negative control), Melting curves (dark blue—test, light brown—control). **D.** Oxidative stress at 0.02 mM for 90'. Amplification curves (green—test, dark red—control, grey—negative control), Melting curves (green—test, dark red—control, grey—negative control). **E.** Oxidative stress at 0.02 mM for 120'. Amplification curves (blue—test, dark red—control, grey—negative control), Melting curves (blue—test, dark red—control, grey—negative control).

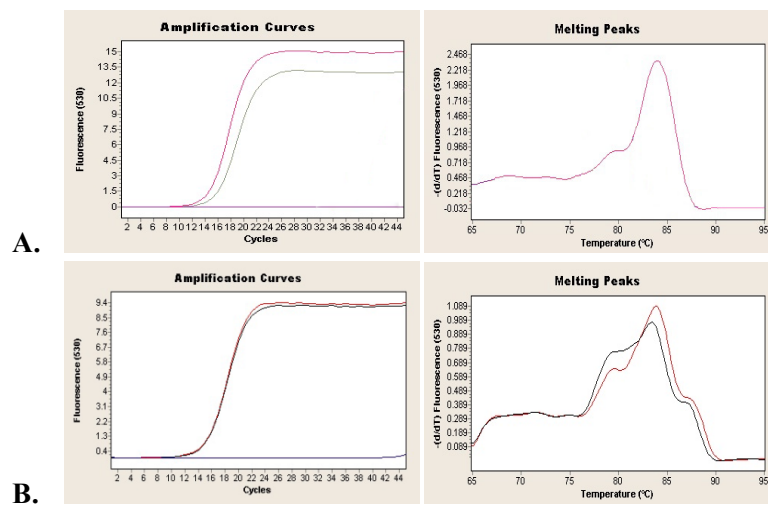


**Figure C.4 Real-time PCR amplification and melting curves for TVN0947 gene under heat-shock. A.** Heat stress at 70°C for 60'. Amplification curves (pink—test, grey—control, purple—negative control), Melting curves (pink—test ) **B.** Heat stress at 70°C for 90'. Amplification curves (red—test, black—control, blue—negative control), Melting curves (red—test, black—control, blue—negative control).

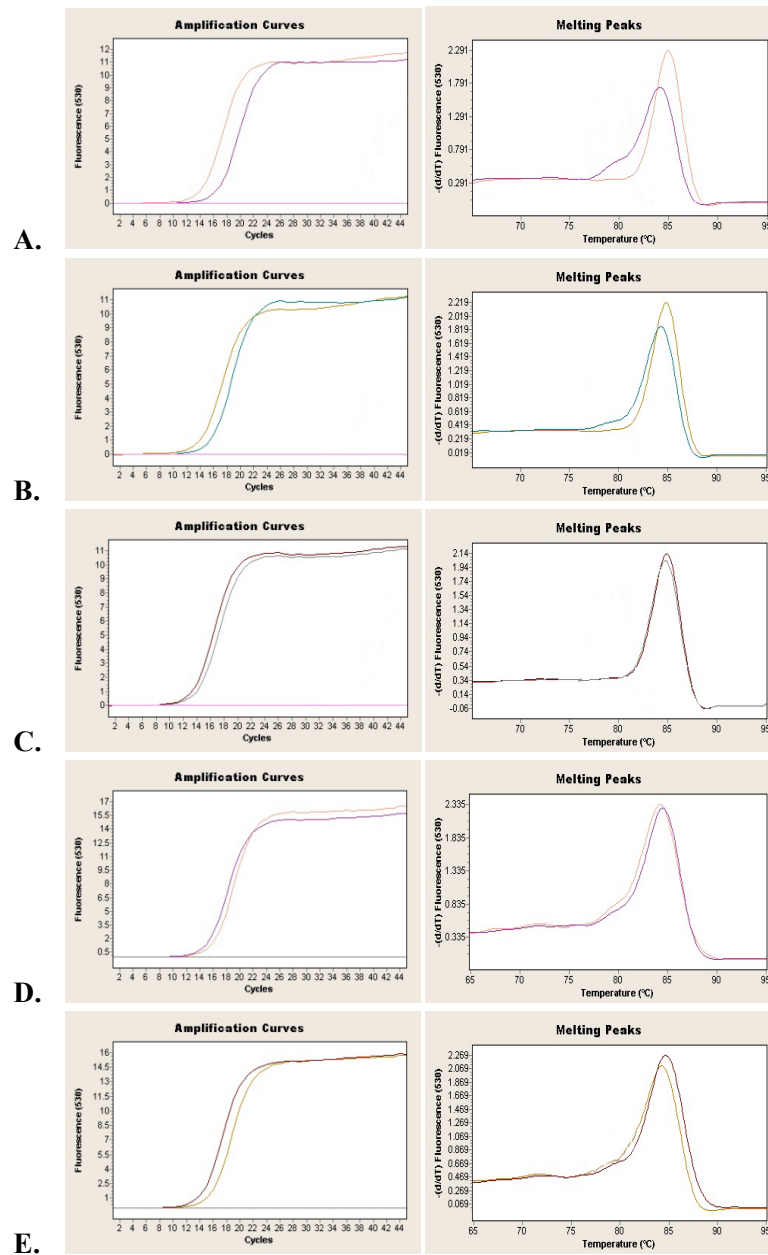


**Figure C.5 Real-time PCR amplification and melting curves for TVN0947 gene under pH stress.** **A.** pH stress at pH 4.0 for 60'. Amplification curves (pink—test, purple—control, pink—negative control), Melting curves (pink—test, purple—control). **B.** pH stress at pH 4.0 for 90'. Amplification curves (light brown—test, green—control, pink—negative control), Melting curves (light brown—test, green—control). **C.** pH stress at pH 4.0 for 120'. Amplification curves (dark red—test, grey—control, pink—negative control), Melting curves (dark red—test, grey—control). **D.** pH stress at pH 5.0 for 30'. Amplification curves (pink—test, purple—control, grey—negative control), Melting curves (pink—test, purple—control). **E.** pH stress at pH 5.0 for 90'. Amplification curves (light brown—test, dark red—control, grey—negative control), Melting curves (light brown—test, dark red—control).

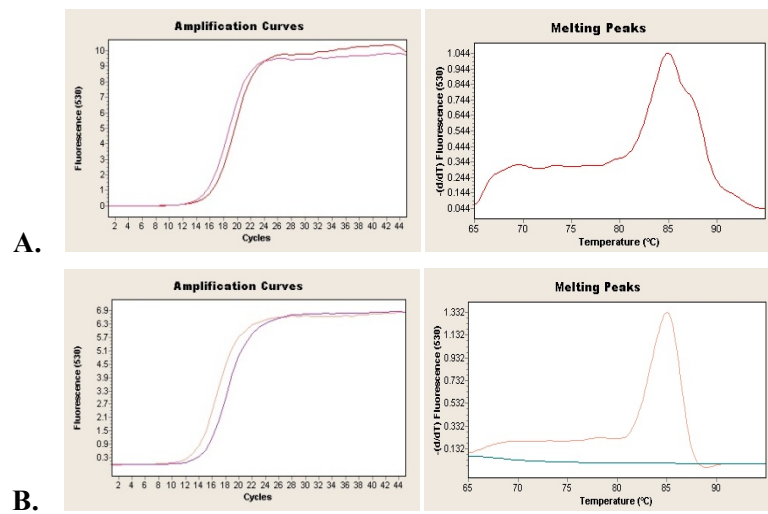


**Figure C.6 Real-time PCR amplification and melting curves for TVN0947 gene under oxidative stress. A.** Oxidative stress at 0.02 mM for 30'. Amplification curves (red—test, purple—control), Melting curves (red—test). **B.** Oxidative stress at 0.02 mM for 90'. Amplification curves (light pink—test, purple—control), Melting curves (light pink—test, green—negative control).

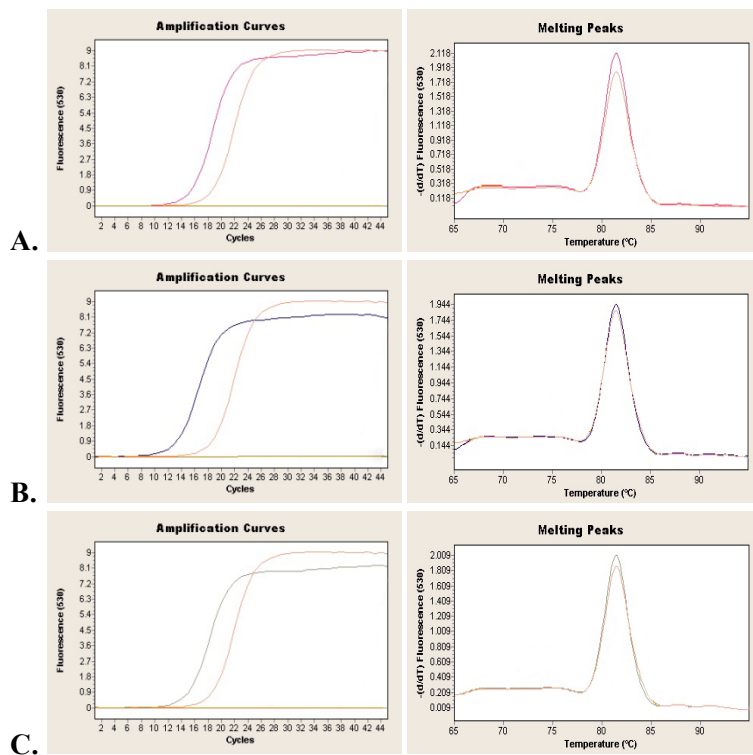


**Figure C.7 Real-time PCR amplification and melting curves for TVN0489 gene under heat-shock (65°C).** **A.** Heat stress at 65°C for 30'. Amplification curves (pink—test, light pink—control, light brown—negative control), Melting curves (pink—test, light pink—control). **B.** Heat stress at 65°C for 90'. Amplification curves (blue—test, light pink—control, light brown—negative control), Melting curves (blue—test, light pink—control). **C.** Heat stress at 65°C for 120'. Amplification curves (grey—test, light pink—control, light brown—negative control), Melting curves (grey—test, light pink—control).

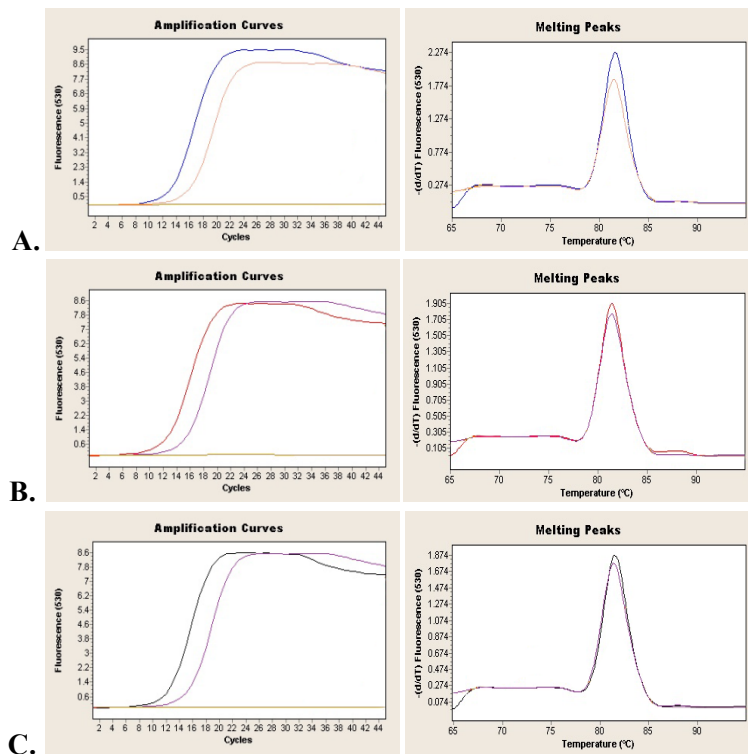


**Figure C.8 Real-time PCR amplification and melting curves for TVN0489 gene under heat-shock (70°C).** A. Heat stress at 70°C for 30'. Amplification curves (blue—test, light pink—control, light brown—negative control), Melting curves (grey—test, light pink—control). B. Heat stress at 70°C for 90'. Amplification curves (red—test, purple—control, light brown—negative control), Melting curves (red—test, purple—control). C. Heat stress at 70°C for 120'. Amplification curves (red—test, purple—control, light brown—negative control), Melting curves (red—test, purple—control).

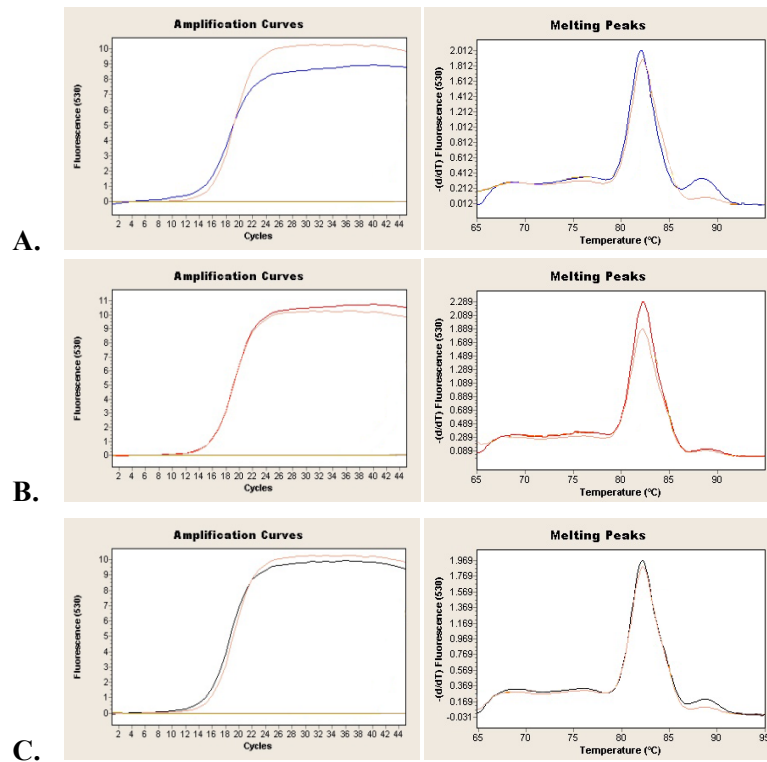


**Figure C.9 Real-time PCR amplification and melting curves for TVN0489 gene under pH stress. A.** pH stress at pH 4.0 for 30'. Amplification curves (blue—test, pink—control, light brown—negative control), Melting curves (blue—test, pink—control). **B.** pH stress at pH 4.0 for 90'. Amplification curves (red—test, pink—control, light brown—negative control), Melting curves (red—test, pink—control). **C.** pH stress at pH 4.0 for 120'. Amplification curves (black—test, pink—control, light brown—negative control), Melting curves (black—test, pink—control).

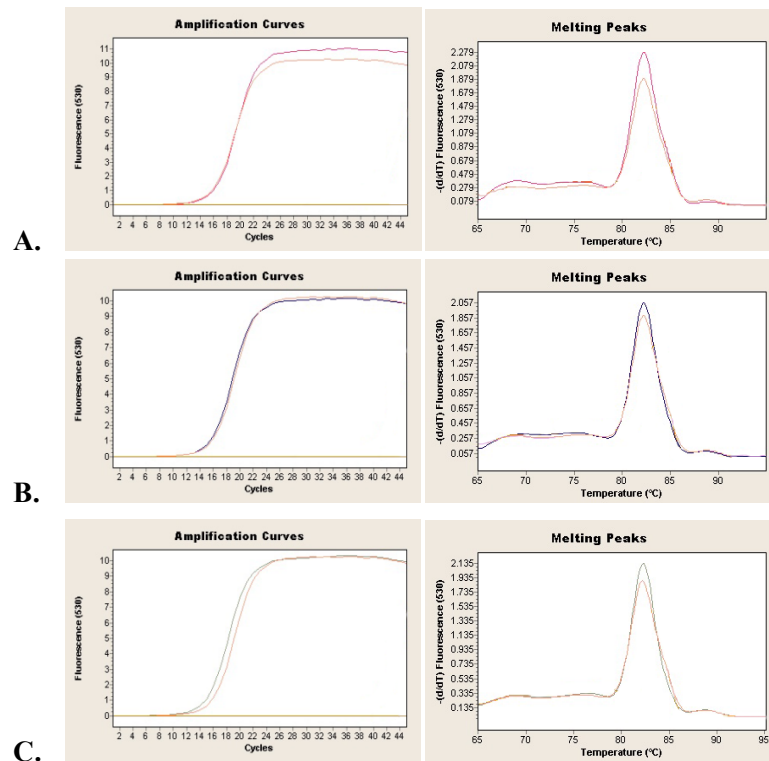


**Figure C.10 Real-time PCR amplification and melting curves for TVN0489 gene under oxidative stress.** A. Oxidative stress at 0.02 mM for 30'. Amplification curves (pink—test, light pink—control, light brown—negative control), Melting curves (pink—test, light pink—control). B. Oxidative stress at 0.02 mM for 90'. Amplification curves (purple—test, light pink—control, light brown—negative control), Melting curves (purple—test, light pink—control). C. Oxidative stress at 0.02 mM for 120'. Amplification curves (grey—test, light pink—control, light brown—negative control), Melting curves (grey—test, light pink—control).

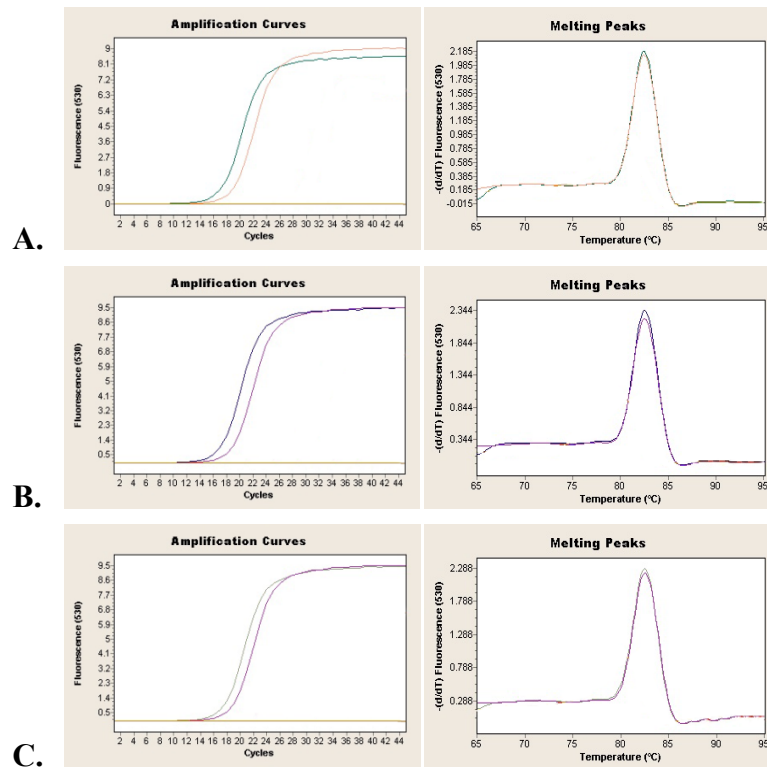


**Figure C.11 Real-time PCR amplification and melting curves for TVN115 gene under heat-shock (65°C).** A. Heat shock at 65°C for 60'. Amplification curves (green—test, light pink—control, light brown—negative control), Melting curves (green—test, light pink—control). B. Heat shock at 65°C for 90'. Amplification curves (blue—test, purple—control, light brown—negative control), Melting curves (blue—test, purple—control). C. Heat shock at 65°C for 120'. Amplification curves (grey—test, purple—control, light brown—negative control), Melting curves (grey—test, purple—control).

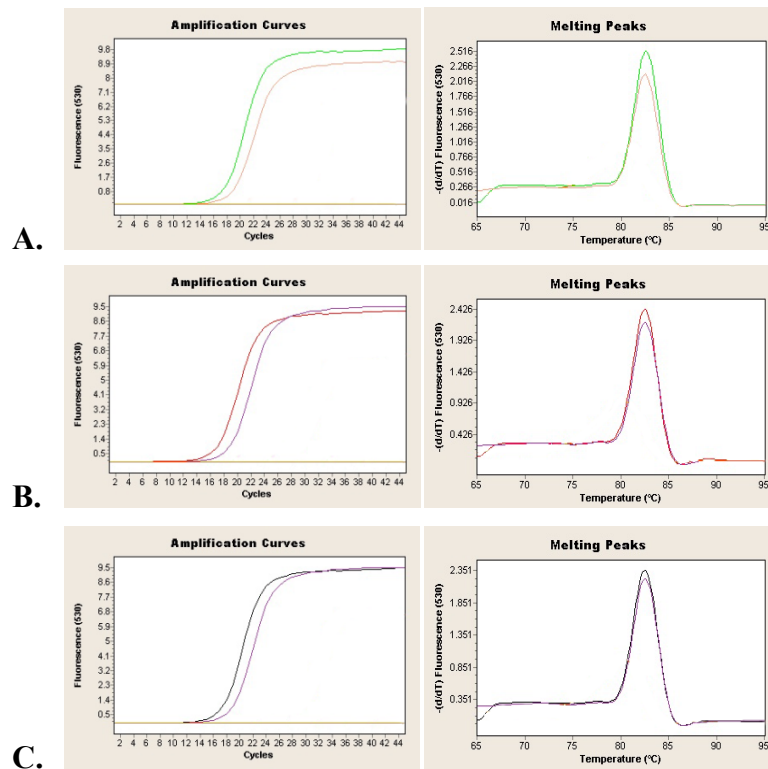


**Figure C.12 Real-time PCR amplification and melting curves for TVN1145 gene under heat-shock (70°C).** **A.** Heat shock at 70°C for 60'. Amplification curves (green—test, light pink—control, light brown—negative control), Melting curves (green—test, light pink—control). **B.** Heat shock at 70°C for 90'. Amplification curves (red—test, purple—control, light brown—negative control), Melting curves (red—test, purple—control). **C.** Heat shock at 70°C for 120'. Amplification curves (black—test, purple—control, light brown—negative control), Melting curves (black—test, purple—control).

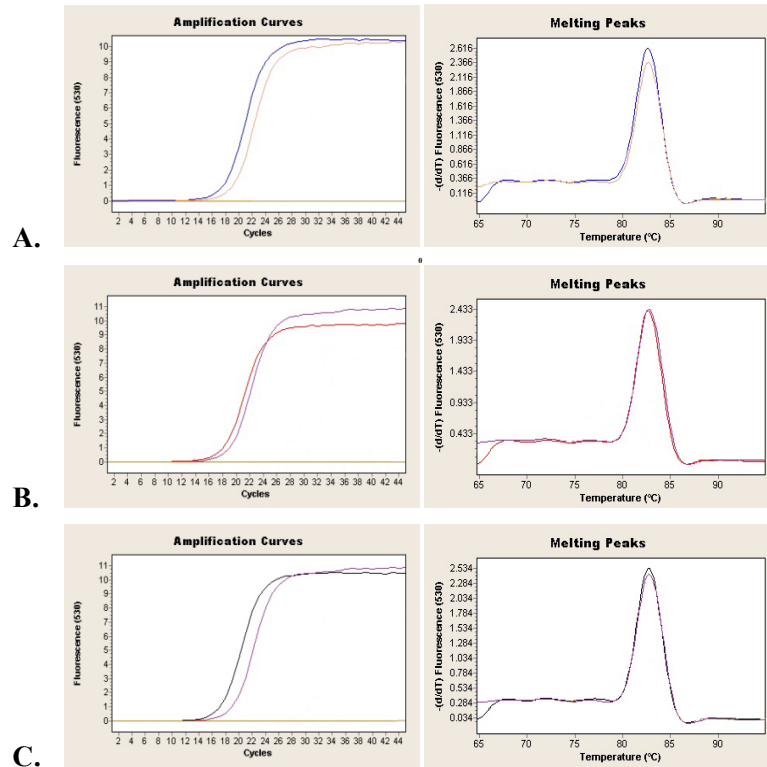


**Figure C.13 Real-time PCR amplification and melting curves for TVN1145 gene under pH stress.** **A.** pH stress at pH 4.0 for 30'. Amplification curves (blue—test, pink—control, light brown—negative control), Melting curves (blue—test, pink—control). **B.** pH stress at pH 4.0 for 90'. Amplification curves (red—test, purple—control, light brown—negative control), Melting curves (red—test, purple—control). **C.** pH stress at pH 4.0 for 120'. Amplification curves (black—test, purple—control, light brown—negative control), Melting curves (black—test, purple—control).

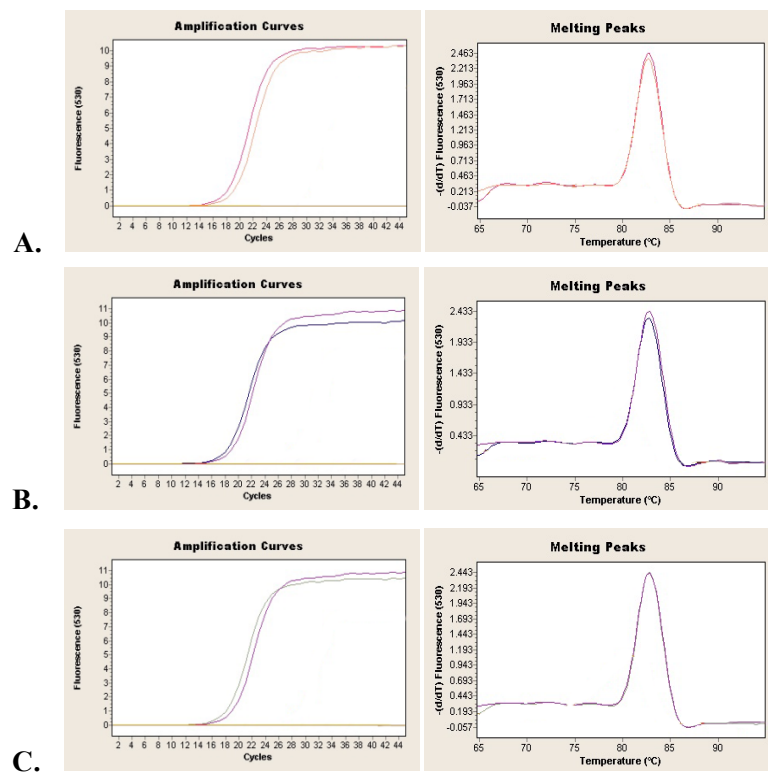


**Figure C.14 Real-time PCR amplification and melting curves for TVN1145 gene under oxidative stress.** **A.** Oxidative stress at 0.02 mM for 30'. Amplification curves (pink—test, light pink—control, light brown—negative control), Melting curves (pink—test, light pink—control). **B.** Oxidative stress at 0.02 mM for 90'. Amplification curves (blue—test, purple—control, light brown—negative control), Melting curves (blue—test, purple—control). **C.** Oxidative stress at 0.02 mM for 120'. Amplification curves (grey—test, purple—control, light brown—negative control), Melting curves (grey—test, purple—control).